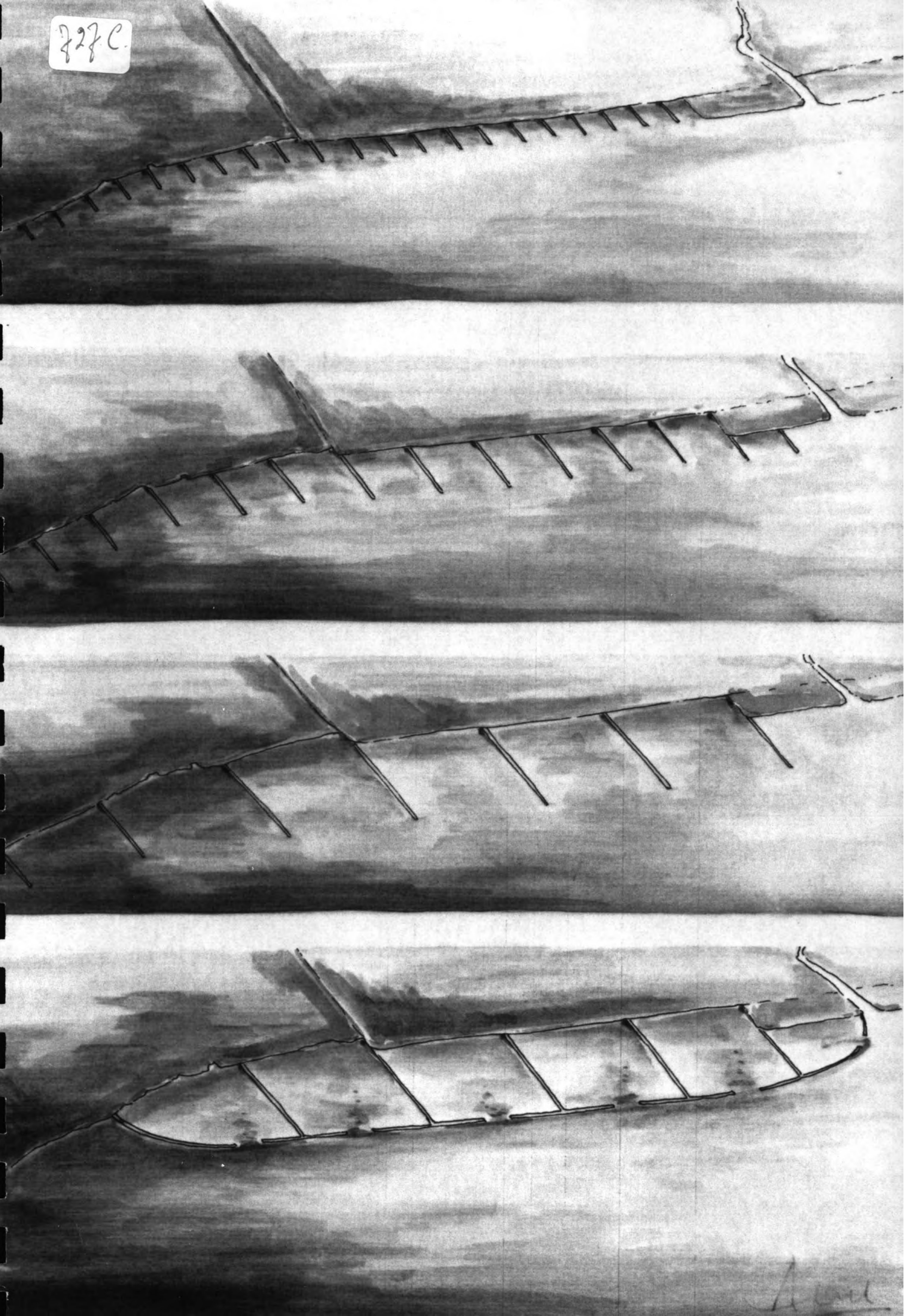

ROTTERDAM PUBLIC WORKS
Harbour Engineering Division

FEASIBILITY STUDY

LANDRECLAMATION SHANGHAI PROVINCE

LAY-OUT Part I
a relation between sedimentation and lay-out

Yvette van den Berg
December 1987

0. SUMMARY

0.1 General

At the Cao Jing district in Shanghai, China, a reclamation project is planned.
The object of this project is to stimulate the natural process of sedimentation.
The object of the present report is to determine the optimum lay-out, which combines a fast accretion of sediments and low construction costs of the dikes (see Fig. 0.1).

In this analysis, the problem is handled by estimating the sedimentation pattern for several lay-outs.
First the water movement is determined by a numerical simulation using the program DUCHESS, next the sediment transports are determined by the program MORPHOR, which uses the results of DUCHESS as a basis.

Following data were available:

	normal conditions	extreme conditions
WATERLEVEL		
low water-level	0.20 m	- 0.60 m
high water-level	3.70 m	5.30 m
CURRENT		
maximum (flood)	1.04 m/s	2.0 m/s
average	0.60 m/s	1.0 m/s
maximum (eb)	- 0.80 m/s	- 1.6 m/s
SEDIMENT CONCENTRATION		
maximum (flood)	1.60 kg/m3	5.0 kg/m3
average	1.00 kg/m3	2.0 kg/m3
maximum (eb)	1.20 kg/m3	4.0 kg/m3

Table 0.1: general data for the Cao Jing district (at a level of -2 m (Wu Song level))

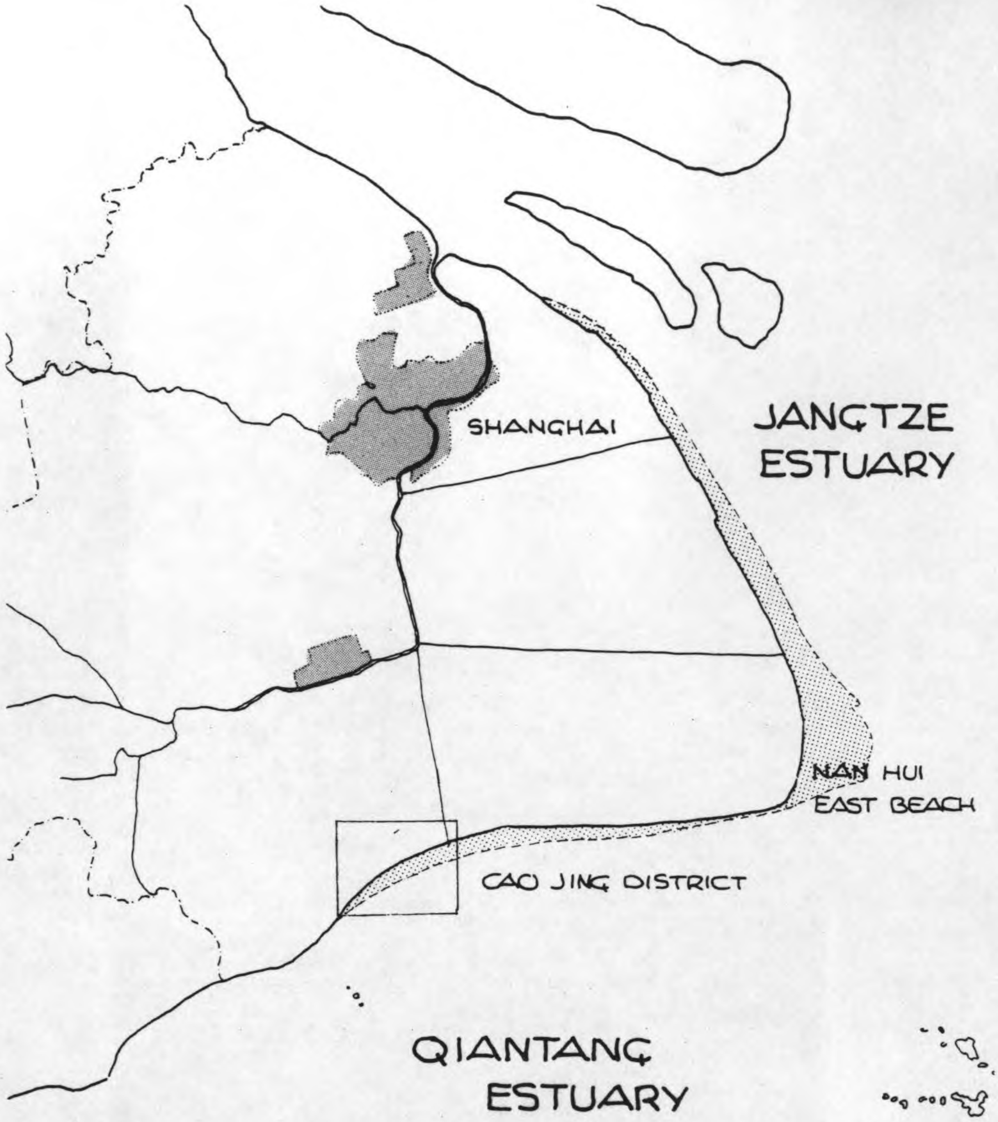
SHANGHAI
JANGTZE ESTUARY
NAN HUI EAST BEACH
CAO JING DISTRICT
QIANTANG ESTUARY

0.1

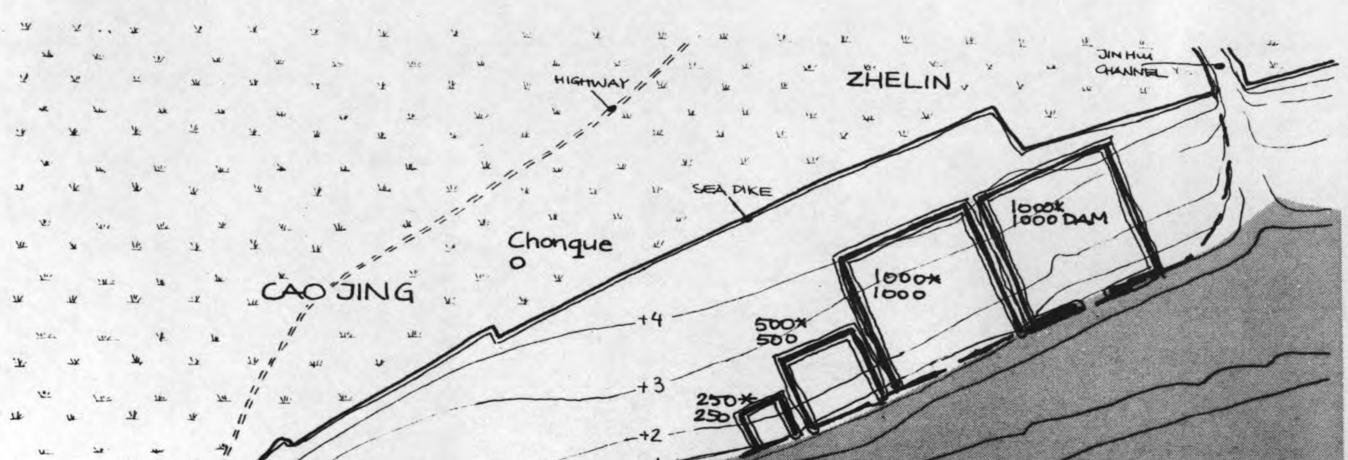
HIGHWAY
ZHELIN
JIN HUI CHANNEL
SEA DIKE
Chonque
CAO JING
1000x 1000 DAM
1000x 1000
500x 500
250x 250
+4
+3
+2
+1
0
-2
-4
-6
-8
Nanku

0.2

0.2 Schematization

The optimization of the dike lay-out concerns the following items:

- the length of the dams;
- the distance between the dams;
- the width of the opening at the seaward end.

In the simulations following lay-outs have been tested:

- 250 x 250 m;
- 500 x 500 m;
- 1,000 x 1,000 m;
- 1,000 x 1,000 m plus a longitudinal dam with an opening at the seaward end, of 333 m (see Fig. 0.2).

For the bottom configuration, the natural situation has been simulated (see Fig. 0.2); the hydraulic and morphological characteristics of the simulation are given in table 0.2 and table 0.3.

In general, the sediments are brought into the reclamation basins by the following mechanisms:

1. exchange of water as a result of storage

   incoming water is rich in sediments, outgoing water is not; as a result of storage the incoming sediments settle to the bottom; accretion results;

2. exchange of water by long-shore currents

   in the basin an eddy develops, driven by the long-shore current. This eddy guarantees a continuous exchange of "new" (sediment rich) water from outside with "old" (sediment poor) water from inside the basin.
   Since the velocity inside the eddy is much smaller (about one third) than in the long-shore current, sediments settle inside the basin; extra sedimentation occurs;

3. exchange of water by difference in density

   the water inside the basin (calm area) has a lower density of sediment than the water outside; as a result a "tongue" of heavy (sediment rich) water will form into the basin, causing extra accretion.

Overview

An overview of the characteristics and schematizations of each of the numerical models is given in the following tabel:

LAY-OUT MODEL	250 * 250	500 * 500	1,000 * 1,000	1,000 * 1,000 + dam
- mesh size: Δx	16.67 m	33.33 m	66.67 m	66.67 m
Δy	16.67 m	33.33 m	66.67 m	66.67 m
- time-step: Δt	20 s	40 s	60 s	60 s
- H-conditions:				
diff. in water-level: Δh	0.033 m	0.067 m	0.133 m	0.133 m
tidal difference : ΔH	4.50 m	4.50 m	4.50 m	4.50 m
tidal period : T	44,700 s	44,700 s	44,700 s	44,700 s
- Q-conditions:	-	-	-	-
- initial conditions:				
mean water-level: H_o	2.00 m	2.00 m	2.00 m	2.00 m
discharge : Qx	0 m2/s	0 m2/s	0 m2/s	0 m2/s
discharge : Qy	0 m2/s	0 m2/s	0 m2/s	0 m2/s
- friction:				
roughness of bottom: K_s	0.05 m	0.05 m	0.05 m	0.05 m
- viscosity: E	0.04 m2/s	0.04 m2/s	0.04 m2/s	0.04 m2/s
- coriolisparameter: C	0	0	0	0
- slipparameter:	FREE SLIP	FREE SLIP	FREE SLIP	FREE SLIP
- computed time: T	3,600 s	3,600 s	7,200 s	7,200 s

Table 0.2: overview of hydraulic characteristics, based on a 25 * 25-nodes-computational grid.

Overview

An overview of the characteristics and schematizations of each of the numerical models is given in the following tabel:

LAY-OUT MODEL	250 * 250	500 * 500	1,000 * 1,000	1,000 * 1,000 plus dam
- mesh_size: Δx Δy	16.67 m 16.67 m	33.33 m 33.33 m	66.67 m 66.67 m	66.67 m 66.67 m
- time-step: Δt	10 s	20 s	40 s	40 s
- C-conditions: C_{in}	377.10^{-6}	377.10^{-6}	377.10^{-6}	377.10^{-6}
- T-conditions: T_{in}	-	-	-	-
- initial conditions: sed.-concentration: C_o transport : Tx transport : Ty	 0 0 m2/s 0 m2/s	 0 0 m2/s 0 m2/s	 0 0 m2/s 0 m2/s	 0 0 m2/s 0 m2/s
- grainsizes: average: D_{50} larger : D_{90}	 50.10^{-6} m 100.10^{-6} m	 50.10^{-6} m 100.10^{-6} m	 50.10^{-6} m 100.10^{-6} m	 50.10^{-6} m 100.10^{-6} m
- fall-velocity: W_s	$1.1.10^{-3}$ m/s	$1.1.10^{-3}$ m/s	$1.1.10^{-3}$ m/s	$1.1.10^{-3}$ m/s
- reference-level: β	0.01	0.01	0.01	0.01
- porosity_sediment: p	0.4	0.4	0.4	0.4
- lateral diffusion: D	1.0 m/s	2.5 m2/s	5.0 m2/s	5.0 m2/s
- morphological conditions: computed time: T pseudo-viscosity: α	 3,600 s 0.21	 3,600 s 0.11	 3,600-7,200 s 0.06	 3,600-7,200 s 0.06
- order of_computation:	1	1	1	1

Table 0.3: overview of morphological characteristics, based on a 25 * 25-nodes-computational grid.

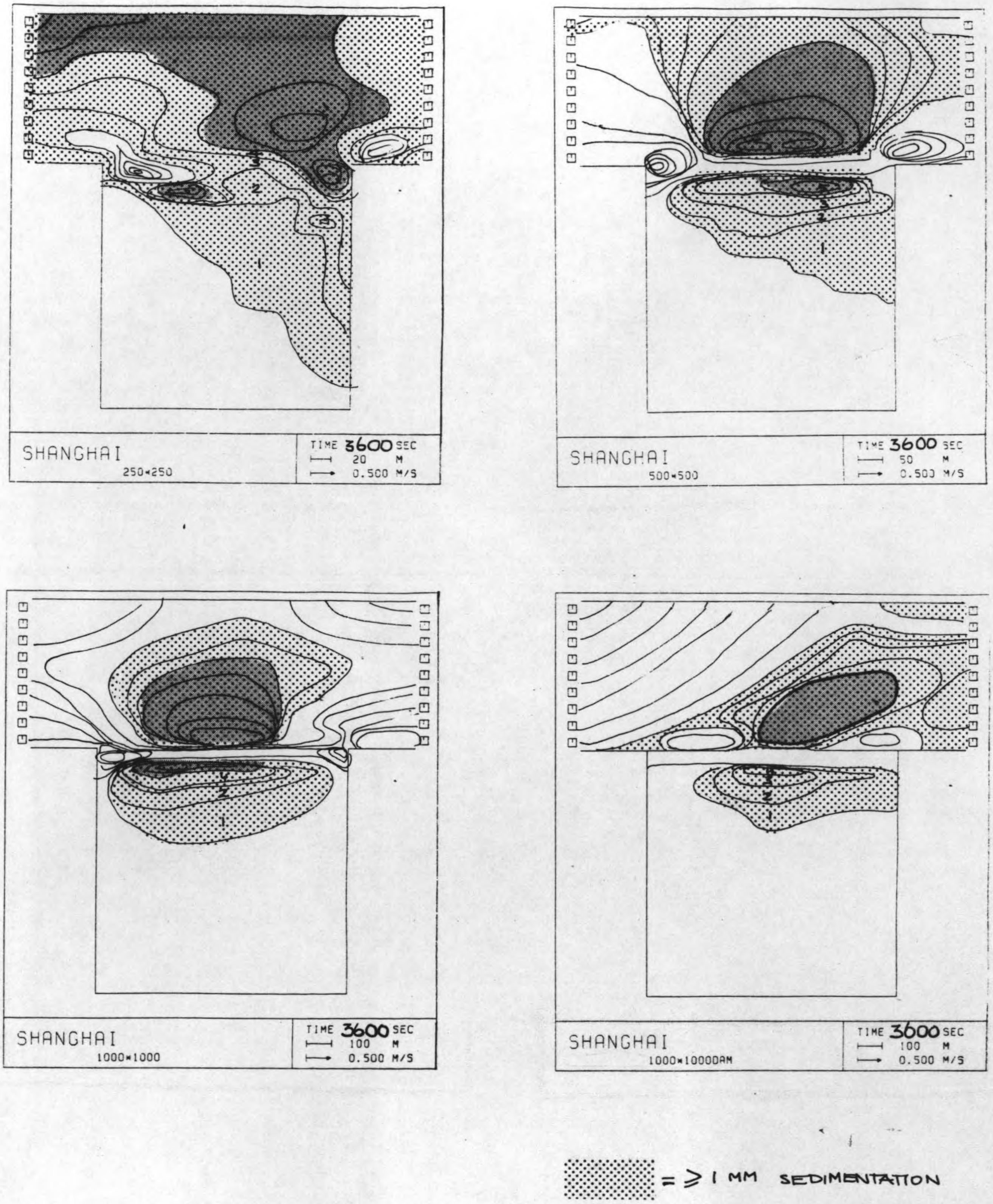
SHANGHAI
250×250
TIME 3600 SEC
20 M
0.500 M/S
SHANGHAI
500×500
TIME 3600 SEC
50 M
0.500 M/S
SHANGHAI
1000×1000
TIME 3600 SEC
100 M
0.500 M/S
SHANGHAI
1000×10000AM
TIME 3600 SEC
100 M
0.500 M/S
= ≥ 1 MM SEDIMENTATION
= ≥ 5 MM SEDIMENTATION

0.3

0.3 Results

The results of the numerical simulations are given in Fig. 0.3; the relations between sedimentation and lay-out are given in Fig. 0.4.

A comparison of the effectivity of each of the lay-out models is given in table 0.4; where the results of the simulations (the total amount of exchange of water and sediments) are given; also these figures are given in case only storage causes an exchange of water and sediments.

LAY-OUT MODEL	250 * 250 m	500 * 500 m	1,000 * 1,000 m	1,000 * 1,000 m plus dam
T = 3,600 s				
simulations				
- DUCHESS				
total in [m3]	188.10^3	541.10^3	$1,847.10^3$	858.10^3
total out [m3]	129.10^3	371.10^3	981.10^3	27.10^3
Δh [mm]	960	948	925	900
- MORPHOR				
total in [m3]	53.0	197.0	673.2	211.0
total out [m3]	5.5	33.5	100.9	-
ΔZ [mm]	0.76	0.65	0.60	0.22
storage				
- water				
total in [m3]	60.610^3	244.10^3	716.10^3	716.10^3
total out [m3]	-	-	-	-
Δh [mm]	969	969	969	969
- sediments				
total in [m3]	22.83	91.50	270.0	270.0
total out [m3]	-	-	-	-
ΔZ [mm]	0.61	0.61	0.45	0.45
T = 7,200 s				
simulations				
- DUCHESS				
total in [m3]	-	$1,019.10^3$	$3,723.10^3$	$1,597.10^3$
total out [m3]	-	671.10^3	$2,138.10^3$	27.10^3
Δh [mm]	-	1,683	1,670	1,656
- MORPHOR				
total in [m3]	-	-	1,468	476.4
total out [m3]	-	-	266.5	-
ΔZ [mm]	-	-	1.34	0.59
storage				
- water				
total in [m3]	106.10^3	426.10^3	$1,576.10^3$	$1,576.10^3$
total out [m3]	-	-	-	-
Δh [mm]	1.696	1.696	1.696	1.696
- sediments				
total in [m3]	40.13	160.5	594	594
total out [m3]	-	-	-	-
ΔZ [mm]	1.07	1.07	0.99	0.99

Table 0.4: total amount of exchanged water [m3] and sediments [m3]; average rise of the bottomlevel [mm] and water-level [mm] in case of DUCHESS, MORPHOR and (only) storage.

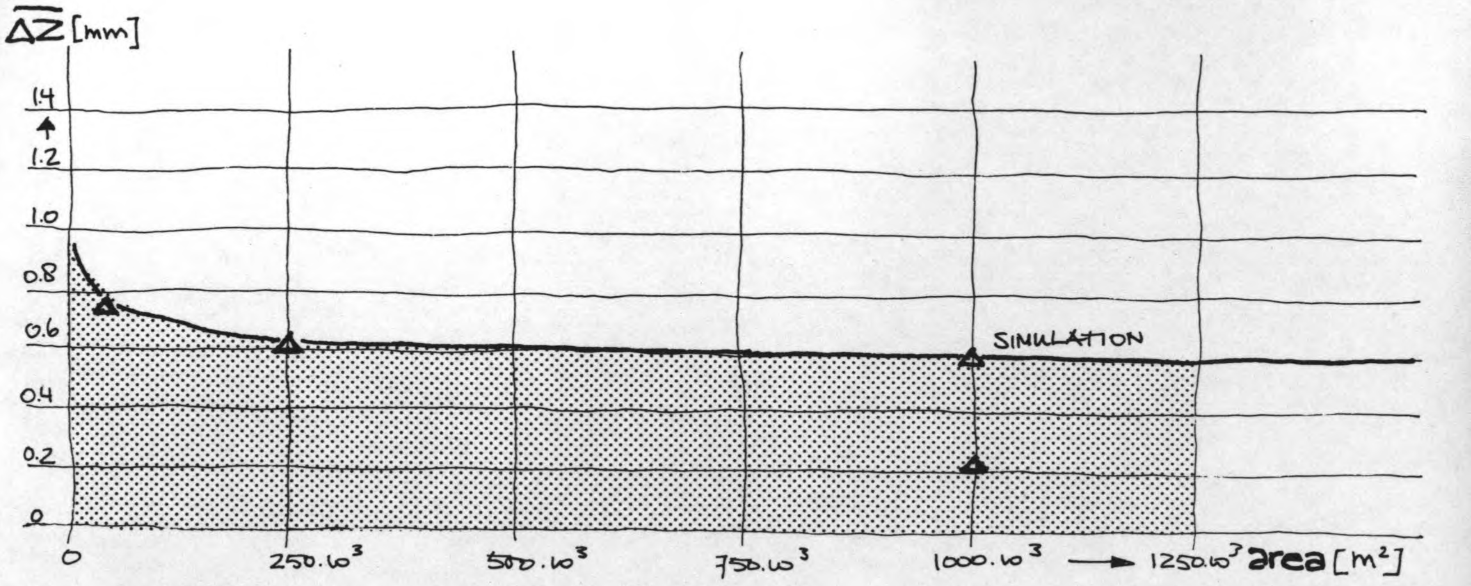

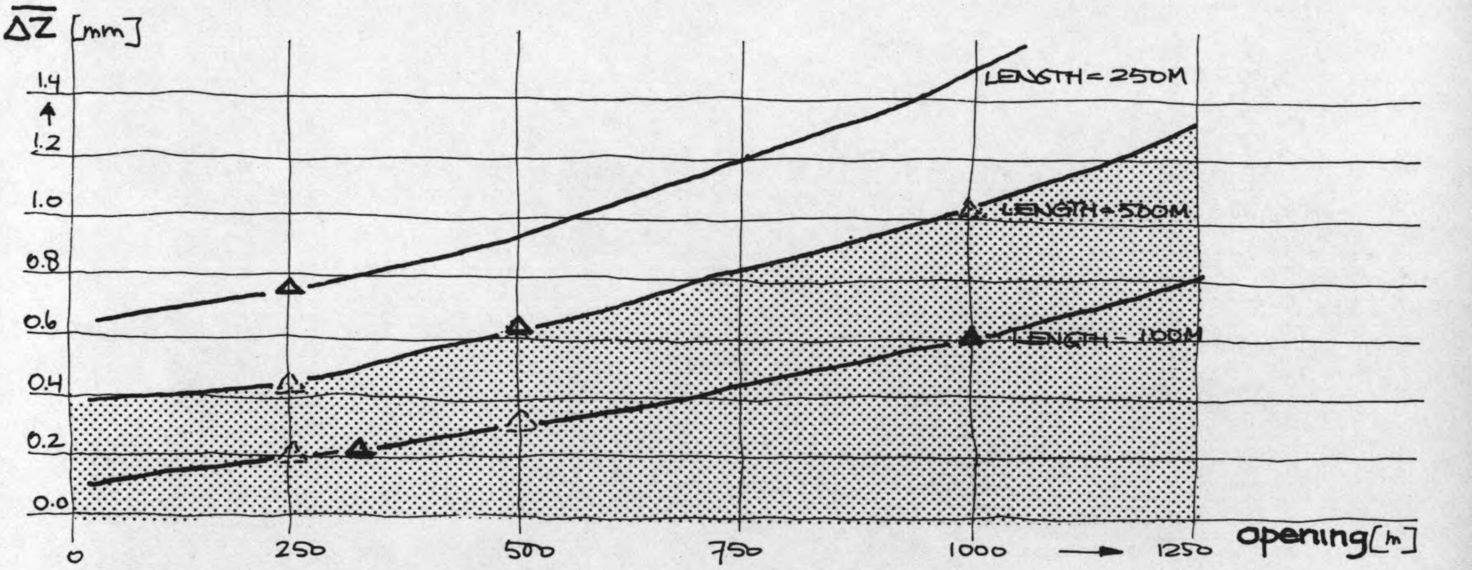

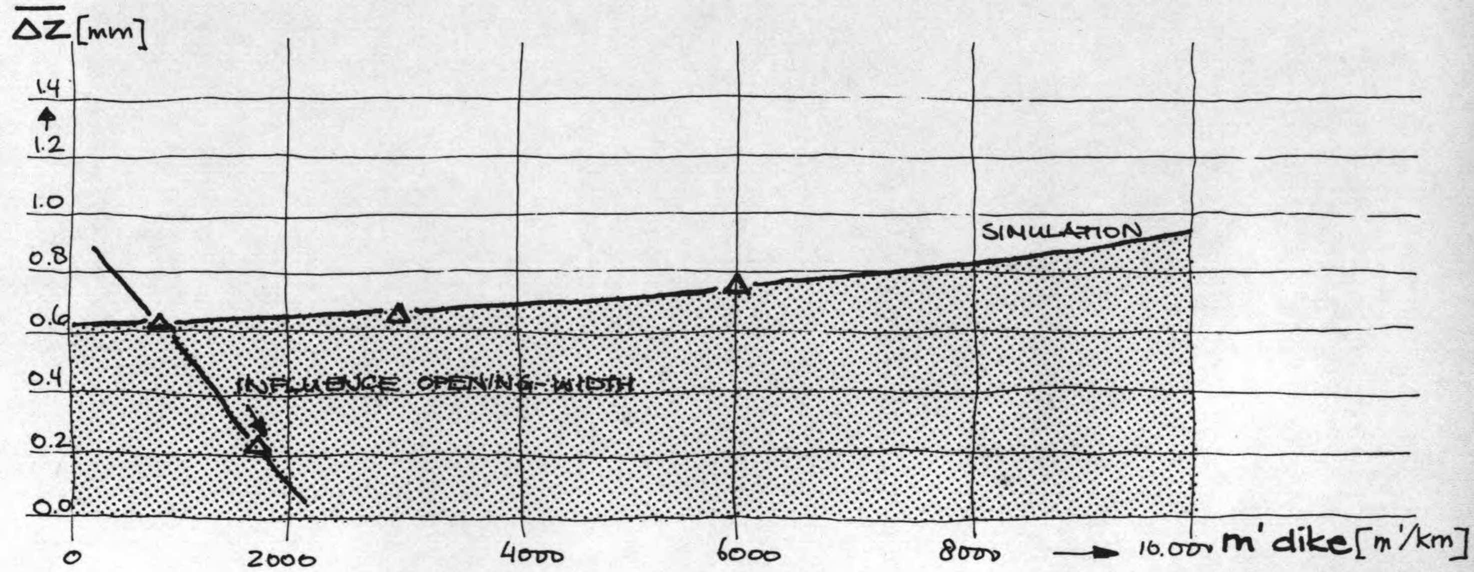

Δ = RESULT SIMULATION

△ = CALCULATED (see table 5.1)

0.4

Due to initial effects the calculated sedimentation is still underpredicted; it is assumed that the results of the "1,000 x 1,000 m plus dam" lay-out are typical for a storage dominated sedimentation pattern (the increase of the sedimentation during the second hour of simulation is comparable to the increase of the storage quantity. In the other lay-outs, the increase of sedimentation is much larger than the storage quantity).

0.4 Conclusions

TIDAL MOTION

On the basis of the numerical calculations (considering the tidal motion, wave influence is neglected) following conclusions can be drawn:

1. sedimentation caused by storage forms an important part of the total sedimentation (causes about 1/3 of the maximum exchange). The actual sedimentation equals or exceeds this quantity (provided that the wave influence is not able to disturb this pattern).
   The penetration of the incoming water by storage is very limited; most of the sedimentation is concentrated in the first few hundreds of meters of the basin (neglecting the wave influence);

2. sedimentation caused by eddy developing forms the main part of the total accretion (causes about 2/3 of the max. exchange). Since the adaption length of the suspension (can be compared to the total length over which the sediments stay in suspension when reaching calm water) is limited to about 300 to 400 m, also the penetration of the sediment-rich water is limited (500 m).
   For the increase of sedimentation by eddy exchanging the opening of the basin must be large; the larger the opening the more extra accretion; when the opening is reduced to 1/3 of the distance, all the advantageous influence of the eddy-developing disappears, only the storage-exchange causes sedimentation.
   The eddy itself also has a limited size (due to the bottom friction) of (a maximum of) 500 m;

3. sedimentation caused by differences in density has not been taken into account; since the programs were of a two-dimensional nature, this effect can't be schematized (a typical three-dimensional problem). It is assumed that this effect on the total sedimentation will be negligible.

As a result, the optimum lay-out can be described as follows (taking into account only the tidal influence) (see Fig. 0.5A):

- length of the basin: as short as possible (500 m);

- distance between the cross-dams: as wide as possible (1,000 m);

- width of the opening at seaward end: as large as possible (small longitudinal dams are avoiding erosion around the cross-dam heads) (≈ 800 m).

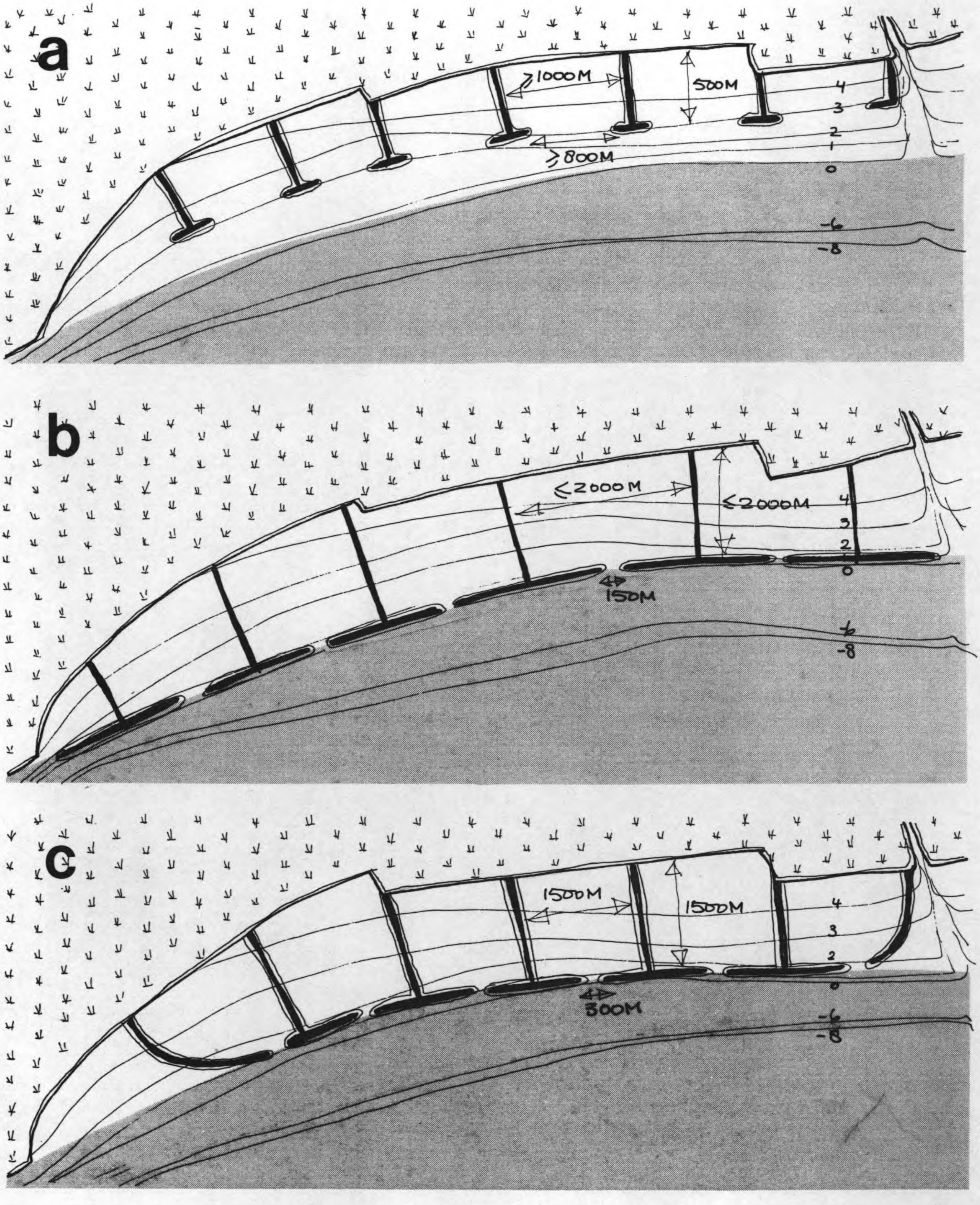
a
≥1000M
500M
≥800M
4
3
2
1
0
-6
-8
b
≤2000M
≤2000M
150M
4
3
2
0
-6
-8
c
1500M
1500M
300M
4
3
2
0
-6
-8

0.5

WAVE INFLUENCE

The waves cause an increased shear stress at the bottom, this causing an increased tendency of the particles to go into suspension.
This effect will cause a reduced sedimentation (sedimentation will only occur where the waves have been reduced considerably).
The optimum lay-out of the reclamation fields on the basis of wave influence is shown in Fig. 0.5B (see report LAY-OUT part II).

COMBINATION

The combined effect of tidal influence and wave influence causes an increased penetration of high sediment concentrated water into the basins, it also causes the necessity of a small opening size at the seaward end of the basins (Fig. 0.5C).
The optimum size of the basin is in the order of 1,500 x 1,500 m, determined by the admissable fetch-length of the waves, and by the maximum size of the eddy (about 500 m). In a larger basin, sedimentation could concentrate at some disadvantageous spots (near the opening, or only at one side of the basin).
The minimum size of the opening is 150 m, based on the admissable storage velocities, and the allowable contraction of the flow (when the opening becomes very small a jet stream develops instead of an eddy); the optimum size of the opening is about 300-500 m.

In order to continue the project, first the wave climate at the Cao Jing district has to be determined, in order to find the width of the openings and the height of the dams.

N.B.: due to the very short numerical simulations, the results of the simulations have no practical value. They show a tendency only. Also the watermovement is so much schematized (a longshore current combined with a rise of the water-level) that it has little relation to the watermovement in the real situation. Due to initial effects, the results of the simulations can't be trusted to be representative; only to follow the tendency of the practical situation.

CONTENT

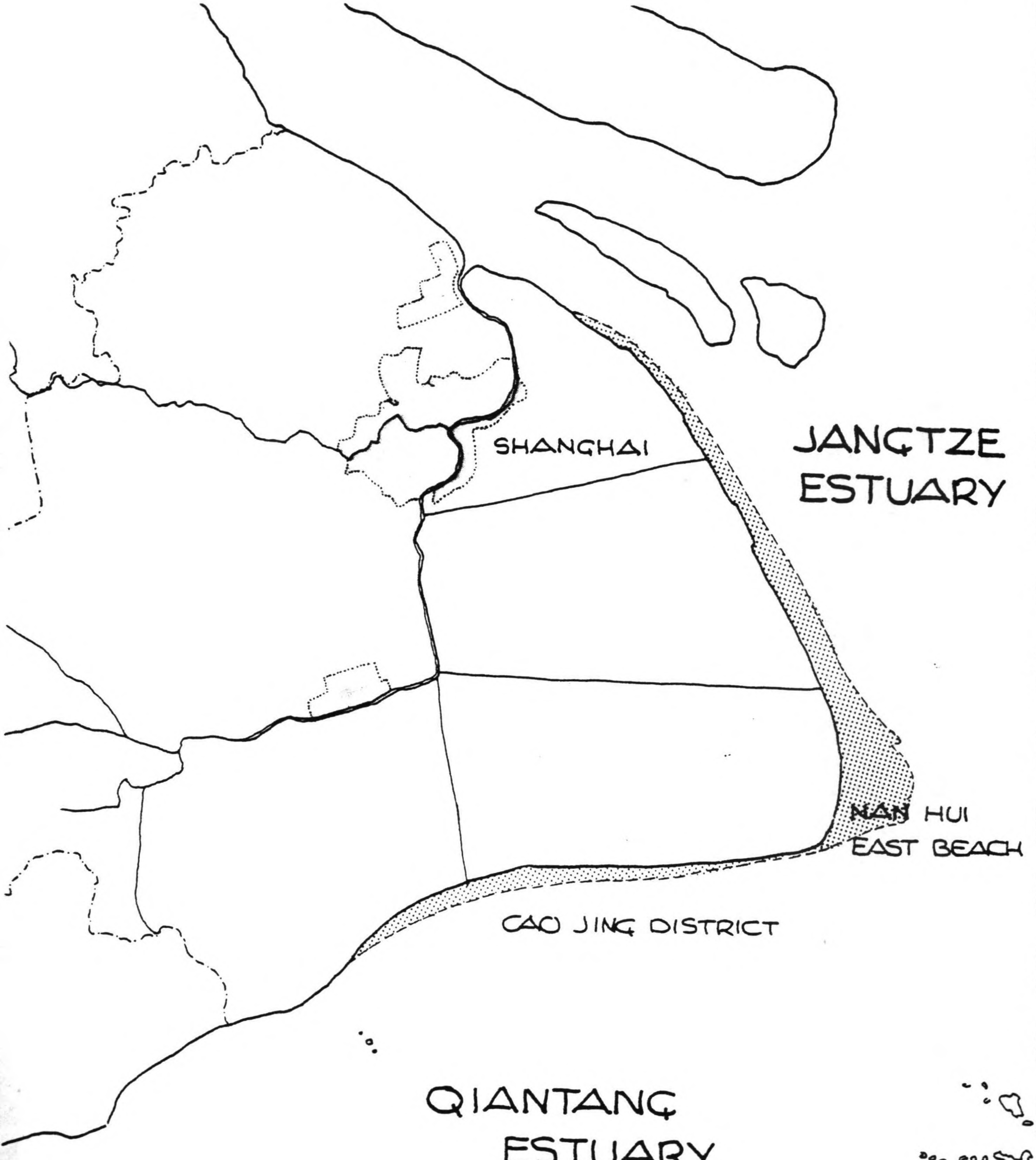

1.1

Overview of the area

1. INTRODUCTION

1.1 Problem

In the delta-area of the river Yangtze Kiang and along the coast of the Hangzhou Bay at Shanghai Province, a reclamation plan is being prepared concerning particularly the Cao Jing district (see Fig. 1.1).
In the forgoing study "study about landreclamation" (lit. (1)) it was suggested to use a system of cross-dams and longitudinal dams to stimulate the natural accretion. These dams consist of geotextile membranes filled with soil (see Fig. 1.2).

The next phase in this project is to perform a feasibility study resulting in a preliminary design of the landreclamation system. This study comprises the following three items:

A. LAY-OUT : the location of the dams in relation to the expected sedimentation. Relations might be found between the speed of siltation and the total length of dams.

B. CONSTRUCTION DESIGN: the dimensions of the soil filled tubes, the kind of geotextile required to resist loadings caused by waves, wind, currents and tidal action.
An optimization might be possible concerning the costs per m' cross-section related to the chance of failure.

C CONSTRUCTION METHOD : ways to fill and handle the tubes in a way that they can be used as construction elements.
An optimization might be possible concerning the total costs of the project related to the way of construction.

This report focusses on the first item: to determine a relation between the configuration of the dams and the expected rate of sedimentation in order to give an advice about a lay-out design.

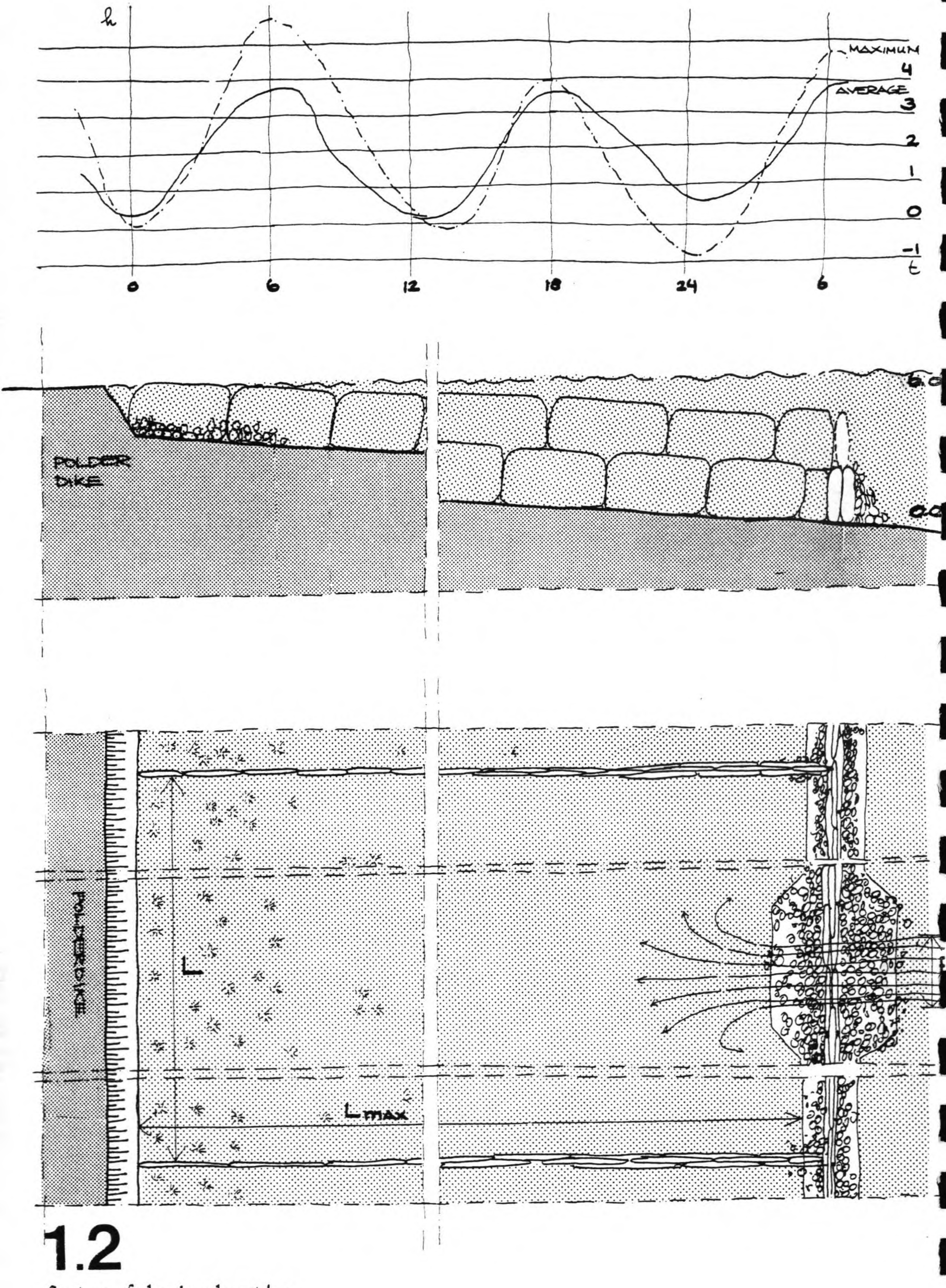

1.2

System of landreclamation

1.2 Approach

Sedimentation is mainly governed by the flow pattern of the water, caused by waves and tidal currents. To determine this flow pattern and the resulting sedimentation pattern, several instruments are available: prototype tests, scale model simulations and numerical simulations.

Starting point for this study is that only the tidal motion is included in the computation of the water and sediment movement, it is presumed that the tidal movement has a dominant effect on the sediment transport on long term. The influence of shorter waves like windwaves and swell is examined in a succeeding report: "LAY-OUT part II" (lit. (2)).

It is chosen to use numerical models available from the Technical University Delft:

1. the two-dimensional tidal program DUCHESS (lit. (3));

2. the two-dimensional morphological program MORPHOR coupled to the program Duchess (lit. (4)).

The model Duchess is used to calculate the flow pattern around and inside the dams, the model Morphor is used to determine the siltation pattern plus the resulting changes in the bottom level. In order to find a relation between the siltation pattern and the configuration of the dams several lay-outs are tested with these models.

Chapter two describes the mathematical models Duchess and Morphor, chapter 3 describes the stepwise schematization of the problem made in order to solve it by means of two-dimensional numerical simulations. Chapter 4 discusses the results of the computations, resulting in an advice about lay-out design in chapter 5.
The appendices A to C go deeper into the theoretical backgrounds: Appendix A discusses the problems that occur when a three-dimensional flow is schematized in two dimensions: the closure problem for depth-averaged flow.
A summary of the thesis on sediment transport, as developed by Van Rijn, is given in appendix B.
Appendix C describes a numerical model for sediment transport that is suitable to be used in two-dimensional flow problems.

This analysis has been performed as an assignment of the co-operation between Rotterdam (harbour engineering division) and Shanghai (bureau of waterconservancy). Originally it was the intention to calculate the tidal velocities of the entire Hangzhou-Bay, resulting in tidal velocities and water-levels at Cao Jing. However enough data were found concerning the tidal motion at Cao Jing. The next phase was to find the optimum lay-out, where eddy-developing was expected to have significant influence.

The programm MORPHOR, which is not in effect yet, came available with the aid of mr. Wang, its inventor.
MORPHOR is a two-dimensional horizontal morphological program, based on a vertical integration of the sediment-movement in (shallow) water. It can be coupled to a two-dimensional, horizontal tidal program, like DUCHESS, by storing the water-data on a tape-unit, which will form the input of MORPHOR. This opportunity, to compute the watermovement inside fictionary basins with stepwise dimensions together with the morphological changes during the tidal motion, seems a logical step to take if one wants to optimize the dimensions of reclamation-basins. By choosing certain intervals between lengthwise dimensions, cross-wise dimensions and opening sizes, one can find the relation between sedimentation and lay-out (provided that the mechanics of the sediment-motion are right).

Unfortunately, the MORPHOR-program does not include wave-action. It is based on the equations of Van Rijn (a publication of Van Rijn is summarized in Appendix B), which are valid for "uniform currents" only (based on the average current velocity in streamwise direction). The tidal motion of the sediments is calculated on the basis of the model of Galapatti (a publication is summarized in Appendix C), which uses the "Van Rijn-results" as an equilibrium solution; the actual situation will reach this equilibrium taking into account an adaption-time and an adaption-length. In a later stage MORPHOR will be including the wave-influence.
However, the results of MORPHOR and DUCHESS can be used to find the eddy-influence; the watermovement; the sedimentation-pattern when the opening-size is small; etc. At least the order of the rate of siltation can be found.

Thus the numerical simulations will give an impression of the possible dimensions of the reclamation fields; the resulting velocities and the size of possible eddies. The wave-calculation will give rise to a more detailed view of the optimum dimensions.

2. THE MATHEMATICAL TOOLS

2.1 The model Duchess

Because of its specific facilities a choice has been made to use the two-dimensional model DUCHESS (lit. (3), lit. (5)). The following are important possibilities of the Duchess-model:

1. the DUCHESS-model computes two-dimensional flow patterns caused by tides and surges. It has been in effect since 1980, the last version originating from Sept. 1986;

2. coupled to the DUCHESS-model a morphological program is available that computes morphological changes in the bottom. It computes concentration and transport rates simultaneously with the water movement;

3. the model allows nesting of coarse and finer grids in the computational grid. The boundary data for the finer grid model can be obtained from the results of a coarse grid model;

4. the program allows certain parts of the computational area to become dry or get inundated during numerical integration;

5. the model can handle a very irregular type of bottom topography, dams in the computational region can be modelled by means of internal boundary-conditions.

The DUCHESS-model is based on two-dimensional long wave equations (integrated in vertical direction).
There are three basic equations in the model. One of them is the continuity equation, which follows from the conservation of mass:

$$\frac{\partial H}{\partial t} + \frac{\partial}{\partial x} Qx + \frac{\partial}{\partial y} Qy = 0 \quad \ldots\ldots (1)$$

The others are the equations of motion in X and Y-direction (vertically integrated).

$$\frac{\partial}{\partial t} Qx + \frac{\partial}{\partial x}\frac{Qx^2}{D} + \frac{\partial}{\partial y}\frac{QxQy}{D} - \frac{\partial}{\partial x}\left[DE \frac{\partial}{\partial x}\frac{Qx}{D}\right]$$

$$- \frac{\partial}{\partial y}\left[DE \frac{\partial}{\partial y}\frac{Qx}{D}\right] + g\, D \frac{\partial}{\partial x}\left[H + P\right] + Fr \mid Q \mid \frac{Qx}{D^2}$$

$$- Co\, Qy + \frac{Wx}{\rho} = 0 \quad \ldots\ldots (2)$$

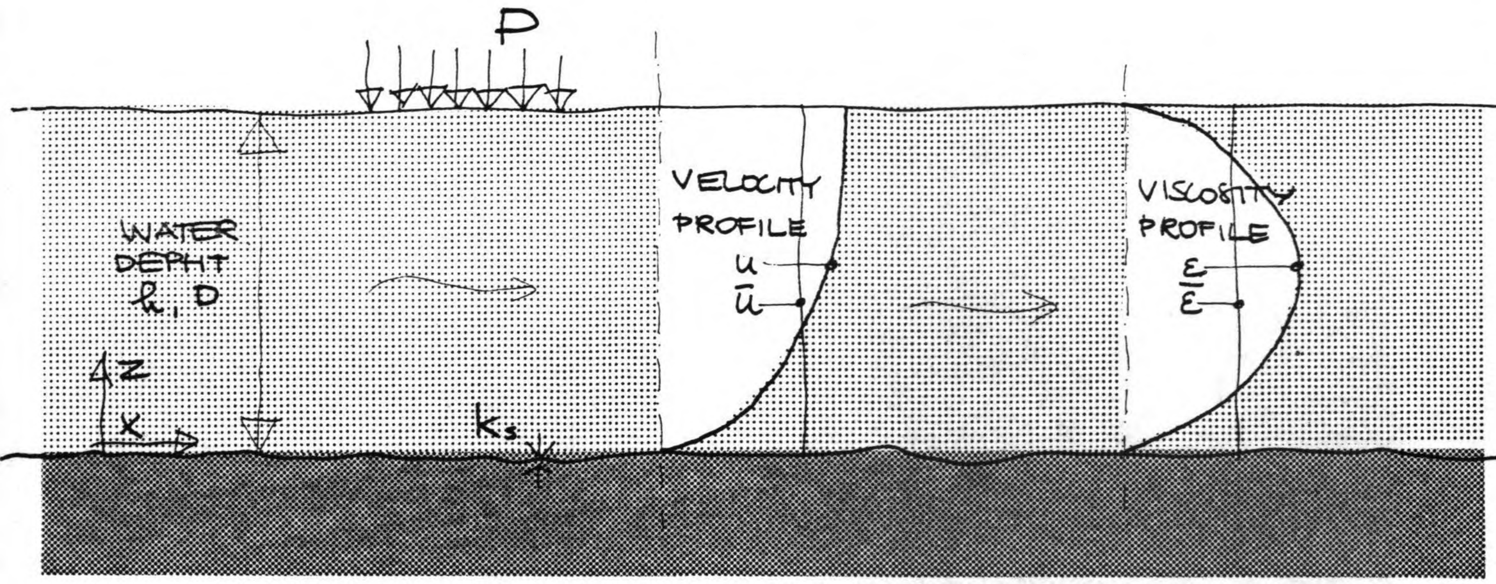

CROSS-SECTION (VERTICAL PLANE)

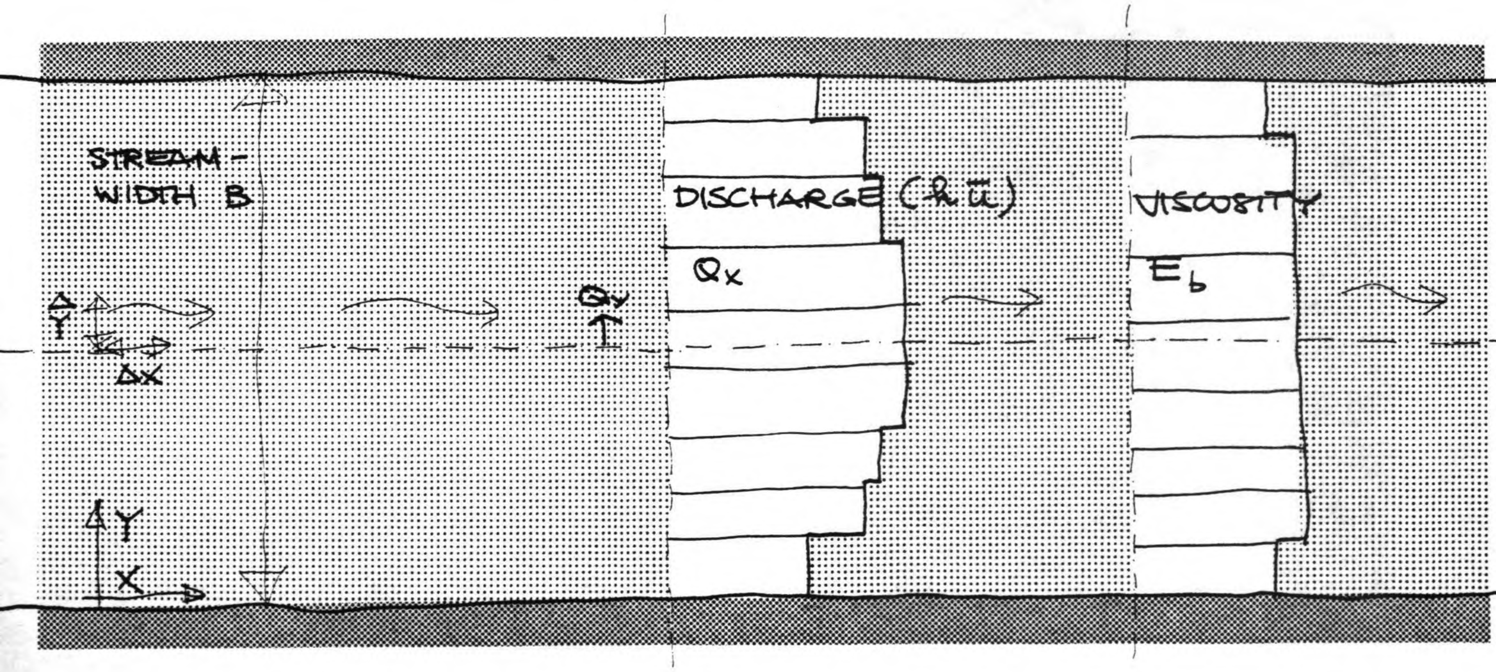

OVERVIEW (HORIZONTAL PLANE)

2.1

DUCHESS: directions and definitions

and

$$\frac{\partial}{\partial t} Qy + \frac{\partial}{\partial x}\frac{QxQy}{D} + \frac{\partial}{\partial y}\frac{Qy^2}{D} - \frac{\partial}{\partial x}\left[DE \frac{\partial}{\partial x}\frac{Qy}{D}\right]$$

$$- \frac{\partial}{\partial y}\left[DE \frac{\partial}{\partial y}\frac{Qy}{D}\right] + g\,D \frac{\partial}{\partial y}\left[H + P\right] + Fr\,|\,Q\,|\,\frac{Qy}{D^2}$$

$$+ Co\,Qx + \frac{Wy}{\rho} = 0 \quad \ldots\ldots\ldots\ldots\ldots\ldots\ldots\ldots \quad (3)$$

The terms present in the equation are the following:

- local acceleration term;
- advective acceleration terms;
- viscosity terms;
- slope and pressure term;
- bottom friction term;
- coriolis term;
- wind shear stress component.

Notations:

g	= gravitational acceleration	[m/s2]
D	= water depth (H - Z)	[m]
Z	= bottom level	[m]
E	= eddy viscosity coefficient	$[m^2/s]$
P	= surface air pressure head = $\frac{p}{\rho g}$	[m]
Fr	= friction coefficient = $\frac{g}{C^2}$	[-]
$\mid Q \mid$	= $\sqrt{Qx^2 + Qy^2}$	$[m^2/s]$
Co	= coriolis coefficient	[m/s2]
Wx and Wy	= X and Y-components of wind shear stress divided by the mass-density of water	$[m^2/s]$
Qx and Qy	= average current velocity multiplied by depth (in X and Y-direction)	[m2/s]
H	= water level	[m]

The equations (1), (2) and (3) are solved by means of an Alternating Direction Implicit Method. Current vector and water level are calculated at alternate points.

In the computational procedures, new values for Qx, Qy and H are calculated at every half time step. In the first half time step computation along the X-direction takes place and in the second half time step computation along the Y-direction.

In the computation along the X-direction the derivatives with respect to X are treated implicitely and the derivatives with respect to Y explicitely and vice versa. The water levels are advanced in time using the continuity equation, the currents using the equations of motion. The partial differential equations are approximated by means of a numerical scheme which is central in space and nearly central in time.

The finite difference approximations to partial differential equations (1)--(3) are given below. Only computation in the X-direction is described since computation in the Y-direction is identical, apart from the swapping of the variables Qx and Qy. The superscript - indicates the known value at time t , the superscript + indicates the as yet unknown value at a time half step ahead (t + ½ Δt).

In the first half time step (implicit in X-direction) the continuity equation (1) is approximated by the following expressions:

$$\left[\frac{H^{+}_{i,j} - H^{-}_{i,j}}{\tfrac{1}{2}\Delta t}\right] + R\left[\frac{Q^{+}_{x_{i,j}} - Q^{+}_{x_{i-1,j}}}{\Delta x}\right] +$$

$$+ (1 - R)\left[\frac{Q^{-}_{x_{i,j}} - Q^{-}_{x_{i-1,j}}}{\Delta x}\right] + \left[\frac{Q^{-}_{y_{i,j}} - Q^{-}_{y_{i,j-1}}}{\Delta y}\right] =$$

$$= 0 \quad \ldots \qquad (4)$$

See (fig. 2.1) for the definitions of directions and the meaning of the superscripts $_{i,j}$ etc. The equation for the computation in the second half time step is found by swapping Qx and Qy and by substituting ($_{i-1,j}$) by ($_{i,j-1}$) etc.

R = 2Θ, where Θ is a coefficient lying between 0.5 and 1 which is used to control the amount of numerical damping. The equation of motion in X-direction (implicit in X-direction) is approximated by:

$$\frac{Q^{+}_{x_{i,j}} - Q^{-}_{x_{i,j}}}{\tfrac{1}{2}\Delta t} + \qquad \text{(local acceleration: } \frac{\partial}{\partial t}\, Qx\text{)}$$

$$+ (Q^{-}_{x_{i,j}} + Q^{-}_{x_{i+1,j}})\, \frac{2R^{1}\left[Q^{+}_{x_{i,j}} + Q^{+}_{x_{i+1,j}}\right] + (1 - 2R^{1})\left[Q^{-}_{x_{i,j}} + Q^{-}_{x_{i+1,j}}\right]}{2D\,\Delta x}$$

$$- (Q^{-}_{x_{i,j}} + Q^{-}_{x_{i-1,j}})\, \frac{2R^{1}\left[Q^{+}_{x_{i,j}} + Q^{+}_{x_{i-1,j}}\right] + (1 - 2R^{1})\left[Q^{-}_{x_{i,j}} + Q^{-}_{x_{i-1,j}}\right]}{2D\,\Delta x}$$

(advective acceleration: $\frac{\partial}{\partial t}\frac{Qx^2}{D}$)

$$+ \frac{\left[Q\bar{x}_{i,j} + Q\bar{x}_{i,j+1}\right] * \left[Q\bar{y}_{i,j} + Q\bar{y}_{i+1,j}\right]}{(D_{i,j} + D_{i+1,j} + D_{i,j+1} + D_{i+1,j+1})\ \Delta y}$$

$$+ \frac{\left[Q\bar{x}_{i,j} + Q\bar{x}_{i,j-1}\right] * \left[Q\bar{y}_{i,j-1} + Q\bar{y}_{i+1,j-1}\right]}{(D_{i,j} + D_{i+1,j} + D_{i,j-1} + D_{i+1,j-1})\ \Delta y}$$

(advective acceleration: $\frac{\partial}{\partial y} \frac{QxQy}{D}$)

$$- \frac{2E_{i,j}\ D_{i,j}}{\Delta x^2} \left[\frac{2Q^+_{x\ i+1,j}}{D_{i+1,j} + D_{i+2,j}} - \frac{2Q^+_{x\ i+1,j}}{D_{i,j} + D_{i+1,j}} \right]$$

$$- \frac{2E_{i-1,j}\ D_{i-1,j}}{\Delta x^2} \left[\frac{2Q^+_{x\ i,j}}{D_{i,j} + D_{i+1,j}} - \frac{2Q^+_{x\ i-1,j}}{D_{i,j} + D_{i-1,j}} \right]$$

(viscosity terms: $DE \ \frac{\partial^2}{\partial x^2} \frac{Qx}{D}$)

$$+ \frac{g(D_{i,j} + D_{i+1,j})}{2\Delta x} \left(\left[P_{i+1,j} - P_{i,j}\right] + R\left[H^+_{i+1,j} - H^+_{i,j}\right] + (1-R)\left[H^{--}_{i+1,j} - H^{--}_{i,j}\right] \right)$$

(slope and pressure term)

$$+ \frac{4\ Fr\ |\ Q\ \cdot|\ \left[2Q^+_{i,j} - Q^-_{i,j}\right]}{(D_{i,j} + D_{i+1,j})^2}$$

(bottom friction term)

$$- \frac{Co}{4} \left[Q\bar{y}_{i,j} + Q\bar{y}_{i+1,j} + Q\bar{y}_{i,j\ 1} + Q\bar{y}_{i+1,j-1}\right]$$

(coriolis term)

$$+ Wx_{i,j} \quad = \quad 0 \ \ldots\ldots\ldots\ldots\ldots \quad (5)$$

(wind shear stress term)

The term R^1 in equation (5) performs a similar function as R. The superscript -- means that values are used at the time ($t - \frac{1}{2}\Delta t$), this is necessary in order to maintain stability, using the values of time (t) causes unstable behaviour. In the numerical experiments R = 1 and R^1 = 1 is used for computations.

The computation in Y-direction (implicit in X-direction) is approximated by (this is still the computation in the <u>first</u> half time step):

$$\frac{\left[\overset{+}{Qy}_{i,j} - \overline{Qy}_{i,j}\right]}{\tfrac{1}{2}\Delta t} \qquad \left(\text{local acceleration } \frac{\partial}{\partial t} Qy\right)$$

$$+\ 2\left(\overline{Qx}_{i,j} + \overline{Qx}_{i,j+1}\right)\left[\frac{R^1\left[\overset{+}{Qy}_{i,j} + \overset{+}{Qy}_{i+1,j}\right] + (1-R^1)\left[\overline{Qy}_{i,j} + \overline{Qy}_{i+1,j}\right]}{\left(D_{i,j} + D_{i,j+1} + D_{i+1,j+1} + D_{i+1,j+1}\right)\Delta x}\right]$$

$$-\ 2\left(\overline{Qx}_{i-1,j} + \overline{Qx}_{i-1,j+1}\right)\left[\frac{R^1\left[\overset{+}{Qy}_{i-1,j} + \overset{+}{Qy}_{i,j}\right] + (1-R^1)\left[\overline{Qy}_{i-1,j} + \overline{Qy}_{i,j}\right]}{\left(D_{i-1,j} + D_{i-1,j+1} + D_{i,j} + D_{i,j+1}\right)\Delta x}\right]$$

$$\left(\text{advective acceleration: } \frac{\partial}{\partial x}\frac{QxQy}{D}\right)$$

$$+\ \frac{\left[\overline{Qy}_{i,j} + \overline{Qy}_{i,j-1}\right] * \left[\overline{Qy}_{i,j} + \overline{Qy}_{i,j+1}\right]}{2D_{i,j+1}\,\Delta y}$$

$$-\ \frac{\left[\overline{Qy}_{i,j} + \overline{Qy}_{i,j-1}\right] * \left[\overline{Qy}_{i,j} + \overline{Qy}_{i,j-1}\right]}{2D_{i,j}\,\Delta y}$$

$$\left(\text{advective acceleration: } \frac{\partial}{\partial y}\frac{Qy^2}{D}\right)$$

$$-\ \frac{E}{2\Delta x^2}\left(D_{i,j} + D_{i,j+1} + D_{i+1,j} + D_{i+1,j+1}\right)\left[\frac{\overset{+}{Qy}_{i+1,j}}{D_{i+1,j} + D_{i+1,j+1}} - \frac{\overset{+}{Qy}_{i,j}}{D_{i,j} + D_{i,j+1}}\right]$$

$$+\ \frac{E}{2\Delta x^2}\left(D_{i,j} + D_{i,j+1} + D_{i+1,j} + D_{i+1,j+1}\right)\left[\frac{\overset{+}{Qy}_{i,j}}{D_{i,j} + D_{i,j+1}} - \frac{\overset{+}{Qy}_{i-1,j}}{D_{i-1,j} + D_{i-1,j+1}}\right]$$

$$\left(\text{viscosity terms: } DE\,\frac{\partial^2}{\partial x^2}\frac{Qy}{D}\right)$$

$$+\ \frac{g\left(D_{i,j} + D_{i,j+1}\right)}{2\Delta x}\left(\overline{H}_{i,j+1} - H_{i,j} + \left[P_{i,j+1} - P_{i,j}\right]\right)$$

(slope and pressure term)

$$+ \frac{4\ Fr\ |\ Q\ |\ \overset{+}{Qy}_{i,j}}{(D_{i,j} + D_{i,j+1})^2}$$ (bottom friction term)

$$+ \frac{Co}{4} \left[Q\bar{x}_{i,j} + Q\bar{x}_{i+1,j} + Q\bar{x}_{i,j-1} - Q\bar{x}_{i+1,j-1} \right]$$ (coriolis term)

$$+ Wy_{i,j} = 0 \quad \ldots\ldots\ldots\ldots\ldots\ldots\ldots\ldots \quad (6)$$ (wind shear stress term)

Analogous equations are used for the computation implicit in Y-direction.
In the manner described above a set of lineair equations is solved efficiently by means of the Thomas-Algorithm, new values for H, Qx and Qy result. This procedure is followed for every line in X-direction, then the time is increased by half a time step and the procedure is applied in Y-direction.

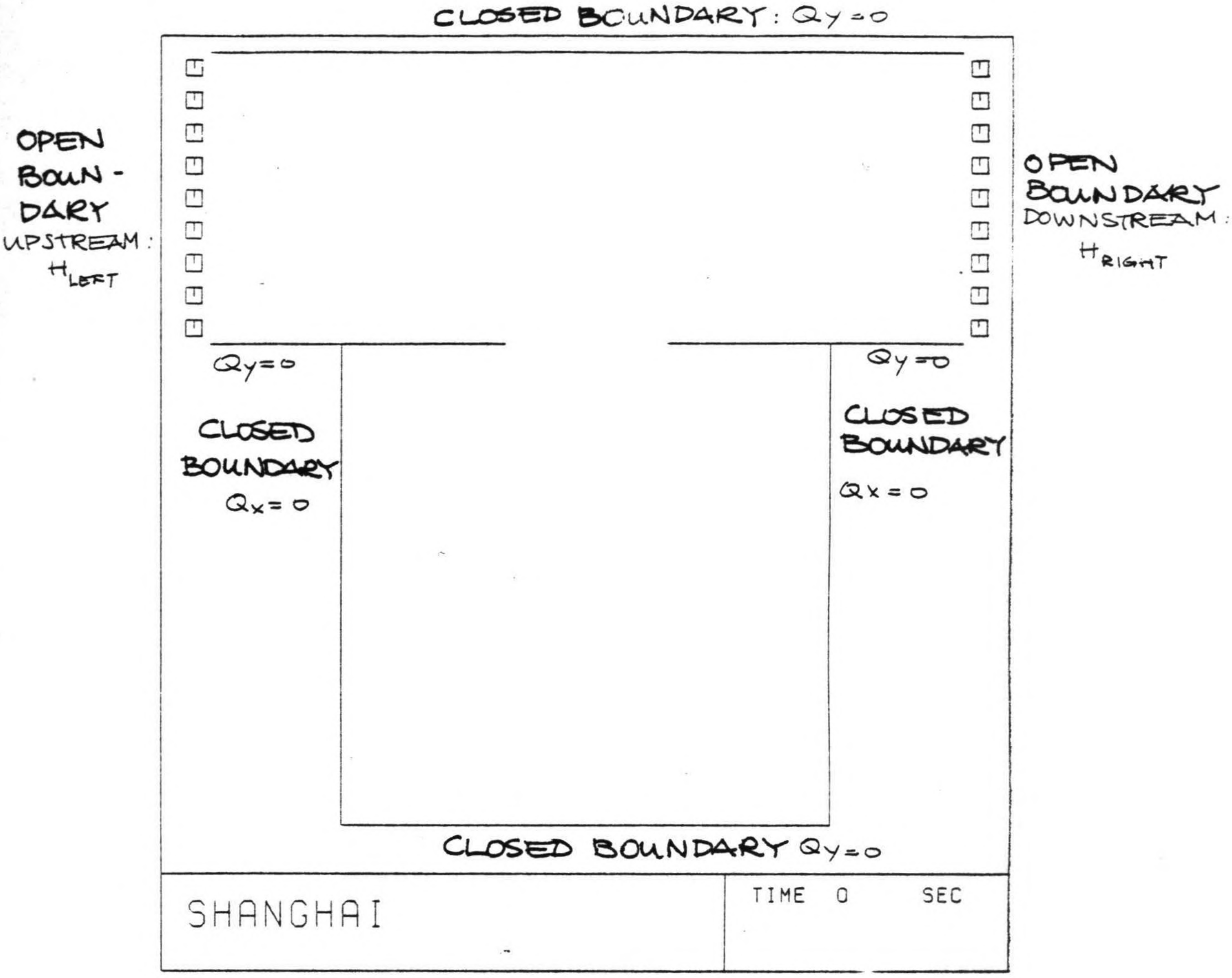

PRESCRIBE INITIAL CONDITION AT COMPLETE FIELD (25*25 POINTS): H, Qx AND Qy
PRESCRIBE BOUNDARY CONDITION AT OPEN BOUNDARIES (2*10 POINTS): H_{LEFT}, H_{RIGHT}

2.2

Input Duchess

INPUT

The model DUCHESS demands following input data:

1. the gridsizes Δx (m)
   Δy (m)
   and orientation: left or right

2. the computational area n_x dimensionless
   n_y dimensionless

3. the bottom level B in each gridpoint given with respect to a certain reference level (B=ZB) (m)

4. the time-step Δt (m)

5. the bottom friction coefficient $Fr = g/C^2$ dimensionless

6. the viscosity coefficient E (m^2/s)

7. the numerical damping in the main acceleration terms and in the convective terms $\theta 1$ and $\theta 2$ dimensionless

8. the wind-stress coefficient $W = w/\rho$ (m^2/s)

9. the atmospheric pressure $P = p/\rho g$ (m)

10. initial conditions for Qx (m^2/s)
    Qy (m^2/s)
    H in each gridpoint (m)

11. boundary conditions for Qx (m^2/s)
    Qy (m^2/s)
    H (m)

OUTPUT

Output data as provided by DUCHESS are:

1. discharge in X-direction Qx for each gridpoint (per unit of width) (m^2/s)

2. discharge in Y-direction Qy for each gridpoint (per unit of width) (m^2/s)

3. waterlevel H in each gridpoint (m)

RESTRICTIONS

The input data of the DUCHESS model must satisfy following requirements.

Time step in relation to mesh size

In order to maintain stability and in the view of the computational accuracy the courant number σ may not become too large; an upper limit is 10.

$$\text{Courant number: } \sigma = c \frac{\Delta t}{\Delta x} \leq 10$$

Time required to minimize the influence of (initial) disturbances

At least several times the time a wave needs to travel through the model must be considered as adjustment time, and as such irrelevant.

Propagation velocity of a wave $c \simeq \sqrt{gd}$

In order to check whether a solution has become periodic, at least a few tidal periods should be simulated.

Bottom schematization

Sharp transitions in the bottom level may cause problems, especially when located near an open boundary. One is advised to smoothen the bottom, if such problems happen. If necessary the boundary should be shifted outward somewhat if one does not want to change the topography of the model and smoothening is still necessary.

2.2 The model MORPHOR

The morphological program MORPHOR is based on an integrated model for suspended transport, as proposed by Galapatti (lit. (6)).

The basic equation for this model is a combination of the two-dimensional flow model and the two-dimensional (vertical) convection-diffusion equation for the sediment concentration in the vertical plane.

$$\frac{\partial c}{\partial t} + u\frac{\partial c}{\partial x} + w\frac{\partial c}{\partial z} = w_s \frac{\partial c}{\partial z} + \frac{\partial}{\partial z}(\varepsilon_z \frac{\partial c}{\partial z}) \quad \ldots\ldots\ldots\ldots\ldots (1)$$

c = sediment concentration
w_s = fall velocity of sediment particles
ε_z = turbulent diffusion coefficient for sediment transfer in vertical direction (see Fig. 2.2)

Galapatti (see Appendix C) proposed to solve this equation by means of an asymptotic solution for the depth-averaged concentration, which resulted in following equation:

first order unsteady solution:

$$\gamma_{11}\overline{c_e} = \gamma_{11}\bar{c} + \gamma_{21}\frac{h}{w_s}\frac{\partial \bar{c}}{\partial t} + \gamma_{22}\frac{\bar{u}h}{w_s}\frac{\partial \bar{c}}{\partial x} \quad \ldots\ldots\ldots\ldots\ldots (2)$$

$\bar{c}$ = depth-averaged concentration
$\overline{c_e}$ = depth-averaged equilibrium concentration
γ_{11} = coefficient concerning zero order concentration profile (see appendix C)
γ_{21} = coefficient concerning first order concentration profile with respect to time (see appendix C)
γ_{22} = coefficient concerning first order concentration profile with respect to location (see appendix C)

γ_{11} can be found from a bed-boundary condition. It is assumed that the bed-load concentration immediately adjusts to the local flow conditions, whereas the suspended load demands a certain length and time to adjust to the new flow conditions.

The bed-boundary can be of a concentration type:

$$\overline{c_e}\gamma_{11} = c_a \Big|_{z\,=\,\text{bottom}} \quad \ldots\ldots\ldots\ldots\ldots\ldots\ldots\ldots\ldots (3A)$$

c_a = sediment concentration of the bed-load
c_e = depth-averaged equilibrium concentration

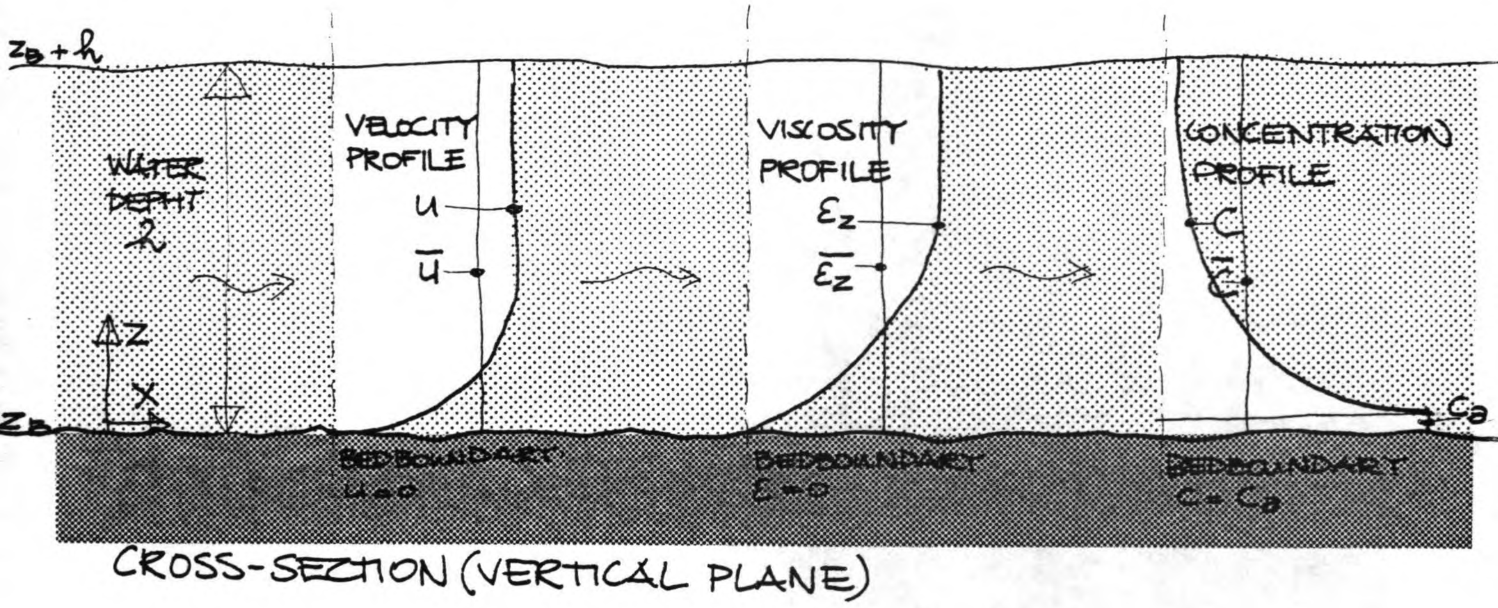

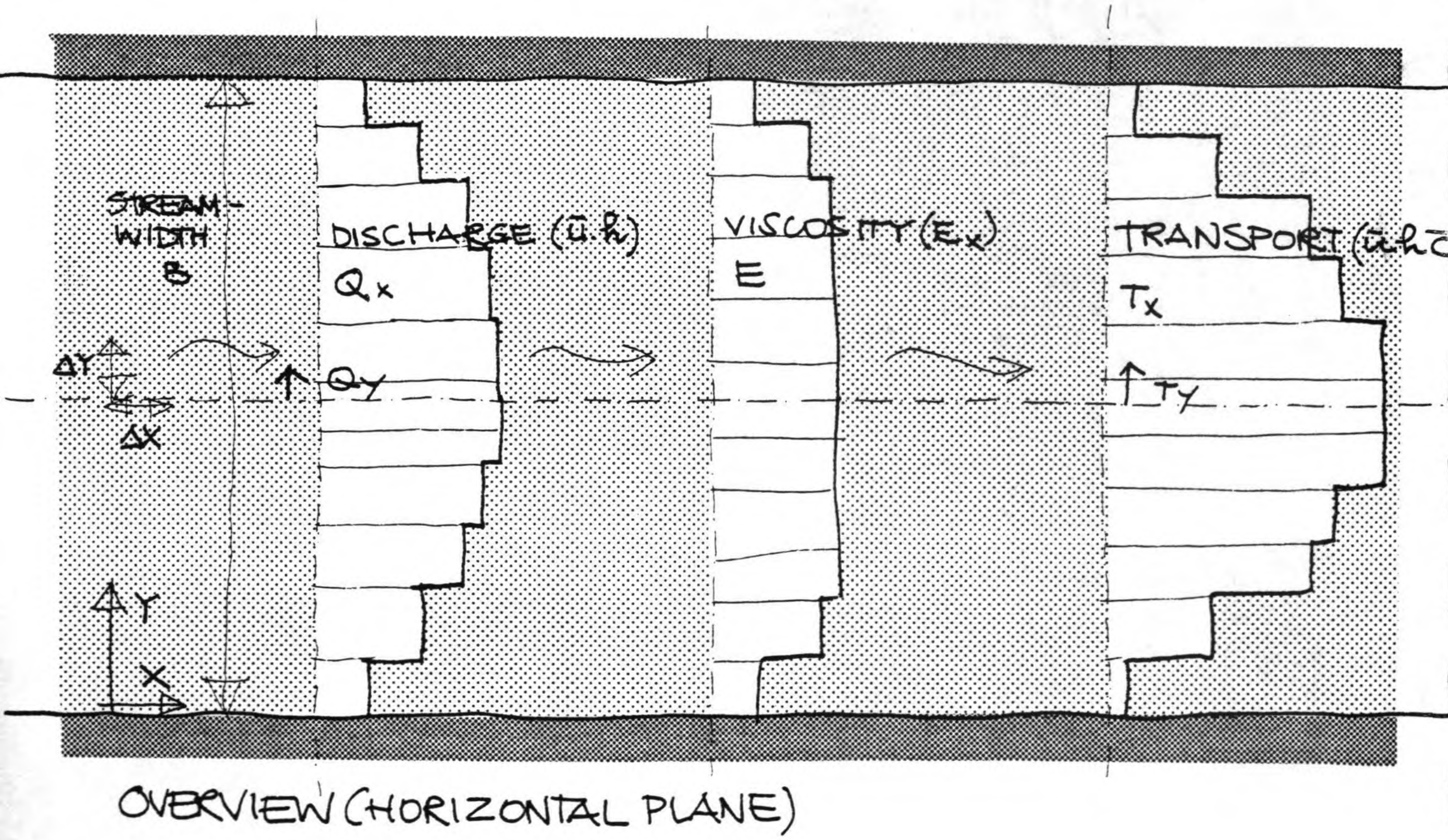

2.3

MORPHOR, directions and definitions

The bed-boundary condition can also be of a gradient type, for example when entrainment at the bottom is obstructed or a sudden change of bottom-material:

$$\left.\frac{\partial c}{\partial z}\right|_{z\,=\,\text{bottom}} = 0 \quad \ldots\ldots (3B)$$

These bed-boundary conditions are applied at a height z_a above the bed, the suspended transport is defined as the transport of particles above this level.

c_a and $\overline{c_e}$ can be found by means of the regular transport-load formulas. Here the method of Van Rijn (lit (8)) is used as described in Appendix B.

c_a can be found, according to Van Rijn:

$$c_a = 0.015\,\frac{D_{50}}{a}\,\frac{T^{1.5}}{D_*^{\,0.3}} \quad \ldots\ldots (4)$$

c_a = sediment concentration of bed-load
a = reference level (see Fig. 2.1)
D_{50} = average particle diameter
T = transport stage parameter (see Appendix B)
D_* = particle parameter (see Appendix B)

$\overline{c_e}$ can be found, according to Van Rijn:

$$\overline{c_e} = \frac{q_b + q_s}{h\overline{u}} \quad \ldots\ldots (5)$$

$\overline{c_e}$ = depth-averaged equilibrium concentration
q_b = (equilibrium) bed-load transport (see Appendix B)
q_s = equilibrium suspended-load transport (see Appendix B)
$\underline{h}$ = waterdepth
u = depth-averaged velocity

γ_{12} and γ_{22} can be found according to Galapatti (see Appendix C).

For the computation of each of these parameters, the local flow variables like u, u_*, w_s, h must be known. These parameters are considerably dependent on the value of especially w_s/u_*. Appendix C specifies the effect of the local flow variables on the parameters.

The model MORPHOR calculates the depth-averaged concentration in each gridpoint by means of the following scheme:

the first-order solution (2) can also be written as

$$\overline{c_e} = \bar{c} + L_A \frac{\partial \bar{c}}{\partial x} + T_A \frac{\partial \bar{c}}{\partial t} \qquad \ldots\ldots (6)$$

$$L_A = \text{adaption-length} = \frac{\gamma_{22}}{\gamma_{11}} \frac{\bar{u}h}{w_s} \qquad \ldots\ldots (6A)$$

$$T_A = \text{adaption-time} = \frac{\gamma_{21}}{\gamma_{11}} \frac{h}{w_s} \qquad \ldots\ldots (6B)$$

A six point-scheme as described in Appendix C is used for expressing this equation in finite-difference form, the expressions for (6) are solved for each time-level independently.

Once the concentration $\bar{c}$ at each gridpoint is known, the sediment transport rate is calculated from

$$S_s = \bar{u}h \left[\alpha_{11}\bar{c} + \alpha_{21} \frac{h}{w_s} \frac{\partial \bar{c}}{\partial t} + \alpha_{22} \frac{\bar{u}h}{w_s} \frac{\partial \bar{c}}{\partial x}\right] \qquad \ldots\ldots (7)$$

$\underline{S}_s$ = suspended load transport
u = depth-averaged velocity
h = waterdepth
α_{11}, α_{21} and α_{22} = coefficients related to sediment transport, see Appendix C

Again this equation is expressed in finite-difference form (see Galapatti, lit. (6)). After S_s is known for each gridpoint, a new bed-level is calculated from

$$\frac{\partial z}{\partial t} + \frac{1}{1 - P_b} \left[\frac{\partial S_s}{\partial x} + \frac{\partial S_b}{\partial x}\right] = 0 \qquad \ldots\ldots (8)$$

P_b = porosity of the bottom
S_b = bed-load transport

Equations (6), (7) and (8) form the basis of the first-order morphological computations of MORPHOR. Appendix C describes the model as developed by Galapatti, with some features of interest.

The finite-difference expression of (8) is (with respect to the X-direction):

$$z_{b_i}^{j+1} = z_{b_i}^{j} - \frac{1}{(1 - P_b)} \frac{\left[S_{i+1}^{j} - S_{i-1}^{j}\right]}{2\Delta x} t$$

$$+ 0.5\alpha \left[z_{b_{i+1}}^{j} - 2z_{b_i}^{j} + z_{b_{i-1}}^{j} \right] \quad \ldots\ldots\ldots\ldots\ldots (9)$$

i = X- (or Y)-level
j = time-level
α = pseudo-viscosity term (see Appendix C) necessary for stability

The model MORPHOR uses the results of DUCHESS as an input.

First the values for H, Qx and Qy are computed by DUCHESS, for each time step. These results are stored on tape. MORPHOR uses the hydraulic data to compute first the depth-averaged concentration C at each time-step (in the same gridpoints as for which H was computed).

The transports Tx and Ty are determined according to eq. (7); during each time-step the transports Tx and Ty are added (integrated in time), becoming TxT and TyT.

The morphological changes in the bed-level are computed at given time-interval. MORPHOR integrates the sediment transport according to eq. (9) and computes the sedimentation or erosion at each grid-point.

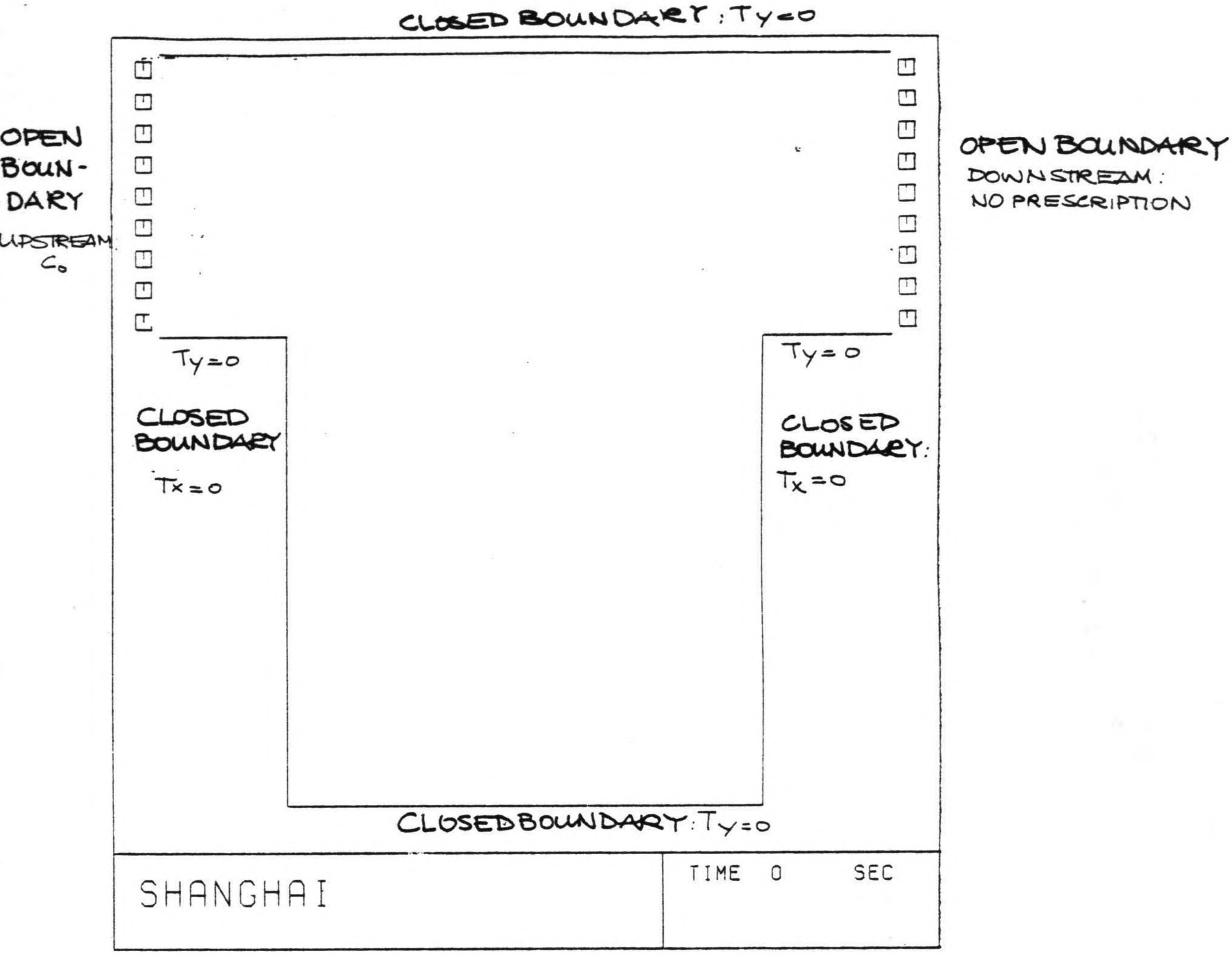

PRESCRIBE INITIAL CONDITION AT COMPLETE FIELD (25 * 25 POINTS): C, Tx AND Ty
PRESCRIBE BOUNDARY-CONDITION AT UPSTREAM OPEN BOUNDARY (10 POINTS): C_0

2.4
Input Morphor

INPUT

Input data for MORPHOR are:

1. morphological time step ΔT (s)

2. the order of the asymptotic solution:
   zero order solution $n = 0$
   first order solution $n = 1$
   second order solution $n = 2$

3. the pseudo-viscosity term in the morphological computation α which must be as small as possible ($\alpha < 1$) (-)

4. specification of the bed-boundary condition: (-)
   concentration type
   gradient type

5. specification of the transport formula used to calculate c_e and c_a: (-)
   Van Rijn
   Engelund and Hansen
   Powerlaw
   zero (if bed-boundary is of gradient type $\overline{c_e} = 0$)

6. the introduction of secondary flow in the calculation (see Appendix A) (-)

7. the diameter parameters of the bed-material
   D_{50} and (m)
   D_{90} (m)

8. the fall-velocity of the material w_s (m/s)

9. relative density of the material $\Delta = \dfrac{\rho s - \rho}{\rho}$ (-)

10. porosity of the bottom P_b (-)

11. correction for the transport with respect to the slope of the bottom α
    $S = S_o \left(1 - \alpha \dfrac{dz}{dx}\right)$ (-)

12. the reference level of the bed-load material
    $a = \beta\ h$ (m)

13. the introduction of extra diffusion in lateral direction;
    diflat = 0.0 means no extra diffusion (m2/s)

14. initial conditions for
    Tx (m^2/s)
    Ty (m^2/s)
    C (m^3/m^3)

15. boundary conditions for
    Tx (m^2/s)
    Ty (m^2/s)
    C (m^3/m^3)

OUTPUT

MORPHOR provides following output:

1. the depth-averaged concentration C at each grid point (m^3/m^3)

2. the total transport in X-direction Tx per unit of width (m^2/s)

3. the total transport in Y-direction Ty per unit of width (m^2/s)

4. the new bed level z_B for each grid point (m)

5. the total integrated transport in X-direction TXT per unit of width (m^2)

6. the total integrated transport in Y-direction TYT per unit of width (m^2)

RESTRICTIONS

In addition to the requirements on the model-variables by DUCHESS, MORPHOR demands as follows.

Time step

The adaption time of the depth-averaged concentration to a new equilibrium concentration is given by, according to Galapatti (see Appendix C), T_A:

$$T_A = \frac{\gamma_{21}}{\gamma_{11}} \frac{h}{w_s}$$

The adaption time is defined by the time that the difference between the actual depth-averaged concentration and the equilibrium concentration needs to decrease by a factor e.

If the time step of the computation (Δt) is more than 2 times this adaption time, a zero order approach ($\bar{c} = \bar{c}_e$) is sufficiently accurate to perform the computation.

If the time step of the computation (Δt) is much smaller than this adaption time ($\Delta t < 0.1\ T_A$), a higher order approach will be necessary.

On the other hand, Wang (lit (9)) has shown that the model (first order) is not valid directly after a sudden change in the flow conditions, change of bed-material, sudden deepening of the bottom or narrowing of the stream-surface (see Appendix C). The error function which describes the deviation between the first order solution and the actual depth-averaged concentration decreases with a factor e after an error time T_*:

$$T_* \simeq h/u_*$$

The time scale of the flow-variation (tidal period) must be much larger than this 'error time'.

Mesh size

According to Galapatti (see Appendix C) the adaption length of the mean concentration of the suspended sediment can be given by

$$L_A = \frac{\gamma_{22}}{\gamma_{11}} \frac{\bar{u}h}{w_s}$$

If the mesh size (Δx, Δy) is larger than 2 times this adaption length, a zero order approach will satisfy to compute the average concentration ($\bar{c} = c_e$).

If the mesh size is much smaller than this adaption length, a higher order approach must be applied ($\Delta < 0.1\ L_A$).

On the other hand, the mesh size may not become too small: Wang (lit (9)) showed that the asymptotic model is not valid directly after a sudden change in flow conditions. The error function decreases with a factor e after a length L_*

$$L_* \simeq \frac{\bar{u}h}{u_*}$$

The length scale of the flow variations must be much larger than this 'error length' L_*. Therefore the mesh size (Δx, Δy) must be larger than this L_*, unless the flow is more or less uniform (straight boundaries).

Ratio particle fall velocity to friction velocity

The model of Galapatti is not valid for $w_s/u_* < 0.3$.
Therefore:

$$w_s/u_* \leq 0.2$$

As Wang showed (lit (9)) then the adaption time and length become of the same order as the error time and length, where the model is not valid.

2.3 Computing facilities

All the numerical computations were carried out using the facilities available at the computer centre of Delft University of Technology, department of Civil Engineering.

The computer

The Delft University of Technology has a fourth generation mainframe computer: IBM 1383 JX.
With a user available memory of 24 Mbytes, it has a virtual memory unit of 16 Mbytes and as such, programs that demand a memory storage up to 16 Mbytes can be run on the mainframe computer.

The computer has compilers in Fortran, Cobol, Pascal, Algol.

Outputs of computations can be obtained either in the form of hard copies (print output) or plots. It can be routed to local line printers. Plotting is done using a remote TECTRONIX terminal. The mainframe has 30 disc-units and 6 tape-units with densities of 6250 (5) and 1600 (1) BPI (bites per inch). Its execution speed is in the order of 3 MIPS (million instructions per second).

The system

The editing and job-scheduling can be done by any system in principle. In this analysis the VSPC-system (Virtual Storage Personal Computing) was used (see lit. (10)).
The total time necessary to become familiar with a system, and to understand the facilities of the computer-centre is about one week, in case the system is new.

The programs

DUCHESS requires a storage-capacity of 800 K, independent of the grid. For a grid of 25 * 25-nodes, each time-step consumes about 1.0 CPU-second.

MORPHOR requires a storage-capacity of 1,920 K, and at least one tape-unit. For a grid of 25 * 25-nodes each time-step consumes about 2.25 CPU-second (dependent on the order of the problem).

The grid can be extended, but the facilities of the output cause a limitation in the maximum of data to be printed; it is only 25 nodes (in x-direction). In y-direction there is no limitation in output; for an economical use of the computer however the grid should not become too long.

3. SCHEMATIZATION

3.1 General

If in some reclamation area, situated in an estuary, siltation is to occur, this implies that sediment, which flows into the area as a result of the water movement, must settle (partially) in this area. The water movement therefore is determining the behaviour of the sediments and must be described accurately by a numerical simulation.
The water movement along the reclamation area can be brought about in three ways (lit (11)).

1. Exchange of water as a result of storage (of the tidal prism)

   The storage in each field is the amount of water that flows in and out the field, caused by changes of the water level in and outside the field. These changes in water levels are caused by tidal movement and by fluctuations in river discharges.

2. Exchange of water as a result of longshore currents

   Water running along the field can cause an eddy to develop inside the field having a vertical axis. As a result water from inside the field is constantly being exchanged with water from outside the field (secondary flow and mixing phenomena play a prominent part in the behaviour of the eddy).

3. Exchange of water as a result of differences in density

   If differences in density exist between the water inside and outside the reclamation field, the water with higher density will penetrate the water with lower density (forming a 'tongue' into the field). Differences in density can be caused by differences in salinity, temperature, sediment concentration and combinations hereof.

As the reclamation area is situated near to the seaward end of the Qiantang estuary (Hangzhou Bay), the influences of fluctuations in salinity will be neglected. The water is considered to be well mixed, with respect to salinity and temperature. Because of the small dimensions of the reclamation fields in relation to the opening sizes, the effect of differences in sediment concentration inside and outside the field will be neglected.
One can therefore suppose the first two processes to be the main causes for the exchange of water and sediment in the fields, and thus determining the resulting water movement.

To separate the effect of storage and eddy developing in the reclamation fields, it has been thought best to perform the numerical computations in three stages.

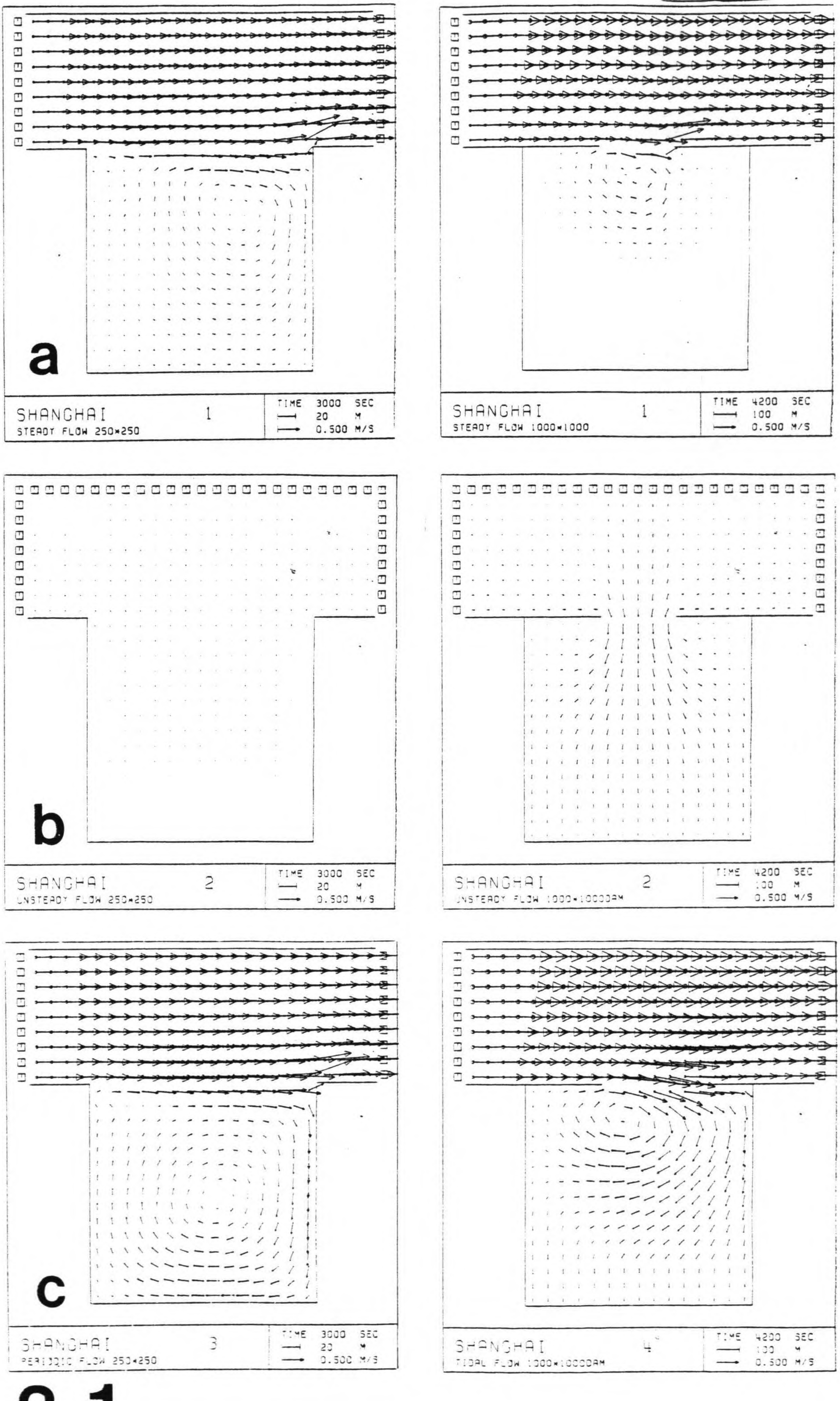

3.1

Typical flow-patterns

A. Simulation of steady flow

A steady flow running along a reclamation field can cause an eddy to develop inside the field (see Fig. 3.1). The formation of an eddy can be advantageous for the sedimentation, depending on the resulting flow velocities inside the field. A slow circling motion exists inside, being fed with sediments from outside. This mechanism might result in more accretion than in the case of an inside flow parallel to the mainflow causing severe erosion around the damheads (see Fig. 3.1A).

This (numerical) simulation should show the time necessary to get rid of the initial effects (after a while, the results of the computation must become invariable) and the time that the eddy needs to develop.

B. Simulation of unsteady flow

An unsteady flow, characterized by a linear rise (or fall) of the water level outside the field is representative for the storage properties of each field and the resulting water velocities inside the field (see Fig. 3.1B).

This simulation should show the water velocities caused by storage exclusively, in order to compare this effect with the water velocities caused by longshore currents.

C. Simulation of the tidal movement

A combination of storage and eddy developing should give a proper image of the behaviour of a field under 'natural' conditions with respect to flow pattern and siltation (or erosion).

It should show the resultant flow velocities inside and outside the reclamation fields (a combination of eddy and storage) and the periodic behaviour of the boundaries, the water level, the flow pattern and the sedimentation pattern.

In order to investigate a relation between lay-out and resulting sedimentation inside the fields, different lay-outs will be subjected to the same flow conditions. The differences in resulting flow pattern inside the fields will be determining for the sedimentation.
After the flow pattern for each lay-out has been determined sufficiently accurate by means of DUCHESS, MORPHOR will give an idea about the sedimentation that might occur.

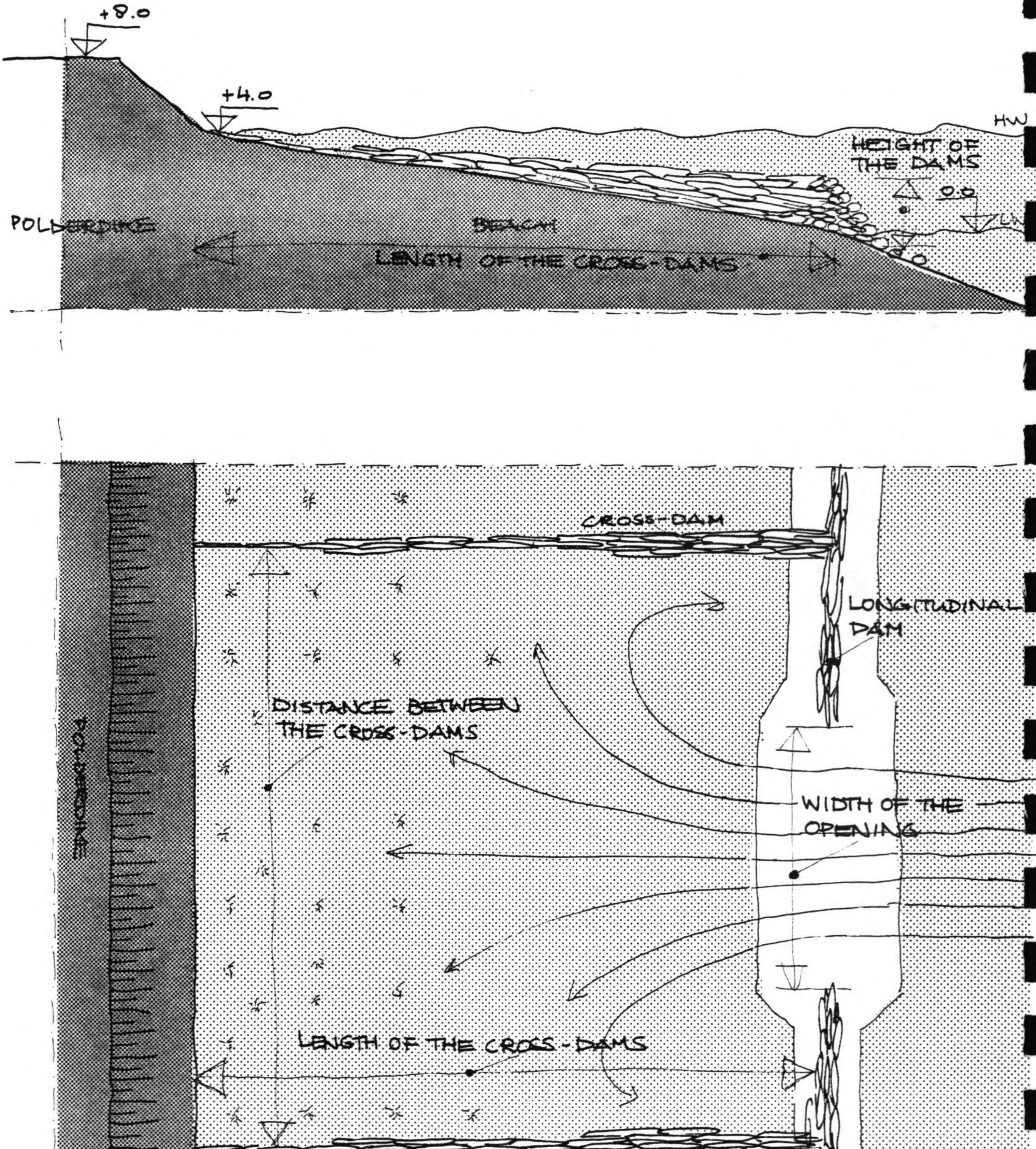

3.2

Characteristics of the reclamation-fields

3.2 Grid and bottom configuration

In the foregoing study "study about landreclamation" (lit (1)) it was already suggested to apply a system of crossdams and longitudinal dams as a reclamation structure (see Fig. 1.2).

The tidal eb and flood currents are running mainly parallel to the coast at Cao Jing, therefore the lay-out of one specific reclamation field (i.e. an area bounded by dams), consists of a four-angular field, two sides are formed by crossdams perpendicular to the coast, one side is formed either by a longitudinal dam parallel to the coastline, or the coastline itself.
The fourth side, at the seaward end of the field, consists of a water-stream-line or short longitudinal dams with an opening (see Fig. 3.2).

Thus the meaning of the word "lay-out" is the exact dimensions of each field, bounded by two crossdams (that have a specific length and distance) and possible longitudinal dams (that have a specific length and distance).

For economic design it is the objective to design a landreclamation structure which combines a quick sedimentation with a minimum total length of dikes per field.

The main problems with respect to lay-out design are:

- the length of the dams;
- the optimum distance between the dams;
- the actual configuration.

To investigate the influence of the length on the behaviour of the sedimentation 3 different lengths are chosen:

250 m;
500 m;
1000 m.

To investigate the influence of the distance between the dams three different distances (between the dams) are chosen:

250 m;
500 m;
1000 m.

The configuration of the dams is not explicitely investigated. It is taken into account as the addition of longitudinal dams. Investigated is the effect of two additional (longitudinal) dams having an opening of 333 m and an inner reclamation field of 1000 * 1000 m. The most economic solution is to use extra longitudinal dams in combination with an 'inner area' as extended as possible (see Fig. 3.3).

Summarizing,the next four lay-out models are chosen to examine the influence of configuration on the sedimentation pattern:

1. 250 * 250 m (cross dams only);
2. 500 * 500 m (cross dams only);
3. 1000 * 1000 m (cross dams only);
4. 1000 * 1000 m plus 2 longitudinal dams with an opening of 333 m (see Fig. 3.3).

N.B.
The lay-out of 500 * 500 m is chosen as a 'reference lay-out' because it is expected that this specific distance, 500 m, is a boundary distance for a free eddy to develop, as the energy fluctuation caused by friction and the energy fluctuation caused by water velocity (which is the main motor for the eddy confirmation) are of the same order of magnitude:

$$\Delta H_{friction} \simeq i \,.\, L = \frac{\bar{u}^2}{C^2 R} \,.\, L = 6 .\, 10^{-2} \text{ m} \quad (C \simeq 50 \sqrt{m}/s)$$

$$\Delta H_{velocity} \simeq \frac{\bar{u}^2}{2g} = 5 \,.\, 10^{-2} \text{ m}$$

L = distance between dams
u = depth-averaged flow velocity
R = hydraulic radius of flow-cross-section
g = acceleration of gravity

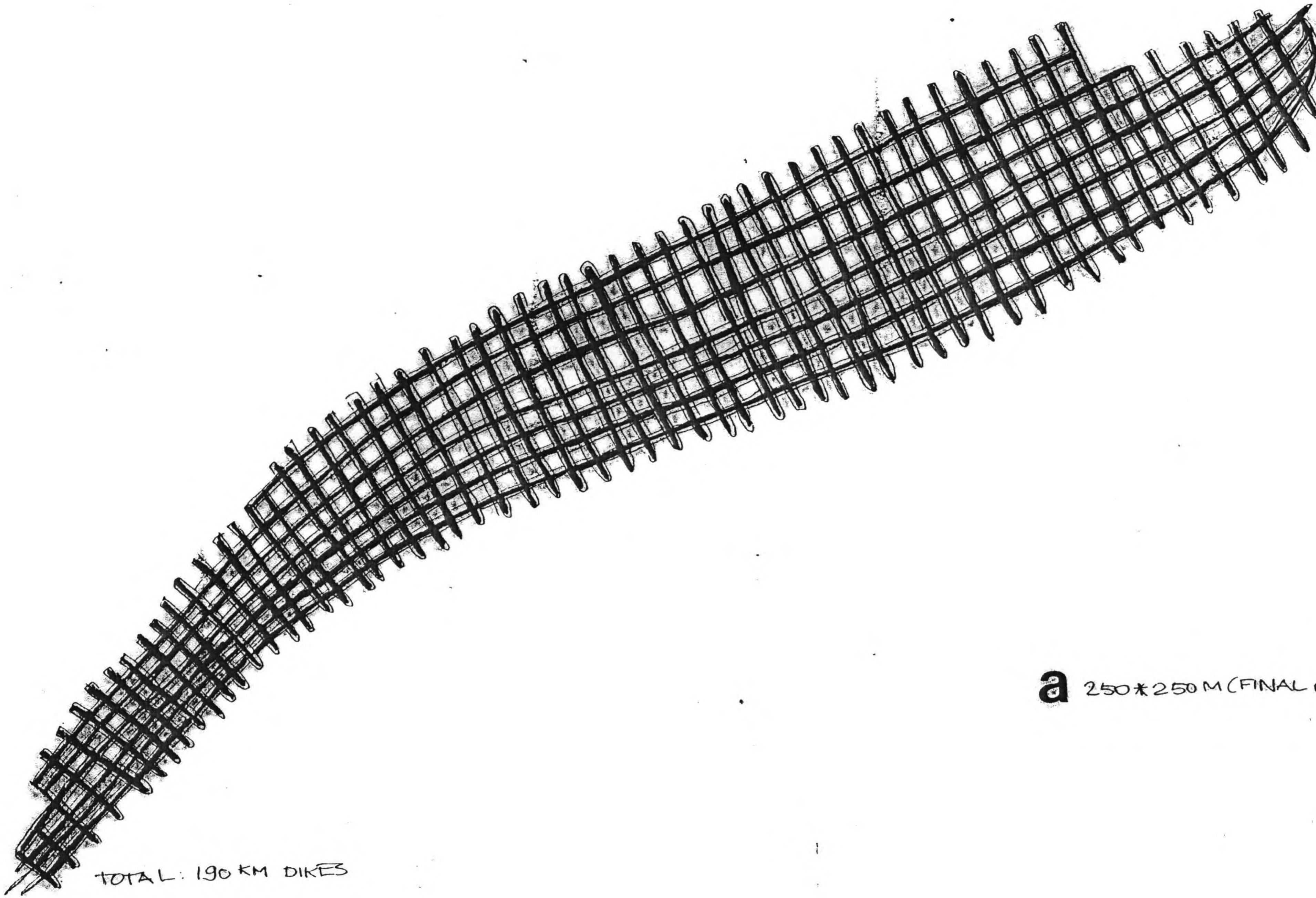

a 250*250 M (FINAL OVERVIEW)

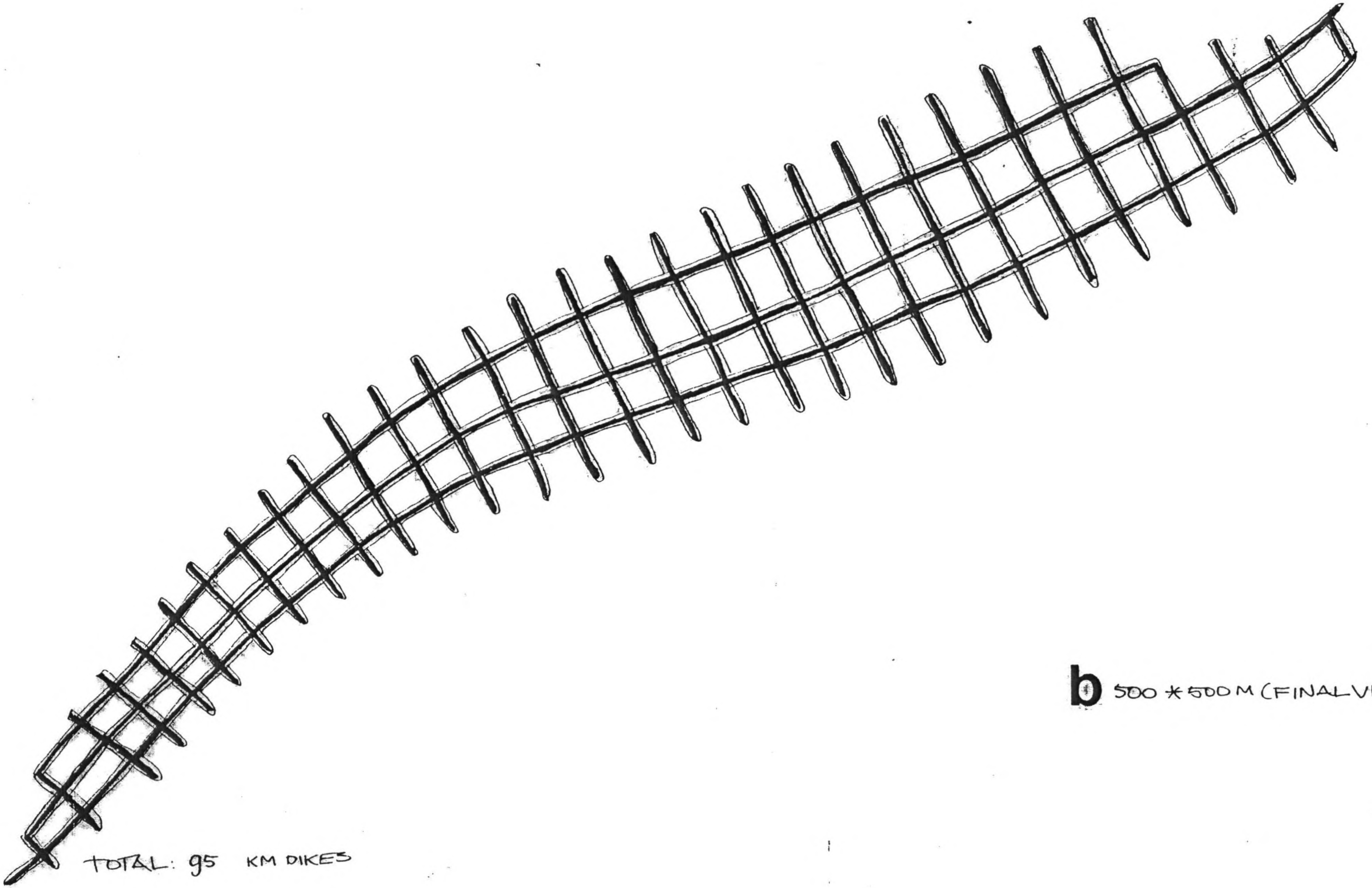

b 500 * 500 M (FINAL VIEW)

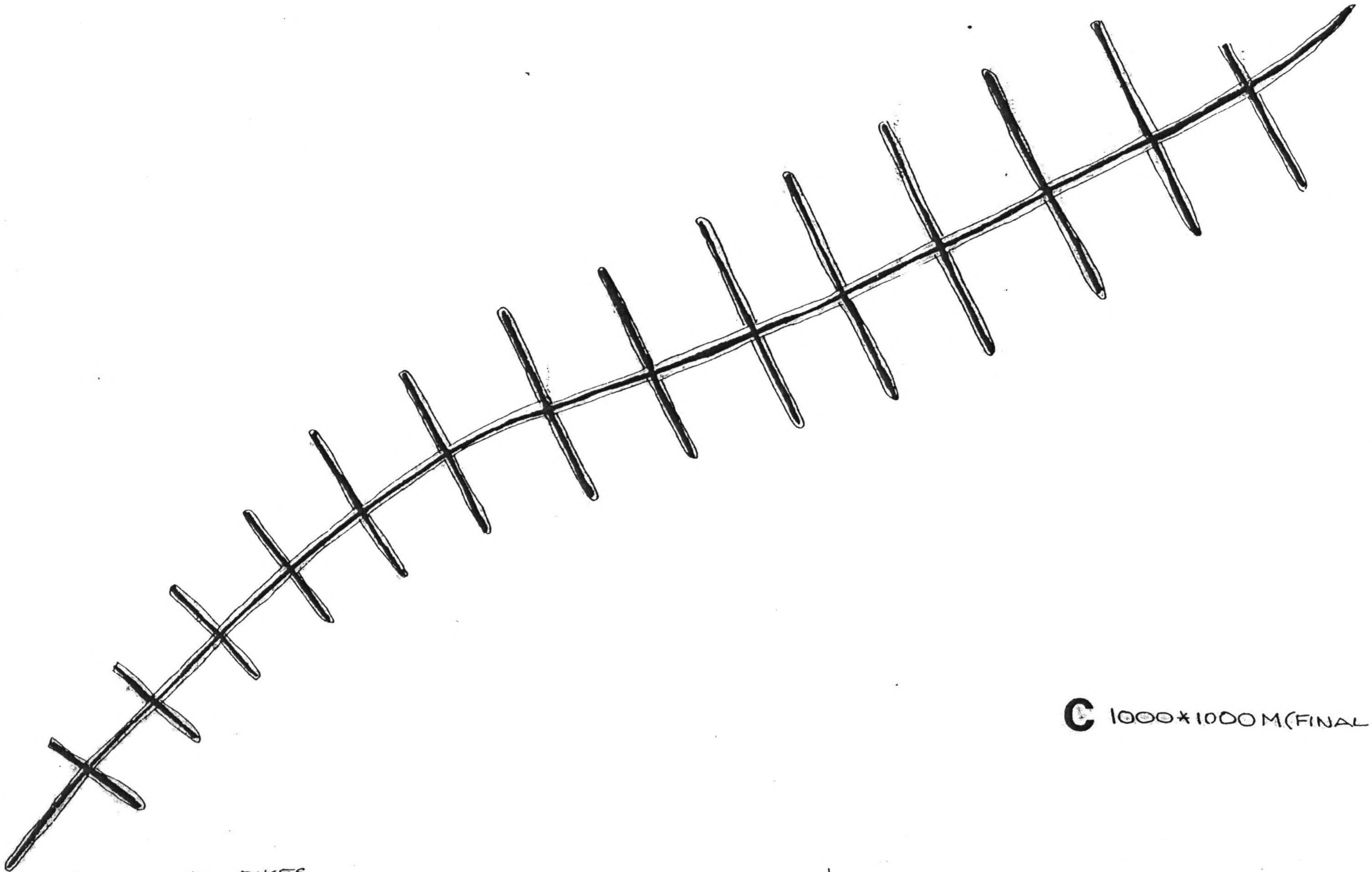

C 1000*1000 M (FINAL VIEW)

TOTAL: 40 km DIKES

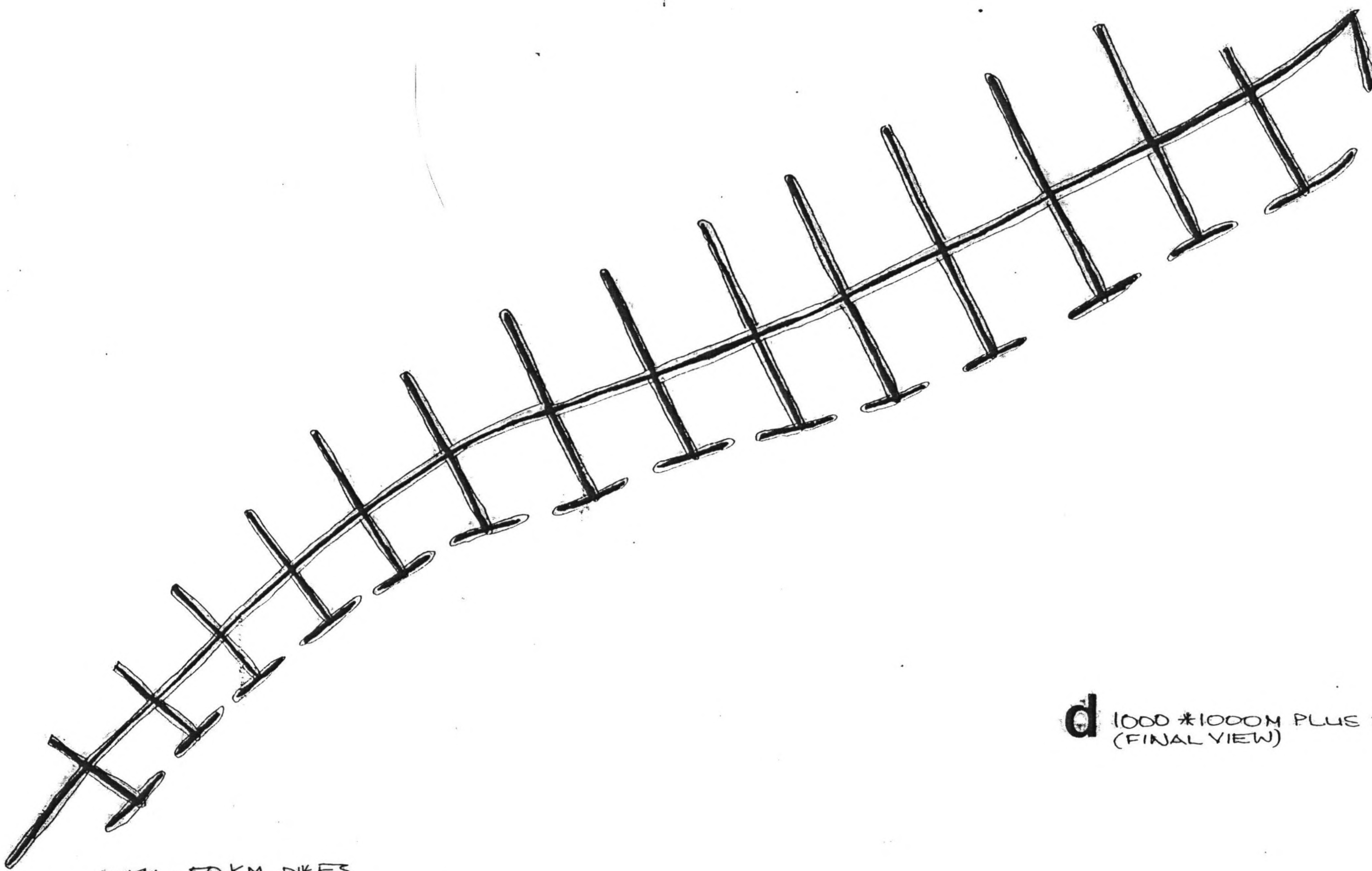

d 1000 * 1000M PLUS DAM
(FINAL VIEW)

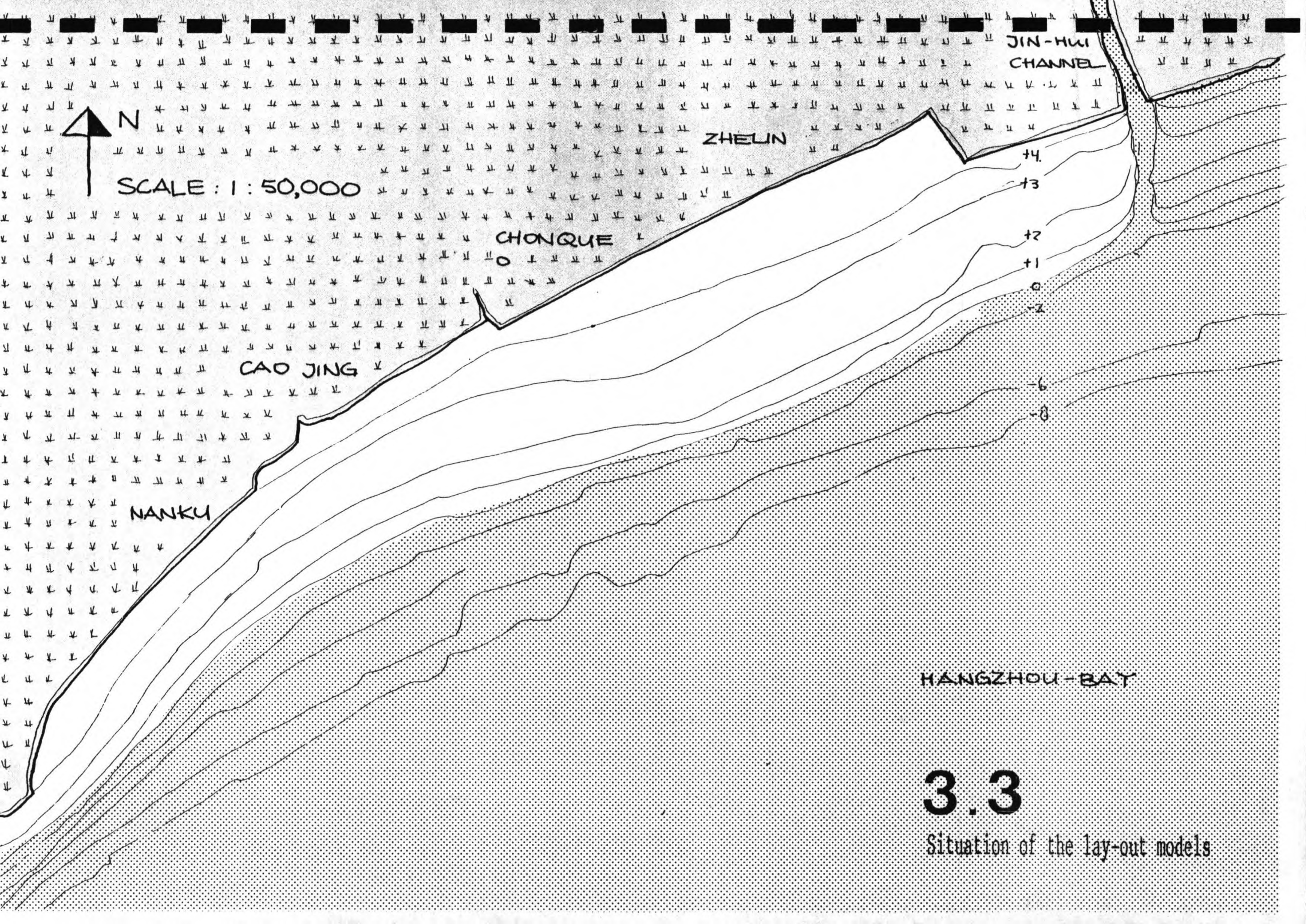

3.3
Situation of the lay-out models

Therefore it is expected that the opening should not exceed 500 m, in order to avoid that the bottom-friction will prevent the eddy to develop along the reclamation-field-opening.

3.2.1 Grid

The maximum computational area that can be reproduced by DUCHESS (and MORPHOR) efficiently is in the order of 25 * 25 computational nodes.
In order to give a proper image of the behaviour of eddies in a two-dimensional flow, the eddy should be covered at least by 5 computational nodes in longitudinal and cross direction. Also the open boundaries of the model must be taken away from the reclamation field, in order to take into account the curvature of the streamlines around the (cross) damheads.

Summarizing it is chosen that the reclamation field itself covers a grid of 15 * 15 nodes, the rest of the flow field is covered by the 25 * 25 meshes of the computational grid (see Fig. 3.4). This results in a mesh size of 16.67 * 16.67 m in the case of a lay-out of 250 * 250 m, a mesh size of 33.33 * 33.33 in the case of a lay-out of 500 * 500 m and a mesh size of 66.67 * 66.67 m in the case of a model of 1000 * 1000 m.

BOUNDARIES (see Fig. 3.4)

a. defines the location of the (cross) dams built of geotextile tubes

They are schematized as impermeable walls (the height of the dams is somewhere around the average highwater level).

b. defines the location of possible longitudinal dams built of geotextile tubes

They are also schematized as being impermeable walls.

c. defines the boundary of the computational area

In the case only cross dams are applied (cases 1, 2, 3) c does not exist as a physical boundary. Nevertheless c is also schematized as an impermeable wall for a better insight in the water movement.
In this model the area surrounded by b and c is excluded from the grid in order to prevent the model from getting too complicated.

d. defines the open boundaries of the model

Here physical boundary conditions can be applied in the model (H- or Q-boundary conditions).

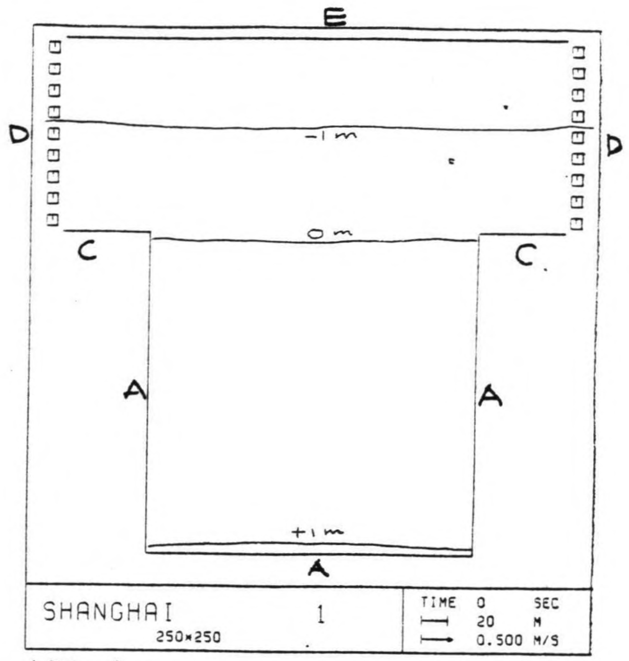

NO. 1.

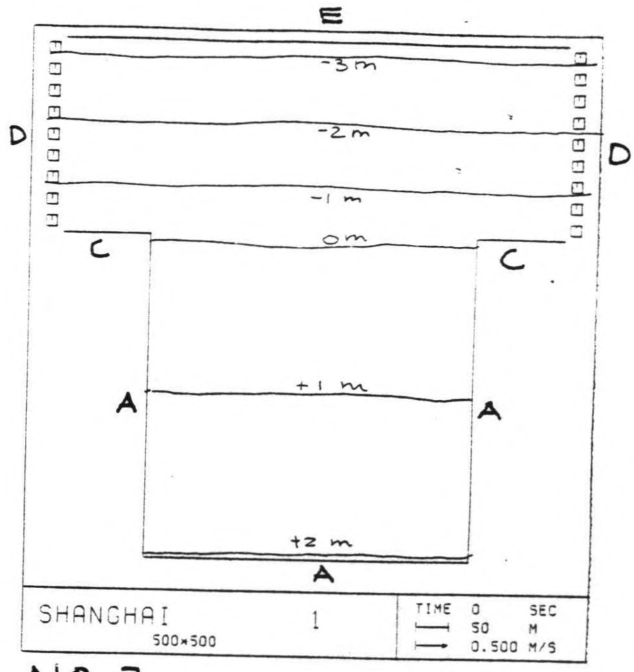

NO. 2

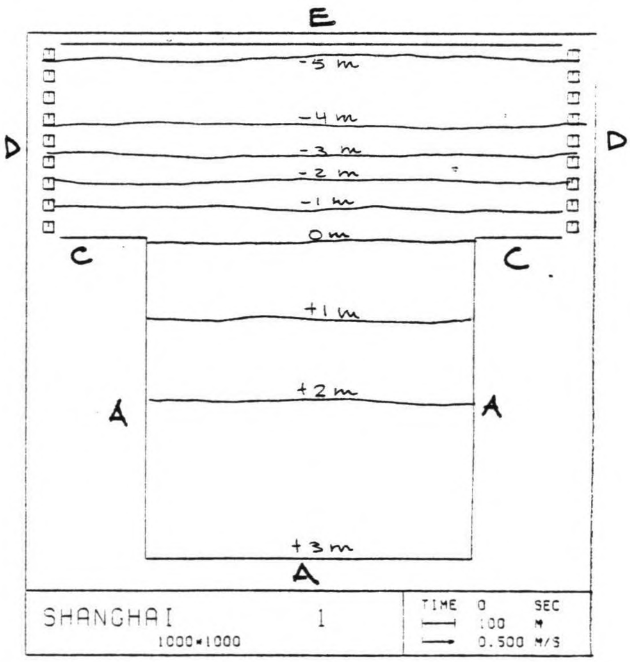

NO. 3

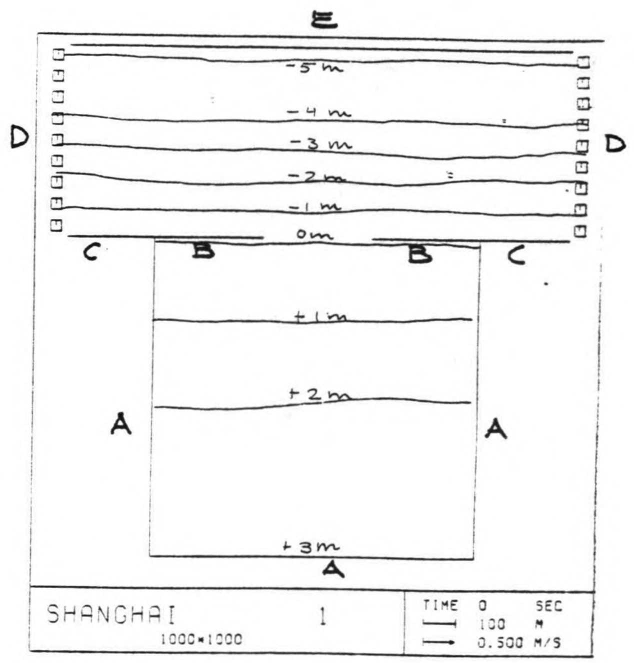

NO. 4

3.4

Boundaries

e. defines the seaward boundary of the model

Actually this also is an open boundary, but to reproduce the flow parallel to the coast properly, in the case of steady flow and tidal flow, it is schematized as a closed boundary, an impermeable wall.
In the case of unsteady flow it is treated in the same way as d.

3.2.2 Bottom

The location of the computational area in the actual bathymetry of the reclamation district is shown in Fig. 3.3. The seaward end of each fictious model is situated along the LW(low water)-line of the mud flat of Cao Jing district. Reasons for this:

- to compare the effectivity of each lay-out the conditions at the open (= influenced by the general water movement) end of the fields must be similar;

- the seaward end of the reclamation area is also situated along the LW-line of the mud flat (level: 0.00 m);

- the conditions for sedimentation are most unfavourable along the edge of the mud flat:
  - . current velocities are large (1.5 - 2.5 m/s);
  - . the tidal difference is maximal (4.5 m average) and here the sediment is permanently under water;
  - . the slope of the bottom is steep.

Thus, in order to compare the effectivity of each of the lay-out models, it is important that the seaward part of each model is situated at the same bottom-level. The results for the bottom-schematization are shown in Fig. 3.4.

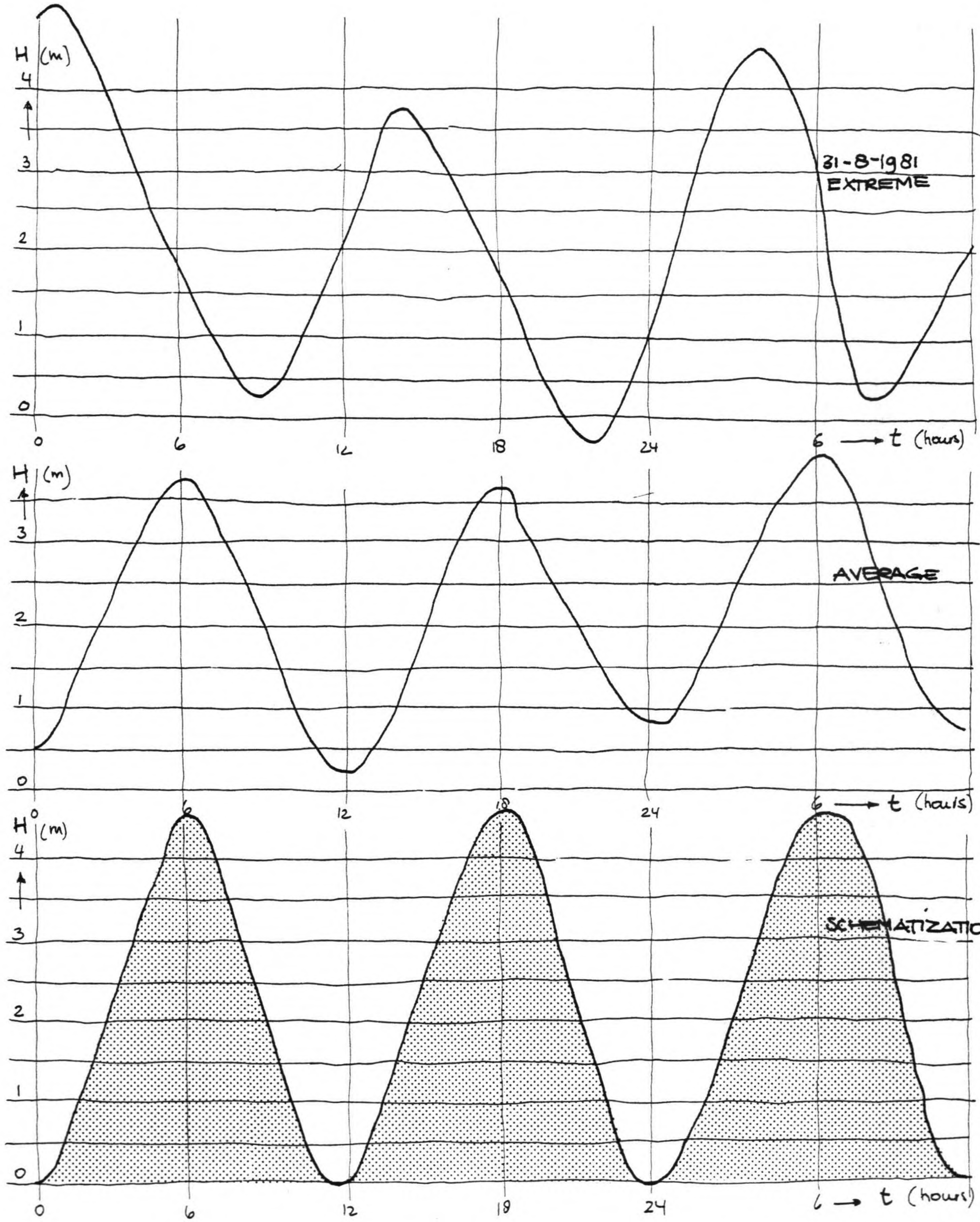

3.5

Tidal movement

3.3 Hydraulic characteristics

In Fig. 3.5 the tidal movement of the water at Cao Jing is given for flood season (typhoon season) and the dry season.

The current velocity measured along the coast where the bottom level is -1 m below the LW-line is

maximum 1.5 m/s during average tides;
maximum 2.0 m/s during extreme tides.

Because of the small mesh sizes (see par. 3.2) the computation of complete tidal periods for each lay-out model is too uneconomic. Of each lay-out only 3600 s (one hour) are computed.

It is thought that these results will be illustrative to compare the effectivity of each lay-out model.

The initial conditions for each numerical simulation are chosen similar: the water level is 2 m above LW (which is about the still-water level);
the currect velocity is 0 m/s, thus the adaption time of the influence of initial conditions can be checked.

3.3.1 H and Q conditions

In the case of two-dimensional models, two boundary conditions must be given in the case of subcritical flow (see lit. (12)).

STEADY FLOW

Steady flow is characterized by constant boundaries in time. In the model it is chosen to prescribe the water level in the left and right open boundaries in the model (see Fig. 3.6A).

$$\Delta H = \frac{u^2}{C^2 R} \cdot L$$

$\bar{u}$ = 1 m/s
C = 50 $\sqrt{}$m/s
R $\simeq$ 5.0 m
L_{tot} = 25 x (16.67, 33.33, 66.67) m

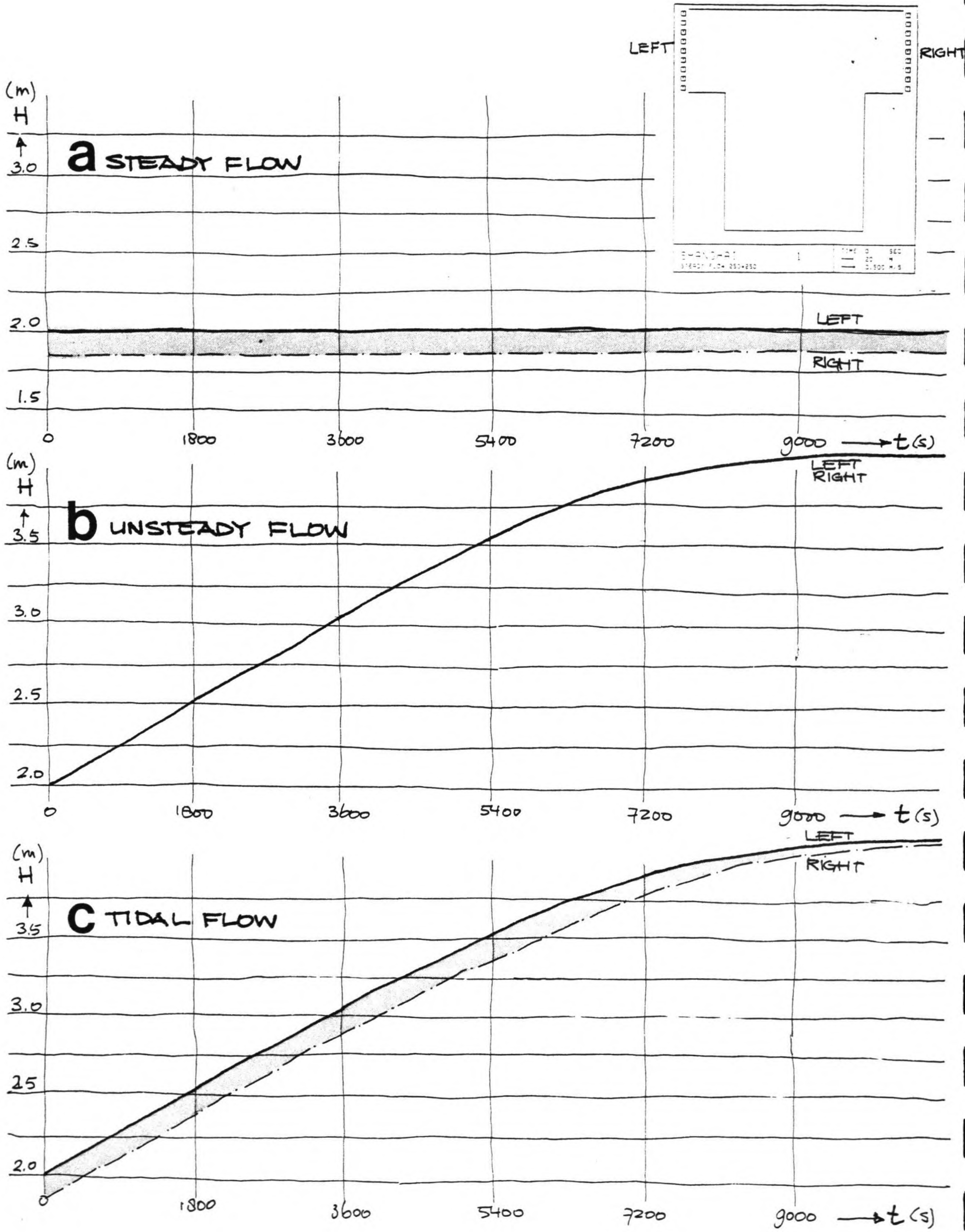

3.6

Flow characteristics

1. 250 * 250 m H_{left} = const. = +2.000 m
   mesh size = 16.67 m H_{right} = const. = +1.967 m

2. 500 * 500 m H_{left} = const. = +2.000 m
   mesh size = 33.33 m H_{right} = const. = +1.933 m

3. 1000 * 1000 m H_{left} = const. = +2.000 m
   mesh size = 66.67 m H_{right} = const. = +1.867 m

4. 1000 * 1000 m + dam similar to 3.
   mesh size = 66.67 m

The initial conditions: H = +2.000 m;
Qx = 0 m^2/s;
Qy = 0 m^2/s.

UNSTEADY FLOW

The tidal movement of the water level H, as shown in Fig. 3.5, is schematized by a homogeneous rise and fall of H. There are no differences in water level along the seaward boundaries. The tide is schematized by a simple wave with a period of 44700 s and one harmonic component having an amplitude of 2.25 m (ΔH = 4.5 m). See Fig. 3.6B.

1. 250 * 250 m $H = 2.25 \sin(2\pi t/44700)$

2. 500 * 500 m $H = 2.25 \sin(2\pi t/44700)$

3. 1000 * 1000 m $H = 2.25 \sin(2\pi t/44700)$

4. 1000 * 1000 m + dam similar to 3.

The initial conditions for each numerical simulation:
the water level H = +2.000 m;
Qx = 0 m^2/s;
Qy = 0 m^2/s.

TIDAL FLOW

The tidal flow is characterized by a harmonic rise and fall of the water level H, plus a difference in water level over the left and right boundary (see Fig. 3.6C).

1. 250 * 250 m

$$H_{left} = 2.25 \sin(2\pi t/44700)$$

$$H_{right} = 2.25 \sin\left(\frac{2\pi t}{44700} - 0.0148\right)$$

2. 500 * 500 m

$$H_{left} = 2.25 \sin(2\pi t/44700)$$

$$H_{right} = 2.25 \sin\left(\frac{2\pi t}{44700} - 0.0296\right)$$

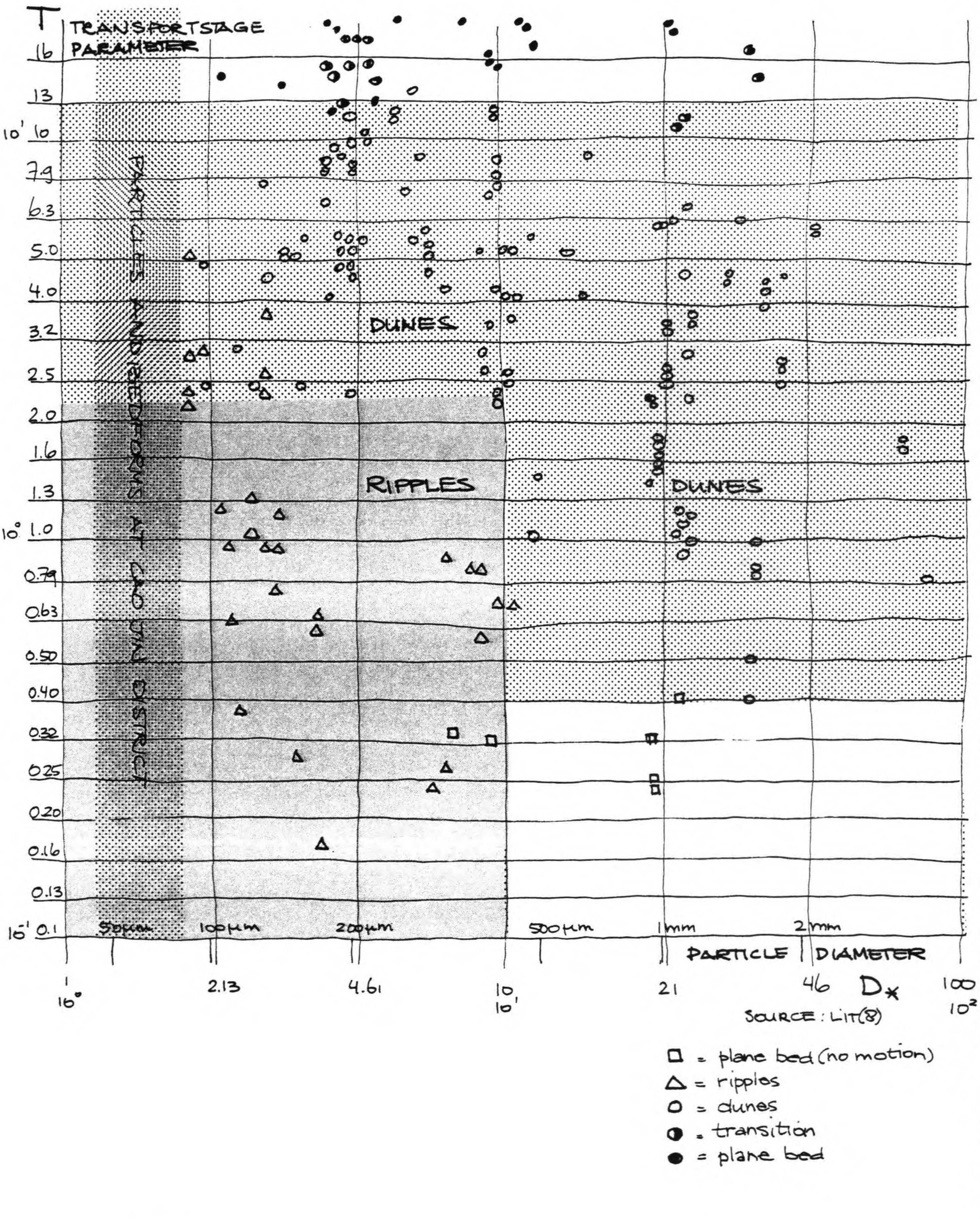

3.7 a

roughness-properties

3. 1000 * 1000 m $\quad H_{left} = 2.25 \sin(2\pi t/44700)$

$$H_{right} = 2.25 \sin\left(\frac{2\pi t}{44700} - 0.0593\right)$$

4. 1000 * 1000 m + dam $\quad$ similar to 3.

Initial conditions: H = +2.000 m;
Qx = 0 m^2/s;
Qy = 0 m^2/s.

3.3.2 Friction, viscosity and coriolis parameter

FRICTION

The friction coefficient is related to the Chézy coefficient $fr = g/C^2$.
In general the Chézy coeffient is described by:

$$C = 18 \log \left[\frac{12\ R}{k_s}\right] \quad \ldots \quad (1)$$

R = hydraulic radius ≃ h (depth) in this model
k_s = roughness of the bottom

According to Van Rijn (lit (8)) the effective roughness of a movable bed surface can be computed by:

$$k_s = 3\ D_{90} + 1.1\ \Delta(1 - e^{-25\Psi}) \quad \ldots \quad (2)$$

D_{90} = 90% particle diameter
Δ = bedform height
ψ = bedform steepness parameter = Δ/λ
λ = bedform length

Herein $3\ D_{90}$ is the roughness related to grains, and
$1.1\ \Delta(1 - e^{-25\psi})$ is the roughness related to the bedform.

$$\frac{\Delta}{d} = 0.11 \left[\frac{D_{50}}{d}\right]^{0.3} (1 - e^{-0.5T})(25 - T) \quad \ldots \quad (3)$$

D_{50} = average particle diameter
d = waterdepth
T = transport stage parameter (see Appendix B)

$$\lambda = 7.3\ d \quad \ldots \quad (4)$$

So the length of the bedform is only related to the flow depth!
The bedform height is dependent on the flow parameters via T.

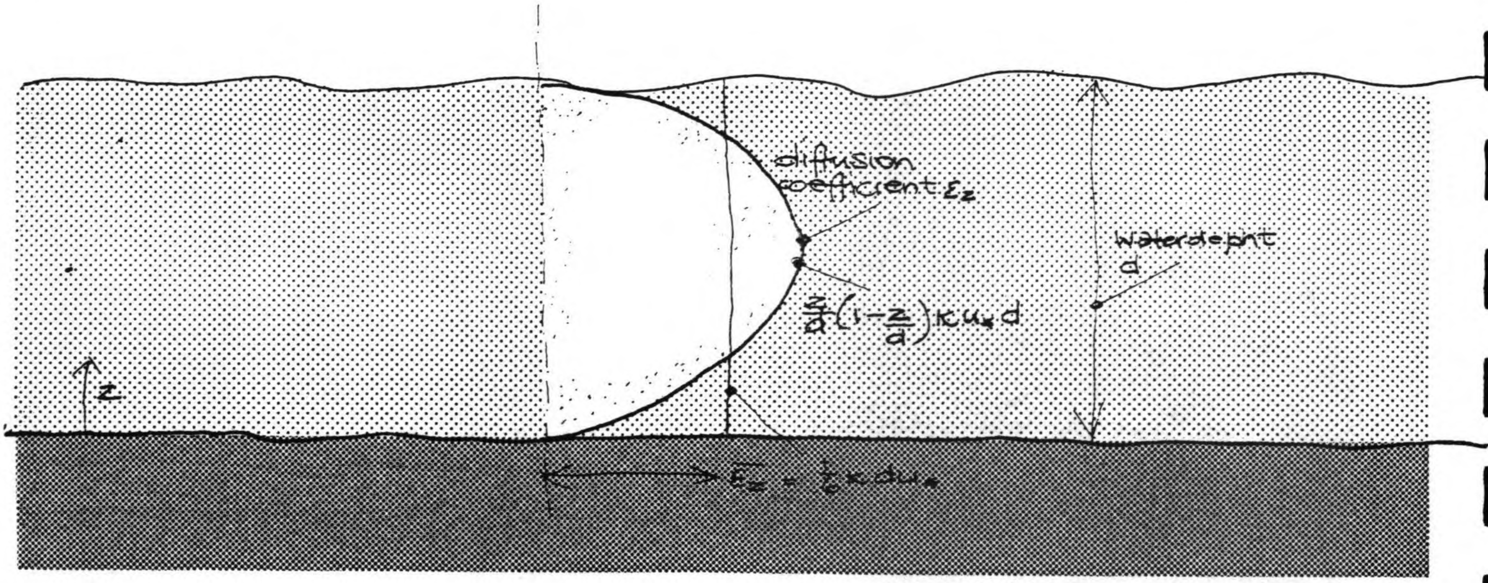

VERTICAL DIRECTION

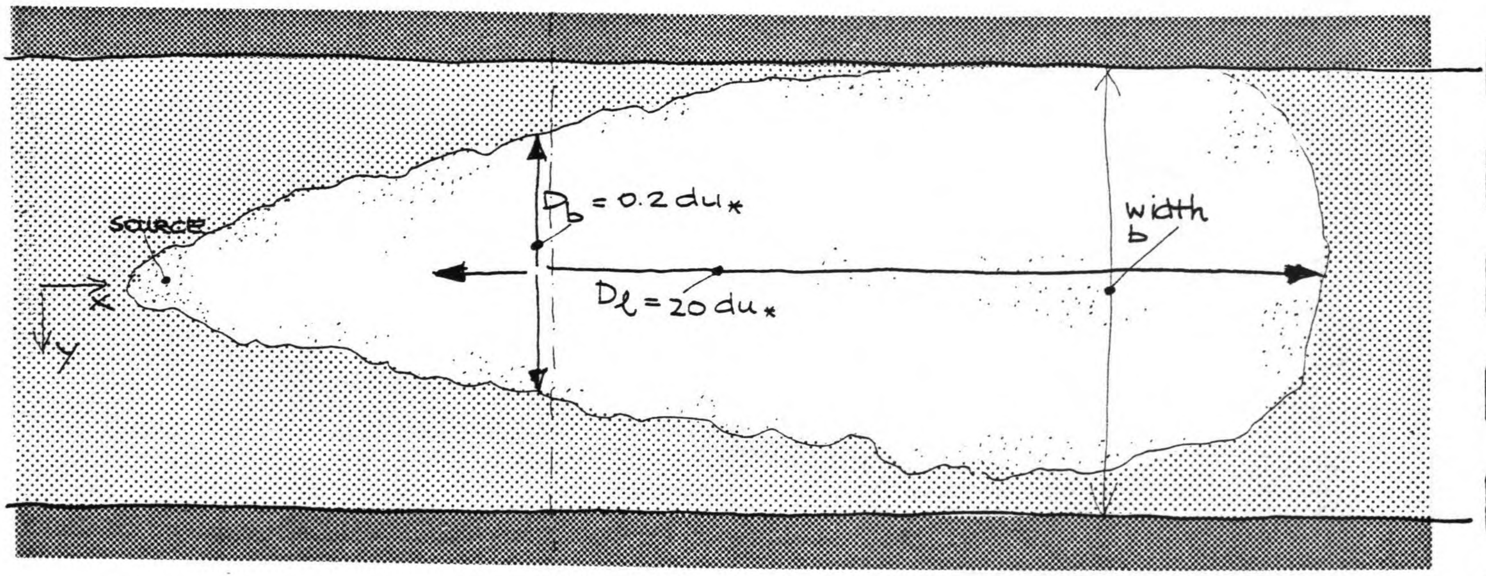

TRANVERSE AND LATERAL DIRECTION

3.7b

viscosity-properties

$$T = \frac{(u'_*)^2 - (u_{*,cr})^2}{(u_{*,cr})^2} \quad \ldots\ldots\ldots\ldots\ldots\ldots \quad (5)$$

u'_* = bed_shear velocity related to grains

$= \frac{\sqrt{g}}{C'} \bar{u}$, $\quad C' = 18 \log \frac{12h}{3D_{90}}$

$u_{*,cr}$ = critical bed shear velocity according to Shields (see Appendix B)

Using eq. (1) t/m eq. (5) and $\bar{u}$ = 1 m/s
h = 3 m
D_{50} = 50 μm
D_{90} = 100 μm

it shows that $k_s \simeq 0.05$ m, which is a reasonable value in this area.
The value for the friction used in the numerical simulations is calculated by:

$$C = 18 \log \left[\frac{12\,R}{0.05}\right]$$

$C_{average} \simeq 50$
$C_{min} = 25$ (R=0.1m)
$C_{max} = 60$ (R=8.0m)

for all over the computational area. It is assumed that the roughness is about 0.05 m all over the reclamation field. This means that $C_{average}$ over the flow section is about 50 $m^{\frac{1}{2}}/s$.

The friction coefficient thus is <u>not</u> constant over the computational grid, but is dependent on the water depth. If the depth becomes smaller than 0.1 m, the friction coefficient is fixed on the one of 0.1 m (threshold depth). Otherwise the friction would become infinite.

VISCOSITY

In general the turbulent viscosity is not constant over the water depth and over the flow field.

Usually it is described by a parabolic distribution over the flow <u>depth</u>:

$$\varepsilon = \frac{z}{d}\left(1 - \frac{z}{d}\right) \kappa\, u_*\, d \quad \ldots\ldots\ldots\ldots\ldots\ldots \quad (6)$$

ε = turbulent diffusion coefficient
z = vertical co-ordinate, 0 at the bottom
d = flow depth
κ = constant of Von Karman = 0.4
u_* = bottom shear velocity
$= \frac{\sqrt{g}}{C} \bar{u}$
$\bar{u}$ = depth averaged flow velocity

The maximum value of ε is:

$$\varepsilon_{max} = 0.25\ \kappa\ u_*\ d \quad \ldots\ldots (7)$$

and the average value over the depth

$$\bar{\varepsilon} = 1/6\ \kappa\ u_*\ d = 0.07|u_*|d \quad \ldots\ldots (8)$$

For the computation of flow fields in vertical direction it is not wise to use a constant viscosity, because ε varies strongly over the depth.

In two-dimensional horizontal flow problems, the viscosity is often taken constant over the flow field. Such is the case with the DUCHESS model (see par. 2.1).
In DUCHESS E stands for the effective viscosity, the horizontal transport of momentum in transverse direction.

In the case of wide channels there is an empirical expression for the diffusion coefficient D_b in transverse direction:

$$D_b = 0.1 \text{ à } 0.2\ d|u_*| \quad \ldots\ldots (9)$$

Because this coefficient is analogous to the effective turbulent viscosity of the two-dimensional models such as DUCHESS, E has this value:

$$E = 0.1 \text{ à } 0.2\ d|u_*| \quad \ldots\ldots (10)$$

This value is two or three times as high as the average value for exchange in vertical direction (eq. (8)), caused by the fact that exchange of momentum is prevented at the bottom and at the water surface. In transverse direction of a flow this is not the case and the value of E can therefore be higher (see lit. (14)).

Summarizing: when $\bar{u} = 1$ m/s, d = 3 m, C = 50 $\sqrt{}$m/s:

E = 0.04 m^2/s (constant over the computational grid).

However, in order to improve stability, it may be necessary to introduce an extra viscosity. According to Kuipers and Vreugdenhill (lit. (15)) this viscosity is dependent on the mesh size and time-step; (α is a weighting-factor).

$$\varepsilon = \alpha \frac{\Delta x^2}{2\Delta t} \quad \ldots\ldots (11)$$

N.B.
When schematizing the viscosity by means of an approximation for the effective turbulent viscosity, it is never physically right to use a constant viscosity. In fact, especially for eddy developping phenomena the viscosity varies over the flow field.For better approximations of E: see Appendix A.

CORIOLIS PARAMETER

In the model the value of C_x and C_y is appointed zero. The influence of the coriolis parameter is not directly important for the results of the calculations; it will only complicate them (since the rest of the external conditions are all simplified).

SLIP PARAMETER

DUCHESS has the option to give a value to a slip parameter CSLIP. It concerns the discharge (velocity) normal to the boundary.

CSLIP = 0 means free slip.
CSLIP = 1 means no slip.

Any real number in between is allowed.

At closed boundaries following boundary conditions are prescribed:

$$u_{\perp} = 0 \quad \text{(12A)}$$

$$u_{//}\,\text{CSLIP} + \Delta(1-\text{CSLIP})\frac{\partial}{\partial n}u_{//} = 0 \;\; (\varepsilon \neq 0) \quad \text{(12B)}$$

$u_{\perp}$ = velocity perpendicular to the boundary
$u_{//}$ = velocity parallel to the boundary
Δ = length related to the distance between boundary and nearest grid point

The models tested in this report have such large grid sizes (16.67 m minimum) that the boundary layers where the no slip condition is valid are very small (compared with the grid).This means: free slip is valid along the closed boundaries.

3.3.3 Time step and stability

TIME STEP

The choice of the time step Δt is dependent on the courant number σ, which is not to exceed 10 while using DUCHESS.

$$\sigma = c \frac{\Delta t}{\Delta x}$$

c = wave propagation velocity $\simeq \sqrt{gd}$
Δt = time step
Δx = (largest) mesh size

This results in following time steps in the simulations:

1. 250 * 250 m — Δt_{max} = 25 s
   mesh size = 16.67 m
   $\sqrt{gd_{max}}$ = 6.32 m/s — Δt = 20 s

2. 500 * 500 m — Δt_{max} = 40 s
   mesh size = 33.33 m
   $\sqrt{gd_{max}}$ = 7.7 m/s — Δt = 40 s

3. 1000 * 1000 m — Δt_{max} = 70 s
   mesh size = 66.66 m
   $\sqrt{gd_{max}}$ = 8.9 m/s — Δt = 60 s

4. 1000 * 1000 m + dam similar to 3.

STABILITY

To get a proper insight in the stability of a two-dimensional numerical scheme is very difficult. An attempt is described in 'Waterloopkundige berekeningen II' (lit (12)). Problems rise in solving the scheme analytically caused by non-linear aspects of the differential equations. For these reasons and for reasons of accuracy the courant number, even in this implicit method, may not become too large.

Another way to improve stability is the introduction of numerical damping, via R and R' (see par. 2.1). In the simulation described in this report this option has not been used.

The final option is to introduce a pseudo-viscosity α in the numerical scheme, via the parameter E, as already pointed out under 'viscosity'.

3.3.4 Overview

An overview of the characteristics and schematizations of each of the numerical models is given in the following table:

LAY-OUT MODEL	250 * 250	500 * 500	1,000 * 1,000	1,000 * 1,000 + dam
- mesh size: Δx	16.67 m	33.33 m	66.67 m	66.67 m
Δy	16.67 m	33.33 m	66.67 m	66.67 m
- time-step: Δt	20 s	40 s	60 s	60 s
- H-conditions:				
slope of water-level: Δh	0.033 m	0.067 m	0.133 m	0.133 m
tide-amplitude : ΔH	4.50 m	4.50 m	4.50 m	4.50 m
tidal period : T	44,700 s	44,700 s	44,700 s	44,700 s
- Q-conditions : Q_{in}	-	-	-	-
- initial conditions:				
still water-level: H_o	2.00 m	2.00 m	2.00 m	2.00 m
discharge : Qx	0 m2/s	0 m2/s	0 m2/s	0 m2/s
discharge : Qy	0 m2/s	0 m2/s	0 m2/s	0 m2/s
- friction:				
roughness of bottom: k_s	0.05 m	0.05 m	0.05 m	0.05 m
- viscosity: E	0.04 m2/s	0.04 m2/s	0.04 m2/s	0.04 m2/s
- coriolisparameter: C	0	0	0	0
- slipparameter:	FREE SLIP	FREE SLIP	FREE SLIP	FREE SLIP
- computed time: T	3,600 s	3,600 s	7,200 s	7,200 s

Table 3.1: overview of hydraulic characteristics, based on a 25 * 25-nodes-computational grid.

GEMEENTEWERKEN ROTTERDAM
AFD. I-02 GEOTECHNIEK

KORRELVERDELINGSDIAGRAM
ISO 565 NEN 2560
MINERALE FRACTIE

WERK CHINA 0-2

BORING

MERK	DIEPTE IN m –	GRIND > 2 mm %	ZAND 0.063-2 mm %	SLIB < 0.016 mm %	LUTUM < 0.002 mm %	HUMUS %	$CaCO_3$ %	U-cijfer	GRONDSOORT
		0.00	24.58	5.33	4.02	1.56	6.82	238.8	ST. SLIBH.UITERST F.ZAND

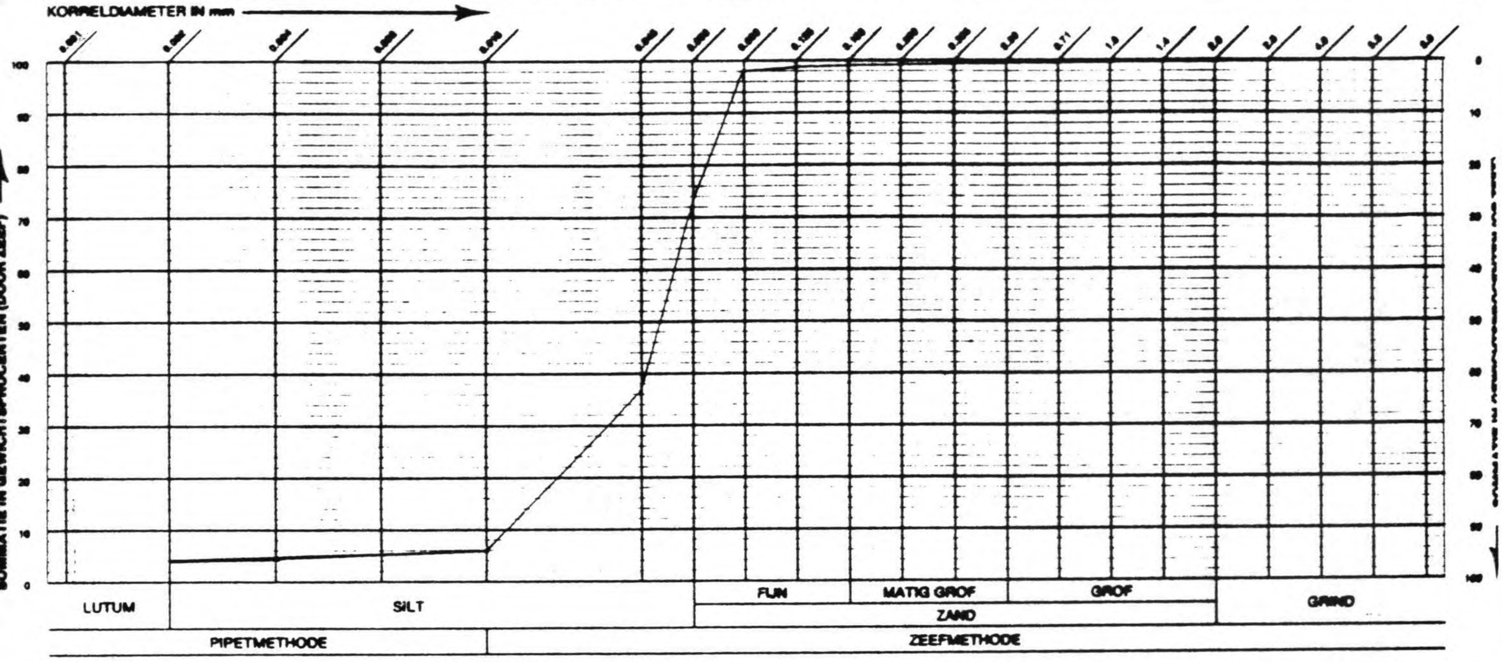

ed 1595 / 2276- 83

GEMEENTEWERKEN ROTTERDAM
AFD. I-02 GEOTECHNIEK

KORRELVERDELINGSDIAGRAM
ISO 565 NEN 2560
MINERALE FRACTIE

WERK CHINA 7

BORING

MERK	DIEPTE IN m –	GRIND > 2 mm %	ZAND 0.063-2 mm %	SLIB < 0.016 mm %	LUTUM < 0.002 mm %	HUMUS %	$CaCO_3$ %	U-cijfer	GRONDSOORT
		0.00	46.16	4.88	3.27	1.89	6.66	188.1	M. SLIBH.UITERST F.ZAND

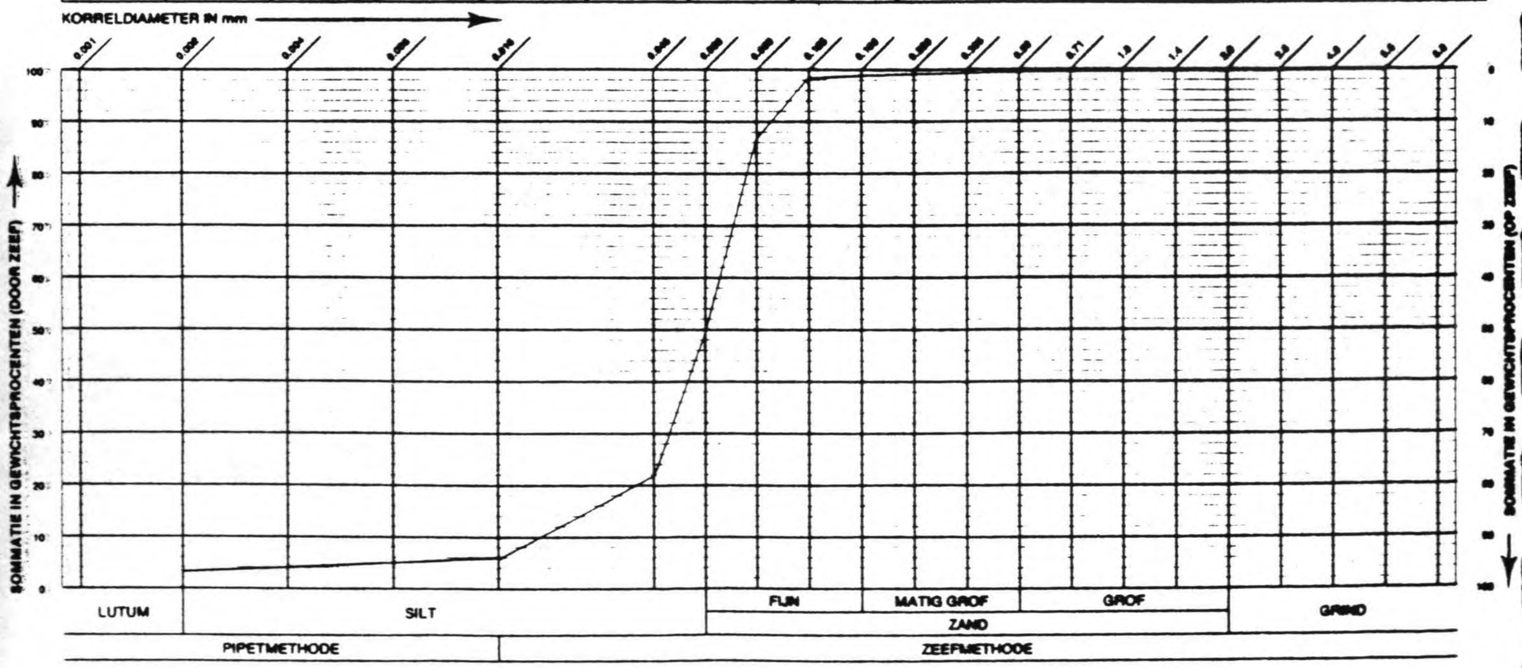

ed 1595 / 2276- 83

3.8 Grainsize distribution

3.4 Morphological characteristics

The program MORPHOR is coupled to DUCHESS, as such all the conditions required by DUCHESS are also valid for MORPHOR. Besides these hydraulic characteristics, characteristics of sediment and transport must be given.

In Fig. 3.8 a typical grain size distribution is given for the coastal area of Cao Jin district.
The following grainsizes may be noted;

D_{50} = 50 . 10^{-6} m;
D_{90} = 100 . 10^{-6} m.

According to local data, the average concentration along the coast of Cao Jing during high tide are varying:
1.000 - 1.200 mg/l is characteristic for 'normal' conditions (see Fig. 3.9). This indicates a concentration C of 377 - 452 . 10^{-6}. As such the initial conditions for each simulation are chosen:

C = 377 . 10^{-6};
Tx = 0 m^2/s (transport in X-direction);
Ty = 0 m^2/s (transport in Y-direction).

(The time necessary for the transport, which is 0 in the beginning, to get homogeneous over the flow direction, is representative for the adaption time of the scheme, the time that initial conditions influence the result.)

3.4.1 C and T conditions

Simulations with MORPHOR are only performed in connection with tidal flow.

According to Galapatti the upstream concentration must be given as a boundary condition for the computation of the depth-averaged concentration and transport rates.

As the exact number of the concentration in time is not known, in this model the concentration is taken constant at both open boundaries (when the tide continues the flow direction changes).

C = 377 . 10^{-6}

(When a zero order approach of the computation is used, MORPHOR will reproduce the equilibrium concentration. This way the value of $C_{boundary}$ = 377 . 10^{-6} can be checked.)

The boundary for the concentration at the bottom is given by the bed-load transport: a BED-BOUNDARY type.

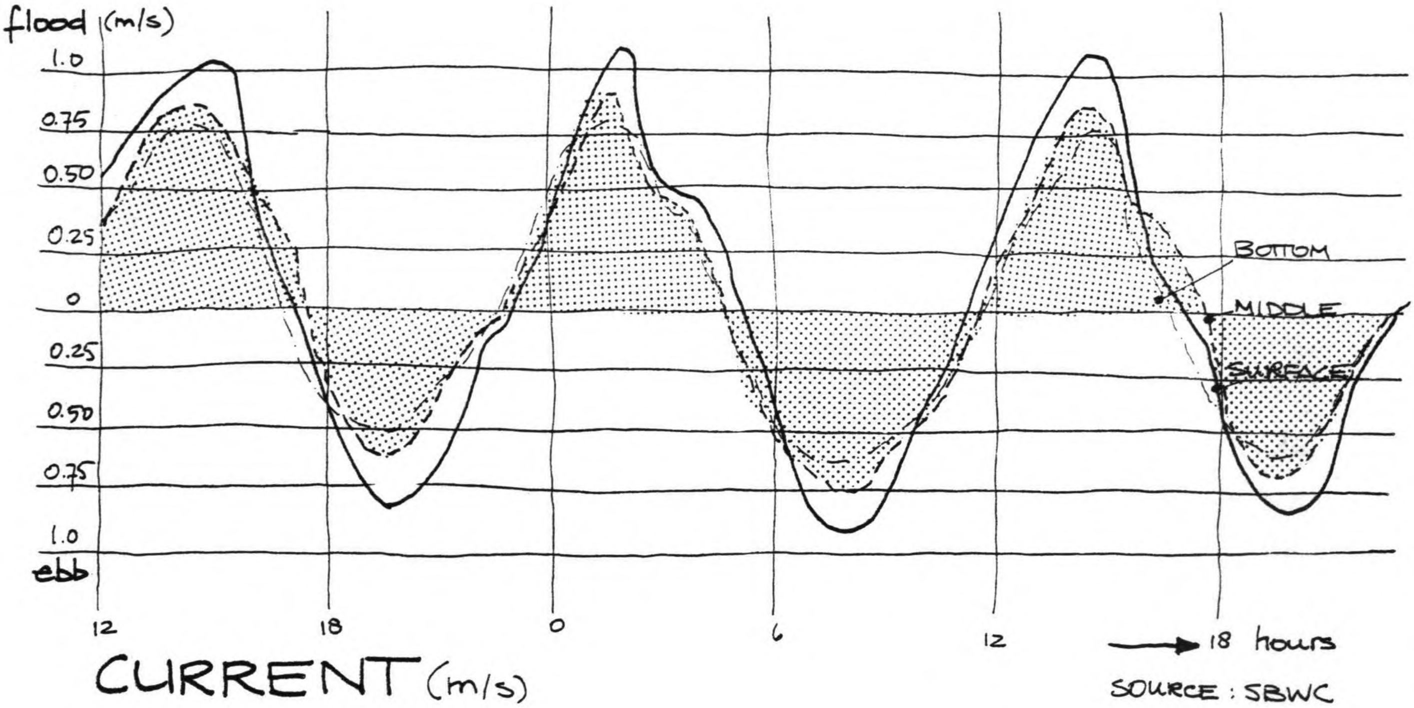

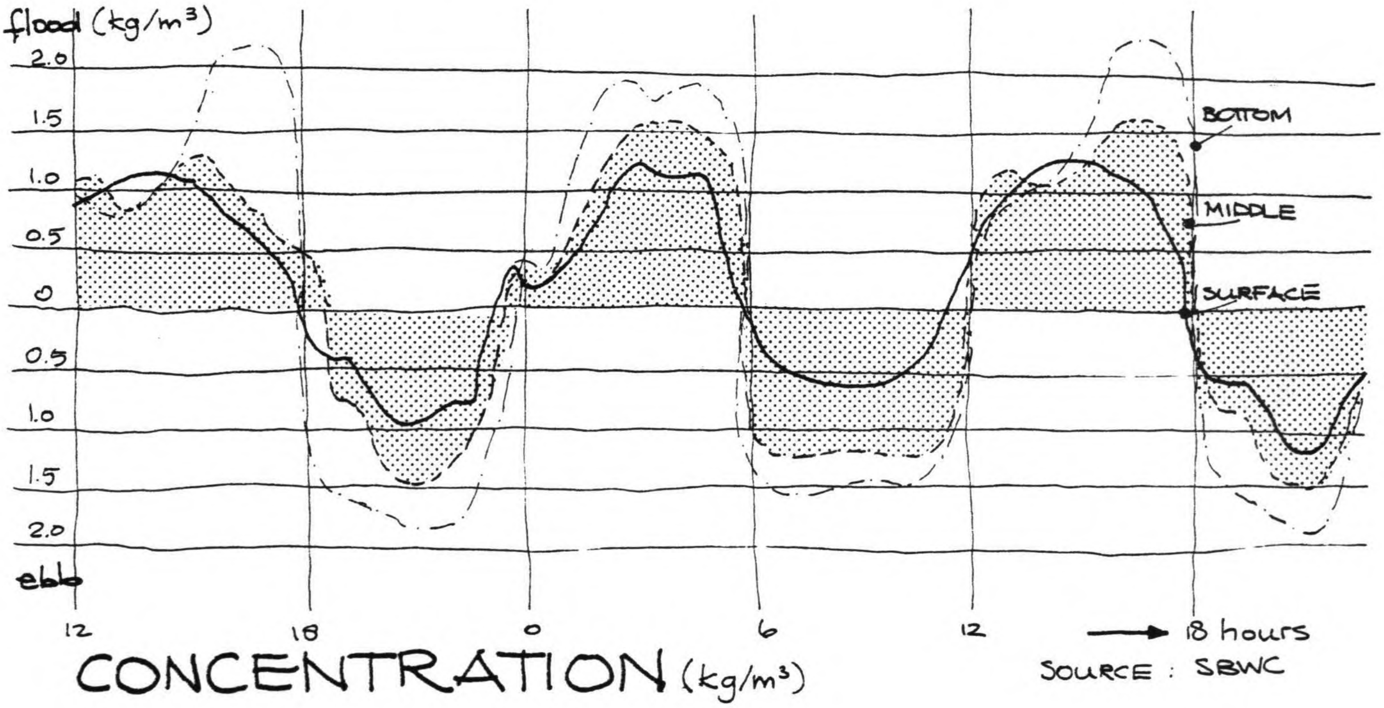

3.9

Concentration and velocity-characteristics

3.4.2 Other parameters

PARTICLE FALL VELOCITY

For $D < 100$ µm the fall velocity of a solitary sand particle is given by Stokes:

$$w_s = \frac{1}{18}\,\frac{(s-1)g\,D_s^{\,2}}{\nu} \qquad (13)$$

s = specific density of grains = ρ_s/ρ = 2.65 (sand)
D_s = diameter of suspended grains
ν = kinematic viscosity of water $\simeq 1 \cdot 10^{-6}$ m²/s

$$\frac{D_s}{D_{50}} = 1 + 0.11\,(\sigma_s - 1)(T - 25) \qquad (14)$$

σ_s = geometric standard deviation of the material $\simeq 2.5$
T = transport stage parameter (see Appendix B)

In the simulations of the model, given $\sigma_s = 2.5$, $\bar{u} = 1$ m/s, $D_{50} = 50 \cdot 10^{-6}$ m, the result is:

$D_s = 32$ µm
and $w_s = 1.1 \cdot 10^{-3}$ m/s (for D = 50 µm: $w_s = 2.3 \cdot 10^{-3}$ m/s)

REFERENCE LEVEL

According to Van Rijn (see Appendix B) the reference level of the bed(-boundary) layer:

$a = 0.5\,\Delta$ or $a = k_s$ and $a \geq 0.01\,d$.

According to Galapatti (see Appendix C, lit (6)) the reference level should be chosen as small as possible
and $0.001d < a < 0.05d$

a = reference level; $\beta = a/d$;
d = flow depth.

For these reasons a was chosen 0.01d (although $k_s = 0.05$ m which is larger than 0.01d in most grid points) (see Fig. 3.10).

POROSITY OF BOTTOM MATERIAL, RELATIVE DENSITY

For the porosity p a value of p = 0.4 is taken. The material at the Cao Jin district is fine sand (silt) with a density of $\rho = 2650$ kg/m³, this means that the relative density

$$\Delta = \frac{\rho_s - \rho}{\rho} = 1.65.$$

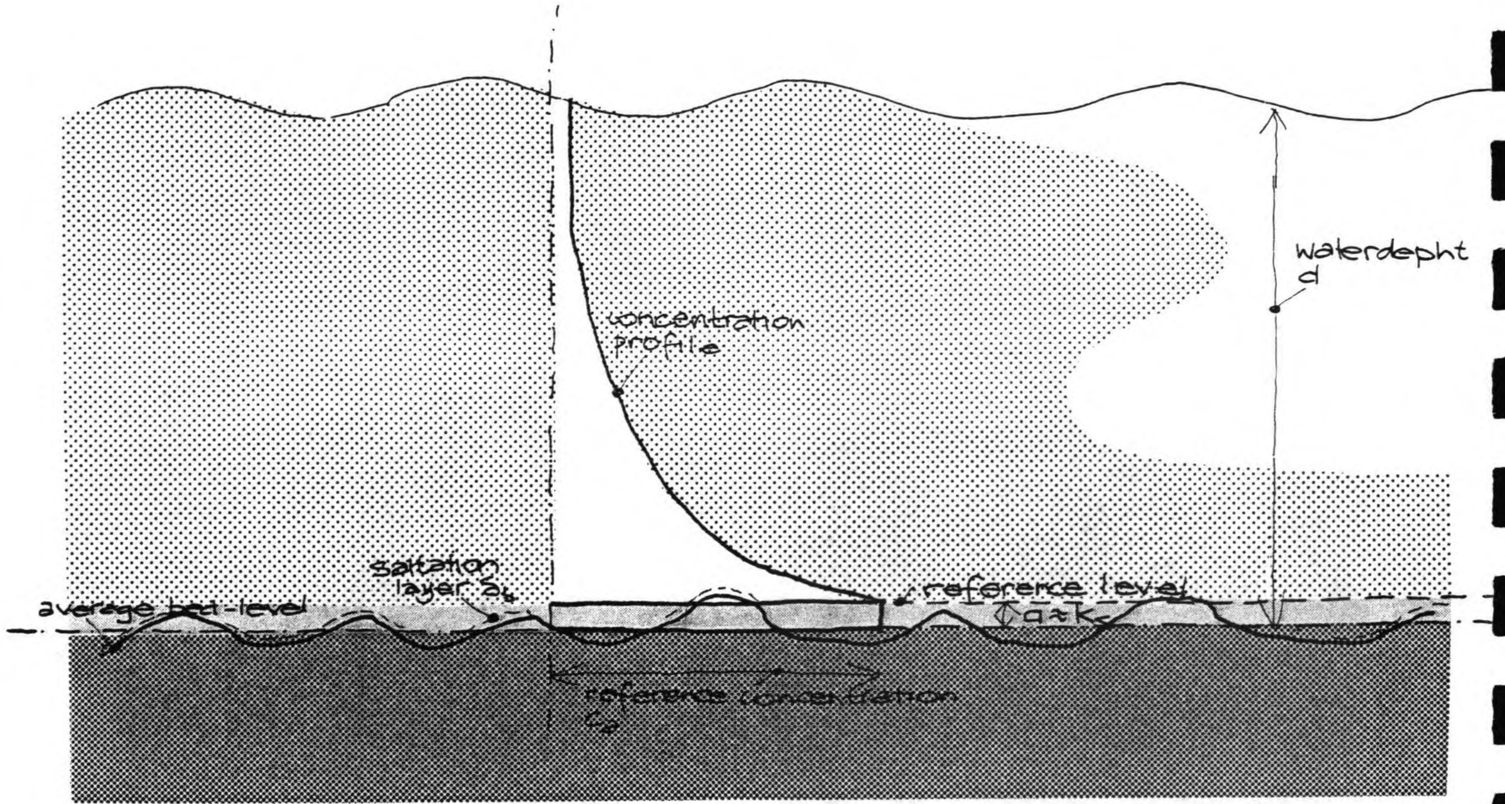

Reference level

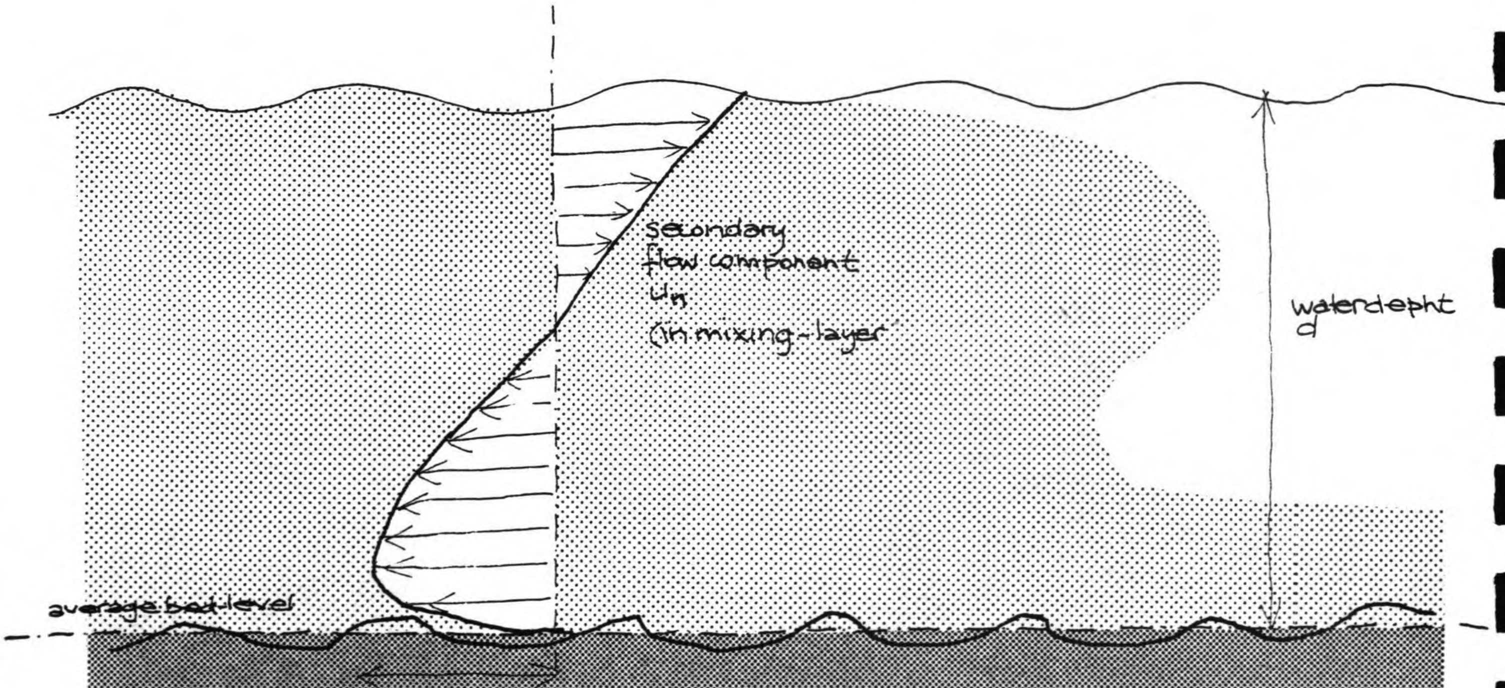

and secondary flow

3.10

ORDER OF THE ASYMPTOTIC SOLUTION

The order of the solution that must be used in the morphological computation is dependent on the mesh size and time step of the schematization and on the flow characteristics.

Galapatti gives for the adaption time and length of the depth-averaged concentration to the equilibrium concentration:

$$L_A = \frac{\gamma_{22}}{\gamma_{11}} \frac{\bar{u}h}{w_s} \quad \text{adaption time} \qquad \text{(C16)}$$

$$T_A = \frac{\gamma_{21}}{\gamma_{11}} \frac{h}{w_s} \quad \text{adaption length} \qquad \text{(C17)}$$

The value of γ_{22}, γ_{21} and γ_{11} are dependent on flow characteristics:
$\bar{u}$, u_* and w_s (see Appendix C).

For $\bar{u}$ = 1 m/s, C = 50 √m/s, d = 3 m it results in:

L_A = 205 m (γ_{22}/γ_{11} = 0.075);
T_A = 136 s (γ_{21}/γ_{11} = 0.05).

This results in the fact that a first order solution is necessary, as the mesh sizes small and therefore the time-step Δt is small also (this is valid for each lay-out model).

(For a check: in the mixing layer between main flow and eddy, $\bar{u}$ ≃ 0.5 m/s, C = 50 √m/s, d = 2 m.)

L_A = 180 m (γ_{22}/γ_{11} = 0.2);
T_A = 300 s (γ_{21}/γ_{11} = 0.17).

A zero order solution is also applied to check the results of the first order approximation, to get an impression of the equilibrium values and to check the deviation of the actual (computed) concentrations from the equilibrium value.

SECONDARY FLOW

In these models the flow is considerably curved, especially where eddies develop (in the mixing layer). As such the influence of secondary flow on the sediment movement will not be negligible. Secondary flow is taken into account (see Appendix A) (see Fig. 3.10).

3.4.3 Time step and stability

TIME STEP

The morphological time-step ΔT can be chosen freely. In these simulations it is taken as 3,600 s (in the case of the computation of tidal motions it is wise to take ΔT as a multiple part of the tidal period).

For the time-step Δt used in calculating the depth-averaged concentration C a courant-number condition applies:

$$\sigma = \bar{u} \frac{\Delta t}{\Delta x} \leq 1 \qquad (15)$$

u = depth-averaged velocity
Δt = time step
Δx = minimum mesh size

As the concentration is calculated by an explicit scheme, this courant-number must be smaller than one to maintain stability.

For the numerical simulations this results in:

1. 250 x 250 m — Δt_{max} = 14.0 s
   mesh size = 16.67 m
   u_{max} = 1.2 m/s — Δt = 10 s

2. 500 x 500 m — Δt_{max} = 27.8 s
   mesh size = 33.33 m
   u_{max} = 1.2 m/s — Δ = 20 s

3. 1000 x 1000 m — Δt_{max} = 55.5 s
   mesh size = 66.67 m
   u_{max} = 1.2 m/s — Δ = 40 s

4. simular to case 3.

One can see that this forms a severe limit to the time step of the morphological computations.
The calculations of the concentration are very sensitive to changes in u, and therefore the depth of the flow. Therefore it is wise to smoothen the bottom for the MORPHOR-computations, which has been done by taking the depth constant in the reclamation fields (the velocities result from the DUCHESS-computations and are realistic).

LATERAL DIFFUSION

An analogy for the diffusion of the sediment-concentration in lateral (in this case lengthwise) direction, can be found from the empirical expression for the dispersion of matter in a turbulent flow:

$$D_l = K\ d\ |u^*| \quad \ldots\ldots\ldots\ldots\ldots\ldots\ldots\ldots\ldots\ldots (16)$$

in which

K = empirical factor, varying from K = 6 (Euler) to K = 100-500 (rivers) (-)
d = waterdepth (m)
u* = bed-shear velocity (m/s).

The scheme which is used to calculate the sediment-concentration is a (implicit) six-point scheme, in which θ, the weighting-factor, is 0.5. The differential-equation is of a convection-diffusion type.
As such, the diffusion parameter D also has to satisfy stability-restrictions in the explicit schemes:

$$\lambda = 2\ D_l \frac{\Delta t}{\Delta x^2} \leq 1 \Rightarrow D_l \leq \frac{\Delta x^2}{2\ \Delta t} \quad \ldots\ldots\ldots\ldots\ldots\ldots (17)$$

Since the weighting-factor θ in the six-point scheme is 0.5, a pseudo-viscosity is introduced (or a pseudo-diffusion)

$$D = \theta \frac{\Delta x^2}{2\ \Delta t} \quad \ldots\ldots\ldots\ldots\ldots\ldots\ldots\ldots\ldots\ldots (18)$$

If we take into account that the diffusion of the scheme consists of the schematized diffusion, plus the numerical diffusion, and that this diffusion should satisfy stability (17), we find (using: u = 1 m/s; d = 3 m; Δx_{250} = 16.67; Δx_{500} = 33.33; $\Delta x_{1,000}$ = 66.67 m, Δt_{250} = 10 s; Δt_{500} = 20 s; $\Delta t_{1,000}$ = 40 s; D_6 = 1.12 m2/s and D_{100} = 20 m2/s):

$D_{250} \leq 7$ m2/s; $D_{500} \leq 14$ m2/s; $D_{1,000} \leq 28$ m2/s.

In the model-simulation the following values are chosen:

1. 250 x 250 m : D = 1 m2/s
2. 500 x 500 m : D = 2,5 m2/s
3. 1,000 x 1,000 m : D = 5 m2/s
4. 1,000 * 1,000 m plus dam: D = 5 m2/s.

Stability morphological computation

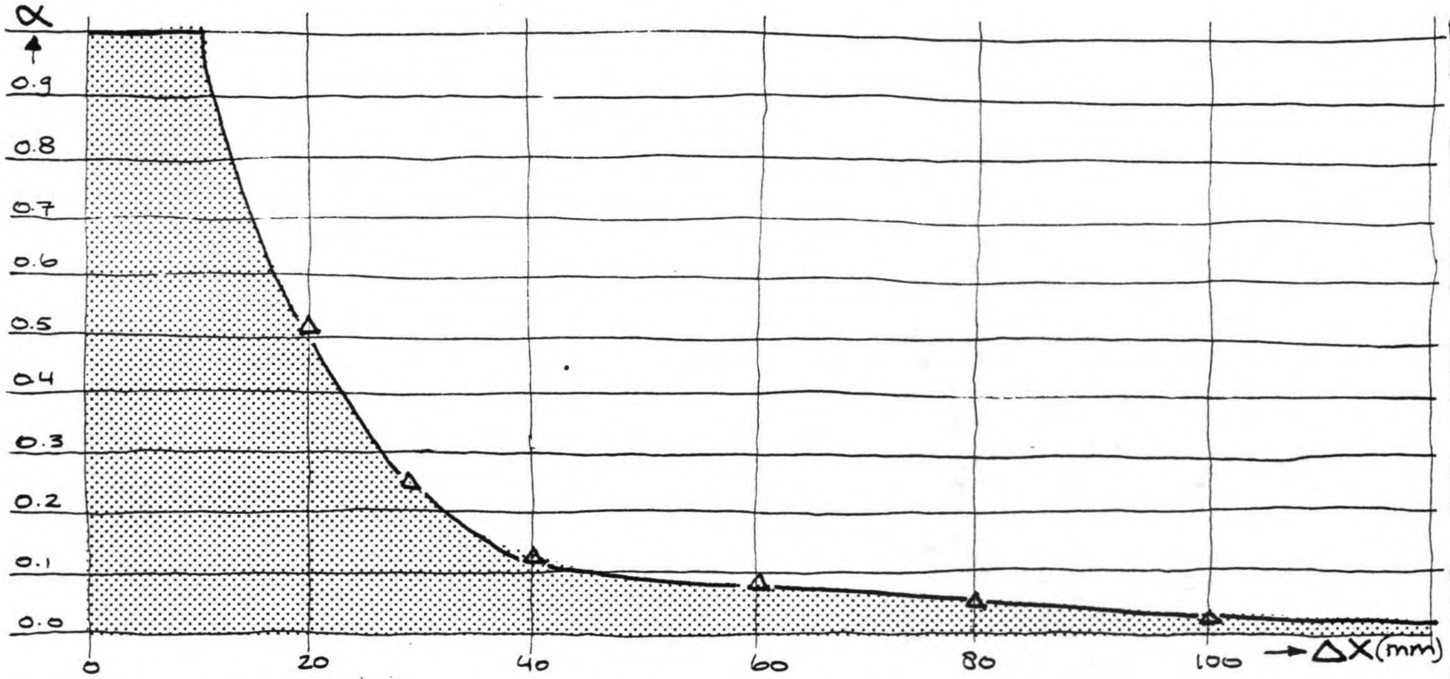

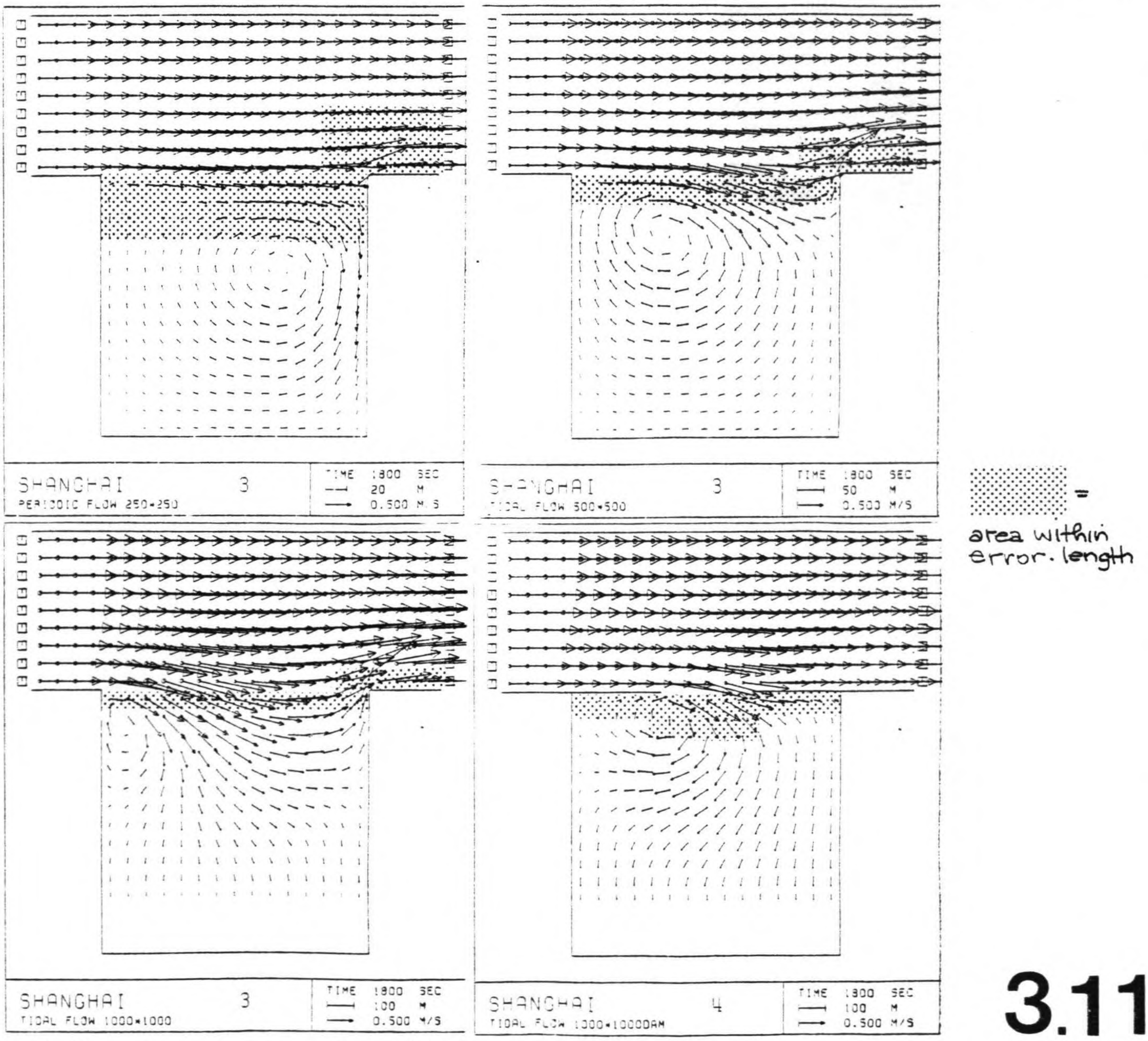

and flow variation over the grid

STABILITY

In order to assure the numerical stability of the morphological computation, a pseudo-viscosity α is introduced, which can be computed by means of a courant number σ for the morphological computation (see Fig. 3.11):

$\alpha = 0.01 + \sigma_m^2 \quad 0.01 \leq \alpha < 1$ . . . .(19)

σ_m = morphological courant number

$\sigma_m = c_m \dfrac{\Delta T}{\Delta x}$ . . . . (20)

c_m = propagation velocity of bottom disturbances

From the powerlaw equation for the transport

$S = a \cdot \bar{u}^b$ . . . . (21)

S = transport
a, b = constants, $b \simeq 5$ (powerlaw)
u = average velocity

it follows
$c_m \simeq b \cdot S/h$ . . . . (22)

The minimum value of $\alpha = 0.01$.
Using $\bar{u} = 1$ m/s, d = h = 3 m, $\bar{c} = 377 \cdot 10^{-6}$, $\Delta T = 3{,}600$ s,
it follows that $(S/h)\ max \simeq 0.8 \cdot 10^{-3}$ m2/s
$c_m \simeq 4.0 \cdot 10^{-3}$ m2/s
$\sigma_m \simeq 14/\Delta x$
$\alpha = (14/\Delta x)^2 + 0.01$

Results for the model simulations:

1. 250 * 250 m — $\alpha = 0.71$
   $\Delta x = 16.67$ m

2. 500 * 500 m — $\alpha = 0.18$
   $\Delta x = 33.33$ m

3. 1,000 * 1,000 m — $\alpha = 0.05$
   $\Delta x = 66.67$ m

4. 1,000 * 1,000 m + dam similar to 3.

VALIDITY OF THE MODEL

According to Wang (Appendix C, lit. (9)) the time and length for which the model is not valid after a (sudden) change in flow conditions:

$T_* \simeq h/u_*$ . . . . error time . . . . (C41)

$L_* \simeq \bar{u}h/u_*$ . . . error length . . . . (C42)

Besides this, the value of w_s/u_*, which is a measurement for the degree of suspension (see Appendix B), must be smaller than 0.2.

Considering $\bar{u}$ = 1 m/s, d = 3 m, C = 50 $\sqrt{m}$/s, w_s = 1.1 . 10^{-3} m/s:

w_s/u_* = 0.017;
T_* = 47.4 s;
L_* = 47 m.

In the mixing layer (where the main flow drives the eddy) the variations in flow conditions are considerable, considering $\bar{u}$ ≈ 0.5 m/s, d = 2 m, C = 50 $\sqrt{m}$/s, w_s = 1.1 . 10^{-3} m/s:

w_s/u_* = 0.035;
T_* = 63 s;
L_* = 32 m.

This shows that the time steps and mesh sizes of the simulations are in the same order as the error length and time.

As the tidal period (44700 s) is very large, the flow variations in time are also large enough to neglect the influence of the error time.

The influence of the error length however is not negligible (see Fig. 3.11), especially in the transition area between main flow and eddy, where flow conditions change in each mesh. The result of the first order solution cannot be trusted in this area. This also is a reason to check the results of a first order approach using a zero order approach.

However, for the computation of morphological changes in the bottom the results will satisfy. Bed level changes are hardly influenced by deviations in sediment concentration. Even in the area that the Galapatti model actually is not valid, it gives the right order of magnitude of the depth-averaged concentration. The model will be more accurate for larger mesh sizes.

3.4.4 Overview

An overview of the characteristics and schematizations of each of the numerical models is given in the following table:

LAY-OUT MODEL	250 * 250	500 * 500	1,000 * 1,000	1,000 * 1,000 plus dam
- mesh size: Δx Δy	16.67 m 16.67 m	33.33 m 33.33 m	66.67 m 66.67 m	66.67 m 66.67 m
- time-step: Δt	10 s	20 s	40 s	40 s
- C-conditions: C_{in}	377.10^{-6}	377.10^{-6}	377.10^{-6}	377.10^{-6}
- T-conditions: T_{in}	-	-	-	-
- initial conditions: sed.-concentration: C_o transport : Tx transport : Ty	 0 0 m2/s 0 m2/s	 0 0 m2/s 0 m2/s	 0 0 m2/s 0 m2/s	 0 0 m2/s 0 m2/s
- grainsizes: average: D_{50} 90% : D_{90}	 50.10^{-6} m 100.10^{-6} m	 50.10^{-6} m 100.10^{-6} m	 50.10^{-6} m 100.10^{-6} m	 50.10^{-6} m 100.10^{-6} m
- fall-velocity: W_s	$1.1.10^{-3}$ m/s	$1.1.10^{-3}$ m/s	$1.1.10^{-3}$ m/s	$1.1.10^{-3}$ m/s
- reference-level: β	0.01	0.01	0.01	0.01
- porosity sediments: p	0.4	0.4	0.4	0.4
- lateral diffusion: D	1.0 m/s	2.5 m2/s	5.0 m2/s	5.0 m2/s
- morphological conditions: computed time: T pseudo-viscosity: α	 3,600 s 0.21	 3,600 s 0.11	 3,600-7,200 s 0.06	 3,600-7,200 s 0.06
- order of computation:	1	1	1	1

Table 3.2: overview of morphological characteristics, based on a 25 * 25-nodes-computational grid.

4. COMPUTATIONS AND RESULTS

4.1 Flow-pattern

Starting point for the numerical computations were the results and calculations as performed in chapter 3.

4.1.1 Results

STEADY FLOW

The results of the steady flow computations are shown in Fig. 4.1. The purpose of this simulation was to find the time that a possible eddy needs to develop, the time the program (DUCHESS) needs to produce steady flow (invariable to time) and the resulting flow-velocities inside the reclamation fields of the various lay-outs, due to a longshore current.

250 * 250 m : it shows that after ≃ 1,800 sec the eddy covers the total field, then the computational results also become rather invariable. Velocities inside the field are in the order of 0.3 m/s, which is about one fourth (¼) of the longitudinal velocity.

500 * 500 m : it shows that the eddy covers the reclamation field after ≃ 3,600 sec, the results then also become more or less steady. Resulting velocities inside the field are in the order of 0.4 m/s.

1.000 * 1.000 m: it shows that the eddy does not cover the entire field; the diameter of the eddy increases until about 300 m in 2,400 sec, apparently then the bottom-friction limits further growth of an eddy, confirming the suspect that 500 m forms a maximum opening size. Resulting velocities are ≃ 0.4 m/s inside the eddy and up to 0.7 m/s near the damheads.

1.000 * 1.000 m plus dam : it shows a complex formation of eddies inside the reclamation field. The results of the computation become rather steady after 2,400 sec Resulting velocities inside the field are in the order of 0.2 m/s (very favourable for sedimentation).

The driving forces that cause an eddy to develop in a sideward expansion are transported to this expansion through a mixing-layer that develops between the mainflow and the sideward expansion.

The total mass of water that must be accelerated and the length of the mixing layer determine the time that an eddy needs to develop. In the case of the 250 * 250 m lay-out, compared with the 500 * 500 m lay-out, the mass of water in the field is about one fourth of that in the 500 * 500 m field, but the length of the mixing layer is at most 250 m, half of the maximum length in the case of 500 * 500 m. So the total time that the eddy needs to develop is about half the time in the 500 * 500 m model, which indicates that the numerical model might reproduce realistic eddy-formation, and the actual time an eddy needs to develop is in the order of the time as shown in Fig. 4.1.

UNSTEADY FLOW

The results are shown in Fig. 4.2 .The purpose of this simulation was to determine velocities inside the reclamation fields due to storage, and the initial effects of unsteady boundary conditions.

250 * 250 m : almost immediately (360 sec) the results become rather invariable. Resulting storage velocities are in the order of 0.05 m/s.

500 * 500 m : initial effects vanish after 360 sec, resulting storage velocities are in the order of 0.1 m/s.

1,000 * 1,000 m: after 360 sec the results become more or less invariable, storage velocities are in the order of 0.2 m/s.

1,000 * 1,000 m plus dam : again it takes about 360 sec before the initial effects have vanished, the resulting storage velocities inside the field are in the order of 0.2 m/s and between the damheads 0.4 m/s.

It shows that the velocities due to storage are smaller than the velocities inside the reclamation fields due to the longshore current, which confirms the expectation that eddy-developing is a major mechanism for the stimulation of sedimentation.

TIDAL FLOW

The tidal motion is simulated by a one-harmonical component having an amplitude of 2.25 m (Fig. 3.6). Purpose of this simulation was to determine the resulting velocities due to a combination of storage and longitudinal currents. The results are shown in Fig. 4.3.

KIP

Tussenvoegen

KIP

Tussenvoegen

KIP

Tussenvoegen

250 * 250 m : the initial effects damp out in about 600 sec, the eddy covers the entire field in about 1,200 sec, after this time the shape of the eddy changes somewhat, but the order of the magnitude of the resulting velocities remain the same: 0.4 m/s (about one third of the main flow-velocity).

500 * 500 m : initial effects damp out in about 600 sec, the eddy develops in about 2,400 sec, resulting in velocities in the order of 0.4 m/s (one third of the main velocity).

1,000 * 1,000 m: again the initial effects vanish after 600 sec, the eddy increases until it reaches a diameter of 400 m, after 2,400 sec. Then the eddy changes its shape and the centre moves in time, but the order of magnitude of the resulting velocities remain the same: 0.4 m/s in the eddy and upto 0.8 m/s in the transitional area. As the waterlevel rises, the eddy becomes larger and the velocities decrease.

1,000 * 1,000 m plus dam : it takes about 600 sec for the initial effects to vanish, after 1,200 sec an eddy forms over the entire innerfield, this eddy increases in velocity until about 3,600 sec, then the results become stable, resulting velocity in the eddy is about 0.4 m/s; in the opening between the longitudinal dams velocities up to 0.8 m/s occur.

It shows that the extra storage increases the eddy-velocities inside the reclamation fields, one could say that both effects can be superimposed. Especially in the smaller lay-outs, the velocities increase considerably by the combined effect (0.3 m/s due to steady flow, 0.4 m/s in the case of periodical flow!). Also the time that the eddy needs to develop decreases as a result of storage. Striking is the lay-out of 1,000 * 1,000 m plus dam, where an eddy develops rather "fast" (1,200 sec) over the entire field (diameter $\simeq$ 1,000 m). Altogether one can say that the rising waterlevel has a positive effect on eddy-developing.

CONCLUSION:

the effect of extra storage has a positive influence on the development of eddies.
The bottom friction limits the size of the eddy. If the opening between the damheads becomes larger than 500 m, extra longitudinal dams are necessary to stimulate eddy-development and to prevent erosion around the damheads.

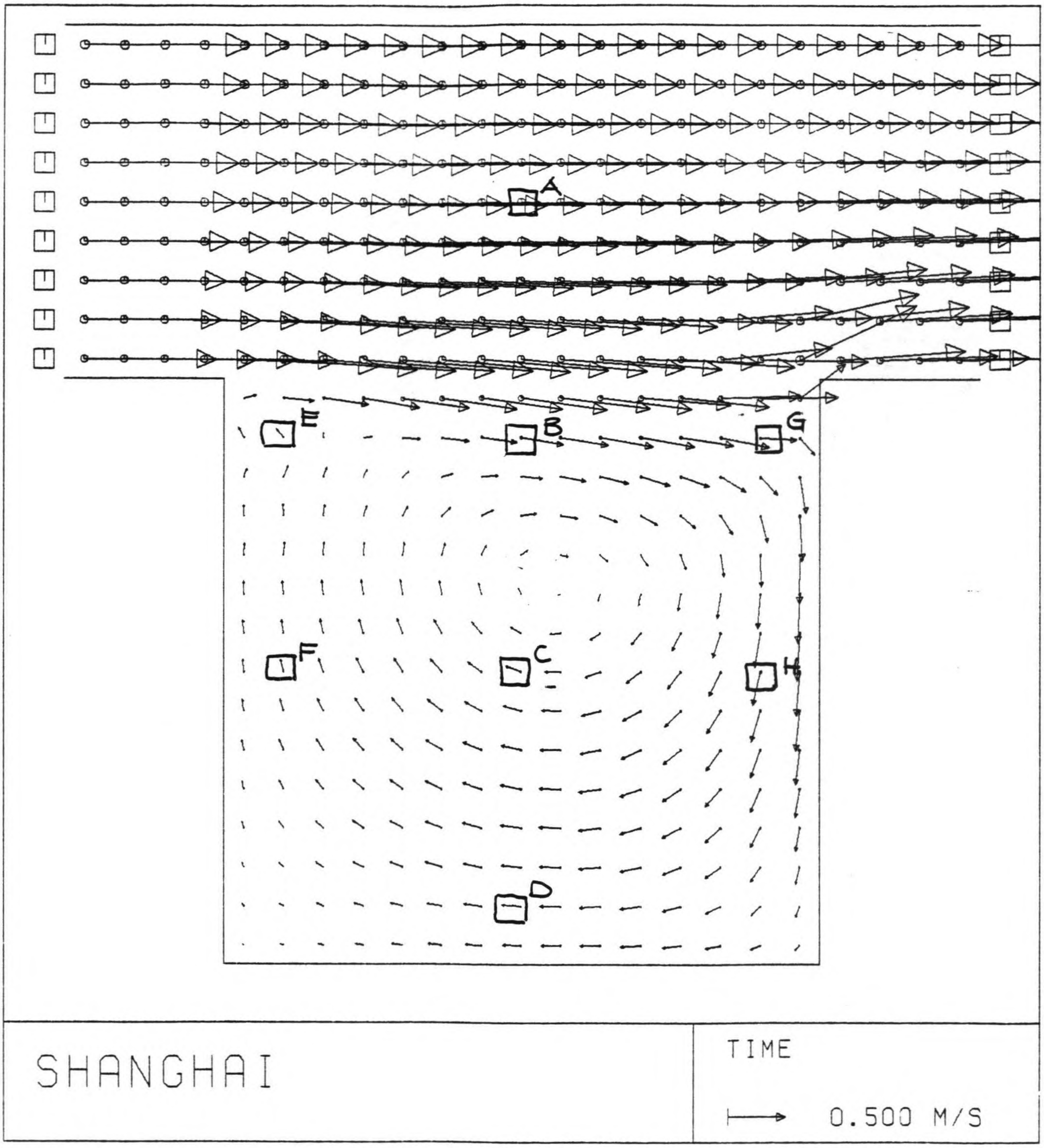

4.4
Overview of the control-points in the computational grid

4.1.2 Sensitivity-analysis

In chapter 3 the input-parameters for the model DUCHESS have been discussed. By means of numerical simulations, the effect of some of these parameters has been investigated. Following items are discussed:

- the influence of the main-flow-velocity;
- the influence of the (bottom) friction;
- the influence of viscosity;
- the influence of the length-distance ratio;
- the influence of the time-step.

In the following table an overview is given of the simulations with respect to the flow-pattern:

LAY-OUT MODEL	250 * 250 m	500 * 500 m	1,000 * 1,000 m	1,000 * 1,000 m plus dam
- mesh_size: Δx Δy	16.67 m 16.67 m	33.33 m 33.33 m	66.67 m 66.67 m	66.67 m 66.67 m
- main_flow-velocity: diff. in waterlevel: Δh $\bar{u}$: diff. in waterlevel: Δh	 0.033 m 1.0 m/s 0.055 m 1.3 m/s	 0.067 m 1.0 m/s 0.111 m 1.4 m/s	 0.133 m 1.0 m/s 0.222 m 1.5 m/s	 0.133 m 1.0 m/s 0.222 m 1.5 m/s
- friction: roughness: k_s bottomlevel opening:	 0.05 m -2.0 m	 0.05 m -2.0 m	 0.05 m -2,0 m -10.0 m	 0.05 m -2.0 m
- viscosity: E	0.04 m2/s	0.04 m2/s 1.0 m2/s 10.0 m2/s	0.04 m2/s	0.04 m2/s
- length-distance ratio:	1:1	1:1	1:1 0.5:1	1:1
- time_step: Δt	10 s 20 s	20 s 40 s	40 s 60 s	40 s 60 s 120 s

Table 4.1: overview of simulations with respect to the analysis of the flow-pattern.

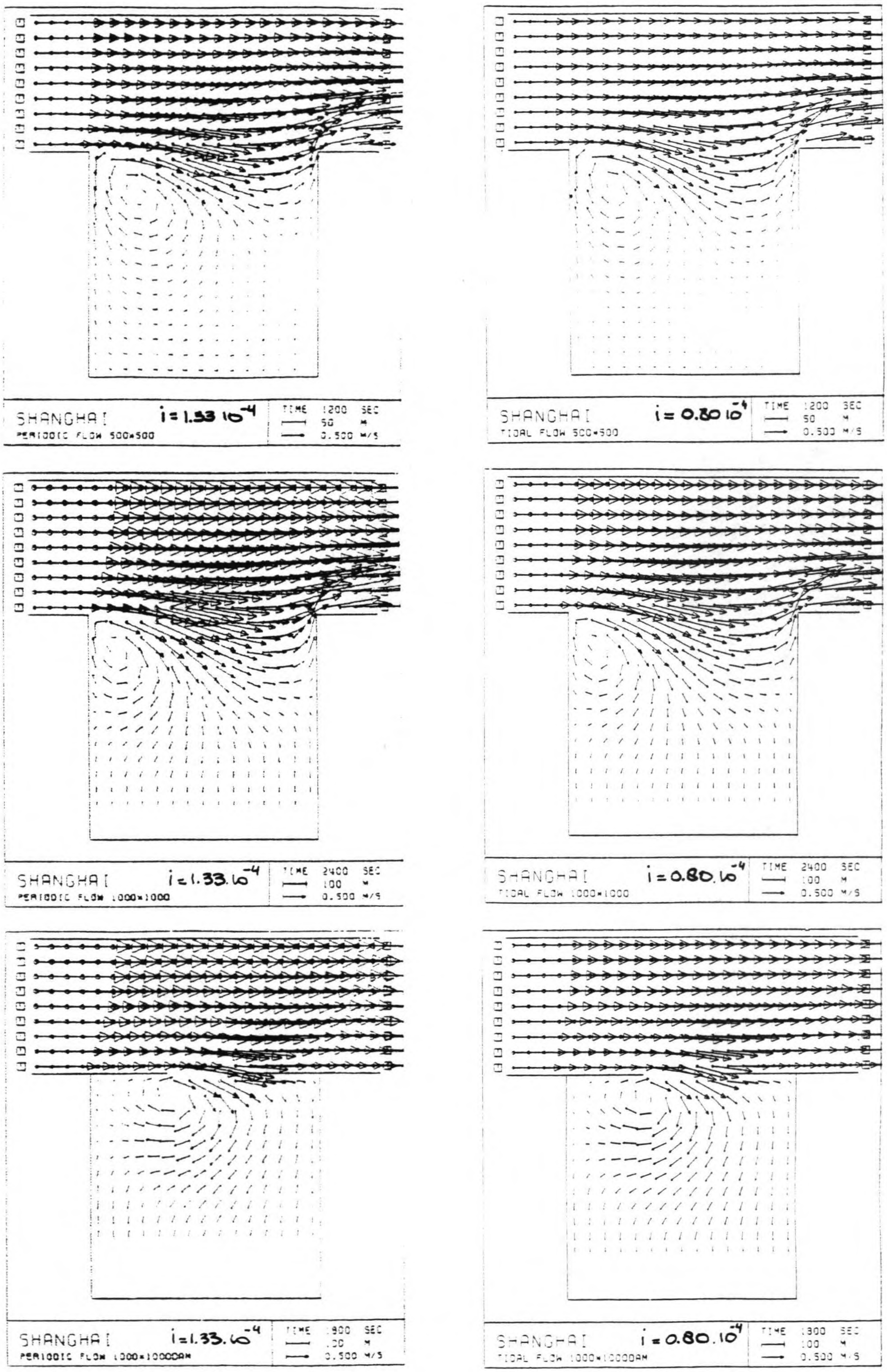

4.5

Influence of the main flow-velocity

INFLUENCE OF THE MAIN-FLOW-VELOCITY (see Fig. 4.5)

The velocity of the main flow is a characteristic parameter for the longshore current. By changing this velocity, the effect can be determined on the development and the velocity-distribution of the eddy inside the reclamation fields. This velocity is schematized by a difference in the waterlevel H at the open boundaries of the model.

The standard model velocity is 1.0 m/s, schematized by a slope of the waterlevel:

$$i = \frac{\bar{u}^2}{C^2R} = 8.0.10^{-5}$$

In this sensitivity analysis, the slope of the waterlevel is increased, thus u = 1.3 m/s:

$$i = \frac{\bar{u}^2}{C^2R} = 1.33.10^{-4}$$

In order to compare the results of the simulations a number of control-points are introduced (see Fig. 4.4) at which the numerical values of the waterlevel H; the horizontal discharge Qx, and the vertical discharge Qy are compared (see table 4.2)

CONCLUSION:

increase of the main flow-velocity causes an increase of the velocities in the eddy (of comparable magnitude). The flow-pattern is not changed, nor the time necessary for the eddy to develop.
So the main flow-velocity only influences the magnitude of the eddy-velocities.

LAY-OUT MODEL		250 * 250		500 * 500		1,000 * 1,000		1,000 * 1,000 plus dam	
		(1)	(2)	(1)	(2)	(1)	(2)	(1)	(2)
point A	H [m]		2.950	2.945	2.929	2.920	2.889	2.906	2.865
	Qx [m2/s]		5.102	5.731	7.144	9.254	11.826	9.718	12.287
	Qy [m2/s]		-0.131	-0.117	-0.135	-0.253	-0.270	-0.235	-0.229
point B	H [m]		2.953	2.946	2.932	2.926	2.900	2.896	2.854
	Qx [m2/s]		0.749	1.296	1.552	1.690	2.044	0.750	0.833
	Qy [m2/s]		-0.566	-0.326	-0.498	-0.843	-0.930	-0.610	-0.559
point C	H [m]		2.952	2.946	2.932	2.925	2.899	2.900	2.862
	Qx [m2/s]		0.106	-0.374	-0.388	-0.071	-0.083	-0.245	-0.255
	Qy [m2/s]		-0.140	0.110	0.087	-0.228	-0.235	-0.086	-0.071
point D	H [m]		2.953	2.949	2.934	2.873	2.880	2.847	2.800
	Qx [m2/s]		-0.636	-0.186	-0.213	-0.001	-0.000	0.000	3.000
	Qy [m2/s]		0.020	0.016	0.014	-0.031	-0.028	-0.028	-0.024
point E	H [m]		2.950	2.948	2.933	2.915	2.887	2.899	2.860
	Qx [m2/s]		-0.179	-0.066	-0.082	0.518	0.542	0.082	0.082
	Qy [m2/s]		0.404	0.141	0.442	-0.046	-0.061	0.127	0.106
point F	H [m]		2.951	2.948	2.933	2.919	2.892	2.898	2.860
	Qx [m2/s]		-0.014	-0.096	-0.115	-0.138	-0.148	-0.054	-0.045
	Qy [m2/s]		0.637	0.248	0.278	0.034	0.056	-0.058	-0.070
point G	H [m]		2.958	2.954	2.941	2.927	2.898	2.914	2.879
	Qx [m2/s]		0.724	0.594	0.640	0.531	0.631	0.152	0.165
	Qy [m2/s]		0.137	0.248	0.439	0.981	1.242	-0.369	-0.707
point H	H [m]		2.953	2.949	2.936	2.930	2.904	2.908	2.873
	Qx [m2/s]		-0.056	-0.105	-0.113	0.007	0.004	-0.057	-0.067
	Qy [m2/s]		-0.637	-0.651	-0.667	-0.140	-0.146	-0.268	-0.286

Table 4.2 influence of main velocity, at T = 3,600 s (tidal motion)
(1): $i = 8.0.10^{-5}$
(2): $i = 1.33.10^{-4}$.

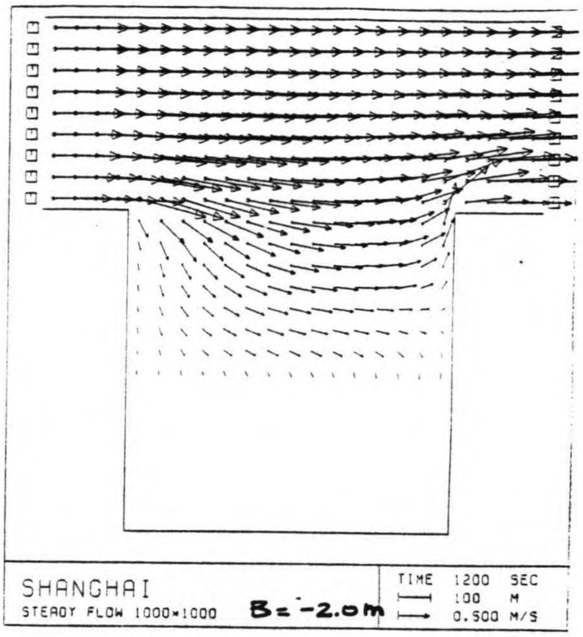
SHANGHAI
STEADY FLOW 1000×1000
B=-2.0m
TIME 1200 SEC
100 M
0.500 M/S

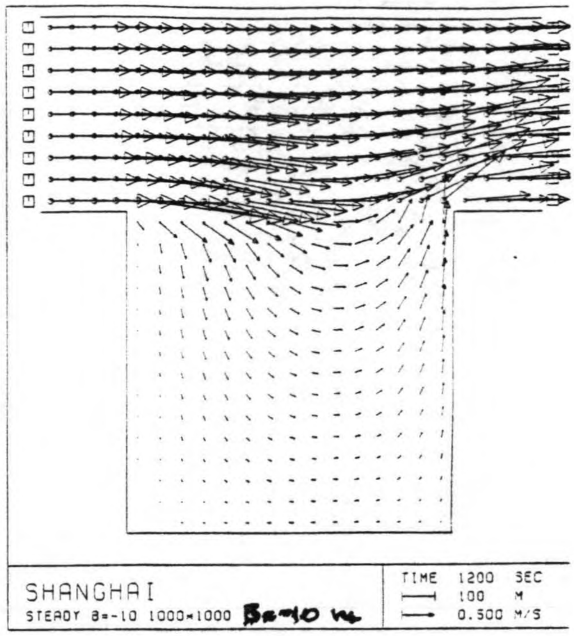
SHANGHAI
STEADY B=-10 1000×1000
TIME 1200 SEC
100 M
0.500 M/S

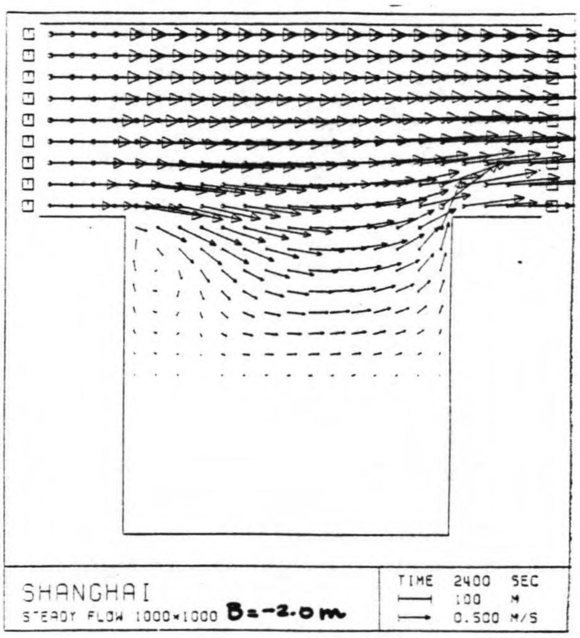
SHANGHAI
STEADY FLOW 1000×1000
B=-2.0m
TIME 2400 SEC
100 M
0.500 M/S

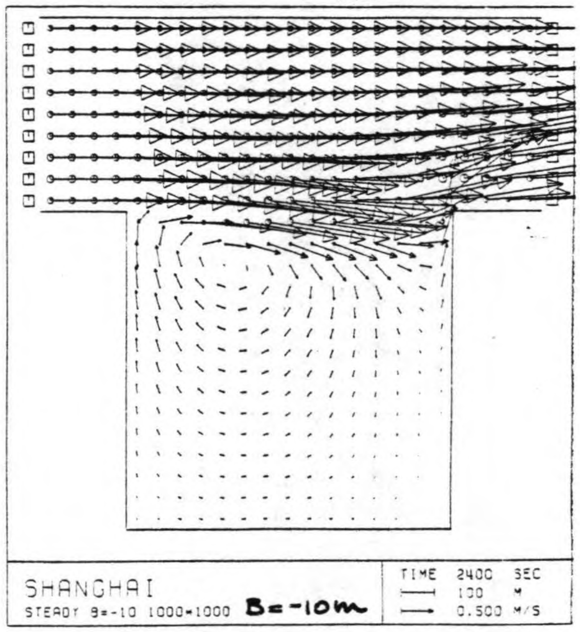
SHANGHAI
STEADY B=-10 1000×1000
B=-10m
TIME 2400 SEC
100 M
0.500 M/S

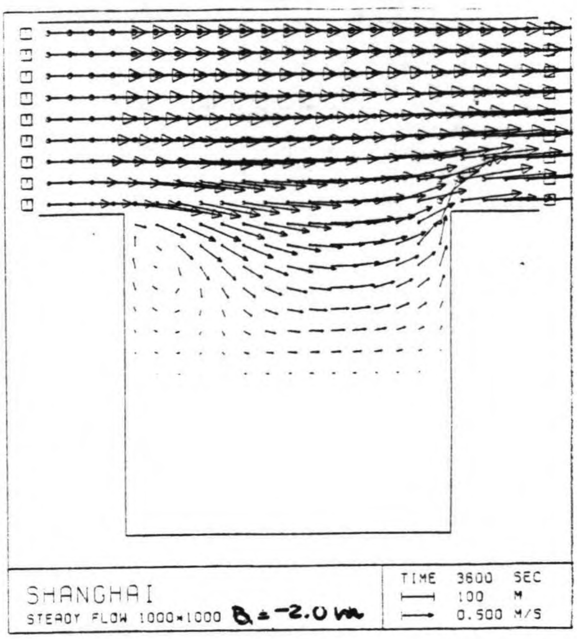
SHANGHAI
STEADY FLOW 1000×1000
B=-2.0m
TIME 3600 SEC
100 M
0.500 M/S

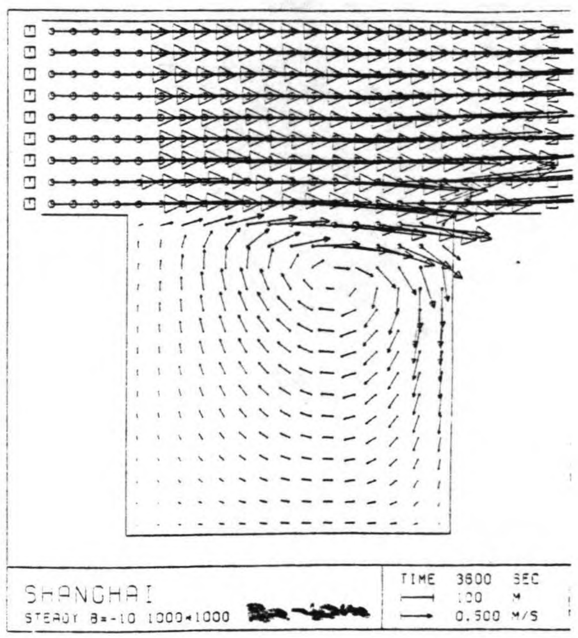
SHANGHAI
STEADY B=-10 1000×1000
TIME 3600 SEC
100 M
0.500 M/S

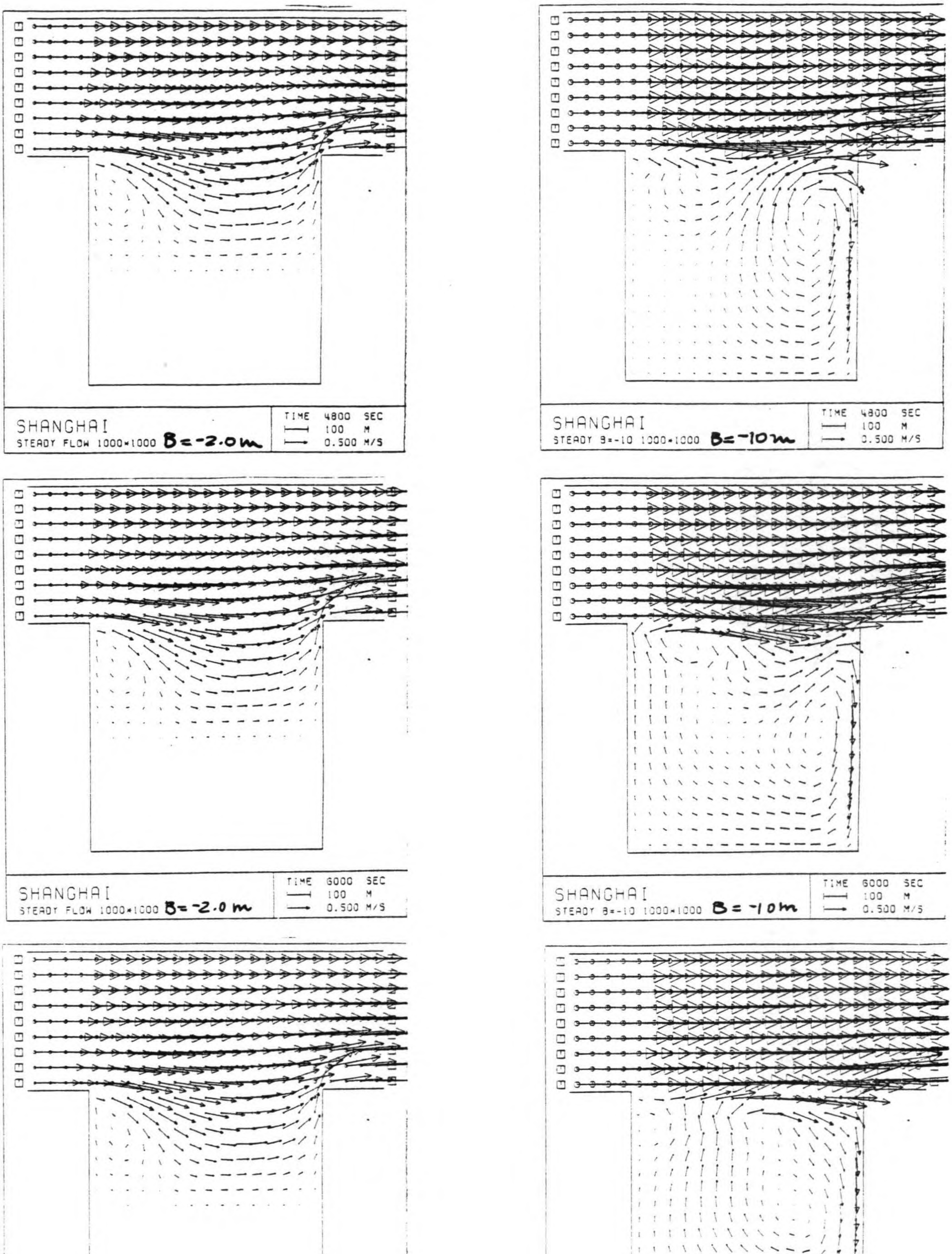

4.6

Influence of the bottom-friction

INFLUENCE OF THE (BOTTOM)-FRICTION (see Fig. 4.6)

The (bottom)-friction is one of the major parameters that dissipates the energy which can cause an eddy to develop (see also appendix A). In this model friction is mainly induced by the bottom.
To check whether the bottom-friction is actually determining the size of the eddy, a very deep bottom (-10.00 m) was applied on the 1,000 * 1,000 lay-out, under the same circumstances as the original simulation (see Fig. 4.6).

The results of this simulation confirms the expectation that the bottom-friction determines the maximum opening between the dams, if eddy-developing is objected. In case of the Cao Jin-district, where the bottomlevel is 2 m below the still-waterlevel, this maximum distance is 500 m.

CONCLUSION:

an increase of the bottom-friction causes a decrease of the size of the eddy. This influence is considerable, especially for very shallow water.

It is important that the bottom-friction is schematized in a proper way, in order to obtain realistic results of a numerical computation.

N.B. the applied roughness of the bottom, k_s = 0.05 m seems a reasonable value. This value will have to be confirmed by measurements.

SIMULATIONS

DUCHESS

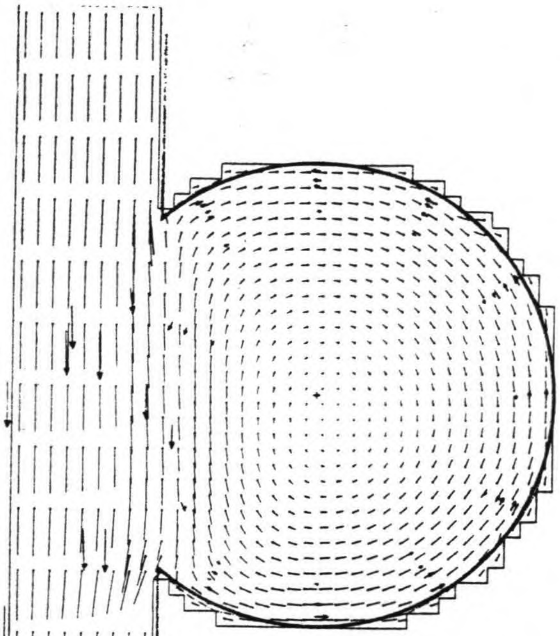

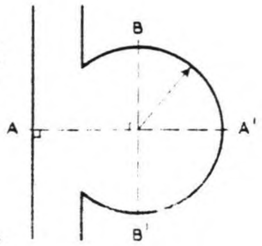

MEASUREMENTS AND SIMULATIONS

—— place of the boundary, when it is assumed that the depth is constant everywhere and the area of the cross-section remains unchanged
—— calculation
⟶ measurement
velocity scale: 1 cm ≙ 0.2 m/s

KUIPERS AND VREUGDENHILL LIT. 16

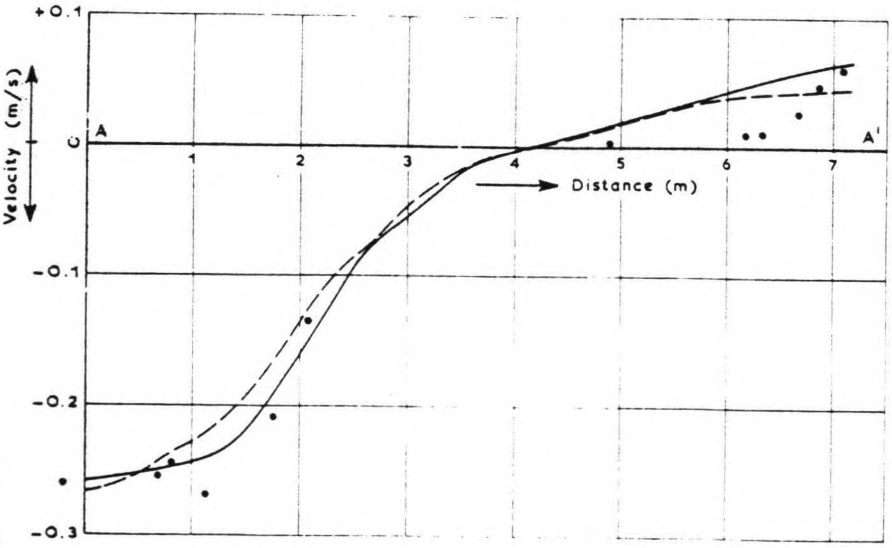

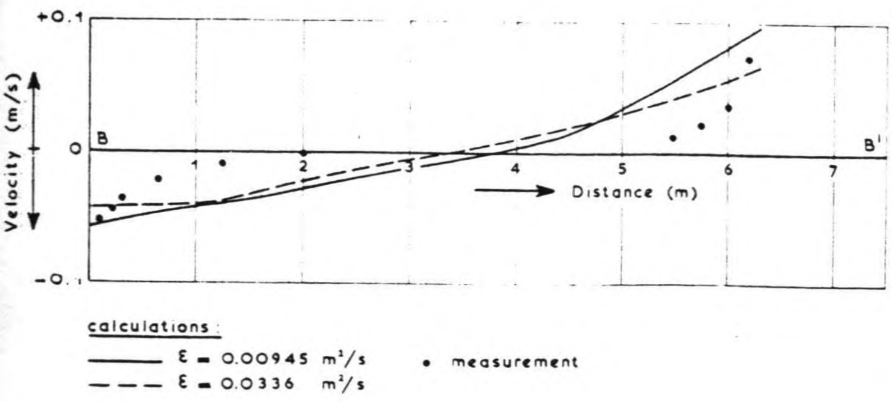

calculations:

—— ε = 0.00945 m²/s • measurement
— — ε = 0.0336 m²/s

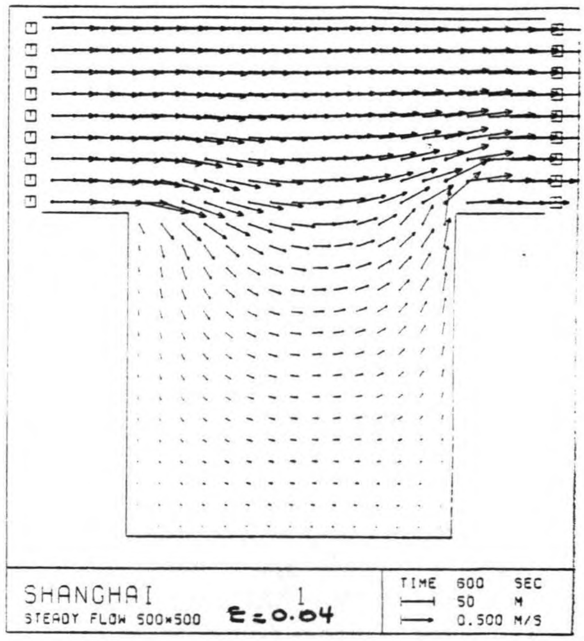

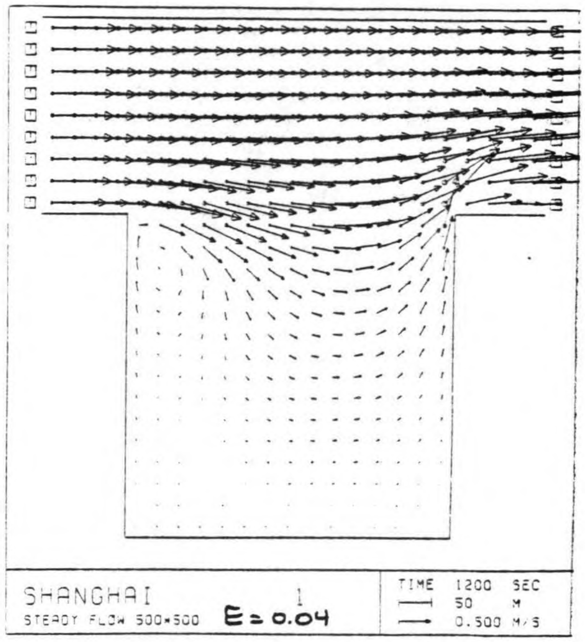

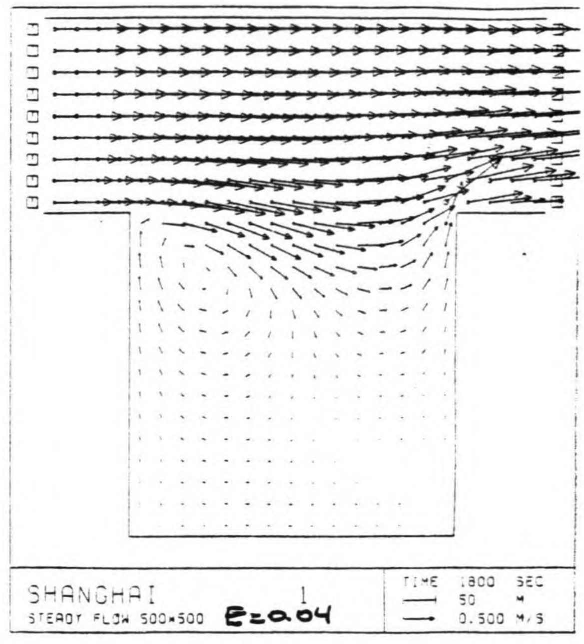

4.7

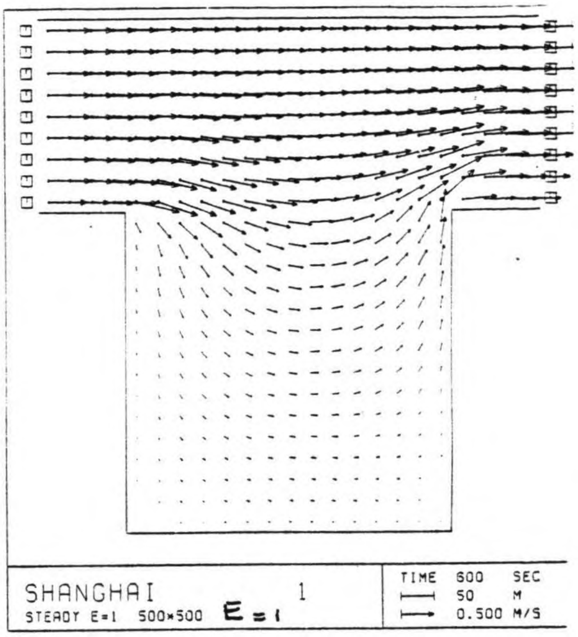
SHANGHAI
1
STEADY E=1 500×500
E=1
TIME 600 SEC
50 M
0.500 M/S

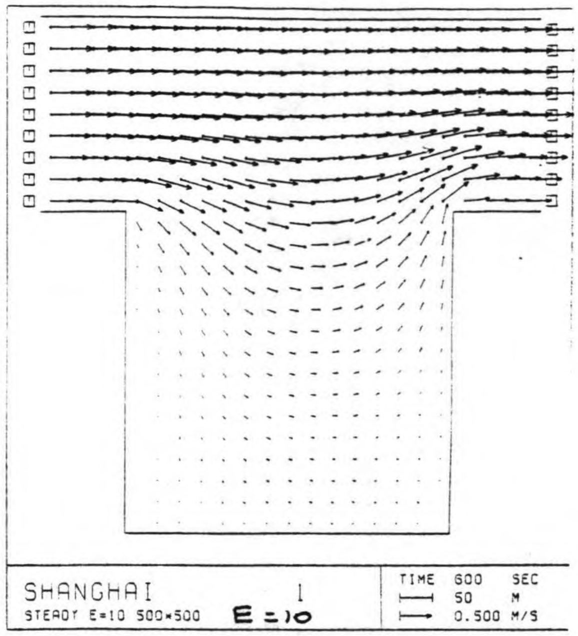
SHANGHAI
1
STEADY E=10 500×500
E=10
TIME 600 SEC
50 M
0.500 M/S

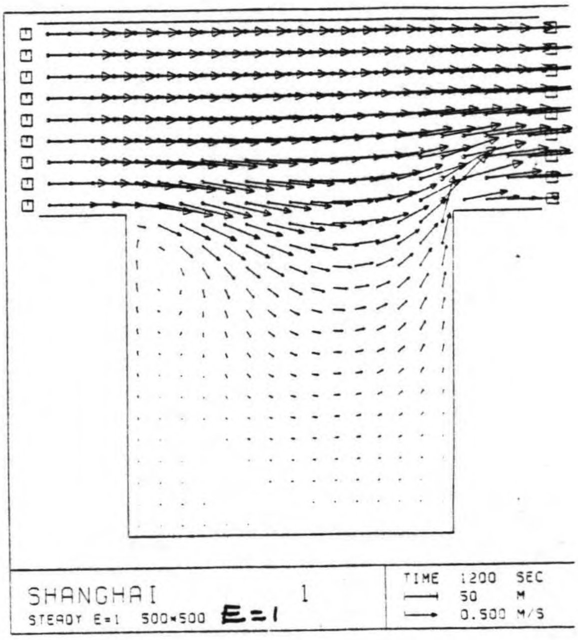
SHANGHAI
1
STEADY E=1 500×500
E=1
TIME 1200 SEC
50 M
0.500 M/S

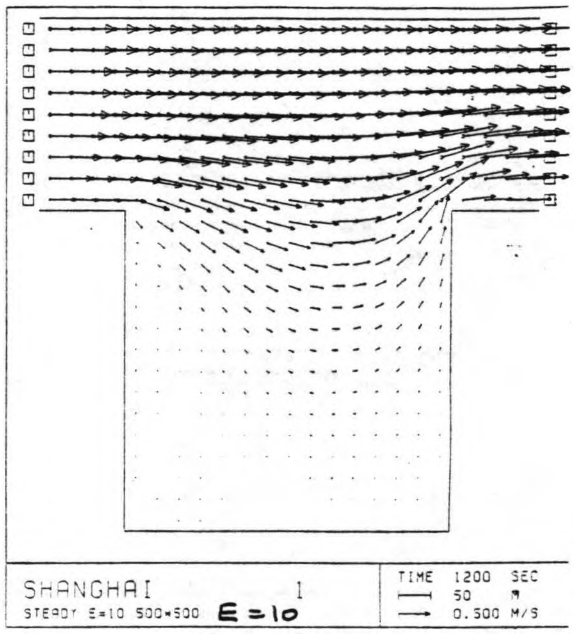
SHANGHAI
1
STEADY E=10 500×500
E=10
TIME 1200 SEC
50 M
0.500 M/S

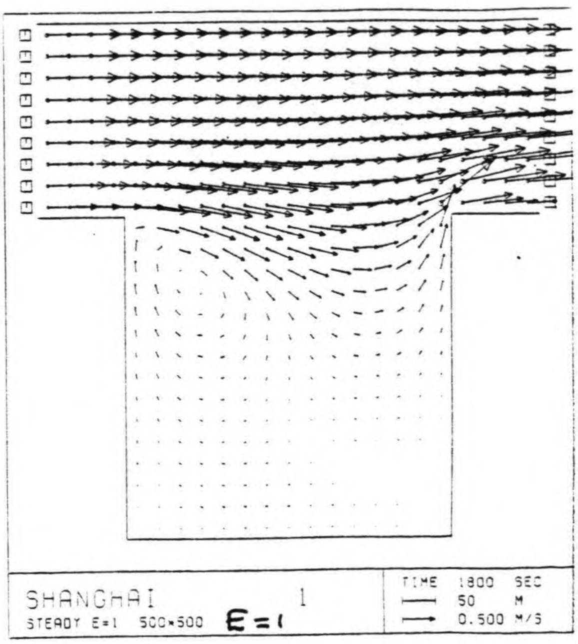
SHANGHAI
1
STEADY E=1 500×500
E=1
TIME 1800 SEC
50 M
0.500 M/S

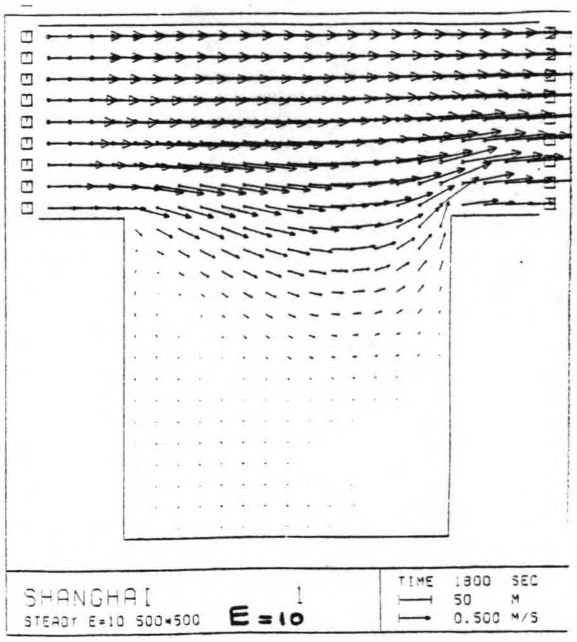
SHANGHAI
1
STEADY E=10 500×500
E=10
TIME 1800 SEC
50 M
0.500 M/S

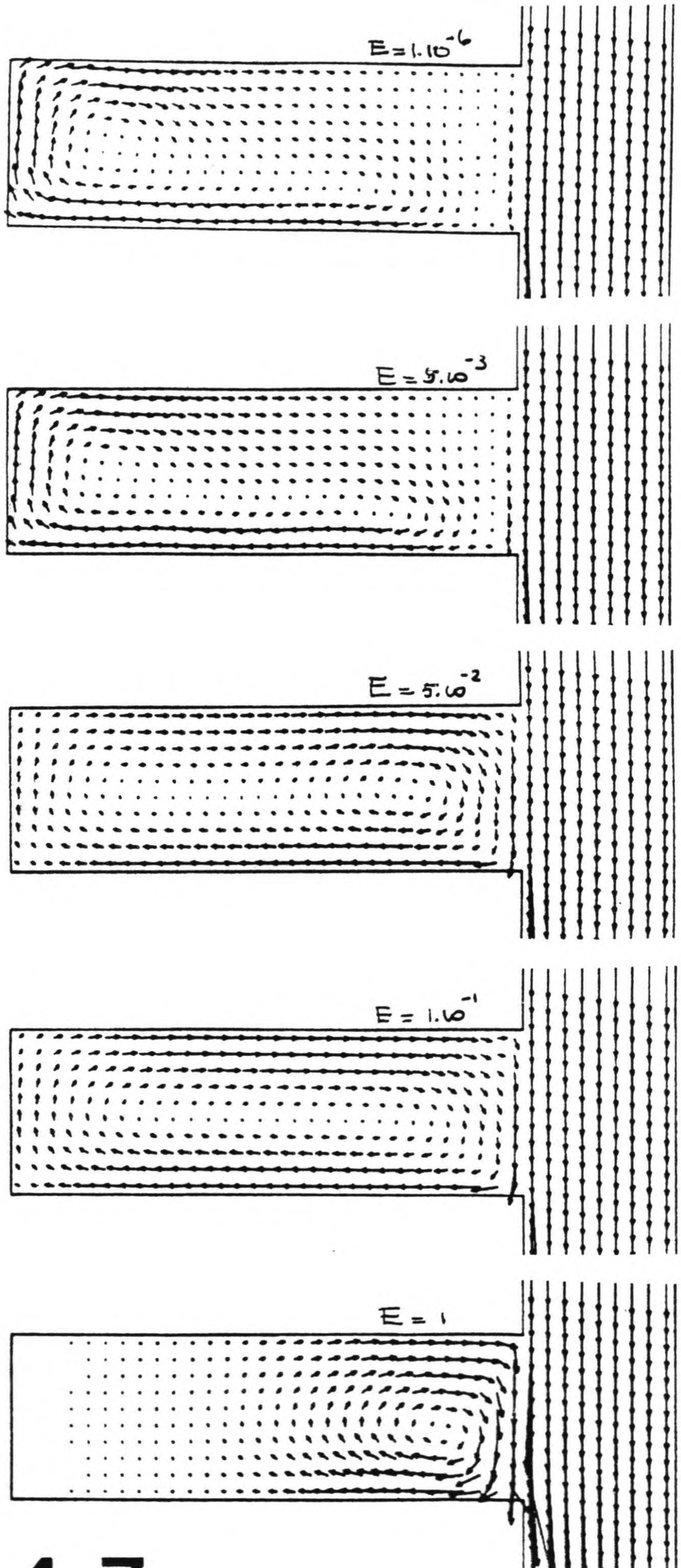

SIMULATIONS

WAQUA, LIT 21

4.7

Influence of viscosity

THE INFLUENCE OF VISCOSITY (see Fig. 4.7)

The viscosity-parameter as schematized in the Duchess-programm, is an artificial "eddy-viscosity", introduced to solve the closure-problem of the depth-averaged-flow (see appendix A). In fact the E-parameter stands for the turbulent viscosity, a parameter to schematize the large scale transfer of momentum as caused by the turbulent (Reynolds) stresses.

As the eddy in this analysis is mainly caused by convection of the main flow, the viscosity-parameter has no direct physical meaning, neither in the function of generating eddies, nor in the function of substituting the Reynolds-stresses. However, the eddy-viscosity does influence the velocity-distribution and the shape of the eddies.

In order to investigate the influence of the viscosity-parameter, different magnitudes of this parameter were used in numerical simulations of the reference lay-out (500 * 500 m). The rest of the parameters were kept constant.

The results of simulations, using E = 1 (m2/s) and E = 10 (m2/s) are shown in Fig. 4.7. It shows that increasing viscosity causes the velocity-distribution to "flatten", and delays the development of eddies. This effect has been observed in Kuipers and Vreugdenhill (lit. (15)) and Stelling and Wang (lit. (16)). The model WAQUA (see Fig. 4.7) is based on the same equations as DUCHESS, it is available from the Delft Hydraulic laboratory. Simulations (source: lit. (21)) with several viscosity parameters show the same tendency as the simulations with DUCHESS.
If the viscosity-parameter of DUCHESS is taken E = 0.04 (m2/s), sometimes two or more eddies develop (see also Fig 4.1 and Fig. 4.6). It seems realistic that several eddies exist if the dimensions of the side-expansion are large.
Altogether it is maybe rather vital that the viscosity-parameter E is schematized in a proper way. Further research will be necessary to determine whether it requires a more extended viscosity-model, or even a three-dimensional model in order to improve the simulation of the velocity-distribution in the eddy.

CONCLUSION:

an increase of the viscosity parameter E causes a smoothening of the velocity-distribution and a suppression of secondary eddies. This influence increases with decreasing mesh-sizes.

It is important that a proper value is taken for this parameter. It seems that an approach as given by eq. 10 forms a reasonable approximation. Measurements on prototypes will have to confirm this approach.

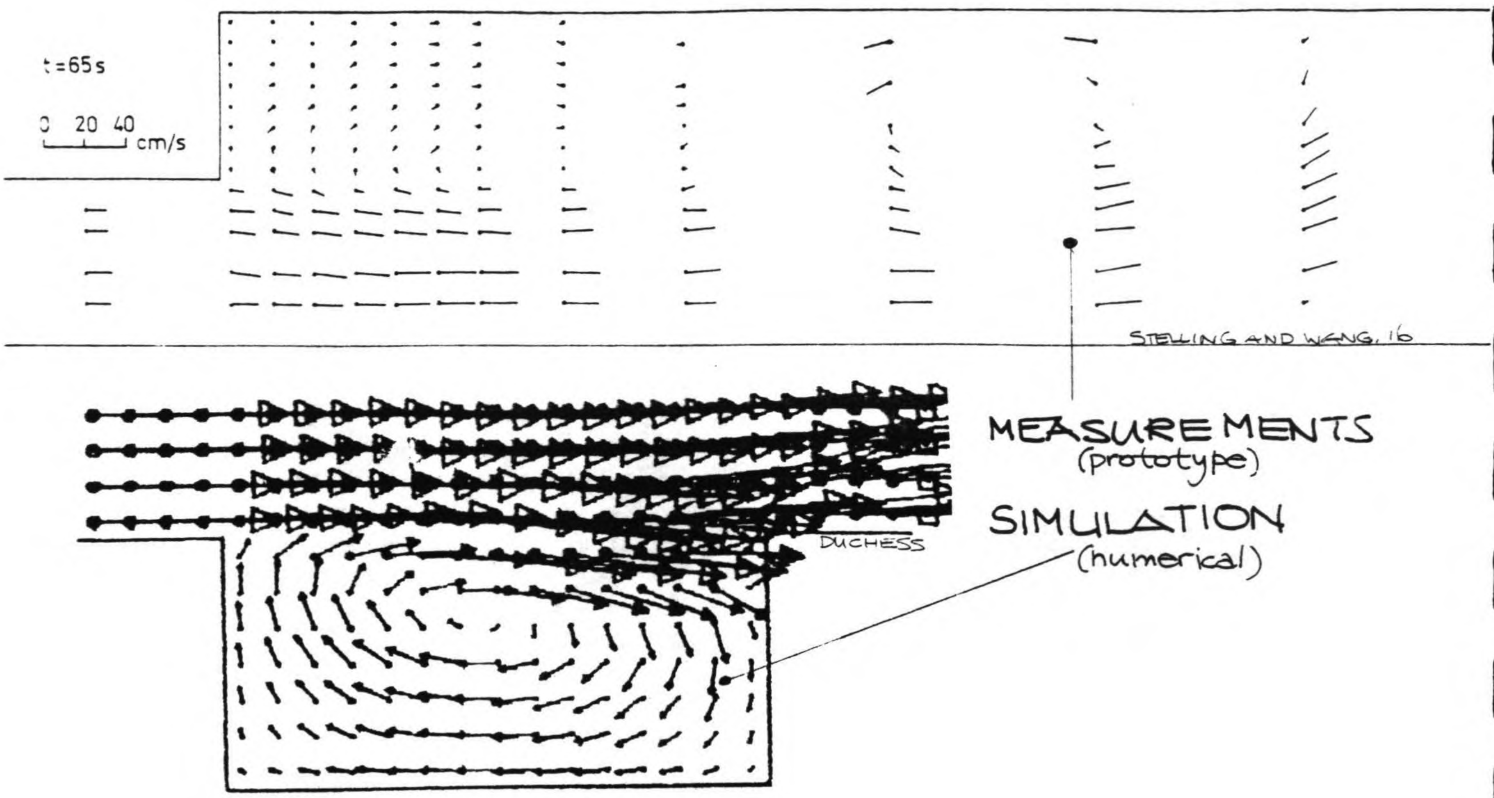

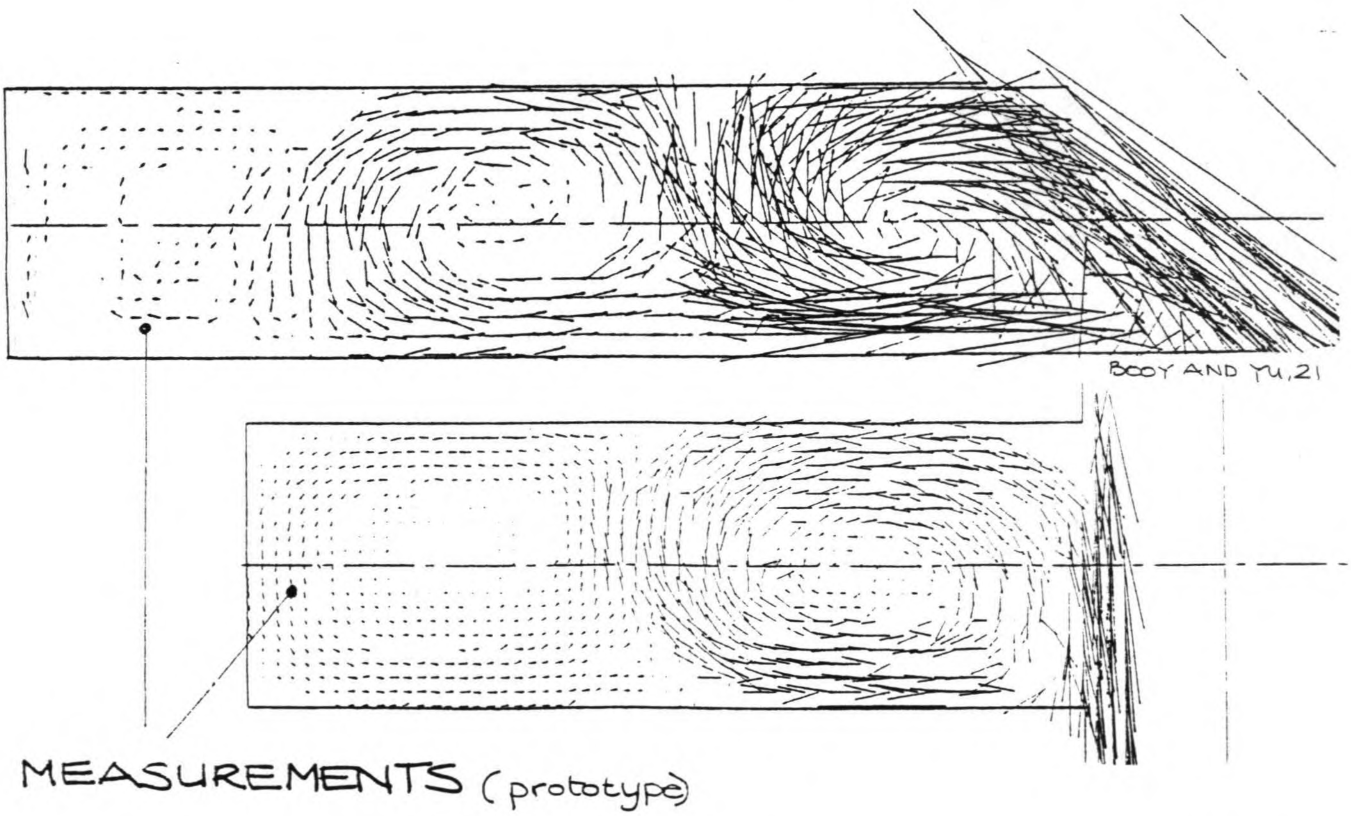

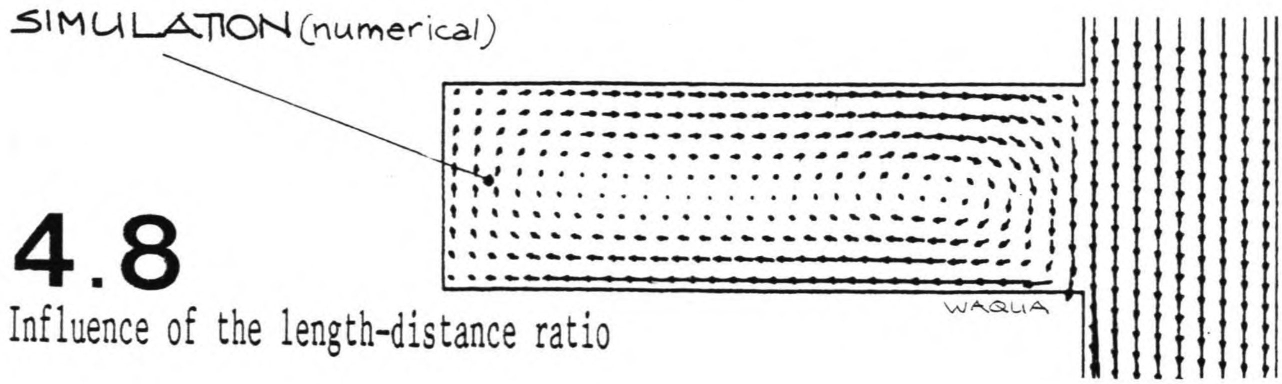

4.8

Influence of the length-distance ratio

INFLUENCE OF THE LENGTH-DISTANCE RATIO (see Fig. 4.8)

In these simulations, the length-to-distance ratio was taken 1:1. One would expect the eddies to change shape when the ratio length-distance varies.
Numerical models (two-dimensional) always reproduce only one, main, eddy (see Fig. 4.8).

From prototype measurements and practice-experiences it is known that eddies tend to take a 1:1-shape. If the basin in which they develop is of an other shape, secondary or even tertiary, eddies develop (see Fig. 4.8). Secondary eddies (this implies eddies with an opposite current direction) develop if the length-distance ratio becomes larger than 2:1 (see Booy and Yu (lit. (21)). Two eddies (of the same direction) develop if the length-distance ratio becomes smaller than 0.5:1, or even in the case 1:1 if the dimensions of the basin (the sideward expansion) are very large (see Fig. 4.1, Fig. 4.6 and Fig. 4.8) (lit.: Stelling and Wang, (16)).

The reason for the discrepancy between the results of numerical simulations and practice could be found in the two-dimensional nature of the model, and the three-dimensional nature of reality. Especially in basins with a length-to-distance ratio of more than 2:1, the influence of secondary flow (see appendix A) which is a typical three-dimensional phenomenon which can't be reproduced by a two-dimensional model, can become large enough to cause the development of secondary eddies as shown in Fig. 4.8.

CONCLUSION:

if the length-to-distance ratio of numerical simulations is considerably different form 1:1, one cannot expect the model to reproduce the realistic eddy-pattern due to the tree-dimensional nature of the eddy-phenomena. In the case of 1:1 ratios the agreement between numerical results and measurement is quite good.

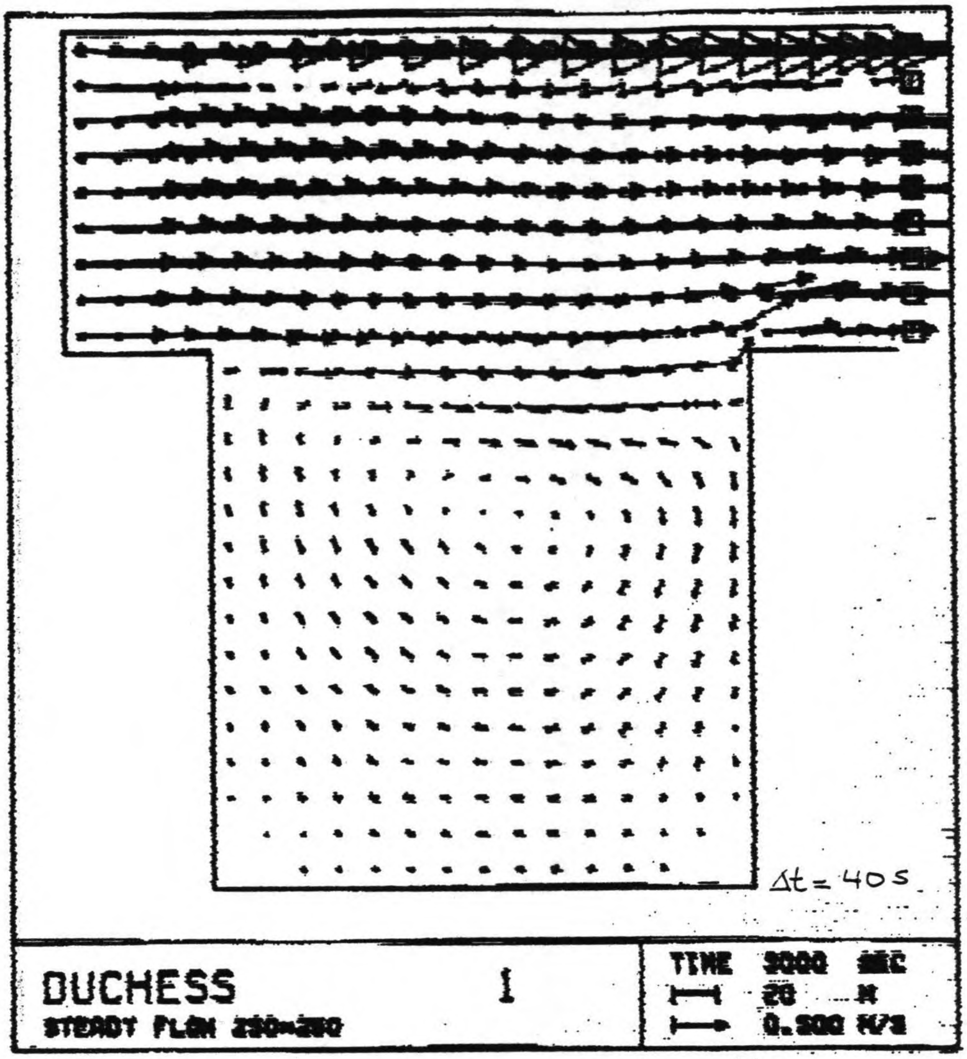

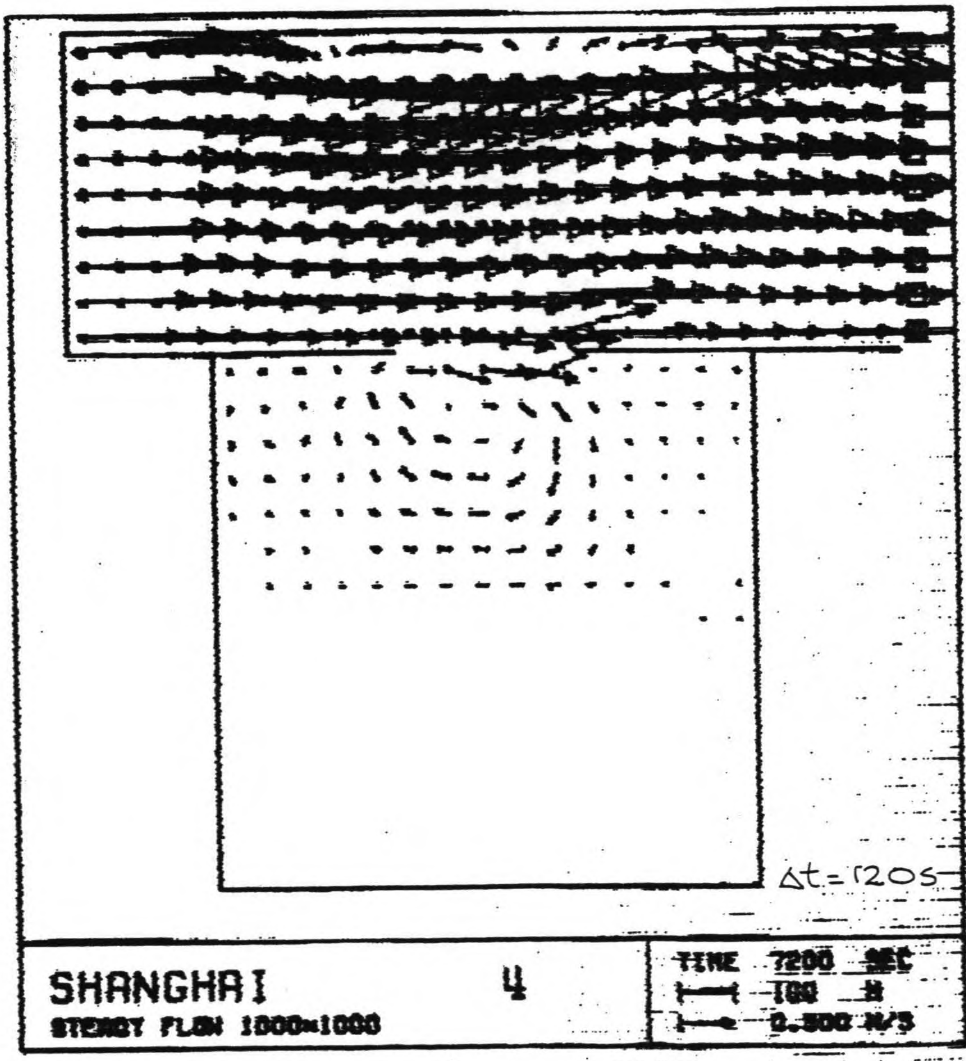

4.9

Influence of the time-step

THE INFLUENCE OF THE TIME STEP (see Fig. 4.9)

In the case of numerical computations, the best way to check the accuracy of the results is to decrease the time-step and to compare the new results with the old ones. In this case, all the time-steps were reduced to half the original value (see page 71). this was due to the fact that for the morphological computations, the original time step was too large (see par. 3.4).
It showed that the results for the flow-velocities were exactly the same.

Also, for the 1,000 * 1,000 plus dam-lay-out', the time-step was doubled. This caused considerable changes in the results, and even instability after T = 7,200 s (see Fig. 4.9).

CONCLUSION:

the time-step found by taking the Courant-numbre $\sigma = 2$ is sufficiently small to ensure the accuracy of the results of the numerical computations. Increasing the time-step causes reduced accuracy and instabilities.

4.2 Sedimentation-pattern

Starting points for the numerical computations of the sedimentation-pattern were the calculations and the results as found in par. 3.4, plus the flowpattern of the tidal flow as found in par. 4.1.

4.2.1. Results

LAY-OUT 250 * 250 m

The results of this simulation, with a length of T = 3,600 s, are shown in Fig. 4.10. The objective of this simulation was to find the time necessary for the initial effects to damp out, and the sedimentation-pattern. In table 4.3 the values in the control-points (see Fig. 4.4) are given.

250 * 250 m	point A	point B	point C	point D
velocity (m/s) bottomlevel (mm) concentration (-)	1.15 +5 378.10^{-6}	0.25 +2 122.10^{-6}	0.05 0 16.10^{-6}	0.30 0 33.10^{-6}
	point E	point F	point G	point H
velocity (m/s) bottomlevel (mm) concentration (-)	0.10 +2 78.10^{-6}	0.21 0 6.10^{-6}	0.26 +5 178.10^{-6}	0.25 +2 91.10^{-6}

Table 4.3: results sediment-concentration at T = 3,600 s of the 250 * 250 lay-out model.

After T = 600 sec the sediment-concentration has "reached" the other end of the model, after T = 1,800 s the concentration of the main flow becomes rather invariable. After T = 3,300 s the concentration of the total model becomes rather invariable (the initial effect has vanished).

The changes of the bottomlevel are also given in Fig. 4.10.

LAY-OUT 500 * 500 m

The results of this simulation, with a length of T = 3,600 s, are shown in Fig. 4.11. The object of this simulation was to find the time necessary for the initial effects to damp out, and of course the sedimentation-pattern. In table 4.4 the values in the controle-points are given:

500 * 500 m	point A	point B	point C	point D
velocity (m/s) bottomlevel (mm) concentration (-)	1.3 +5 438.10^{-6}	0.45 +5 161.10^{-6}	0.21 0 32.10^{-6}	0.15 0 1.10^{-6}
	point E	point F	point G	point H
velocity (m/s) bottomlevel (mm) concentration (-)	0.10 0 88.10^{-6}	0.11 0 3.10^{-6}	0.30 +3 168.10^{-6}	0.33 +1 74.10^{-6}

Table 4.4: results sediment-concentration at T = 3,600 s of the 500 * 500 lay-out model.

After T = 600 s the sediment concentration has "reached" the other end of the model and after T = 2,100 s. The value of this concentration in the main flow becomes more or less stable. Inside the basin the sediment-concentration becomes rather invariable at the most interesting parts after T = 2,700 s.

The changes of the bottomlevel are also shown in Fig. 4.11. It is obvious that sedimentation does not occur in the total basin. The estimated adaption-length inside the basin (eddy) is about 200 m and the adaption-time 300 s (this implies the time and length the average concentration needs to adapt to the new concentration profile; inside the eddy, flow velocities decrease and the sediments will settle). Since the total size of the basin is 500 x 500 m, sedimentation will occur in only a part of the basin.

LAY-OUT 1,000 * 1,000 m

The results of this simulation, with a length of T = 3,600 s and 7,200 s, are shown in Fig. 4.12. The objective of this simulation was to find the time necessary for the initial effects to damp out, and the sedimentation-pattern. In table 4.5 the values of the results of the simulation in the control-points are given:

1,000 * 1,000 m	point A	point B	point C	point D
velocity (m/s) bottomlevel (mm) concentration (-)	1.60 +6 541.10^{-6}	0.70 +7 285.10^{-6}	0.22 0 19.10^{-6}	0.10 0 0
	point E	point F	point G	point H
velocity (m/s) bottomlevel (mm) concentration (-)	0.12 +4 103.10^{-6}	0.11 0 5.10^{-6}	0.45 0 81.10^{-6}	0.14 0 1.10^{-6}

Table 4.5: results sediment-concentration at T = 3,600 s of the 1,000 * 1,000 lay-out model.

After T $\simeq$ 900 s the sediment-concentration has "reached" the other end of the model and in the main flow the sediment-concentration becomes stable after T = 2,200 s. Inside the basin the concentration in the most interesting parts becomes stable after T = 2,800 s.

The changes of the bottom-level are also shown in Fig. 4.12A and 4.12B. Also a computation has been made with a total length of T = 7,200 s. It shows that the total sedimentation is doubled after this time (the sedimentation is nearly proportional to time). It also shows that a large part of the basin is useless with respect to sedimentation.

LAY-OUT 1,000 * 1,000 m PLUS DAM

The results of the simulations, with a length of T = 3,600 s and T = 7,200 s, are shown in Fig. 4.13. The objective of this simulation was to find the sedimentation-pattern and the time necessary for the initial effects to vanish. In table 4.6 an overview is given of the results in the control-points:

1,000 * 1,000 m plus dam	point A	point B	point C	point D
velocity (m/s) bottomlevel (mm) concentration (-)	1.60 +2 569.10^{-6}	0.30 +3 148.10^{-6}	0.25 0 5.10^{-6}	0.10 0 0
	point E	point F	point G	point H
velocity (m/s) bottomlevel (mm) concentration (-)	0.05 0 47.10^{-6}	0.06 0 0	0.22 +1 147.10^{-6}	0.25 0 5.10^{-6}

Table 4.6: results sediment-concentration at T = 3,600 s for the 1,000 * 1,000 plus dam lay-out model.

After T $\simeq$ 900 s the sediment-concentration "reaches" the other end of the model, and the magnitude of the concentration in the main flow becomes stable after T = 2,600 s. Inside the basin this is the case already after 1,800 s.

The changes of the bottom-level are also shown in Fig. 4.13A and Fig. 4.13B. Again a large part of the basin is not useful for sedimentation. Calculations (see page 89) show that the total amount of sediment which has accreted, is comparable to the amount of sediment that would have been carried into the basin by storage.
It seems logical that the smaller the openings, the less the advantageous influence of the eddy-developing becomes, and the more the total amount of sedimentation equals the magnitude of the "storage"-contribution.

MORPHOR DELFT UNIVERSITY OF TECHNOLOGY PROJECT: SHANGHAI RUN: 4
250*250 MET SEDIMENT
TIME= 0. SEC

VARIABLE: CS UNIT: 0.1000E-05

	1	2	3	4	5	6	7	8	9	10	11	12	13	14	15	16	17	18	19	20	21	22	23	24	25
1	[illegible]																								
4	[illegible]																								
7	[illegible]																								
10	[illegible]																								
13	[illegible]																								
16	[illegible]																								
19	[illegible]																								
22	[illegible]																								
25	[illegible]																								

MORPHOR DELFT UNIVERSITY OF TECHNOLOGY PROJECT: SHANGHAI RUN: 4
250*250 MET SEDIMENT
TIME= 600. SEC

VARIABLE: CS UNIT: 0.1000E-05

	1	2	3	4	5	6	7	8	9	10	11	12	13	14	15	16	17	18	19	20	21	22	23	24	25
1	[illegible]																								
4	[illegible]																								
7	[illegible]																								
10	[illegible]																								
13	[illegible]																								
16	[illegible]																								
19	[illegible]																								
22	[illegible]																								
25	[illegible]																								

MORPHOR DELFT UNIVERSITY OF TECHNOLOGY PROJECT: SHANGHAI RUN: 4
250*250 MET SEDIMENT
TIME= 1200. SEC

VARIABLE: CS UNIT: 0.1000E-05

	1	2	3	4	5	6	7	8	9	10	11	12	13	14	15	16	17	18	19	20	21	22	23	24	25
1	[illegible]																								
4	[illegible]																								
7	[illegible]																								
10	[illegible]																								
13	[illegible]																								
16	[illegible]																								
19	[illegible]																								
22	[illegible]																								
25	[illegible]																								

MORPHOR DELFT UNIVERSITY OF TECHNOLOGY PROJECT: SHANGHAI RUN: 4
250*250 MET SEDIMENT
TIME= 1800. SEC

VARIABLE: CS UNIT: 0.1000E-05

	1	2	3	4	5	6	7	8	9	10	11	12	13	14	15	16	17	18	19	20	21	22	23	24	25
1	[illegible]																								
4	[illegible]																								
7	[illegible]																								
10	[illegible]																								
13	[illegible]																								
16	[illegible]																								
19	[illegible]																								
22	[illegible]																								
25	[illegible]																								

MORPHOR DELFT UNIVERSITY OF TECHNOLOGY PROJECT: SHANGHAI RUN: 4
250*250 MET SEDIMENT
TIME= 2400. SEC

VARIABLE: CS UNIT: 0.1000E-05

	1	2	3	4	5	6	7	8	9	10	11	12	13	14	15	16	17	18	19	20	21	22	23	24	25
1	[illegible]																								
4	[illegible]																								
7	[illegible]																								
10	[illegible]																								
13	[illegible]																								
16	[illegible]																								
19	[illegible]																								
22	[illegible]																								
25	[illegible]																								

MORPHOR DELFT UNIVERSITY OF TECHNOLOGY PROJECT: SHANGHAI RUN: 4
250*250 MET SEDIMENT
TIME= 3000. SEC

VARIABLE: CS UNIT: 0.1000E-05

	1	2	3	4	5	6	7	8	9	10	11	12	13	14	15	16	17	18	19	20	21	22	23	24	25
1	[illegible]																								
4	[illegible]																								
7	[illegible]																								
10	[illegible]																								
13	[illegible]																								
16	[illegible]																								
19	[illegible]																								
22	[illegible]																								
25	[illegible]																								

MORPHOR DELFT UNIVERSITY OF TECHNOLOGY PROJECT: SHANGHAI RUN: 4
250*250 MET SEDIMENT
TIME= 3600. SEC

VARIABLE: CS UNIT: 0.1000E-05

	1	2	3	4	5	6	7	8	9	10	11	12	13	14	15	16	17	18	19	20	21	22	23	24	25
1	[illegible]																								
4	[illegible]																								
7	[illegible]																								
10	[illegible]																								
13	[illegible]																								
16	[illegible]																								
19	[illegible]																								
22	[illegible]																								
25	[illegible]																								

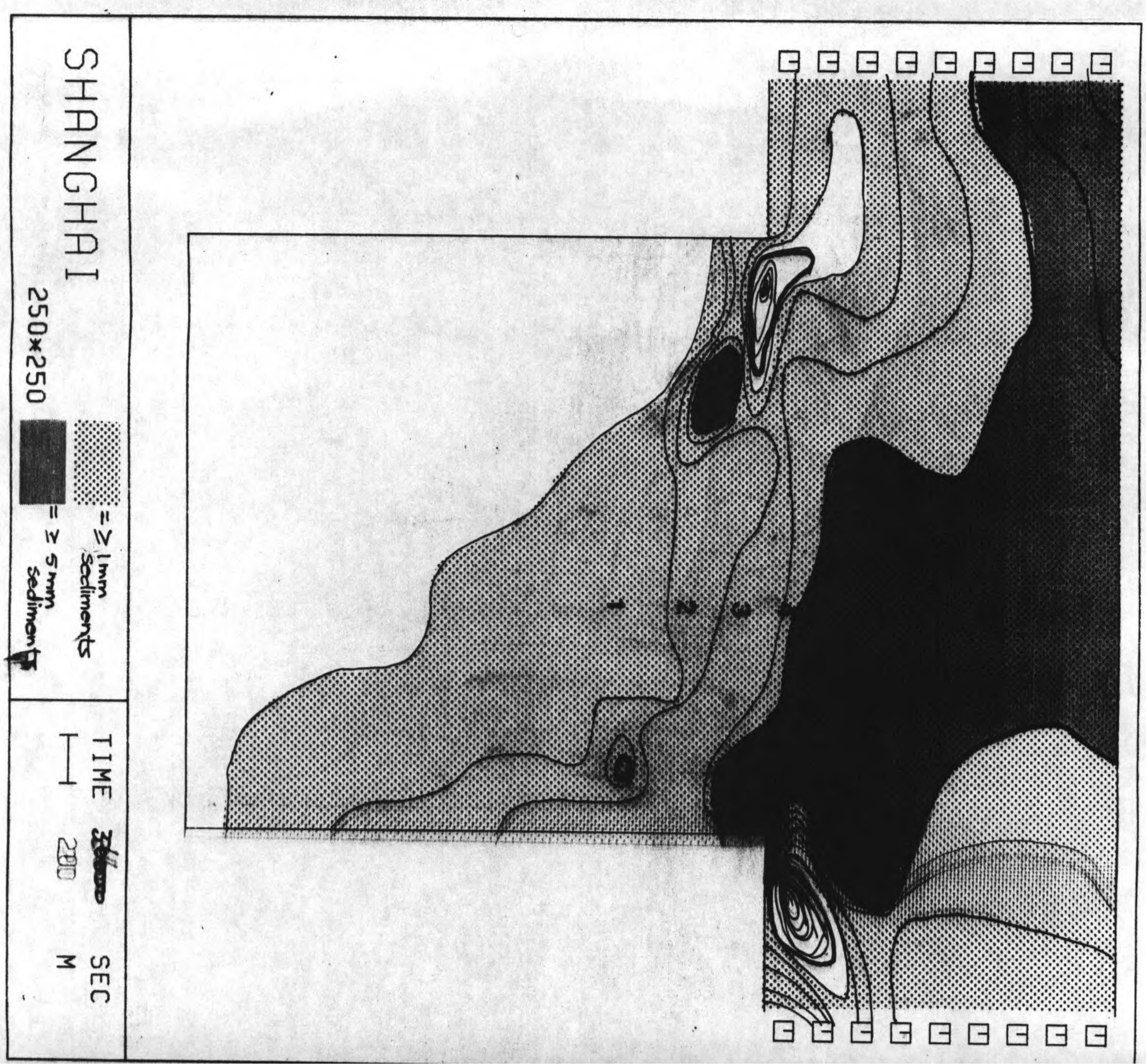

4.10
Results sedimentation 250 × 250 m lay-out

MORPHOR DELFT UNIVERSITY OF TECHNOLOGY PROJECT: SHANGHAI RUN: 4
500*500 PET SEDIMENT
TIME= 0. SEC

VARIABLE: CS UNIT: 0.1000E-05

Columns 1 2 3 4 5 6 7 8 9 10 11 12 13 14 15 16 17 18 19 20 21 22 23 24 25; rows 1 4 7 10 13 16 19 22 25

[illegible]

MORPHOR DELFT UNIVERSITY OF TECHNOLOGY PROJECT: SHANGHAI RUN: 4
500*500 PET SEDIMENT
TIME= 600. SEC

VARIABLE: CS UNIT: 0.1000E-05

Columns 1 2 3 4 5 6 7 8 9 10 11 12 13 14 15 16 17 18 19 20 21 22 23 24 25; rows 1 4 7 10 13 16 19 22 25

[illegible]

MORPHOR DELFT UNIVERSITY OF TECHNOLOGY PROJECT: SHANGHAI RUN: 4
500*500 PET SEDIMENT
TIME= 1200. SEC

VARIABLE: CS UNIT: 0.1000E-05

Columns 1 2 3 4 5 6 7 8 9 10 11 12 13 14 15 16 17 18 19 20 21 22 23 24 25; rows 1 4 7 10 13 16 19 22 25

[illegible]

MORPHOR DELFT UNIVERSITY OF TECHNOLOGY PROJECT: SHANGHAI RUN: 4
500*500 PET SEDIMENT
TIME= 1800. SEC

VARIABLE: CS UNIT: 0.1000E-05

Columns 1 2 3 4 5 6 7 8 9 10 11 12 13 14 15 16 17 18 19 20 21 22 23 24 25; rows 1 4 7 10 13 16 19 22 25

[illegible]

MORPHOR DELFT UNIVERSITY OF TECHNOLOGY PROJECT: SHANGHAI RUN: 4
500*500 PET SEDIMENT
TIME= 2400. SEC

VARIABLE: CS UNIT: 0.1000E-05

Columns 1 2 3 4 5 6 7 8 9 10 11 12 13 14 15 16 17 18 19 20 21 22 23 24 25; rows 1 4 7 10 13 16 19 22 25

[illegible]

MORPHOR DELFT UNIVERSITY OF TECHNOLOGY PROJECT: SHANGHAI RUN: 4
500*500 PET SEDIMENT
TIME= 3000. SEC

VARIABLE: CS UNIT: 0.1000E-05

Columns 1 2 3 4 5 6 7 8 9 10 11 12 13 14 15 16 17 18 19 20 21 22 23 24 25; rows 1 4 7 10 13 16 19 22 25

[illegible]

MORPHOR DELFT UNIVERSITY OF TECHNOLOGY PROJECT: SHANGHAI RUN: 4
500*500 PET SEDIMENT
TIME= 3600. SEC

VARIABLE: CS UNIT: 0.1000E-05

Columns 1 2 3 4 5 6 7 8 9 10 11 12 13 14 15 16 17 18 19 20 21 22 23 24 25; rows 1 4 7 10 13 16 19 22 25

[illegible]

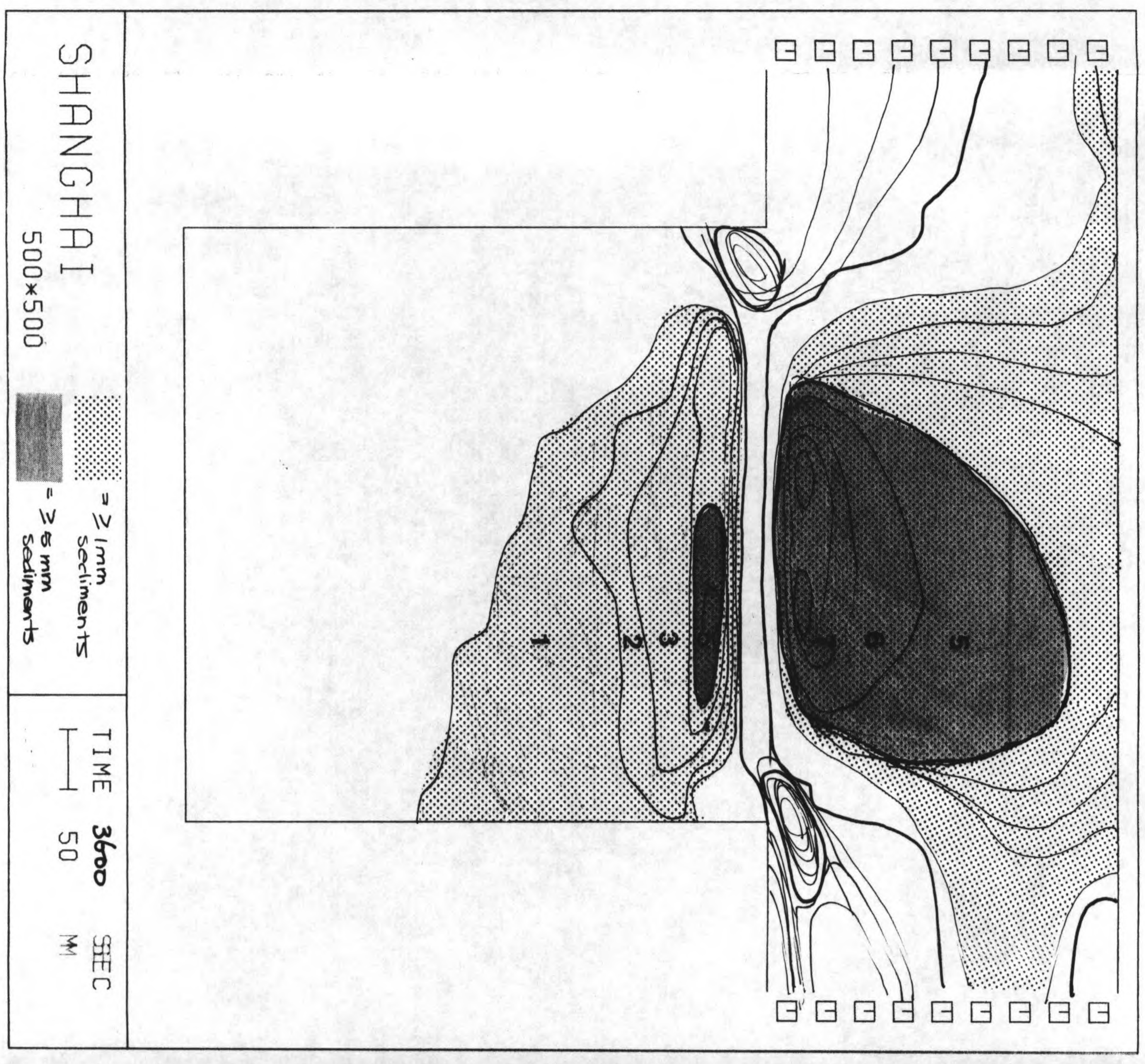

4.11

Results sedimentation 500 * 500 m lay-out

MORPHOR DELFT UNIVERSITY OF TECHNOLOGY PROJECT: SHANGHAI RUN: 4
1000*1000 MET SEDIMENT
TIME= 0. SEC
VARIABLE: CS UNIT: 0.1000E-05

MORPHOR DELFT UNIVERSITY OF TECHNOLOGY PROJECT: SHANGHAI RUN: 4
1000*1000 MET SEDIMENT
TIME= 600. SEC
VARIABLE: CS UNIT: 0.1000E-05

MORPHOR DELFT UNIVERSITY OF TECHNOLOGY PROJECT: SHANGHAI RUN: 4
1000*1000 MET SEDIMENT
TIME= 1200. SEC
VARIABLE: CS UNIT: 0.1000E-05

MORPHOR DELFT UNIVERSITY OF TECHNOLOGY PROJECT: SHANGHAI RUN: 4
1000*1000 MET SEDIMENT
TIME= 1800. SEC
VARIABLE: CS UNIT: 0.1000E-05

MORPHOR DELFT UNIVERSITY OF TECHNOLOGY PROJECT: SHANGHAI RUN: 4
1000*1000 MET SEDIMENT
TIME= 2400. SEC
VARIABLE: CS UNIT: 0.1000E-05

MORPHOR DELFT UNIVERSITY OF TECHNOLOGY PROJECT: SHANGHAI RUN: 4
1000*1000 MET SEDIMENT
TIME= 3000. SEC
VARIABLE: CS UNIT: 0.1000E-05

MORPHOR DELFT UNIVERSITY OF TECHNOLOGY PROJECT: SHANGHAI RUN: 4
1000*1000 MET SEDIMENT
TIME= 3600. SEC
VARIABLE: CS UNIT: 0.1000E-05

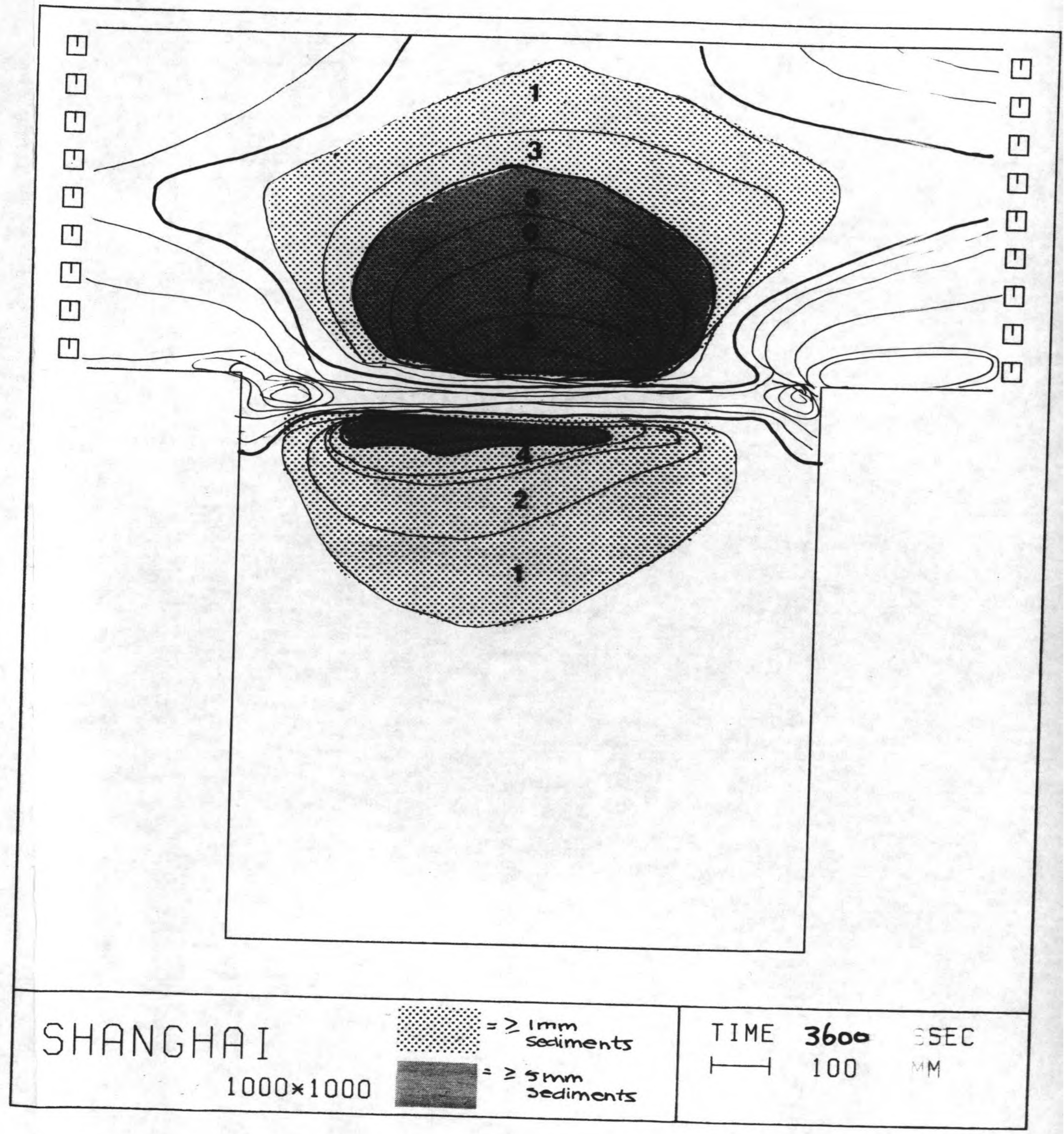

4.12a

Results sedimentation 1,000 * 1,000 m² lay-out

MORPHOR DELFT UNIVERSITY OF TECHNOLOGY PROJECT: SHANGHAI RUN: 4
1000*1000 MET SEDIMENT
TIME= 4200. SEC

VARIABLE: CS UNIT: 0.1000E-05

	1	2	3	4	5	6	7	8	9	10	11	12	13	14	15	16	17	18	19	20	21	22	23	24	25
1																									
						C	C	0	0	0	0	0	0	0	0	0	0	0	0	0					
						C	0	0	0	0	0	0	0	0	0	0	0	0	0	0					
4						C	0	0	0	0	0	0	0	0	0	0	0	0	0	0					
						C	0	0	0	0	1	1	0	0	0	0	0	0	0	0					
						C	0	1	1	1	2	2	2	1	1	1	1	0	0	0					
7						1	1	2	3	4	5	5	5	4	3	2	2	1	1	0					
						[illegible]	3	5	8	10	12	13	12	11	9	7	4	3	2	1					
						4	6	11	16	21	25	27	26	24	20	15	11	7	4	2					
10						7	13	21	31	40	46	49	48	44	38	30	22	14	8	5					
						12	21	35	51	65	75	79	78	72	63	52	40	27	15	9					
						17	30	51	76	96	109	114	113	106	94	80	63	45	27	14					
13						22	38	66	100	128	145	152	151	143	130	112	92	68	43	23					
						31	47	80	129	166	190	200	200	190	173	152	126	96	65	37					
						69	94	141	196	238	265	275	272	257	235	206	172	134	93	51					
16						222	256	299	345	380	396	394	379	354	325	288	251	202	159	108					
	377	412	443	470	502	524	542	551	550	537	515	488	457	425	393	360	328	286	256	249	278	279	266	252	240
	377	410	439	465	490	511	525	530	527	518	504	486	467	445	424	400	377	352	333	325	343	361	369	371	373
19	377	409	437	463	485	504	518	526	529	527	520	511	499	485	471	455	439	422	409	400	405	415	425	431	437
	377	408	435	459	481	499	513	523	528	530	529	524	518	510	501	491	481	472	465	460	461	466	472	477	483
	377	405	431	454	474	491	505	516	524	529	531	531	529	525	521	516	511	506	503	502	504	507	512	517	522
22	377	402	425	446	465	481	496	507	516	523	527	530	531	531	529	528	526	525	525	526	528	532	537	543	549
	377	401	424	444	462	478	492	504	513	521	526	530	533	534	535	535	535	536	537	539	543	547	553	558	565
	377	400	421	440	458	472	487	499	509	517	523	528	531	534	536	537	539	540	542	546	549	555	559	567	572
25	377	398	418	436	452	467	481	492	502	510	517	523	527	531	534	536	539	541	544	548	553	558	563	569	575

MORPHOR DELFT UNIVERSITY OF TECHNOLOGY PROJECT: SHANGHAI RUN: 4
1000*1000 MET SEDIMENT
TIME= 4800. SEC

VARIABLE: CS UNIT: 0.1000E-05

	1	2	3	4	5	6	7	8	9	10	11	12	13	14	15	16	17	18	19	20	21	22	23	24	25
1																									
						C	0	0	0	0	0	0	0	0	0	0	0	0	0	0					
						C	0	0	0	0	0	0	0	0	0	0	0	0	0	0					
4						C	0	0	0	0	0	0	0	0	0	0	0	0	0	0					
						C	0	0	1	1	1	1	1	1	1	0	0	0	0	0					
						C	1	1	2	2	2	3	3	2	2	2	1	1	0	0					
7						1	2	3	4	5	6	7	7	6	5	4	3	2	1	1					
						2	3	6	8	11	14	15	15	14	12	9	7	5	3	2					
						4	7	11	17	22	26	29	29	27	24	19	15	10	6	4					
10						7	12	20	29	38	45	49	50	47	42	35	27	19	12	8					
						11	19	31	46	59	70	75	77	73	66	57	45	33	21	13					
						15	26	43	65	84	99	106	108	104	95	83	69	52	34	20					
13						20	32	54	83	111	130	140	142	137	127	113	96	74	50	29					
						30	42	68	108	144	170	183	186	180	168	150	128	101	72	44					
						69	89	125	172	211	239	252	253	243	226	201	171	137	98	58					
16						216	242	276	314	345	364	367	357	337	312	280	246	201	160	109					
	377	404	427	449	473	490	504	512	512	503	486	463	437	409	380	349	320	280	252	241	269	270	259	246	234
	377	402	425	446	467	485	496	500	498	490	478	463	446	427	407	385	364	341	323	314	331	347	354	355	357
19	377	402	425	446	465	481	492	499	501	500	494	486	476	464	450	436	421	406	394	385	389	398	406	412	418
	377	402	424	444	462	478	490	498	503	505	504	500	495	487	479	471	462	453	446	442	443	447	452	457	463
	377	400	421	441	458	473	485	494	501	506	508	507	506	503	499	494	490	486	483	482	483	486	491	496	501
22	377	398	417	435	451	465	478	488	496	502	506	508	509	509	508	507	505	504	504	506	508	512	517	522	528
	377	397	416	434	449	463	475	486	494	501	506	510	512	513	514	514	515	516	517	520	523	528	532	539	543
	377	396	414	431	446	460	472	482	491	498	504	508	512	514	516	518	519	521	524	527	531	535	542	545	555
25	377	395	411	427	441	454	466	476	485	493	499	504	509	512	515	517	520	523	526	530	534	539	543	551	554

MORPHOR DELFT UNIVERSITY OF TECHNOLOGY PROJECT: SHANGHAI RUN: 4
1000*1000 MET SEDIMENT
TIME= 5400. SEC

VARIABLE: CS UNIT: 0.1000E-05

	1	2	3	4	5	6	7	8	9	10	11	12	13	14	15	16	17	18	19	20	21	22	23	24	25
1																									
						C	0	0	0	0	0	0	0	0	0	0	0	0	0	0					
						C	0	0	0	0	0	0	0	0	0	0	0	0	0	0					
4						C	0	0	0	0	0	0	0	0	0	0	0	0	0	0					
						C	0	0	1	1	1	1	1	1	1	1	1	0	0	0					
						1	1	1	2	2	3	3	3	3	3	2	2	1	1	1					
7						1	2	3	4	5	7	7	8	7	6	5	4	3	2	2					
						2	3	6	8	11	13	15	16	15	13	11	9	7	5	4					
						4	6	10	15	20	25	27	29	28	25	21	17	13	9	7					
10						7	11	18	26	34	41	45	47	46	43	37	30	23	16	11					
						10	16	26	39	51	62	69	71	70	65	57	48	37	25	18					
						13	21	36	54	72	86	95	99	97	91	82	69	55	38	25					
13						17	27	44	67	92	112	124	128	127	120	109	94	76	54	34					
						28	36	56	86	119	144	160	166	164	156	142	124	100	75	49					
						66	81	105	144	179	205	221	226	221	209	189	164	134	99	62					
16						201	222	246	275	303	322	328	324	310	290	263	233	193	156	107					
	377	395	410	425	443	453	461	466	465	459	446	428	406	382	357	329	303	267	241	227	252	253	243	232	222
	377	394	409	424	439	453	460	462	460	454	443	430	415	398	381	361	343	321	305	295	308	322	329	330	332
19	377	395	412	427	441	453	461	466	467	465	460	453	443	433	421	408	395	380	369	361	364	372	379	384	389
	377	395	412	427	441	452	461	468	471	472	471	467	462	456	448	440	432	425	418	414	415	418	422	427	432
	377	395	411	425	439	450	460	467	472	475	476	476	474	471	467	463	459	456	453	452	453	456	459	463	468
22	377	393	408	422	434	445	455	463	469	474	477	478	479	478	478	476	475	474	474	475	477	480	484	489	495
	377	393	408	421	434	445	454	463	469	474	478	481	483	484	484	484	485	485	486	489	491	496	500	506	511
	377	392	406	419	431	442	452	460	467	473	477	481	483	485	487	488	490	491	493	496	500	503	509	514	520
25	377	391	404	416	428	438	447	456	463	469	474	478	481	484	486	488	490	493	496	499	503	508	512	518	523

MORPHOR DELFT UNIVERSITY OF TECHNOLOGY PROJECT: SHANGHAI RUN: 4
1000*1000 MET SEDIMENT
TIME= 6000. SEC

VARIABLE: CS UNIT: 0.1000E-05

	1	2	3	4	5	6	7	8	9	10	11	12	13	14	15	16	17	18	19	20	21	22	23	24	25
1																									
						C	0	0	0	0	0	0	0	0	0	0	0	0	0	0					
						C	0	0	0	0	0	0	0	0	0	0	0	0	0	0					
4						C	0	0	0	0	0	1	1	1	0	0	0	0	0	0					
						C	0	1	1	1	1	1	1	1	1	1	1	1	0	0					
						1	1	1	2	3	3	3	4	3	3	3	2	2	1	1					
7						1	2	3	4	5	7	7	8	8	7	6	5	4	3	2					
						[illegible]	3	5	8	10	13	14	15	15	14	12	10	8	6	5					
						4	6	9	14	18	22	25	27	27	25	22	19	15	11	9					
10						6	9	15	22	29	36	41	43	43	41	37	31	25	19	14					
						9	14	22	32	43	53	60	64	64	61	55	48	38	28	21					
						11	18	29	43	58	73	82	88	88	85	78	68	55	41	30					
13						15	22	35	52	72	93	106	112	114	110	102	90	75	56	39					
						26	32	46	67	95	119	136	145	146	141	131	116	97	75	53					
						64	75	93	122	151	175	191	198	197	188	173	153	127	97	64					
16						189	206	223	244	266	282	290	289	279	264	242	216	181	148	103					
	377	385	393	401	413	417	421	423	421	415	404	390	372	351	330	306	282	250	226	211	233	235	227	217	208
	377	386	395	404	413	421	425	425	422	416	407	395	382	367	352	335	318	299	284	273	285	296	302	303	305
19	377	388	398	408	416	424	429	432	432	429	424	417	409	399	389	377	365	352	342	334	335	342	347	352	356
	377	389	400	410	419	427	432	436	438	438	436	432	428	422	415	408	400	393	387	382	382	385	388	392	396
	377	389	400	410	419	427	433	438	441	443	443	442	440	437	434	430	426	422	419	418	418	420	423	427	431
22	377	388	398	408	417	424	431	437	441	444	446	447	446	446	444	443	441	440	439	440	442	444	447	452	456
	377	388	399	408	417	425	432	438	442	446	449	450	451	451	451	451	451	451	452	454	456	459	463	467	472
	377	388	398	407	416	424	431	437	442	446	449	451	453	454	455	456	456	457	459	461	464	467	471	476	481
25	377	387	396	405	413	420	427	433	438	443	446	449	452	453	455	456	458	460	462	464	468	471	475	480	485

MORPHOR DELFT UNIVERSITY OF TECHNOLOGY PROJECT: SHANGHAI RUN: 4
1000*1000 MET SEDIMENT
TIME= 6600. SEC

VARIABLE: CS UNIT: 0.1000E-05

	1	2	3	4	5	6	7	8	9	10	11	12	13	14	15	16	17	18	19	20	21	22	23	24	25
1																									
						C	0	0	0	0	0	0	0	0	0	0	0	0	0	0					
						C	0	0	0	0	0	0	0	0	0	0	0	0	0	0					
4						C	0	0	0	0	1	1	1	1	1	0	0	0	0	0					
						C	0	1	1	1	1	1	2	2	1	1	1	1	1	1					
						1	1	1	2	2	3	3	4	4	3	3	3	2	2	2					
7						1	2	3	4	5	6	7	8	8	7	7	6	5	4	3					
						2	3	5	7	9	11	13	14	14	14	13	11	9	8	7					
						3	5	8	12	16	19	22	24	25	24	22	19	16	13	11					
10						5	8	13	18	24	30	35	38	39	38	35	31	26	21	17					
						7	11	18	26	35	44	51	56	57	56	52	46	38	30	25					
						10	14	23	34	46	59	69	75	78	76	71	64	54	42	33					
13						14	19	28	41	54	74	88	96	99	98	92	84	71	56	43					
						24	29	39	55	77	98	114	123	127	125	118	106	91	73	55					
						61	71	85	107	130	150	163	171	172	167	155	139	118	93	65					
16						175	190	203	218	233	247	254	254	247	236	217	197	166	138	97					
	377	377	377	379	384	383	383	381	378	372	363	350	335	317	299	278	258	230	208	193	211	213	207	198	191
	377	378	380	383	387	390	391	369	385	378	369	359	347	334	320	305	290	273	259	249	258	267	272	273	274
19	377	381	385	389	393	396	398	398	396	393	387	381	373	364	354	343	333	321	311	304	305	309	314	317	321
	377	382	388	393	397	401	404	405	405	403	401	396	391	385	379	372	365	358	352	348	347	349	352	354	358
	377	383	389	394	399	404	407	409	410	410	409	407	405	401	397	393	389	386	382	381	381	382	384	387	390
22	377	383	388	394	399	403	407	410	412	413	414	413	412	411	409	407	405	403	402	402	403	405	407	410	414
	377	383	389	395	400	405	409	412	415	416	418	418	418	417	416	415	415	414	414	415	417	419	422	426	430
	377	383	389	395	400	405	409	412	415	417	419	420	420	420	420	420	420	421	422	423	425	428	431	435	438
25	377	382	388	393	398	402	406	410	413	415	417	419	420	421	421	422	422	423	425	427	429	432	435	439	442

MORPHOR DELFT UNIVERSITY OF TECHNOLOGY PROJECT: SHANGHAI RUN: 4
1000*1000 MET SEDIMENT
TIME= 7200. SEC

VARIABLE: CS UNIT: 0.1000E-05

	1	2	3	4	5	6	7	8	9	10	11	12	13	14	15	16	17	18	19	20	21	22	23	24	25
1																									
						C	0	0	0	0	0	0	0	0	0	0	0	0	0	0					
						C	0	0	0	0	0	0	0	0	0	0	0	0	0	0					
4						C	0	0	0	0	1	1	1	1	1	1	0	0	0	0					
						C	0	1	1	1	1	1	2	2	2	1	1	1	1	1					
						1	1	1	2	2	3	3	3	4	3	3	3	3	2	2					
7						1	1	2	3	4	5	6	7	7	7	7	6	5	5	4					
						[illegible]	3	4	6	8	10	11	13	13	13	12	11	10	9	8					
						3	4	7	10	13	16	19	21	22	22	21	19	17	14	13					
10						4	7	10	15	20	25	30	33	34	34	32	29	26	22	19					
						6	9	14	21	28	36	42	47	50	49	47	43	37	31	27					
						8	12	18	27	36	47	57	63	67	67	64	58	51	42	35					
13						12	16	23	32	43	59	72	80	85	85	82	75	66	54	45					
						23	27	34	47	63	81	95	104	108	108	103	95	83	69	55					
						57	66	78	94	112	128	139	146	148	145	136	123	106	86	63					
16						160	173	182	193	204	214	219	220	215	207	192	175	149	125	90					
	377	368	362	357	356	349	345	341	336	329	321	310	297	282	267	249	232	207	188	173	188	190	185	178	172
	377	371	366	363	362	360	358	354	348	340	332	322	311	300	287	274	261	245	233	223	229	237	241	241	242
19	377	374	372	371	370	369	368	365	361	356	350	344	336	327	318	309	299	288	279	272	272	275	278	281	284
	377	376	376	376	375	376	375	374	372	369	365	360	355	349	342	336	329	322	317	312	311	312	313	315	318
	377	377	378	379	380	380	381	380	379	377	375	372	369	365	360	356	352	348	345	343	342	342	344	345	348
22	377	378	379	380	381	382	383	383	383	382	381	379	377	375	372	370	367	365	364	363	363	364	366	368	371
	377	378	380	382	383	384	386	386	386	386	386	385	383	382	380	379	377	376	375	376	376	378	380	383	385
	377	379	380	382	384	385	386	387	388	388	388	387	387	386	385	384	383	383	383	383	384	386	388	391	394
25	377	378	380	381	382	384	385	386	387	387	387	387	387	387	386	386	386	386	386	387	389	391	393	395	398

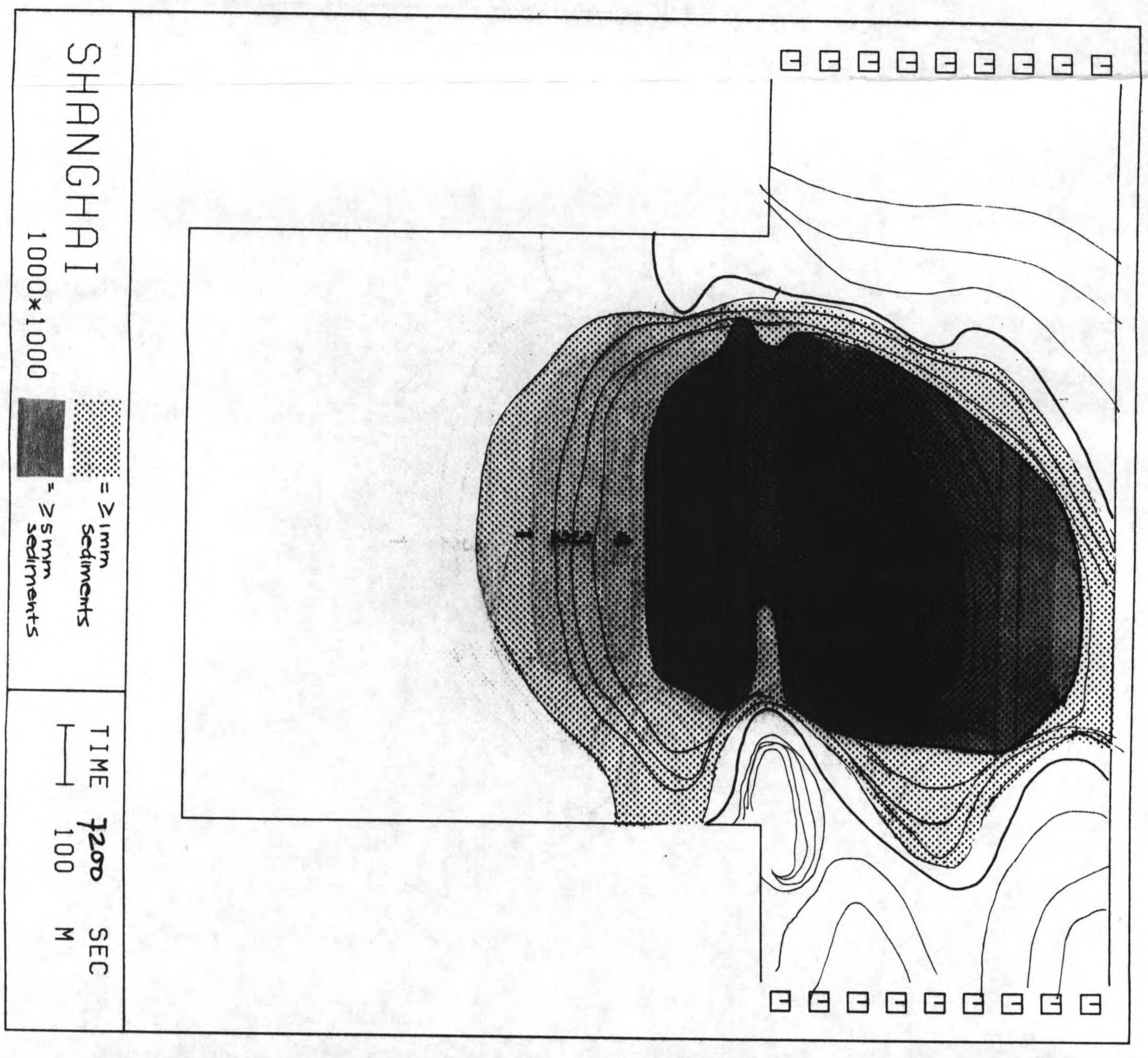

4.12b

MORPHOR DELFT UNIVERSITY OF TECHNOLOGY PROJECT: SHANGHAI RUN: 4
1000*1000 DAM MET SEDIMENT
TIME= 0. SEC

VARIABLE: CS UNIT: 0.1000E-05

	1	2	3	4	5	6	7	8	9	10	11	12	13	14	15	16	17	18	19	20	21	22	23	24	25
1																									
4																									
7																									
10						0	0	0	0	0	0	0	0	0	0	0	0	0	0	0					
						0	0	0	0	0	0	0	0	0	0	0	0	0	0	0					
						0	0	0	0	0	0	0	0	0	0	0	0	0	0	0					
13						0	0	0	0	0	0	0	0	0	0	0	0	0	0	0					
						0	0	0	0	0	0	0	0	0	0	0	0	0	0	0					
						0	0	0	0	0	0	0	0	0	0	0	0	0	0	0					
16						0	0	0	0	0	0	0	0	0	0	0	0	0	0	0					
	0	0	0	0	0	0	0	0	0	0	0	0	0	0	0	0	0	0	0	0	0	0	0	0	0
	0	0	0	0	0	0	0	0	0	0	0	0	0	0	0	0	0	0	0	0	0	0	0	0	0
19	0	0	0	0	0	0	0	0	0	0	0	0	0	0	0	0	0	0	0	0	0	0	0	0	0
	0	0	0	0	0	0	0	0	0	0	0	0	0	0	0	0	0	0	0	0	0	0	0	0	0
	0	0	0	0	0	0	0	0	0	0	0	0	0	0	0	0	0	0	0	0	0	0	0	0	0
22	0	0	0	0	0	0	0	0	0	0	0	0	0	0	0	0	0	0	0	0	0	0	0	0	0
	0	0	0	0	0	0	0	0	0	0	0	0	0	0	0	0	0	0	0	0	0	0	0	0	0
	0	0	0	0	0	0	0	0	0	0	0	0	0	0	0	0	0	0	0	0	0	0	0	0	0
25	0	0	0	0	0	0	0	0	0	0	0	0	0	0	0	0	0	0	0	0	0	0	0	0	0

MORPHOR DELFT UNIVERSITY OF TECHNOLOGY PROJECT: SHANGHAI RUN: 4
1000*1000 DAM MET SEDIMENT
TIME= 600. SEC

VARIABLE: CS UNIT: 0.1000E-05

	1	2	3	4	5	6	7	8	9	10	11	12	13	14	15	16	17	18	19	20	21	22	23	24	25
1																									
4																									
7																									
						0	0	0	0	0	0	0	0	0	0	0	0	0	0	0					
						0	0	0	0	0	0	0	0	0	0	0	0	0	0	0					
10						0	0	0	0	0	0	0	0	0	0	0	0	0	0	0					
						0	0	0	0	0	0	0	0	0	0	0	0	0	0	0					
						0	0	0	0	0	0	0	0	0	0	0	0	0	0	0					
13						0	0	0	0	0	0	0	0	0	0	0	0	0	0	0					
						0	0	0	0	0	3	2	0	0	0	0	0	0	0	0					
						0	0	0	0	3	14	11	0	1	0	0	0	0	0	0					
16						5	3	2	3	8	36	33	4	7	0	0	0	0	0	0					
	377	317	253	187	127	78	52	42	45	56	70	55	17	14	2	2	1	1	2	2	2	3	3	3	3
	377	323	263	197	132	80	47	32	28	28	28	22	30	9	5	4	3	3	3	3	3	3	3	3	3
19	377	328	271	205	137	81	44	25	18	16	15	12	15	6	5	3	3	3	2	2	2	2	2	2	2
	377	333	278	212	142	82	41	21	13	11	10	8	9	5	4	3	3	2	2	2	2	2	2	2	2
	377	336	284	218	146	83	40	19	11	8	7	6	6	4	3	2	2	2	2	1	2	2	1	1	1
22	377	339	288	223	149	84	40	17	9	6	5	4	5	3	2	2	2	2	2	1	1	1	1	1	1
	377	340	291	225	151	85	40	17	8	5	4	4	4	3	2	2	2	2	1	1	1	1	1	1	1
	377	341	293	227	152	85	40	16	7	5	4	3	3	2	2	2	2	1	1	1	1	1	1	1	1
25	377	342	294	229	153	86	40	16	7	4	3	3	3	2	2	2	1	1	1	1	1	1	1	1	0

MORPHOR DELFT UNIVERSITY OF TECHNOLOGY PROJECT: SHANGHAI RUN: 4
1000*1000 DAM MET SEDIMENT
TIME= 1200. SEC

VARIABLE: CS UNIT: 0.1000E-05

	1	2	3	4	5	6	7	8	9	10	11	12	13	14	15	16	17	18	19	20	21	22	23	24	25
1																									
4																									
7						0	0	0	0	0	0	0	0	0	0	0	0	0	0	0					
						0	0	0	0	0	0	0	0	0	0	0	0	0	0	0					
						0	0	0	0	0	0	0	0	0	0	0	0	0	0	0					
10						0	0	0	0	0	0	0	0	0	0	0	0	0	0	0					
						0	0	0	0	0	1	1	1	0	0	0	0	0	0	0					
						0	0	0	1	2	3	4	3	2	1	0	0	0	0	0					
13						0	0	1	2	6	10	13	12	8	3	2	0	0	0	0					
						2	2	3	6	14	25	34	33	23	11	6	2	1	1	0					
						10	9	9	11	21	46	64	65	51	28	18	9	5	4	3					
16						57	54	49	44	46	76	107	110	92	58	47	35	28	25	21					
	377	354	332	311	292	264	240	221	207	204	210	209	191	168	147	144	140	137	135	134	138	139	140	140	139
	377	359	340	322	306	290	275	261	250	240	230	215	194	171	155	147	143	140	140	139	139	138	137	136	136
19	377	362	346	330	315	300	286	273	259	245	230	214	195	174	157	146	138	132	129	128	127	125	124	123	123
	377	363	349	334	320	305	291	277	263	247	230	211	192	172	153	139	128	121	117	114	112	111	110	109	109
	377	364	350	336	322	308	294	280	264	248	230	211	190	168	149	132	120	111	106	102	100	98	97	96	96
22	377	365	351	337	323	310	296	281	266	249	231	210	188	165	144	126	112	102	95	91	89	87	86	85	84
	377	365	351	338	324	310	296	282	266	250	231	210	187	164	142	123	108	97	90	85	83	81	79	78	78
	377	365	352	338	324	311	297	283	267	250	232	211	187	163	140	120	104	93	85	81	77	75	74	73	73
25	377	365	352	338	325	311	297	283	268	251	232	211	187	163	139	118	102	90	82	78	74	72	70	68	65

MORPHOR DELFT UNIVERSITY OF TECHNOLOGY PROJECT: SHANGHAI RUN: 4
1000*1000 DAM MET SEDIMENT
TIME= 1800. SEC

VARIABLE: CS UNIT: 0.1000E-05

	1	2	3	4	5	6	7	8	9	10	11	12	13	14	15	16	17	18	19	20	21	22	23	24	25
1																									
4																									
						0	0	0	0	0	0	0	0	0	0	0	0	0	0	0					
						0	0	0	0	0	0	0	0	0	0	0	0	0	0	0					
7						0	0	0	0	0	0	0	0	0	0	0	0	0	0	0					
						0	0	0	0	0	0	0	0	0	0	0	0	0	0	0					
						0	0	0	0	0	0	0	0	0	0	0	0	0	0	0					
10						0	0	0	0	0	1	1	1	1	1	0	0	0	0	0					
						0	0	0	1	2	3	4	5	4	3	1	1	0	0	0					
						0	0	1	2	5	8	13	15	14	9	5	3	1	1	1					
13						1	2	3	6	11	21	34	40	39	27	16	9	5	4	3					
						5	6	7	12	23	46	75	87	87	64	39	24	16	13	11					
						24	24	23	24	36	87	139	157	156	125	83	56	41	35	32					
16						100	99	99	95	98	169	235	258	252	208	153	115	94	86	80					
	377	388	394	397	397	382	372	367	369	382	406	417	398	358	312	279	260	248	238	229	230	230	231	233	234
	377	390	399	406	410	412	412	412	414	419	424	419	401	373	344	318	301	291	283	277	271	267	265	264	263
19	377	392	404	413	419	424	426	428	429	429	427	419	406	388	368	349	334	322	313	306	299	293	289	285	282
	377	393	405	415	423	428	431	432	432	430	427	420	409	395	381	366	352	341	331	322	314	307	301	296	291
	377	392	405	414	421	427	430	431	431	428	424	418	409	398	387	375	362	351	341	332	323	316	308	301	295
22	377	390	402	410	417	422	425	426	426	423	419	413	405	396	386	376	365	354	344	335	326	318	310	302	295
	377	390	401	410	416	420	423	424	423	420	416	410	403	394	385	376	366	356	346	336	327	319	310	301	293
	377	389	399	407	413	418	420	420	419	417	412	407	400	392	384	375	365	356	346	336	327	319	310	300	292
25	377	388	397	405	410	414	416	417	415	413	409	403	397	390	382	373	364	354	344	335	326	317	309	300	290

MORPHOR DELFT UNIVERSITY OF TECHNOLOGY PROJECT: SHANGHAI RUN: 4
1000*1000 DAM MET SEDIMENT
TIME= 2400. SEC

VARIABLE: CS UNIT: 0.1000E-05

	1	2	3	4	5	6	7	8	9	10	11	12	13	14	15	16	17	18	19	20	21	22	23	24	25
1																									
4																									
						0	0	0	0	0	0	0	0	0	0	0	0	0	0	0					
						0	0	0	0	0	0	0	0	0	0	0	0	0	0	0					
7						0	0	0	0	0	0	0	0	0	0	0	0	0	0	0					
						0	0	0	0	0	0	0	0	0	0	0	0	0	0	0					
						0	0	0	0	0	1	1	1	1	1	1	0	0	0	0					
10						0	0	0	1	1	2	3	4	5	4	3	2	1	1	1					
						0	0	1	2	4	7	10	13	14	12	9	6	4	3	2					
						1	1	3	6	11	18	27	34	36	32	24	16	11	8	8					
13						3	4	6	11	21	37	55	70	75	68	52	37	27	22	20					
						10	10	12	19	33	59	92	116	127	119	97	73	56	47	45					
						35	36	35	36	44	72	122	158	179	173	150	124	102	91	89					
16						121	126	126	121	116	142	196	237	261	246	215	189	171	162	163					
	377	390	400	406	410	399	391	385	383	387	402	417	420	408	383	361	348	339	332	326	328	330	331	331	329
	377	393	405	416	425	431	437	442	447	453	461	464	459	448	432	417	405	395	388	381	377	374	372	370	369
19	377	397	414	429	441	452	461	469	476	483	488	490	487	481	472	463	454	446	439	432	426	421	418	414	411
	377	400	420	437	452	465	476	486	494	501	506	508	507	504	499	493	487	481	475	469	463	458	453	449	445
	377	401	422	441	457	471	484	494	503	510	516	519	520	519	516	513	509	505	500	495	489	485	480	475	471
22	377	400	421	440	456	471	484	495	504	512	518	522	524	525	524	522	519	516	512	508	504	499	495	490	486
	377	401	423	442	459	474	487	498	507	515	521	525	528	529	529	527	525	522	519	515	511	507	503	498	494
	377	401	422	441	459	473	486	497	506	514	520	525	528	529	530	529	527	525	522	519	516	512	508	503	499
25	377	399	420	438	454	468	481	492	502	510	516	521	525	527	528	528	527	525	523	520	517	514	509	504	498

MORPHOR DELFT UNIVERSITY OF TECHNOLOGY PROJECT: SHANGHAI RUN: 4
1000*1000 DAM MET SEDIMENT
TIME= 3000. SEC

VARIABLE: CS UNIT: 0.1000E-05

	1	2	3	4	5	6	7	8	9	10	11	12	13	14	15	16	17	18	19	20	21	22	23	24	25
1																									
4						[illegible]	[illegible]	[illegible]	[illegible]	[illegible]	[illegible]	[illegible]	[illegible]	[illegible]	[illegible]	[illegible]	[illegible]	[illegible]	[illegible]	[illegible]					
7						[illegible]	[illegible]	[illegible]	[illegible]	[illegible]	[illegible]	[illegible]	[illegible]	[illegible]	[illegible]	[illegible]	[illegible]	[illegible]	[illegible]	[illegible]					
10						[illegible]	[illegible]	[illegible]	[illegible]	[illegible]	[illegible]	[illegible]	[illegible]	[illegible]	[illegible]	[illegible]	[illegible]	[illegible]	[illegible]	[illegible]					
13						[illegible]	[illegible]	[illegible]	[illegible]	[illegible]	[illegible]	[illegible]	[illegible]	[illegible]	[illegible]	[illegible]	[illegible]	[illegible]	[illegible]	[illegible]					
16						[illegible]	[illegible]	[illegible]	[illegible]	[illegible]	[illegible]	[illegible]	[illegible]	[illegible]	[illegible]	[illegible]	[illegible]	[illegible]	[illegible]	[illegible]					
19	[illegible]	[illegible]	[illegible]	[illegible]	[illegible]	[illegible]	[illegible]	[illegible]	[illegible]	[illegible]	[illegible]	[illegible]	[illegible]	[illegible]	[illegible]	[illegible]	[illegible]	[illegible]	[illegible]	[illegible]	[illegible]	[illegible]	[illegible]	[illegible]	[illegible]
22	[illegible]	[illegible]	[illegible]	[illegible]	[illegible]	[illegible]	[illegible]	[illegible]	[illegible]	[illegible]	[illegible]	[illegible]	[illegible]	[illegible]	[illegible]	[illegible]	[illegible]	[illegible]	[illegible]	[illegible]	[illegible]	[illegible]	[illegible]	[illegible]	[illegible]
25	[illegible]	[illegible]	[illegible]	[illegible]	[illegible]	[illegible]	[illegible]	[illegible]	[illegible]	[illegible]	[illegible]	[illegible]	[illegible]	[illegible]	[illegible]	[illegible]	[illegible]	[illegible]	[illegible]	[illegible]	[illegible]	[illegible]	[illegible]	[illegible]	[illegible]

MORPHOR DELFT UNIVERSITY OF TECHNOLOGY PROJECT: SHANGHAI RUN: 4
1000*1000 DAM MET SEDIMENT
TIME= 3600. SEC

VARIABLE: CS UNIT: 0.1000E-05

	1	2	3	4	5	6	7	8	9	10	11	12	13	14	15	16	17	18	19	20	21	22	23	24	25
1																									
4						[illegible]	[illegible]	[illegible]	[illegible]	[illegible]	[illegible]	[illegible]	[illegible]	[illegible]	[illegible]	[illegible]	[illegible]	[illegible]	[illegible]	[illegible]					
7						[illegible]	[illegible]	[illegible]	[illegible]	[illegible]	[illegible]	[illegible]	[illegible]	[illegible]	[illegible]	[illegible]	[illegible]	[illegible]	[illegible]	[illegible]					
10						[illegible]	[illegible]	[illegible]	[illegible]	[illegible]	[illegible]	[illegible]	[illegible]	[illegible]	[illegible]	[illegible]	[illegible]	[illegible]	[illegible]	[illegible]					
13						[illegible]	[illegible]	[illegible]	[illegible]	[illegible]	[illegible]	[illegible]	[illegible]	[illegible]	[illegible]	[illegible]	[illegible]	[illegible]	[illegible]	[illegible]					
16						[illegible]	[illegible]	[illegible]	[illegible]	[illegible]	[illegible]	[illegible]	[illegible]	[illegible]	[illegible]	[illegible]	[illegible]	[illegible]	[illegible]	[illegible]					
19	[illegible]	[illegible]	[illegible]	[illegible]	[illegible]	[illegible]	[illegible]	[illegible]	[illegible]	[illegible]	[illegible]	[illegible]	[illegible]	[illegible]	[illegible]	[illegible]	[illegible]	[illegible]	[illegible]	[illegible]	[illegible]	[illegible]	[illegible]	[illegible]	[illegible]
22	[illegible]	[illegible]	[illegible]	[illegible]	[illegible]	[illegible]	[illegible]	[illegible]	[illegible]	[illegible]	[illegible]	[illegible]	[illegible]	[illegible]	[illegible]	[illegible]	[illegible]	[illegible]	[illegible]	[illegible]	[illegible]	[illegible]	[illegible]	[illegible]	[illegible]
25	[illegible]	[illegible]	[illegible]	[illegible]	[illegible]	[illegible]	[illegible]	[illegible]	[illegible]	[illegible]	[illegible]	[illegible]	[illegible]	[illegible]	[illegible]	[illegible]	[illegible]	[illegible]	[illegible]	[illegible]	[illegible]	[illegible]	[illegible]	[illegible]	[illegible]

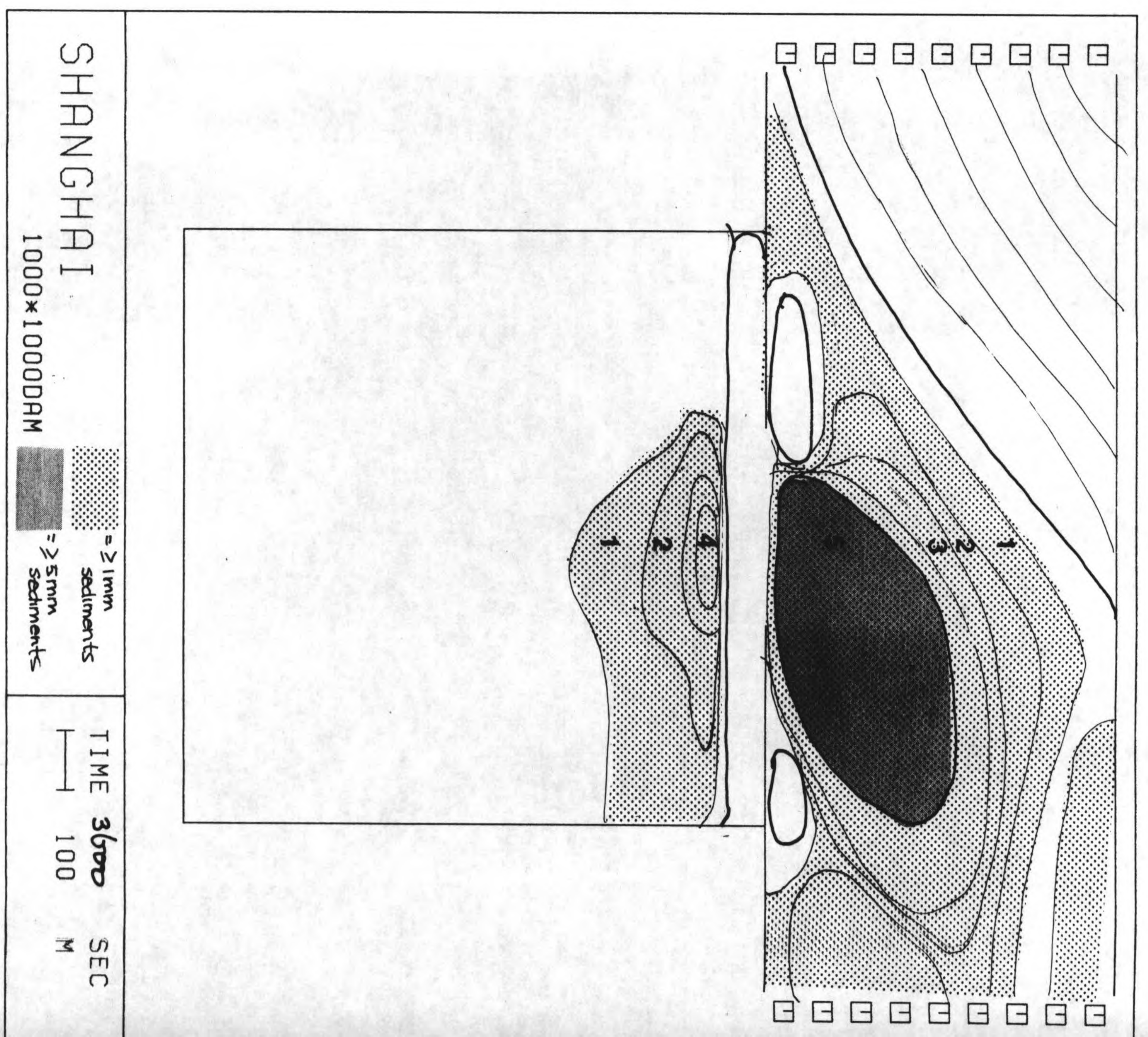

4.13

Results sedimentation 1,000 * 1,000 m plus dam lay-out

MORPHOR DELFT UNIVERSITY OF TECHNOLOGY PROJECT: SHANGHAI RUN: 4
1000*1000 DAM MET SEDIMENT
TIME= 4200. SEC

VARIABLE: CS UNIT: 0.1000E-05

	1	2	3	4	5	6	7	8	9	10	11	12	13	14	15	16	17	18	19	20	21	22	23	24	25
1																									
2						C	0	0	0	0	0	0	0	0	0	0	0	0	0	0					
3						C	0	0	0	0	0	0	0	0	0	0	0	0	0	0					
4						C	0	0	0	0	0	0	0	0	0	0	0	0	0	0					
5						C	0	0	0	0	0	0	0	0	0	0	0	0	0	0					
6						C	0	0	0	0	0	0	0	1	1	1	1	1	1	1					
7						C	0	0	0	0	1	1	1	2	2	2	2	2	2	2					
8						C	0	0	1	1	2	3	3	4	5	5	5	5	6	6					
9						C	0	1	2	3	4	6	8	9	10	11	12	12	13	14					
10						1	1	2	4	6	9	12	15	19	21	22	23	24	26	28					
11						1	2	4	7	11	16	22	28	34	38	40	40	41	44	47					
12						3	4	7	11	17	26	36	47	56	63	64	63	63	66	71					
13						6	8	11	16	25	37	54	71	85	96	95	91	88	91	99					
14						17	18	20	24	33	48	71	99	119	135	133	125	117	119	132					
15						48	49	50	51	54	68	97	137	161	183	177	164	153	153	171					
16						137	143	146	147	142	164	196	233	254	276	252	225	205	201	223					
17	377	387	395	401	405	396	390	386	386	392	406	419	425	421	407	379	360	347	339	334	335	336	337	337	336
18	377	390	401	411	419	426	432	438	445	452	461	466	466	460	449	433	420	410	402	396	392	389	387	385	383
19	377	395	411	426	438	450	460	469	478	487	494	499	500	498	492	485	477	470	464	459	455	451	449	446	444
20	377	399	420	438	454	468	482	493	504	514	522	527	531	531	530	526	522	518	515	511	508	506	503	501	499
21	377	402	425	445	464	481	496	510	523	534	543	550	555	558	560	559	558	557	555	554	552	550	549	548	546
22	377	403	426	448	469	487	504	519	533	545	555	564	571	576	580	582	583	584	584	584	583	583	582	582	581
23	377	405	430	454	475	495	513	529	544	557	568	578	585	591	596	600	602	604	604	605	605	606	605	605	605
24	377	405	431	455	477	498	516	533	548	562	574	584	593	599	605	609	613	615	618	618	621	619	622	621	621
25	377	404	429	453	475	495	513	530	546	560	572	583	592	600	606	612	616	620	622	626	625	629	627	629	628

MORPHOR DELFT UNIVERSITY OF TECHNOLOGY PROJECT: SHANGHAI RUN: 4
1000*1000 DAM MET SEDIMENT
TIME= 4800. SEC

VARIABLE: CS UNIT: 0.1000E-05

	1	2	3	4	5	6	7	8	9	10	11	12	13	14	15	16	17	18	19	20	21	22	23	24	25
1																									
2						C	0	0	0	0	0	0	0	0	0	0	0	0	0	0					
3						C	0	0	0	0	0	0	0	0	0	0	0	0	0	0					
4						C	0	0	0	0	0	0	0	0	0	0	0	0	0	0					
5						C	0	0	0	0	0	0	0	0	0	0	0	0	0	1					
6						C	0	0	0	0	0	1	1	1	1	1	1	1	2	2					
7						C	0	0	0	1	1	1	2	2	3	3	4	4	5	5					
8						C	0	1	1	2	2	3	4	6	7	8	9	10	11	12					
9						C	1	1	2	3	5	7	9	12	14	16	17	19	21	23					
10						1	1	2	4	6	9	13	17	21	25	28	30	33	36	39					
11						2	2	4	7	11	16	22	29	36	42	45	48	50	54	58					
12						3	4	7	11	17	25	35	46	56	64	68	69	70	74	80					
13						7	8	11	15	23	34	49	66	81	94	97	95	94	97	106					
14						18	19	20	24	31	43	62	89	108	128	130	126	121	123	136					
15						49	50	51	52	53	64	84	121	144	170	170	163	154	155	172					
16						136	141	144	144	140	154	177	212	231	256	240	220	204	200	221					
17	377	382	385	388	390	379	372	367	366	368	378	389	396	396	387	363	346	335	327	323	325	326	326	325	324
18	377	385	392	399	405	409	413	418	422	428	435	440	441	436	427	415	403	394	387	382	378	375	373	370	369
19	377	390	402	413	423	432	440	448	455	463	469	474	475	474	470	463	457	451	446	442	438	434	432	429	427
20	377	395	411	426	439	451	462	472	482	490	497	503	506	507	506	504	501	498	495	492	489	486	484	482	480
21	377	398	417	434	450	465	478	490	501	511	519	526	531	534	536	536	536	535	534	533	532	530	529	527	526
22	377	399	419	438	455	471	486	500	512	523	533	541	548	553	557	559	561	562	562	563	562	563	561	563	561
23	377	401	423	444	462	480	496	511	524	536	546	555	563	568	574	577	580	581	585	583	587	583	589	582	589
24	377	401	424	445	465	483	500	515	529	541	552	562	570	577	583	588	590	596	594	602	595	606	594	610	593
25	377	401	423	444	463	481	498	513	527	540	552	562	571	578	585	590	596	598	603	602	609	604	614	603	617

MORPHOR DELFT UNIVERSITY OF TECHNOLOGY PROJECT: SHANGHAI RUN: 4
1000*1000 DAM MET SEDIMENT
TIME= 5400. SEC

VARIABLE: CS UNIT: 0.1000E-05

	1	2	3	4	5	6	7	8	9	10	11	12	13	14	15	16	17	18	19	20	21	22	23	24	25
1																									
2						C	0	0	0	0	0	0	0	0	0	0	0	0	0	0					
3						C	0	0	0	0	0	0	0	0	0	0	0	0	0	0					
4						C	0	0	0	0	0	0	0	0	0	0	0	0	0	0					
5						C	0	0	0	0	0	0	0	0	1	1	1	1	1	1					
6						C	0	0	0	0	1	1	1	1	2	2	2	3	3	3					
7						C	0	0	0	1	1	2	2	3	4	5	6	7	7	8					
8						C	0	1	1	2	3	4	5	7	8	10	12	14	15	17					
9						1	1	1	2	4	5	7	10	13	16	19	22	24	27	29					
10						1	1	2	4	7	10	13	18	22	27	31	35	38	42	45					
11						2	3	4	7	11	15	21	28	35	42	47	51	55	59	63					
12						3	5	7	10	15	22	31	42	52	61	67	70	73	78	84					
13						7	8	11	14	20	30	42	56	71	84	91	93	94	98	108					
14						18	19	20	23	28	37	50	69	87	109	116	118	117	122	135					
15						49	50	50	51	51	59	71	99	117	142	147	147	145	149	168					
16						132	136	138	139	134	145	157	183	196	221	211	198	189	189	211					
17	377	375	374	373	371	358	349	343	339	340	345	352	356	356	351	332	319	310	305	301	303	304	305	305	304
18	377	379	381	384	386	387	389	391	393	396	401	404	404	401	394	383	374	367	361	357	353	351	349	347	346
19	377	385	392	398	404	410	415	420	425	430	435	438	440	438	435	430	425	420	416	413	410	407	405	403	401
20	377	389	401	411	421	429	437	445	452	458	464	468	471	471	471	469	467	465	462	460	458	456	455	453	452
21	377	392	407	420	432	443	453	463	472	479	486	492	496	499	500	501	501	501	500	499	498	498	497	497	495
22	377	394	410	424	438	451	463	474	484	493	501	508	514	518	522	524	526	527	528	528	529	528	531	527	532
23	377	396	414	430	446	460	473	485	496	506	514	522	529	534	538	542	544	547	548	550	549	553	549	558	545
24	377	397	415	432	448	463	477	490	501	512	521	530	537	543	548	552	556	559	562	562	567	563	574	558	583
25	377	396	414	431	447	462	476	489	501	512	522	530	538	545	551	556	560	564	566	570	570	576	570	583	567

MORPHOR DELFT UNIVERSITY OF TECHNOLOGY PROJECT: SHANGHAI RUN: 4
1000*1000 DAM MET SEDIMENT
TIME= 6000. SEC

VARIABLE: CS UNIT: 0.1000E-05

	1	2	3	4	5	6	7	8	9	10	11	12	13	14	15	16	17	18	19	20	21	22	23	24	25
1																									
2						C	0	0	0	0	0	0	0	0	0	0	0	0	0	0					
3						C	0	0	0	0	0	0	0	0	0	0	0	0	0	0					
4						C	0	0	0	0	0	0	0	0	0	0	0	0	1	1					
5						C	0	0	0	0	0	1	1	1	1	1	1	1	2	2					
6						C	0	0	0	1	1	1	1	2	2	3	3	4	4	5					
7						C	0	0	1	1	1	2	3	4	5	6	7	9	10	11					
8						C	0	1	1	2	3	4	6	8	10	12	14	17	19	20					
9						1	1	1	2	4	5	8	10	14	17	21	24	27	31	33					
10						1	1	2	4	6	9	13	17	22	27	32	37	41	45	48					
11						2	2	4	6	10	14	20	26	33	40	46	51	55	60	65					
12						3	4	6	9	14	20	27	36	46	55	62	67	71	77	83					
13						7	8	10	13	18	25	34	46	59	72	80	85	88	94	104					
14						18	19	20	22	25	32	41	53	69	90	100	104	107	114	128					
15						48	49	49	50	50	56	65	87	100	122	128	129	131	138	156					
16						128	129	132	132	128	140	148	168	176	197	188	177	170	173	194					
17	377	370	363	358	353	338	327	319	314	313	317	321	324	323	318	302	290	283	277	274	276	278	278	278	278
18	377	374	371	370	368	367	366	365	366	367	370	371	370	367	360	351	342	336	331	326	323	321	319	317	316
19	377	379	382	384	387	389	392	394	397	400	403	404	405	403	400	395	390	385	381	378	375	372	370	369	367
20	377	384	391	397	403	408	413	418	423	427	430	433	435	435	434	432	429	427	425	422	420	419	417	416	414
21	377	387	397	406	414	422	429	436	442	448	453	457	460	461	462	462	462	461	460	460	459	458	457	456	455
22	377	389	400	411	421	430	439	448	455	462	468	473	477	481	483	485	486	487	487	488	488	488	488	488	487
23	377	391	404	417	429	439	449	459	467	475	481	487	492	496	500	502	504	506	507	508	509	509	510	509	511
24	377	392	406	419	432	443	454	464	473	481	489	495	501	506	510	513	516	518	520	521	523	524	524	526	525
25	377	392	405	419	431	443	453	464	473	482	489	496	503	508	513	517	520	523	525	528	529	531	532	532	534

MORPHOR DELFT UNIVERSITY OF TECHNOLOGY PROJECT: SHANGHAI RUN: 4
1000*1000 DAM MET SEDIMENT
TIME= 6600. SEC

VARIABLE: CS UNIT: 0.1000E-05

	1	2	3	4	5	6	7	8	9	10	11	12	13	14	15	16	17	18	19	20	21	22	23	24	25
1																									
2						C	0	0	0	0	0	0	0	0	0	0	0	0	0	0					
3						C	0	0	0	0	0	0	0	0	0	0	0	0	0	0					
4						C	0	0	0	0	0	0	0	0	0	1	1	1	1	1					
5						C	0	0	0	0	0	0	1	1	1	1	2	2	2	2					
6						C	0	0	0	0	1	1	2	2	3	3	4	5	6	6					
7						C	0	0	1	1	2	2	3	4	6	7	9	10	12	13					
8						C	0	1	1	2	3	4	6	8	10	13	16	18	21	23					
9						1	1	1	2	3	5	7	10	14	17	21	25	29	32	35					
10						1	1	2	4	6	9	12	16	21	26	31	36	41	45	48					
11						2	2	4	6	9	13	17	23	30	37	43	48	53	58	63					
12						3	4	6	8	12	17	23	31	40	48	56	62	67	73	79					
13						7	8	9	12	15	21	28	38	49	61	70	76	81	88	97					
14						18	19	19	20	23	28	35	44	56	74	85	92	97	105	119					
15						47	47	47	48	47	53	59	75	85	103	109	113	117	125	143					
16						122	121	124	124	120	129	133	148	153	170	163	156	152	156	177					
17	377	364	352	343	334	317	304	294	287	284	285	286	288	286	283	270	260	254	249	247	249	250	251	251	251
18	377	368	361	355	349	345	341	338	336	335	335	335	334	330	324	316	309	303	299	295	292	290	288	287	286
19	377	374	371	369	368	367	366	366	366	367	368	368	367	365	362	357	353	349	345	342	339	337	335	333	332
20	377	378	380	382	384	385	387	389	391	393	395	396	397	396	395	392	390	388	385	383	381	380	378	377	375
21	377	382	387	391	395	400	404	407	411	414	417	419	421	422	422	422	421	420	419	418	417	416	415	414	414
22	377	384	390	397	403	409	414	419	424	429	433	436	439	441	443	444	444	444	445	445	444	444	444	444	444
23	377	386	394	402	410	417	424	430	436	441	446	450	453	456	459	460	462	463	463	464	464	465	465	465	465
24	377	387	396	405	414	421	429	436	442	448	453	458	462	466	468	471	473	475	476	477	478	478	479	480	480
25	377	387	396	405	413	421	429	436	443	449	455	460	464	468	472	475	477	479	481	483	484	485	486	487	487

MORPHOR DELFT UNIVERSITY OF TECHNOLOGY PROJECT: SHANGHAI RUN: 4
1000*1000 DAM MET SEDIMENT
TIME= 7200. SEC

VARIABLE: CS UNIT: 0.1000E-05

	1	2	3	4	5	6	7	8	9	10	11	12	13	14	15	16	17	18	19	20	21	22	23	24	25
1																									
2						C	0	0	0	0	0	0	0	0	0	0	0	0	0	0					
3						C	0	0	0	0	0	0	0	0	0	0	0	0	0	0					
4						C	0	0	0	0	0	0	0	0	1	1	1	1	1	1					
5						C	0	0	0	0	0	1	1	1	1	2	2	2	3	3					
6						C	0	0	0	1	1	1	2	2	3	4	5	6	7	7					
7						C	0	0	1	1	2	2	3	5	6	8	10	11	13	14					
8						1	0	1	1	2	3	4	6	8	11	13	16	19	22	23					
9						1	1	1	2	3	5	7	10	13	17	21	25	29	32	34					
10						1	1	2	3	5	8	11	15	19	24	29	34	39	43	46					
11						2	2	3	5	7	11	15	20	26	33	39	45	50	55	59					
12						3	4	5	7	10	14	20	26	34	42	49	55	61	67	73					
13						7	8	9	11	13	18	24	31	40	51	59	66	73	80	89					
14						18	18	18	19	21	25	30	37	47	61	71	78	85	94	107					
15						46	45	45	45	44	49	53	66	73	87	92	96	102	111	129					
16						116	113	115	116	111	118	120	132	134	147	141	135	133	138	157					
17	377	358	341	328	316	296	280	269	260	255	254	254	254	251	248	237	229	223	219	217	219	220	221	221	221
18	377	363	350	340	331	323	317	311	307	304	302	300	298	294	288	281	274	269	265	261	258	256	255	253	252
19	377	368	361	354	349	345	341	338	336	334	333	332	330	327	324	319	315	311	307	304	302	299	297	295	294
20	377	373	370	367	365	363	362	361	361	360	360	359	358	357	355	352	349	347	344	342	340	338	336	335	334
21	377	377	376	377	377	378	378	379	380	381	382	382	382	382	381	380	378	377	376	374	373	372	371	370	369
22	377	379	381	383	385	387	389	392	394	396	397	399	400	401	401	401	401	400	400	399	399	398	398	397	397
23	377	381	385	388	392	395	399	402	405	408	410	412	414	415	416	417	417	418	418	418	418	417	417	417	417
24	377	382	387	391	396	400	404	408	411	415	418	420	423	425	426	427	428	429	430	430	430	430	431	431	431
25	377	382	387	391	396	401	405	409	413	417	420	423	426	428	430	432	433	434	435	436	437	437	437	438	438

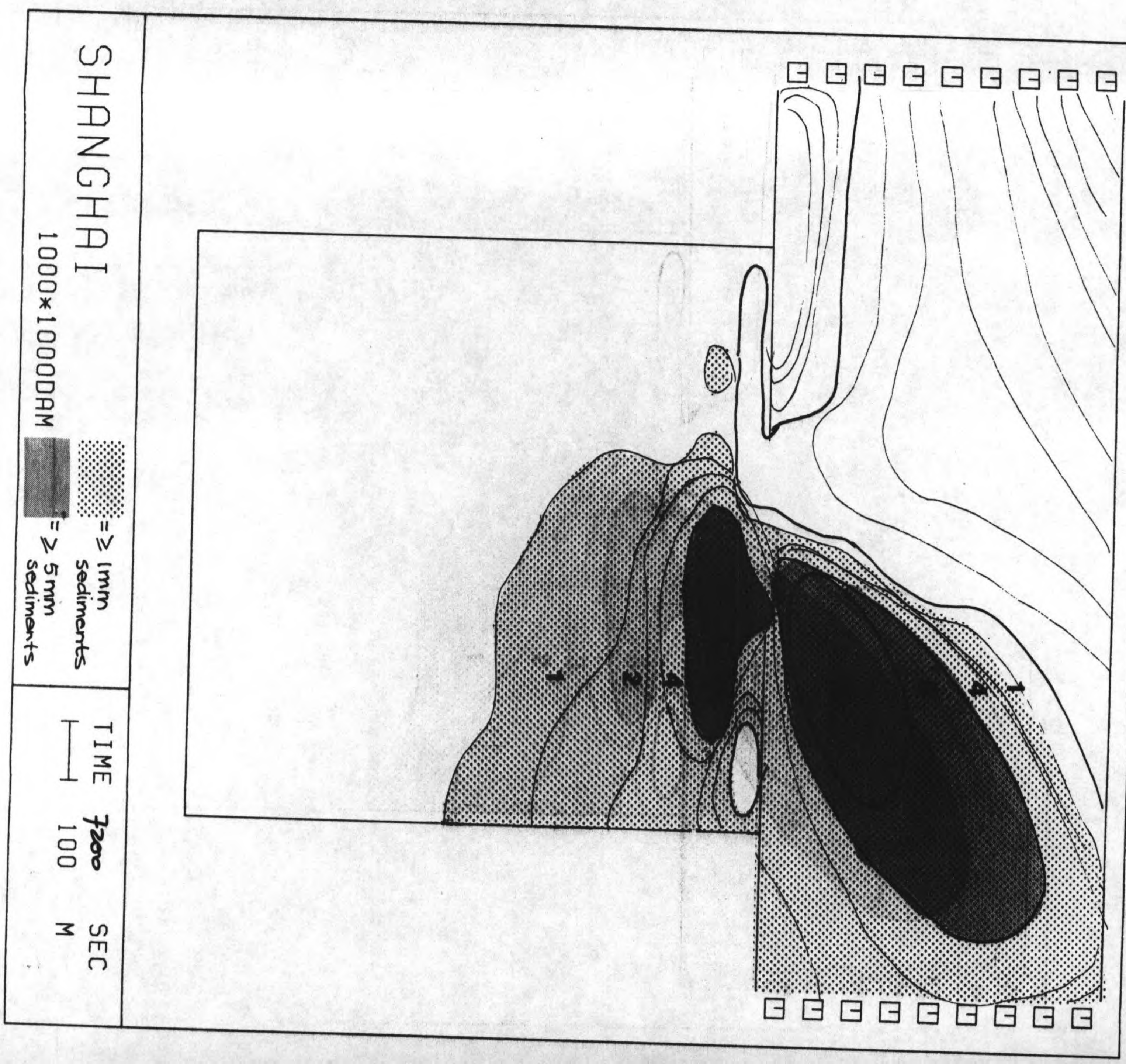

4.13b

CONCLUSION

In the following table 4.7, a comparison is given of the total exchange of water and sediment in and out the fields during the numerical simulations with DUCHESS and MORPHOR. Also the average increase of the water-level and the bottomlevel are given.

The second set of data are based on a storage-analogy (the only mechanism of exchange is storage).

LAY-OUT MODEL	250 * 250 m	500 * 500 m	1,000 * 1,000 m	1,000 * 1,000 m plus dam
T = 3,600 s				
simulations				
- DUCHESS				
total in [m3]	188.10³	541.10³	1,847.10³	858.10³
total out [m3]	129.10³	371.10³	981.10³	27.10³
Δh [mm]	960	948	925	900
- MORPHOR				
total in [m3]	53.0	197.0	673.2	211.0
total out [m3]	5.5	33.5	100.9	-
ΔZ [mm]	0.76	0.65	0.60	0.22
storage				
- water				
total in [m3]	60.610³	244.10³	716.10³	716.10³
total out [m3]	-	-	-	-
Δh [mm]	969	969	969	969
- sediments				
total in [m3]	22.83	91.50	270.0	270.0
total out [m3]	-	-	-	-
ΔZ [mm]	0.61	0.61	0.45	0.45
T = 7,200 s				
simulations				
- DUCHESS				
total in [m3]	-	1,019.10³	3,723.10³	1,597.10³
total out [m3]	-	671.10³	2,138.10³	27.10³
Δh [mm]	-	1,683	1,670	1,656
- MORPHOR				
total in [m3]	-	-	1,468	476.4
total out [m3]	-	-	266.5	-
ΔZ [mm]	-	-	1.34	0.59
storage				
- water				
total in [m3]	106.10³	426.10³	1,576.10³	1,576.10³
total out [m3]	-	-	-	-
Δh [mm]	1.696	1.696	1.696	1.696
- sediments				
total in [m3]	40.13	160.5	594	594
total out [m3]	-	-	-	-
ΔZ [mm]	1.07	1.07	0.99	0.99

Table 4.7: total amount of exchanged water [m3] and sediment [m3] and the average rise of water-level Δh [mm] plus bottomlevel ΔZ [mm], in case of DUCHESS, MORPHOR and the storage-analogy.

*): parts of the basin, so the average rise of the bottomlevel is smaller than in the case of lay-outs.
Per square meter.

In case of storage, it is assumed that all of the sediment settles to the bottom; in this case the total amount of sediment can be calculated by:

$$S_{storage} = (C_{in} - C_{out})\ \Delta h.A \qquad (23)$$

S = total number of m3 sediment brought in by storage [m3]
C_{in} = incoming concentration of sediments = 377.10^{-6} [-]
C_{out} = outgoing concentration of sediments = 0.10^{-6} [-]
Δh = rise of the waterlevel if T = 3,600 s: Δh = 0.97 m and if T = 7,200 s: Δh = 1,69 m [m]
A = surface of the basin [m2].

The average sedimentation can be calculated by:

$$\overline{\Delta Z} = \frac{S_{total}}{(1-p)A} \qquad (24)$$

$\overline{\Delta Z}$ = average rise of the bottomlevel over the total surface of the basins [m]
S = total number of m3 sediment settled on the bottom [m3]
p = porosity = 0.4 [-]
A = surface of the basin [m2].

In case of MORPHOR, the programm gives the rise of the bottomlevel per mesh. This can be re-calculated to ΔZ (see table 4.7). MORPHOR also gives the total transports in x- and y-direction; by integration the total incoming amount of sediment, and the outgoing amount can be determined (see table 4.7).

The sedimentation after T = 3,600 s and T = 7,200 s as given by MORPHOR is underpredicted; this is due to the initial effects. (In MORPHOR the initial value of the concentration is zero; the time necessary for the concentration along the basin to adapt to the boundary-value of 377.10^{-6} is rather long; so that the total amount of sedimented material is too low.)
However, in order to compare the effectivity of each lay-out model, the results of MORPHOR can be used.

Doing so, table 4.7 shows that the storage-mechanism is an important feature, but the exchange by the eddy is much stronger. The larger the basin, the more this is true. For sedimentation it is advantageous that a large amount of sediment-rich water enters the basin, whereas the concentration of the outgoing water should be low.
From this point of view, the distance between the cross-dams should be as large as possible (say, in the order of 1,500 to 2,000 m). Such a lay-out provides a streampattern in which the longshore current spreads over the fields, being reduced by the cross-dams sufficiently to cause sedimentation in the fields.

By the limited adaption-length of the sediment-concentration, the sediment does not penetrate deep into the basins (in the order of 500 m). From this point of view the length of the fields should be short, at least not longer than 500 m.

Furthermore, the opening-size at the seaward end is a significant parameter. If this opening is reduced to one third of the distance between the cross-dams, only the storage-mechanism remains as transport-system of the sediment. In such a case the advantageous effect of the eddy, the longshore current, is completely vanished. From this point of view the opening at the seaward end should be as large as possible.

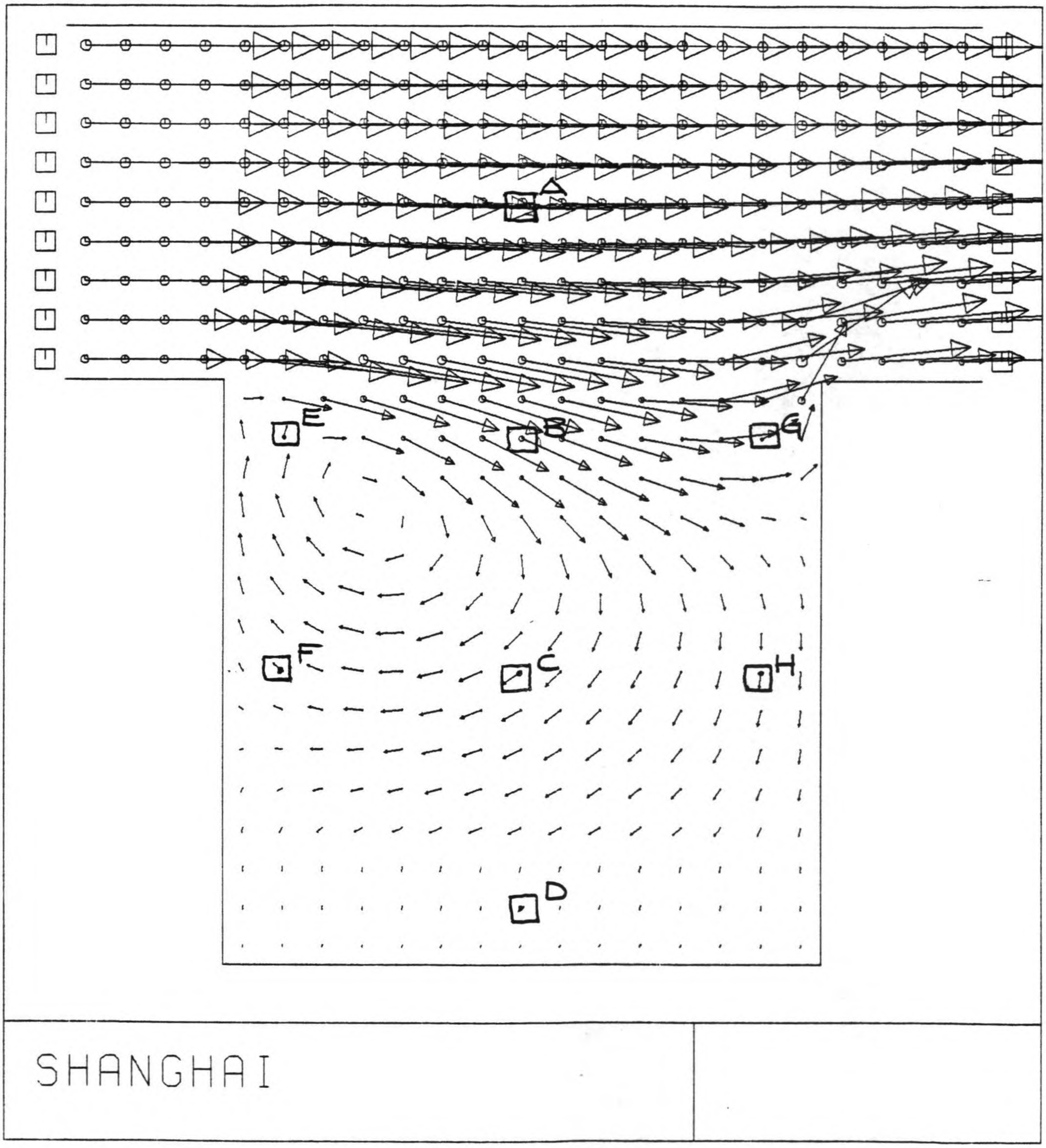

4.14

Overview of the control-points in the computational grid

4.2.2 Sensitivity-analysis

In chapter 3 the input-parameters for the model MORPHOR have been discussed. By means of numerical simulations, the influence of some of these parameters has been investigated. Following items are discussed:

- the influence of the grainsize D_{50} and D_{90};
- the influence of the fall-velocity W_s;
- the influence of secondary flow;
- the influence of the order of the model;
- the influence of the transport formula;
- the influence of lateral diffusion D;
- the influence of the time-step Δt.

In the following table 4.8 an overview is given of the simulations with respect to the sedimentation-pattern:

LAY-OUT MODEL	250 * 250 m	500 * 500 m	1,000 * 1,000 m	1,000 * 1,000 m plus dam
mesh size: Δx Δy	16.67 m 16.67 m	33.33 m 33.33 m	66.67 m 66.67 m	66.67 m 66.67 m
grainsizes: D_{50} D_{90} D_{50} D_{90}	50.10^{-6} m 100.10^{-6} m	50.10^{-6} m 100.10^{-6} m 500.10^{-6} m $1,000.10^{-6}$ m	50.10^{-6} m 100.10^{-6} m	50.10^{-6} m 100.10^{-6} m
- fall-velocity: W_s	$1,110^{-3}$ m/s	$1,110^{-3}$ m/s $1,110^{-4}$ m/s	$1,110^{-3}$ m/s	$1,110^{-3}$ m/s
secondary flow:	yes	yes no	yes	yes
order of model: N	1	1 0	1	1
transport formula:	v. Rijn	v. Rijn	v. Rijn	v. Rijn
- lateral diffusion: D	1 m2/s 25 m2/s	2.5 m2/s 25 m2/s 100 m2/s	5 m2/s	5 m2/s
time step: Δt	10 s 20 s	20 s 40 s	40 s 60 s	40 s 60 s

Table 4.8: overview of simulations with respect to the sensitivity-analysis of the sedimentation-pattern.

MORPHOR   DELFT UNIVERSITY OF TECHNOLOGY   PROJECT: SHANGHAI   RUN: 4
500*500 MET SEDIMENT
TIME=   600. SEC

d_{50} = 500 μm
d_{90} = 1000 μm

VARIABLE: CS   UNIT: 0.1000E-05

	1	2	3	4	5	6	7	8	9	10	11	12	13	14	15	16	17	18	19	20	21	22	23	24	25
1																									
						C	0	0	0	0	0	0	0	0	0	0	0	0	0	C					
						C	0	0	0	0	0	0	0	0	0	0	0	0	0	C					
4						C	0	0	0	0	0	0	0	0	0	0	0	0	0	C					
						C	0	0	0	0	0	0	0	0	0	0	0	0	0	C					
						C	0	0	0	0	0	0	0	0	0	0	0	0	0	C					
7						C	0	0	0	0	0	0	0	0	0	0	0	0	0	C					
						C	0	0	0	0	0	0	0	0	0	0	0	0	0	C					
						C	0	0	0	0	0	0	0	0	0	0	0	0	0	C					
10						C	0	0	0	0	0	0	0	0	0	0	0	0	0	C					
						1	2	2	1	0	0	0	0	0	0	0	0	0	0	C					
						5	8	8	6	3	1	0	0	0	0	0	0	0	0	C					
13						16	30	32	23	13	6	2	1	0	0	0	0	0	0	C					
						50	89	94	73	45	23	10	4	1	0	0	0	0	0	C					
						134	205	207	168	114	66	33	14	5	2	1	0	0	1	0					
16						349	373	355	293	211	135	78	41	20	10	5	4	5	8	67					
	377	409	433	460	514	566	560	478	361	248	158	94	54	31	18	13	12	17	32	147	127	96	75	67	64
	377	401	417	427	429	410	366	301	227	158	102	63	38	25	18	16	18	26	42	119	137	129	112	99	92
19	377	386	389	386	375	352	316	265	205	147	99	64	42	30	24	22	23	29	39	73	93	96	91	84	80
	377	376	370	360	341	318	282	236	184	133	91	60	41	30	25	23	24	28	33	47	60	66	67	65	64
	377	369	359	345	325	300	264	221	172	125	86	57	39	29	25	23	23	26	29	35	43	48	50	51	51
22	377	366	353	337	317	290	254	212	165	120	82	55	38	28	24	22	22	23	25	26	33	37	40	41	42
	377	365	350	333	313	285	249	207	161	116	79	52	36	26	22	20	20	21	22	24	27	30	32	34	35
	377	364	349	332	311	283	247	204	158	114	77	50	34	24	20	18	18	18	19	21	23	25	26	26	29
25	377	364	348	331	310	282	246	203	157	113	76	49	32	23	19	17	16	17	17	18	19	20	20	20	19

T= 600s

MORPHOR   DELFT UNIVERSITY OF TECHNOLOGY   PROJECT: SHANGHAI   RUN: 4
500*500 MET SEDIMENT
TIME=   1200. SEC

VARIABLE: CS   UNIT: 0.1000E-05

	1	2	3	4	5	6	7	8	9	10	11	12	13	14	15	16	17	18	19	20	21	22	23	24	25
1																									
						C	0	0	0	0	0	0	0	0	0	0	0	0	0	C					
						C	0	0	0	0	0	0	0	0	0	0	0	0	0	C					
4						C	0	0	0	0	0	0	0	0	0	0	0	0	0	C					
						C	0	0	0	0	0	0	0	0	0	0	0	0	0	C					
						C	0	0	0	0	0	0	0	0	0	0	0	0	0	C					
7						C	0	1	1	1	1	1	0	0	0	0	0	0	0	C					
						1	1	2	3	4	4	3	2	1	0	0	0	0	0	C					
						2	4	8	12	16	16	13	9	5	2	1	0	0	0	C					
10						6	12	24	37	50	53	45	32	19	10	4	1	0	0	C					
						14	31	62	99	131	140	124	94	61	34	16	6	2	0	C					
						29	68	139	221	285	300	271	217	152	54	49	21	8	2	1					
13						53	125	257	404	498	517	478	402	305	207	121	60	26	8	2					
						88	197	369	590	712	750	713	624	503	372	244	140	69	26	8					
						160	304	534	773	940	1000	961	857	717	564	406	264	147	67	37					
16						452	575	847	1120	1279	1296	1200	1066	903	741	578	427	287	198	211					
	377	581	759	919	1071	1205	1367	1512	1574	1531	1412	1257	1093	933	765	646	527	420	368	566	657	622	538	449	382
	377	556	715	857	993	1112	1214	1271	1272	1228	1155	1065	967	863	761	663	579	513	481	592	718	796	811	791	771
19	377	524	658	781	893	978	1042	1061	1093	1082	1050	1002	943	877	807	735	668	613	580	602	668	742	802	838	860
	377	493	568	693	777	845	898	933	950	949	932	902	861	815	766	718	673	630	614	615	639	675	716	753	760
	377	467	547	620	689	738	780	810	829	836	831	816	793	763	731	698	667	641	625	622	631	647	666	690	709
22	377	448	511	560	619	661	695	722	740	750	752	746	733	714	653	671	650	632	620	618	620	628	639	652	665
	377	434	466	532	572	607	636	659	677	686	693	691	684	673	659	643	629	616	606	601	602	607	614	623	631
	377	425	448	506	540	569	595	615	631	643	649	650	647	639	629	618	606	597	589	583	581	583	587	593	599
25	377	418	445	488	519	564	567	566	601	613	620	621	621	616	609	599	590	582	574	566	563	562	565	568	570

T= 1200s

MORPHOR   DELFT UNIVERSITY OF TECHNOLOGY   PROJECT: SHANGHAI   RUN: 4
500*500 MET SEDIMENT
TIME=   1800. SEC

VARIABLE: CS   UNIT: 0.1000E-05

	1	2	3	4	5	6	7	8	9	10	11	12	13	14	15	16	17	18	19	20	21	22	23	24	25
1																									
						C	0	0	0	0	0	0	0	0	0	0	0	0	0	0					
						C	0	0	0	0	0	0	0	0	0	0	0	0	0	0					
4						C	0	0	0	0	0	0	0	0	0	0	0	0	0	0					
						C	0	0	1	1	1	1	1	1	1	1	0	0	0	0					
						C	1	1	2	3	4	5	5	5	4	2	1	1	0	0					
7						1	2	4	7	10	13	16	18	16	13	9	5	2	1	0					
						3	5	10	18	28	37	46	50	47	38	27	16	8	3	1					
						6	12	25	43	65	88	108	118	113	96	71	44	23	10	4					
10						12	24	49	86	131	177	215	233	227	199	155	103	57	26	10					
						20	41	83	145	221	297	355	385	383	348	287	205	124	60	24					
						30	58	116	204	312	414	489	537	548	518	450	349	231	123	52					
13						41	71	135	235	358	471	572	649	687	677	619	514	374	221	97					
						68	90	143	227	332	464	614	743	818	832	786	685	538	357	171					
						166	176	206	265	364	550	757	926	1016	1032	977	869	708	486	238					
16						520	528	534	602	761	976	1173	1303	1341	1310	1221	1099	919	724	434					
	377	606	801	969	1123	1226	1308	1381	1463	1551	1625	1657	1638	1575	1485	1378	1263	1115	995	906	992	990	950	895	840
	377	569	740	897	1043	1162	1260	1344	1418	1479	1519	1529	1512	1472	1417	1350	1278	1200	1133	1096	1153	1208	1230	1228	1232
19	377	554	711	850	974	1082	1176	1257	1326	1381	1420	1441	1445	1432	1406	1373	1333	1289	1252	1229	1250	1289	1323	1346	1367
	377	533	673	798	911	1012	1099	1172	1234	1285	1325	1352	1367	1370	1362	1348	1329	1308	1291	1283	1294	1318	1344	1367	1387
	377	515	639	750	851	941	1020	1088	1147	1196	1236	1266	1286	1298	1302	1300	1295	1290	1286	1287	1296	1313	1334	1355	1374
22	377	499	609	708	799	879	951	1014	1068	1115	1155	1186	1211	1228	1240	1247	1250	1253	1257	1264	1274	1289	1306	1327	1346
	377	486	584	673	754	827	892	951	1002	1047	1086	1118	1145	1166	1182	1194	1203	1211	1219	1229	1241	1255	1272	1292	1311
	377	474	563	643	715	783	843	898	947	990	1028	1061	1088	1112	1131	1146	1159	1170	1181	1192	1204	1219	1236	1256	1277
25	377	464	544	618	685	747	803	856	903	946	983	1017	1046	1071	1092	1110	1126	1139	1152	1164	1178	1193	1211	1230	1249

T= 1800s

MORPHOR   DELFT UNIVERSITY OF TECHNOLOGY   PROJECT: SHANGHAI   RUN: 4
500*500 MET SEDIMENT
TIME=   1800. SEC

d_{50} = 50 μm
d_{90} = 100 μm

VARIABLE: CS   UNIT: 0.1000E-05

	1	2	3	4	5	6	7	8	9	10	11	12	13	14	15	16	17	18	19	20	21	22	23	24	25
1																									
						C	0	0	0	0	0	0	0	0	0	0	0	0	0	0					
						C	0	0	0	0	0	0	0	0	0	0	0	0	0	0					
4						C	0	0	0	0	0	0	0	0	0	0	0	0	0	0					
						C	0	0	0	0	0	0	0	0	0	0	0	0	0	0					
						C	0	0	1	1	1	2	2	1	1	1	0	0	0	0					
7						C	1	1	2	3	4	5	5	5	4	3	1	1	0	0					
						1	2	3	6	8	11	13	14	14	11	8	5	2	1	C					
						2	4	8	13	19	25	31	33	32	27	20	13	7	3	1					
10						4	8	15	25	37	49	59	64	62	54	43	29	16	7	3					
						6	13	24	41	62	82	96	103	102	93	77	56	34	17	7					
						9	18	34	58	87	113	131	142	144	136	118	92	62	34	15					
13						13	22	39	67	100	129	154	171	179	175	160	134	98	59	27					
						22	28	43	66	95	129	166	196	212	213	201	176	139	93	45					
						54	56	64	80	106	153	202	241	260	262	247	220	180	124	61					
16						173	171	168	181	216	264	307	334	339	330	306	275	230	181	108					
	377	392	404	414	423	421	418	416	420	428	435	435	424	405	380	351	320	281	249	220	236	234	223	209	196
	377	388	398	407	416	423	427	429	431	432	430	424	412	396	377	356	334	309	289	272	280	288	290	287	286
19	377	388	397	405	412	417	420	423	425	424	422	417	409	398	385	371	355	339	325	313	312	316	320	321	324
	377	386	394	400	405	411	414	415	416	415	413	409	403	395	366	376	364	353	343	335	332	332	334	335	337
	377	385	391	396	400	403	406	407	407	406	404	400	396	390	383	375	367	359	352	346	343	341	341	342	343
22	377	383	388	392	394	397	398	399	398	397	395	392	388	384	378	372	366	360	355	350	347	345	344	345	345
	377	382	385	388	390	391	392	392	392	390	388	386	383	379	374	369	364	360	355	351	349	347	345	345	346
	377	381	383	385	385	387	387	387	386	385	383	381	378	375	371	367	363	358	355	351	348	346	345	345	346
25	377	379	381	382	383	383	383	383	382	381	379	377	374	371	368	365	361	357	354	351	348	346	345	345	345

T= 1800s

4.15

Influence of the grainsize

INFLUENCE OF THE GRAINSIZE (see Fig. 4.15)

The grainsize is one of the parameters determining the rate of entrainment. In the model MORPHOR, this rate is determined by the shields-relation (see appendix B). As the size of the particles is very small (D_{50} = 50 μm, $D_* \simeq 1.27$) the critical shear-stress velocity will decrease for increasing grainsize! So for larger particles it will be easier to go into suspension than for the small particles of the simulation (the so-called "plastering"-effect of the small particles: the roughness is so small that a laminar layer develops along the bottom, thus increasing the (critical) shear-stress necessary to go into suspension) (see also appendix B).

This effect is considerable, as shown in Fig. 4.15, where D_{50} = 500 μm and D_{90} = 1,000 μm (ten times as much as in the original simulation) is compared to the original situation. In table 4.9 the values for C (the concentration) are given in the control-points.

The sedimentation occuring after T = 1,800 s turns out to be larger than in the original case after T = 3,600 s.

CONCLUSION:

the influence of the grainsizes on the sedimentation-pattern is considerable; increase of the grainsize causes increase of the average concentration and increase of the sedimentation.

It is important that the grainsizes are schematized in the proper way, in order to obtain realistic results of the numerical computations with MORPHOR.

influence of grainsize		D_{50} = 50 µm	D_{50} = 500 µm
- point A	C [-]	396.10^{-6}	$1{,}286.10^{-6}$
	Tx [m2/s]	$1{,}839.10^{-6}$	$6{,}041.10^{-6}$
	Ty [m2/s]	-55.10^{-6}	-252.10^{-6}
- point B	C [-]	241.10^{-6}	926.10^{-6}
	Tx [m2/s]	338.10^{-6}	$1{,}310.10^{-6}$
	Ty [m2/s]	-225.10^{-6}	-885.10^{-6}
- point C	C [-]	33.10^{-6}	118.10^{-6}
	Tx [m2/s]	-8.10^{-6}	-27.10^{-6}
	Ty [m2/s]	-13.10^{-6}	-49.10^{-6}
- point D	C [-]	0.10^{-6}	0.10^{-6}
	Tx [m2/s]	0.10^{-6}	0.10^{-6}
	Ty [m2/s]	0.10^{-6}	0.10^{-6}
- point E	C [-]	56.10^{-6}	176.10^{-6}
	Tx [m2/s]	28.10^{-6}	59.10^{-6}
	Ty [m2/s]	-2.10^{-6}	9.10^{-6}
- point F	C [-]	4.10^{-6}	12.10^{-6}
	Tx [m2/s]	-1.10^{-6}	-2.10^{-6}
	Ty [m2/s]	1.10^{-6}	3.10^{-6}
- point G	C [-]	124.10^{-6}	486.10^{-6}
	Tx [m2/s]	144.10^{-6}	569.10^{-6}
	Ty [m2/s]	67.10^{-6}	263.10^{-6}
- point H	C [-]	3.10^{-6}	10.10^{-6}
	Tx [m2/s]	1.10^{-6}	2.10^{-6}
	Ty [m2/s]	-1.10^{-6}	-3.10^{-6}

Table 4.9: values of C, Tx and Ty as found in the original simulation and for increased grainsize, at T = 1,800 s.

MORPHOR DELFT UNIVERSITY OF TECHNOLOGY PROJECT: SHANGHAI RUN: 4 : $w_s = 1.1\ 10^{-4}$ m/s
500*500 MET SEDIMENT
TIME= 600. SEC

VARIABLE: CS UNIT: 0.1000E-05

	1	2	3	4	5	6	7	8	9	10	11	12	13	14	15	16	17	18	19	20	21	22	23	24	25
1																									
						C	0	0	0	0	0	0	0	0	0	0	0	0	0	C					
						C	0	0	0	0	0	0	0	0	0	0	0	0	0	0					
4						C	0	0	0	0	0	0	0	0	0	0	0	0	0	0					
						C	0	0	0	0	0	0	0	0	0	0	0	0	0	0					
						C	0	0	0	0	0	0	0	0	0	0	0	0	0	0					
7						C	0	0	0	0	0	0	0	0	0	0	0	0	0	0					
						C	0	0	0	0	0	0	0	0	0	0	0	0	0	0					
						C	C	0	0	0	0	0	0	0	0	0	0	0	0	0					
10						C	0	0	0	0	0	0	0	0	0	0	0	0	0	0					
						1	1	1	0	0	0	0	0	0	0	0	0	0	0	0					
						3	4	4	2	1	0	0	0	0	0	0	0	0	0	0					
13						10	15	15	10	5	2	1	0	0	0	0	0	0	0	0					
						28	44	43	31	18	9	4	1	0	0	0	0	0	0	0					
						74	100	94	73	47	26	12	5	2	1	0	0	0	0	3					
16						178	179	161	127	88	53	29	14	7	3	2	1	1	2	17					
	377	351	327	307	297	285	261	217	162	109	67	37	20	11	6	4	4	5	9	36	33	26	21	19	18
	377	353	329	308	285	258	224	180	132	88	53	30	16	9	6	5	5	8	12	31	35	34	30	27	25
19	377	352	328	305	280	252	219	178	134	91	56	33	18	11	8	7	7	8	11	20	25	26	24	23	22
	377	352	328	304	279	250	216	176	132	91	57	33	19	12	8	7	7	8	10	13	16	16	18	18	18
	377	353	329	305	280	251	216	176	132	91	57	33	19	12	8	7	7	8	8	10	12	13	14	14	14
22	377	354	331	308	283	253	218	177	133	92	58	34	19	12	8	7	7	7	7	8	5	10	11	12	12
	377	355	333	310	286	256	221	179	135	93	58	34	19	11	8	5	6	6	7	7	8	9	9	10	10
	377	356	335	313	289	260	224	182	137	94	59	34	19	11	7	6	6	6	6	6	7	7	6	8	8
25	377	357	337	316	292	262	226	184	138	95	60	34	19	11	7	5	5	5	5	5	6	6	6	6	6

T = 600 s

MORPHOR DELFT UNIVERSITY OF TECHNOLOGY PROJECT: SHANGHAI RUN: 4
500*500 MET SEDIMENT
TIME= 1200. SEC

VARIABLE: CS UNIT: 0.1000E-05

	1	2	3	4	5	6	7	8	9	10	11	12	13	14	15	16	17	18	19	20	21	22	23	24	25
1																									
						C	0	0	0	0	0	0	0	0	0	0	0	0	0	0					
						C	0	0	0	0	0	0	0	0	0	0	0	0	0	0					
4						C	0	0	0	0	0	0	0	0	0	0	0	0	0	0					
						C	0	0	0	0	0	0	0	0	0	0	0	0	0	0					
						C	C	0	0	0	0	0	0	0	0	0	0	0	0	0					
7						C	0	0	0	1	1	0	0	0	0	0	0	0	0	0					
						C	1	1	2	2	2	2	1	1	0	0	0	0	0	0					
						1	3	5	7	8	8	7	4	3	1	0	0	0	0	0					
10						4	7	13	18	23	24	20	15	9	5	2	1	0	0	0					
						8	16	30	44	55	57	50	39	26	15	7	3	1	0	0					
						16	32	60	89	108	111	100	82	59	38	20	9	3	1	C					
13						26	56	105	152	175	177	164	140	109	76	47	24	10	3	1					
						41	84	158	208	236	242	230	204	168	127	87	52	26	10	3					
						68	121	193	256	298	312	299	270	229	165	137	92	53	24	12					
16						172	208	283	353	391	393	368	329	283	237	189	142	97	64	57					
	377	393	406	419	433	441	461	482	486	469	435	392	346	300	257	215	177	140	118	149	170	161	140	117	100
	377	390	402	413	424	435	443	443	433	413	387	357	326	293	261	229	200	174	157	171	195	209	210	204	198
19	377	386	394	402	409	413	414	410	402	389	372	352	330	306	281	256	232	209	193	188	196	207	217	222	224
	377	381	385	388	390	391	389	385	377	367	353	337	319	300	280	260	242	225	211	203	201	202	206	209	212
	377	377	377	376	375	373	369	364	357	348	337	325	311	295	280	264	249	235	223	214	209	205	203	202	201
22	377	374	372	369	365	361	356	350	344	336	326	316	304	291	278	265	253	241	230	222	215	209	204	200	197
	377	373	368	364	359	354	348	342	335	328	319	310	300	289	278	266	255	245	235	226	218	212	205	200	155
	377	372	367	361	355	350	344	337	331	323	315	307	297	287	277	267	257	247	238	229	220	213	206	199	192
25	377	371	366	360	354	347	341	335	328	321	313	305	296	287	277	267	258	248	239	230	221	213	205	197	169

T = 1200 s

MORPHOR DELFT UNIVERSITY OF TECHNOLOGY PROJECT: SHANGHAI RUN: 4
500*500 MET SEDIMENT
TIME= 1800. SEC

VARIABLE: CS UNIT: 0.1000E-05

	1	2	3	4	5	6	7	8	9	10	11	12	13	14	15	16	17	18	19	20	21	22	23	24	25
1																									
						C	0	0	0	0	0	0	0	0	0	0	0	0	0	0					
						C	0	0	0	0	0	0	0	0	0	0	0	0	0	0					
4						0	0	0	0	0	0	0	0	0	0	0	0	0	0	0					
						C	C	0	0	1	1	1	1	1	1	0	0	0	0	0					
						C	1	1	1	2	2	3	3	2	2	1	1	0	0	0					
7						1	1	2	4	5	7	8	8	8	6	4	2	1	1	0					
						2	3	6	9	13	17	20	21	20	16	12	7	4	2	1					
						4	6	12	19	28	36	43	46	44	38	28	19	10	5	2					
10						6	12	22	36	52	67	79	84	81	72	58	40	23	11	5					
						10	19	35	57	83	107	123	130	129	118	99	74	47	25	11					
						14	25	47	78	114	145	164	173	175	165	146	117	81	46	22					
13						19	31	54	90	134	167	186	202	210	207	190	162	122	77	38					
						30	38	57	87	121	156	193	225	243	246	233	206	166	115	59					
						68	70	79	97	125	175	230	274	297	300	285	255	211	149	77					
16						201	195	190	204	242	296	344	376	384	375	351	318	268	214	130					
	377	400	418	434	449	451	451	453	459	469	479	481	472	454	428	398	366	324	289	253	271	269	257	243	228
	377	394	410	425	439	450	457	463	469	472	473	468	457	442	423	402	379	354	332	313	320	329	331	328	327
19	377	394	408	420	431	440	448	454	458	461	461	458	451	442	430	416	400	384	370	357	356	360	364	366	368
	377	391	403	414	424	432	438	443	446	448	448	446	442	436	427	418	407	397	387	380	377	377	379	361	382
	377	389	399	408	415	422	428	432	434	436	436	434	431	427	421	414	407	400	394	389	386	385	385	386	387
22	377	387	395	403	409	414	418	421	423	424	424	423	421	418	414	409	404	399	394	391	388	387	386	367	368
	377	385	392	398	403	407	410	413	415	415	415	415	413	411	407	404	400	396	392	389	387	386	385	386	367
	377	384	389	394	399	401	404	406	408	408	408	408	406	404	402	399	396	393	390	387	385	384	383	384	365
25	377	382	387	391	394	397	399	401	402	403	403	402	401	400	398	395	393	390	388	385	383	382	382	362	382

T = 1800 s

MORPHOR DELFT UNIVERSITY OF TECHNOLOGY PROJECT: SHANGHAI RUN: 4 : $w_s = 1.1\ 10^{-3}$ m/s
500*500 MET SEDIMENT
TIME= 1800. SEC

VARIABLE: CS UNIT: 0.1000E-05

	1	2	3	4	5	6	7	8	9	10	11	12	13	14	15	16	17	18	19	20	21	22	23	24	25
1																									
						C	0	0	0	0	0	0	0	0	0	0	0	0	0	0					
						C	0	0	0	0	0	0	0	0	0	0	0	0	0	0					
4						C	0	0	0	0	0	0	0	0	0	0	0	0	0	0					
						C	0	0	0	0	0	0	0	0	0	0	0	0	0	0					
						C	0	0	1	1	1	2	2	1	1	1	0	0	0	0					
7						C	1	1	2	3	4	5	5	5	4	3	1	1	0	0					
						1	2	3	6	8	11	13	14	14	11	8	5	2	1	C					
						2	4	8	13	19	25	31	33	32	27	20	13	7	3	1					
10						4	8	15	25	37	49	59	64	62	54	43	29	16	7	3					
						6	13	24	41	62	82	96	103	102	93	77	56	34	17	7					
						9	18	34	58	87	113	131	142	144	136	118	92	62	34	15					
13						13	22	39	67	100	129	154	171	179	175	160	134	98	59	27					
						22	28	43	66	95	129	166	196	212	213	201	176	139	93	45					
						54	56	64	80	106	153	202	241	260	262	247	220	180	124	61					
16						173	171	168	181	216	264	307	334	339	330	306	275	230	181	108					
	377	392	404	414	429	421	418	416	420	428	435	435	424	405	380	351	320	281	249	220	236	234	223	209	196
	377	388	358	407	415	423	427	429	431	432	430	424	412	396	377	356	334	309	289	272	280	288	290	287	286
19	377	388	397	405	412	417	420	423	425	424	422	417	409	398	385	371	355	339	325	313	312	316	320	321	324
	377	386	394	400	405	411	414	415	416	415	413	409	403	395	366	376	364	353	343	335	332	332	334	335	337
	377	385	391	396	400	403	406	407	407	406	404	400	396	390	383	375	367	359	352	346	343	341	341	342	343
22	377	383	388	392	394	397	398	399	398	397	395	392	388	384	378	372	366	360	355	350	347	345	344	345	345
	377	382	385	388	390	391	392	392	392	390	388	386	383	379	374	369	364	360	355	351	349	347	345	345	346
	377	381	383	385	385	387	387	387	386	385	383	381	378	375	371	367	363	358	355	351	348	346	345	345	346
25	377	379	381	382	383	383	383	383	382	381	379	377	374	371	368	365	361	357	354	351	348	346	345	345	345

T = 1800 s

4.16

Influence of the fall-velocity

INFLUENCE OF THE FALL-VELOCITY (see Fig. 4.16)

The fall-velocity is, together with the shear-stress-velocity, a parameter which determines the rate of suspension of the flow. Increasing the fall-velocity influences the equilibrium between settling and entrainment of the particles, and causes a lower concentration.
In this analysis, the influence of the particle-fall-velocity is determined by decreasing the fall-velocity with a factor of 10. The results of this simulation are given in Fig. 4.16 and in table 4.10, compared with the "normal" fall-velocity w_s = $1.1 \cdot 10^{-3}$ (m/s).

It shows that the effect of increasing the fall-velocity by a factor 10 is hardly noticeable; some increase of concentration can be found. The effect on the (bottom) sedimentation is negligible.

CONCLUSION:

the influence of the particle fall-velocity on the sedimentation pattern is rather small, decrease of the fall-velocity causes a small increase of the average concentration, and a small increase of the penetration in the reclamation field.

As the results do not seem to be very sensitive to the fall-velocity value, this parameter can be schematized rather crude.

MORPHOR DELFT UNIVERSITY OF TECHNOLOGY PROJECT: SHANGHAI RUN: TEST *no secondary flow*
500*500 NET SEDIMENT
TIME= 100. SEC

VARIABLE: CS UNIT: 0.1000E-05

	1	2	3	4	5	6	7	8	9	10	11	12	13	14	15	16	17	18	19	20	21	22	23	24	25
1																									
						0	0	0	0	0	0	0	0	0	0	0	0	0	0	0					
						0	0	0	0	0	0	0	0	0	0	0	0	0	0	0					
4						0	0	0	0	0	0	0	0	0	0	0	0	0	0	0					
						0	0	0	0	0	0	0	0	0	0	0	0	0	0	0					
						0	0	0	0	0	0	0	0	0	0	0	0	0	0	0					
7						0	0	0	0	0	0	0	0	0	0	0	0	0	0	0					
						0	0	0	0	0	0	0	0	0	0	0	0	0	0	0					
						0	0	0	0	0	0	0	0	0	0	0	0	0	0	0					
10						0	0	0	0	0	0	0	0	0	0	0	0	0	0	0					
						0	0	0	0	0	0	0	0	0	0	0	0	0	0	0					
						0	0	0	0	0	0	0	0	0	0	0	0	0	0	0					
13						0	0	0	0	0	0	0	0	0	0	0	0	0	0	0					
						0	0	0	0	0	0	0	0	0	0	0	0	0	0	0					
						0	0	0	0	0	0	0	0	0	0	0	0	0	0	0					
16						0	0	0	0	0	0	0	0	0	0	0	0	0	0	0					
	377	78	7	0	0	0	0	0	0	0	0	0	0	0	0	0	0	0	0	0	0	0	0	0	0
	377	78	7	0	0	0	0	0	0	0	0	0	0	0	0	0	0	0	0	0	0	0	0	0	0
19	377	78	7	0	0	0	0	0	0	0	0	0	0	0	0	0	0	0	0	0	0	0	0	0	0
	377	79	7	0	0	0	0	0	0	0	0	0	0	0	0	0	0	0	0	0	0	0	0	0	0
	377	79	7	0	0	0	0	0	0	0	0	0	0	0	0	0	0	0	0	0	0	0	0	0	0
22	377	79	7	0	0	0	0	0	0	0	0	0	0	0	0	0	0	0	0	0	0	0	0	0	0
	377	80	7	0	0	0	0	0	0	0	0	0	0	0	0	0	0	0	0	0	0	0	0	0	0
	377	80	7	0	0	0	0	0	0	0	0	0	0	0	0	0	0	0	0	0	0	0	0	0	0
25	377	80	7	0	0	0	0	0	0	0	0	0	0	0	0	0	0	0	0	0	0	0	0	0	0

T=100s

MORPHOR DELFT UNIVERSITY OF TECHNOLOGY PROJECT: SHANGHAI RUN: TEST
500*500 NET SEDIMENT
TIME= 200. SEC

VARIABLE: CS UNIT: 0.1000E-05

	1	2	3	4	5	6	7	8	9	10	11	12	13	14	15	16	17	18	19	20	21	22	23	24	25
1																									
						0	0	0	0	0	0	0	0	0	0	0	0	0	0	0					
						0	0	0	0	0	0	0	0	0	0	0	0	0	0	0					
4						0	0	0	0	0	0	0	0	0	0	0	0	0	0	0					
						0	0	0	0	0	0	0	0	0	0	0	0	0	0	0					
						0	0	0	0	0	0	0	0	0	0	0	0	0	0	0					
7						0	0	0	0	0	0	0	0	0	0	0	0	0	0	0					
						0	0	0	0	0	0	0	0	0	0	0	0	0	0	0					
						0	0	0	0	0	0	0	0	0	0	0	0	0	0	0					
10						0	0	0	0	0	0	0	0	0	0	0	0	0	0	0					
						0	0	0	0	0	0	0	0	0	0	0	0	0	0	0					
						0	0	0	0	0	0	0	0	0	0	0	0	0	0	0					
13						0	0	0	0	0	0	0	0	0	0	0	0	0	0	0					
						0	0	0	0	0	0	0	0	0	0	0	0	0	0	0					
						0	0	0	0	0	0	0	0	0	0	0	0	0	0	0					
16						0	0	0	0	0	0	0	0	0	0	0	0	0	0	0					
	377	235	98	27	5	1	0	0	0	0	0	0	0	0	0	0	0	0	0	0	0	0	0	0	0
	377	235	98	26	5	1	0	0	0	0	0	0	0	0	0	0	0	0	0	0	0	0	0	0	0
19	377	235	97	26	5	1	0	0	0	0	0	0	0	0	0	0	0	0	0	0	0	0	0	0	0
	377	235	97	26	4	0	0	0	0	0	0	0	0	0	0	0	0	0	0	0	0	0	0	0	0
	377	235	96	26	4	0	0	0	0	0	0	0	0	0	0	0	0	0	0	0	0	0	0	0	0
22	377	236	96	25	4	0	0	0	0	0	0	0	0	0	0	0	0	0	0	0	0	0	0	0	0
	377	236	96	25	4	0	0	0	0	0	0	0	0	0	0	0	0	0	0	0	0	0	0	0	0
	377	236	96	25	4	0	0	0	0	0	0	0	0	0	0	0	0	0	0	0	0	0	0	0	0
25	377	236	96	25	4	0	0	0	0	0	0	0	0	0	0	0	0	0	0	0	0	0	0	0	0

T=200s

MORPHOR DELFT UNIVERSITY OF TECHNOLOGY PROJECT: SHANGHAI RUN: TEST
500*500 NET SEDIMENT
TIME= 300. SEC

VARIABLE: CS UNIT: 0.1000E-05

	1	2	3	4	5	6	7	8	9	10	11	12	13	14	15	16	17	18	19	20	21	22	23	24	25
1																									
						0	0	0	0	0	0	0	0	0	0	0	0	0	0	0					
						0	0	0	0	0	0	0	0	0	0	0	0	0	0	0					
4						0	0	0	0	0	0	0	0	0	0	0	0	0	0	0					
						0	0	0	0	0	0	0	0	0	0	0	0	0	0	0					
						0	0	0	0	0	0	0	0	0	0	0	0	0	0	0					
7						0	0	0	0	0	0	0	0	0	0	0	0	0	0	0					
						0	0	0	0	0	0	0	0	0	0	0	0	0	0	0					
						0	0	0	0	0	0	0	0	0	0	0	0	0	0	0					
10						0	0	0	0	0	0	0	0	0	0	0	0	0	0	0					
						0	0	0	0	0	0	0	0	0	0	0	0	0	0	0					
						0	0	0	0	0	0	0	0	0	0	0	0	0	0	0					
13						0	0	0	0	0	0	0	0	0	0	0	0	0	0	0					
						0	0	0	0	0	0	0	0	0	0	0	0	0	0	0					
						1	0	0	0	0	0	0	0	0	0	0	0	0	0	0					
16						7	3	1	0	0	0	0	0	0	0	0	0	0	0	0					
	377	309	224	138	73	33	12	3	1	0	0	0	0	0	0	0	0	0	0	0	0	0	0	0	0
	377	311	224	133	64	24	7	1	0	0	0	0	0	0	0	0	0	0	0	0	0	0	0	0	0
19	377	313	224	131	60	21	6	1	0	0	0	0	0	0	0	0	0	0	0	0	0	0	0	0	0
	377	314	224	129	59	20	5	1	0	0	0	0	0	0	0	0	0	0	0	0	0	0	0	0	0
	377	315	224	128	57	19	5	1	0	0	0	0	0	0	0	0	0	0	0	0	0	0	0	0	0
22	377	316	224	127	56	19	5	1	0	0	0	0	0	0	0	0	0	0	0	0	0	0	0	0	0
	377	316	224	127	55	19	5	1	0	0	0	0	0	0	0	0	0	0	0	0	0	0	0	0	0
	377	317	225	127	55	18	5	1	0	0	0	0	0	0	0	0	0	0	0	0	0	0	0	0	0
25	377	318	225	127	55	18	5	1	0	0	0	0	0	0	0	0	0	0	0	0	0	0	0	0	0

T=300s

MORPHOR DELFT UNIVERSITY OF TECHNOLOGY PROJECT: SHANGHAI RUN: 4 *with secondary flow*
500*500 NET SEDIMENT
TIME= 300. SEC

VARIABLE: CS UNIT: 0.1000E-05

	1	2	3	4	5	6	7	8	9	10	11	12	13	14	15	16	17	18	19	20	21	22	23	24	25
1																									
						0	0	0	0	0	0	0	0	0	0	0	0	0	0	0					
						0	0	0	0	0	0	0	0	0	0	0	0	0	0	0					
4						0	0	0	0	0	0	0	0	0	0	0	0	0	0	0					
						0	0	0	0	0	0	0	0	0	0	0	0	0	0	0					
						0	0	0	0	0	0	0	0	0	0	0	0	0	0	0					
7						0	0	0	0	0	0	0	0	0	0	0	0	0	0	0					
						0	0	0	0	0	0	0	0	0	0	0	0	0	0	0					
						0	0	0	0	0	0	0	0	0	0	0	0	0	0	0					
10						0	0	0	0	0	0	0	0	0	0	0	0	0	0	0					
						0	0	0	0	0	0	0	0	0	0	0	0	0	0	0					
						0	0	0	0	0	0	0	0	0	0	0	0	0	0	0					
13						0	0	0	0	0	0	0	0	0	0	0	0	0	0	0					
						0	0	0	0	0	0	0	0	0	0	0	0	0	0	0					
						1	0	0	0	0	0	0	0	0	0	0	0	0	0	0					
16						7	3	1	0	0	0	0	0	0	0	0	0	0	0	0					
	377	309	224	138	73	33	12	3	1	0	0	0	0	0	0	0	0	0	0	0	0	0	0	0	0
	377	311	224	133	64	24	7	1	0	0	0	0	0	0	0	0	0	0	0	0	0	0	0	0	0
19	377	313	224	131	60	21	6	1	0	0	0	0	0	0	0	0	0	0	0	0	0	0	0	0	0
	377	314	224	129	59	20	5	1	0	0	0	0	0	0	0	0	0	0	0	0	0	0	0	0	0
	377	315	224	128	57	19	5	1	0	0	0	0	0	0	0	0	0	0	0	0	0	0	0	0	0
22	377	316	224	127	56	19	5	1	0	0	0	0	0	0	0	0	0	0	0	0	0	0	0	0	0
	377	316	224	127	56	19	5	1	0	0	0	0	0	0	0	0	0	0	0	0	0	0	0	0	0
	377	317	225	127	55	18	5	1	0	0	0	0	0	0	0	0	0	0	0	0	0	0	0	0	0
25	377	318	225	127	55	18	5	1	0	0	0	0	0	0	0	0	0	0	0	0	0	0	0	0	0

T=300s

PORFHOR DELFT UNIVERSITY OF TECHNOLOGY   PROJECT: SHANGHAI   RUN: TEST   no secondary flow
500*500 MET SEDIMENT
TIME= 400. SEC

VARIABLE: CS   UNIT: 0.1000E-05

	1	2	3	4	5	6	7	8	9	10	11	12	13	14	15	16	17	18	19	20	21	22	23	24	25
1																									
2						C	0	0	0	0	0	0	0	0	0	0	0	0	0	C					
3						C	0	0	0	0	0	0	0	0	0	0	0	0	0	C					
4						C	0	0	0	0	0	0	0	0	0	0	0	0	0	C					
5						C	0	0	0	0	0	0	0	0	0	0	0	0	0	C					
6						C	0	0	0	0	0	0	0	0	0	0	0	0	0	C					
7						C	0	0	0	0	0	0	0	0	0	0	0	0	0	C					
8						C	0	0	0	0	0	0	0	0	0	0	0	0	0	C					
9						C	0	0	0	0	0	0	0	0	0	0	0	0	0	C					
10						C	0	0	0	0	0	0	0	0	0	0	0	0	0	C					
11						C	0	0	0	0	0	0	0	0	0	0	0	0	0	C					
12						C	0	0	0	0	0	0	0	0	0	0	0	0	0	C					
13						1	0	0	0	0	0	0	0	0	0	0	0	0	0	C					
14						4	3	1	0	0	0	0	0	0	0	0	0	0	0	C					
15						18	13	6	2	1	0	0	0	0	0	0	0	0	0	C					
16						61	42	22	9	3	1	0	0	0	0	0	0	0	0	C					
17	377	336	291	244	201	150	91	44	18	7	2	0	0	0	0	0	0	0	0	C					
18	377	337	290	236	175	115	62	27	10	3	1	1	0	0	0	0	0	0	0	C					
19	377	338	292	235	170	107	56	24	9	3	1	0	0	0	0	0	0	0	0	C	0	0	0	0	0
20	377	339	293	234	167	103	52	22	8	2	1	0	0	0	0	0	0	0	0	C	0	0	0	0	0
21	377	341	295	235	165	100	50	21	7	2	1	0	0	0	0	0	0	0	0	C	0	0	0	0	0
22	377	343	297	236	165	99	49	20	7	2	1	0	0	0	0	0	0	0	0	C	0	0	0	0	0
23	377	344	299	237	165	99	49	20	7	2	1	0	0	0	0	0	0	0	0	C	0	0	0	0	0
24	377	345	301	239	165	99	49	20	7	2	1	0	0	0	0	0	0	0	0	C	0	0	0	0	0
25	377	346	302	240	167	99	49	20	7	2	1	0	0	0	0	0	0	0	0	C	0	0	0	0	0

T=100s

PORFHOR DELFT UNIVERSITY OF TECHNOLOGY   PROJECT: SHANGHAI   RUN: TEST
500*500 MET SEDIMENT
TIME= 500. SEC

VARIABLE: CS   UNIT: 0.1000E-05

	1	2	3	4	5	6	7	8	9	10	11	12	13	14	15	16	17	18	19	20	21	22	23	24	25
1																									
2						C	0	0	0	0	0	0	0	0	0	0	0	0	0	0					
3						C	0	0	0	0	0	0	0	0	0	0	0	0	0	0					
4						C	0	0	0	0	0	0	0	0	0	0	0	0	0	0					
5						C	0	0	0	0	0	0	0	0	0	0	0	0	0	0					
6						C	0	0	0	0	0	0	0	0	0	0	0	0	0	0					
7						C	0	0	0	0	0	0	0	0	0	0	0	0	0	0					
8						C	0	0	0	0	0	0	0	0	0	0	0	0	0	0					
9						C	0	0	0	0	0	0	0	0	0	0	0	0	0	0					
10						C	0	0	0	0	0	0	0	0	0	0	0	0	0	0					
11						C	0	0	0	0	0	0	0	0	0	0	0	0	0	0					
12						1	1	1	0	0	0	0	0	0	0	0	0	0	0	0					
13						4	5	3	2	1	0	0	0	0	0	0	0	0	0	0					
14						17	19	13	7	3	1	0	0	0	0	0	0	0	0	0					
15						51	55	41	23	11	4	1	0	0	0	0	0	0	0	0					
16						134	121	68	54	27	12	5	2	1	0	0	0	0	0	1					
17	377	345	315	289	271	243	195	134	78	40	18	7	3	1	1	0	0	1	1	7					
18	377	346	315	284	249	206	154	100	56	27	12	5	2	1	1	1	1	1	2	5	5	4	3	3	3
19	377	346	316	283	245	199	148	97	55	27	12	5	3	2	1	1	1	1	1	3	5	5	4	4	3
20	377	347	317	283	244	196	144	94	53	26	12	5	3	2	1	1	1	1	1	2	3	3	3	3	3
21	377	348	319	285	245	196	143	92	51	25	11	5	3	2	1	1	1	1	1	1	2	2	2	2	2
22	377	350	321	288	247	197	143	92	51	25	11	5	2	2	1	1	1	1	1	1	2	2	2	2	2
23	377	351	324	291	249	199	144	92	51	25	11	5	2	1	1	1	1	1	1	1	1	1	1	1	1
24	377	353	326	294	252	201	145	93	52	25	11	5	2	1	1	1	1	1	1	1	1	1	1	1	1
25	377	354	328	296	254	203	146	93	52	25	11	4	2	1	1	1	1	1	1	1	1	1	1	1	0

T=200s

PORFHOR DELFT UNIVERSITY OF TECHNOLOGY   PROJECT: SHANGHAI   RUN: TEST
500*500 MET SEDIMENT
TIME= 600. SEC

VARIABLE: CS   UNIT: 0.1000E-05

	1	2	3	4	5	6	7	8	9	10	11	12	13	14	15	16	17	18	19	20	21	22	23	24	
1																									
2						C	C	0	0	0	0	0	0	0	0	0	0	0	0	0					
3						C	0	0	0	0	0	0	0	0	0	0	0	0	0	0					
4						C	0	0	0	0	0	0	0	0	0	0	0	0	0	0					
5						C	0	0	0	0	0	0	0	0	0	0	0	0	0	0					
6						C	0	0	0	0	0	0	0	0	0	0	0	0	0	0					
7						C	0	0	0	0	0	0	0	0	0	0	0	0	0	0					
8						C	0	0	0	0	0	0	0	0	0	0	0	0	0	0					
9						C	0	0	0	0	0	0	0	0	0	0	0	0	0	0					
10						C	0	0	0	0	0	0	0	0	0	0	0	0	0	0					
11						C	1	1	0	0	0	0	0	0	0	0	0	0	0	0					
12						[illegible]	3	3	2	1	0	0	0	0	0	0	0	0	0	0					
13						8	13	12	8	4	2	1	0	0	0	0	0	0	0	0					
14						23	38	37	27	16	8	3	1	0	0	0	0	0	0	0					
15						61	88	84	65	41	22	10	4	1	0	0	0	0	0	[illegible]					
16						161	163	146	114	78	46	25	12	5	3	1	1	1	2	14					
17	377	346	317	294	280	266	241	199	147	98	59	32	17	9	5	3	3	4	7	32	28	21	17	15	1(
18	377	348	321	297	272	244	210	168	122	60	48	26	14	7	5	4	4	6	9	26	30	28	25	22	2(
19	377	348	322	296	270	241	207	168	125	84	51	29	16	9	6	5	5	7	9	16	21	22	20	19	18
20	377	349	323	297	270	241	207	167	125	65	52	30	16	10	7	6	6	6	8	11	14	15	15	15	15
21	377	350	325	299	273	243	208	168	126	86	53	30	17	10	7	6	6	6	7	8	10	11	12	12	12
22	377	352	327	302	275	246	211	170	128	87	54	31	17	10	7	6	5	6	6	7	8	9	9	9	10
23	377	353	330	306	280	250	214	173	130	89	55	31	17	10	6	5	5	5	5	6	6	7	8	8	8
24	377	354	332	309	283	254	218	176	132	90	56	32	17	9	6	5	4	4	5	5	5	6	6	7	7
25	377	355	334	312	287	257	221	179	134	91	57	32	17	9	6	4	4	4	4	4	5	5	5	5	4

T=300s

PORFHOR DELFT UNIVERSITY OF TECHNOLOGY   PROJECT: SHANGHAI   RUN: .   with secondary flow
500*500 MET SEDIMENT
TIME= 600. SEC

VARIABLE: CS   UNIT: 0.1000E-05

	1	2	3	4	5	6	7	8	9	10	11	12	13	14	15	16	17	18	19	20	21	22	23	24	25
1																									
2						C	0	0	0	0	0	0	0	0	0	0	0	0	0	C					
3						C	0	0	0	0	0	0	0	0	0	0	0	0	0	C					
4						C	0	0	0	0	0	0	0	0	0	0	0	0	0	C					
5						C	0	0	0	0	0	0	0	0	0	0	0	0	0	C					
6						C	0	0	0	0	0	0	0	0	0	0	0	0	0	C					
7						C	0	0	0	0	0	0	0	0	0	0	0	0	0	C					
8						C	0	0	0	0	0	0	0	0	0	0	0	0	0	C					
9						C	0	0	0	0	0	0	0	0	0	0	0	0	0	C					
10						C	0	0	0	0	0	0	0	0	0	0	0	0	0	C					
11						C	1	1	0	0	0	0	0	0	0	0	0	0	0	C					
12						[illegible]	3	3	2	1	0	0	0	0	0	0	0	0	0	C					
13						8	13	12	8	4	2	1	0	0	0	0	0	0	0	C					
14						23	38	37	27	16	8	3	1	0	0	0	0	0	0	C					
15						61	88	84	65	41	22	10	4	1	0	0	0	0	0	[illegible]					
16						161	163	146	114	78	46	25	12	5	3	1	1	1	2	14					
17	377	346	317	294	280	266	241	199	147	98	59	32	17	9	5	3	3	4	7	[illegible]	28	21	17	15	14
18	377	348	321	297	272	244	210	168	122	60	48	26	14	7	5	4	4	6	9	[illegible]	30	28	25	22	[illegible]
19	377	348	322	296	270	241	207	168	125	84	51	29	16	9	6	5	5	7	9	16	21	22	20	19	18
20	377	349	323	297	270	241	207	167	125	65	52	30	16	10	7	6	6	6	8	11	14	15	15	15	15
21	377	350	325	299	273	243	208	168	126	86	53	30	17	10	7	6	6	6	7	8	10	11	12	12	12
22	377	352	327	302	275	246	211	170	128	87	54	31	17	10	7	6	5	6	6	7	8	9	9	9	10
23	377	353	330	306	280	250	214	173	130	89	55	31	17	10	6	5	5	5	5	6	6	7	8	8	8
24	377	354	332	309	283	254	218	176	132	90	56	32	17	9	6	5	4	4	5	5	5	6	6	7	7
25	377	355	334	312	287	257	221	179	134	91	57	32	17	9	6	4	4	4	4	4	5	5	5	5	4

T=300s

4.17

Influence of secondary flow

INFLUENCE OF SECONDARY FLOW (see Fig. 4.17)

As described in appendix A, secondary flow is a typical three-dimensional phenomenon, and can't be described by a two-dimensional model. However, its influence on the sedimentation-pattern could be significant; at the bottom of a circular flow, a net inward movement results from the secondary effect.

According to appendix A, the secondary flow-component can be approximated by:

$$U_n = 2 \frac{|\bar{U}_s| h}{\kappa^2 R_s} \cdot f_b \left(\frac{z}{h}, \alpha\right) \qquad (25)$$

$$\alpha = \frac{\sqrt{g}}{\kappa C}$$

U_n = secondary flow component [m/s]
$\bar{U}_s$ = average main flow component [m/s]
h = waterdepth [m]
κ = constant of Von Karman = 0.4
g = acceleration of gravity [m/s2]
C = Chézy roughness parameter [$\sqrt{m}$/s]
R_s = radius of curvature of the main flow [m]
f_b = function which describes the profile of the secondary flow-component as a function of the waterdepth, here it is taken a linear function with $f_{b,max}$ = 0.5.

Assuming $|\bar{U}_s| \approx 0.6$ m/s; $h \approx 2$ m;
$C = 50\sqrt{m}$/s; R_s = 125, 250 and 500 m (radius of the eddy), the secondary flow-component at the bottom is in the order of:

U_n = 0.06 m/s (lay-out 250 * 250 m)
U_n = 0.03 m/s (lay-out 500 * 500 m)
U_n = 0.015 m/s (lay-out 1,000 * 1,000 m).

This normal velocity causes a fluid exchange (outward at the upper half of the eddy, inward along the bottom) of:

$$E_{sec.flow} \approx \tfrac{1}{2}\, u_{n,max} \cdot \tfrac{1}{2}\, h \qquad (27)$$

and

$E_{sec.flow}$ = 0.03 m2/s (lay-out 250 x 250)

$E_{sec.flow}$ = 0.015 m2/s (lay-out 500 x 500)

$E_{sec.flow}$ = 0.008 m2/s (lay-out 1,000 x 1,000)

These values are comparable to the exchange of fluid caused by the turbulent viscosity (E = 0.04 m2/s), especially in case of the smaller lay-out.

The effect on the concentration of sediments however, is hardly noticeable. The effect on the transports of sediment is noticeable, but still of a very small order (see table 4.11 and Fig. 4.17).
It seems that for the determination of the sedimentation pattern the subtle deviations of the main flow velocity are negligible. Eq. (25) shows that the main parameters are the main flow velocity $\bar{u}$, the waterdepth h and the radius of curvature R_s.
So for deep water, and strongly curved flows, where the average velocity is large, the influence of secondary flow can be very important, and also the movement of the sediments will be strongly influenced. This will be the case for riverbends, flows through pipelines, etc.

CONCLUSION

In case of shallow and slowmoving eddies, the influence of secondary flow can be neglected with respect to the sedimentation pattern. A small calculation however, is necessary in order to estimate the influence, before neglecting it.

influence of secondary flow		secondary flow	no secondary flow
- point E	C [-]	$88 \cdot 10^{-6}$	$88 \cdot 10^{-6}$
	Tx [m2/s]	$18 \cdot 10^{-6}$	$18 \cdot 10^{-6}$
	Ty [m2/s]	$-63 \cdot 10^{-6}$	$-65 \cdot 10^{-6}$

Table 4.11: values of C, Tx and Ty as found in point E, where the main flow is strongly curved at T = 600 s

MORPHOR DELFT UNIVERSITY OF TECHNOLOGY PROJECT: SHANGHAI RUN: 4 Zero order
500*500 WET SEDIMENT
TIME= 600. SEC

VARIABLE: CS UNIT: 0.1000E-05

	1	2	3	4	5	6	7	8	9	10	11	12	13	14	15	16	17	18	19	20	21	22	23	24	25
1																									
						C	0	0	0	0	0	0	0	0	0	0	0	0	0	0					
						C	0	0	0	0	0	0	0	0	0	0	0	0	0	0					
4						C	0	0	0	0	0	0	0	0	0	0	0	0	0	0					
						C	0	0	0	0	0	0	0	0	0	0	0	0	0	0					
						C	0	0	0	0	0	0	0	0	0	0	0	0	0	0					
7						C	0	0	0	0	0	0	0	0	0	0	0	0	0	0					
						C	0	0	0	0	0	0	0	0	0	0	0	0	0	0					
						C	0	0	0	0	0	0	0	0	0	0	0	0	0	0					
10						C	0	0	0	0	0	0	0	0	0	0	0	0	0	0					
						C	0	0	0	0	0	0	0	0	0	0	0	0	0	0					
						C	0	0	0	0	0	0	0	0	0	0	0	0	0	0					
13						C	0	0	0	0	0	0	0	0	0	0	0	0	0	0					
						C	0	0	0	0	0	0	0	0	0	0	0	0	0	0					
						C	0	0	0	0	0	0	0	0	0	0	0	0	0	19					
16						C	14	49	53	41	29	20	14	11	9	8	8	11	10	125					
	377	142	142	153	215	308	279	182	106	62	40	28	22	18	16	17	19	32	47	284	81	49	43	46	48
	377	138	140	141	135	112	76	48	32	25	20	18	18	18	19	23	29	44	60	177	152	121	99	90	88
19	377	110	109	107	102	93	81	66	53	43	36	31	29	28	28	31	36	47	57	102	116	108	96	89	87
	377	88	87	85	80	73	65	56	48	41	36	33	31	30	31	34	38	46	52	71	86	88	84	80	79
	377	72	71	69	65	62	57	52	46	41	37	34	33	32	33	35	38	44	48	58	68	73	73	72	72
22	377	61	60	59	57	54	51	47	44	40	37	35	34	33	34	35	38	42	45	51	56	63	65	66	66
	377	53	52	52	51	49	46	44	42	39	36	34	33	33	33	35	37	39	43	46	51	55	58	60	61
	377	48	47	47	45	45	43	41	39	37	35	33	32	32	32	33	35	37	40	43	46	50	53	56	57
25	377	44	43	43	42	41	40	38	37	35	34	32	31	31	31	32	34	36	38	40	42	44	44	41	38

T=600s

MORPHOR DELFT UNIVERSITY OF TECHNOLOGY PROJECT: SHANGHAI RUN: 4
500*500 WET SEDIMENT
TIME= 1200. SEC

VARIABLE: CS UNIT: 0.1000E-05

	1	2	3	4	5	6	7	8	9	10	11	12	13	14	15	16	17	18	19	20	21	22	23	24	25
1																									
						C	0	0	0	0	0	0	0	0	0	0	0	0	0	0					
						C	0	0	0	0	0	0	0	0	0	0	0	0	0	0					
4						C	0	0	0	0	0	0	0	0	0	0	0	0	0	0					
						C	0	0	0	0	0	0	0	0	0	0	0	0	0	0					
						C	0	0	0	0	0	0	0	0	0	0	0	0	0	0					
7						C	0	0	0	0	0	0	0	0	0	0	0	0	0	0					
						C	0	0	0	0	0	0	0	0	0	0	0	0	0	0					
						C	0	0	0	0	0	0	0	0	0	0	0	0	0	0					
10						C	0	0	0	0	0	0	0	0	0	0	0	0	0	0					
						C	0	0	0	0	0	0	0	0	0	0	0	0	0	0					
						C	0	0	0	0	0	0	0	0	0	0	0	0	0	0					
13						C	0	0	0	0	0	0	0	0	0	0	0	0	0	0					
						C	0	0	0	0	3	5	4	2	0	0	0	0	0	0					
						C	0	0	8	46	66	61	49	34	24	14	8	3	4	13					
16						C	17	121	256	307	269	201	145	104	60	63	55	57	69	251					
	377	436	431	431	445	510	608	658	598	459	320	216	153	113	93	82	83	115	120	757	306	116	39	18	13
	377	435	431	431	443	463	464	419	340	261	201	161	135	117	106	103	106	150	152	372	453	434	359	291	265
19	377	406	410	416	418	406	383	355	323	288	255	226	204	187	174	170	167	193	205	265	332	375	386	369	354
	377	367	367	367	365	356	341	323	300	272	244	220	201	187	178	178	180	196	219	253	286	310	329	338	337
	377	326	325	324	320	312	301	288	273	255	238	222	210	200	194	194	198	208	227	254	279	293	304	318	323
22	377	293	292	290	287	281	273	264	253	242	230	220	211	205	202	203	208	217	230	251	273	287	297	310	316
	377	270	268	266	263	259	254	247	239	231	224	217	211	207	206	208	213	222	232	247	264	280	293	305	311
	377	252	251	249	245	244	240	235	230	224	218	213	209	206	206	208	214	222	232	243	257	273	286	298	306
25	377	238	237	236	233	232	229	225	221	216	212	209	206	205	206	209	214	221	231	236	248	263	279	287	289

T=1200s

TIME= 1800. SEC

VARIABLE: CS UNIT: 0.1000E-05

	1	2	3	4	5	6	7	8	9	10	11	12	13	14	15	16	17	18	19	20	21	22	23	24	25
1																									
						C	0	0	0	0	0	0	0	0	0	0	0	0	0	0					
						C	0	0	0	0	0	0	0	0	0	0	0	0	0	0					
4						C	0	0	0	0	0	0	0	0	0	0	0	0	0	0					
						C	0	0	0	0	0	0	0	0	0	0	0	0	0	0					
						C	0	0	0	0	0	0	0	0	0	0	0	0	0	0					
7						C	0	0	0	0	0	0	0	0	0	0	0	0	0	0					
						C	0	0	0	0	0	0	0	0	0	0	0	0	0	0					
						C	0	0	0	0	0	0	0	0	0	0	0	0	0	0					
10						C	0	0	0	0	0	0	0	0	0	0	0	0	0	0					
						C	0	0	0	0	0	0	0	0	0	0	0	0	0	0					
						C	0	0	0	0	0	0	0	0	0	0	0	0	0	0					
13						C	0	0	0	0	0	0	0	0	0	0	0	0	0	0					
						C	0	0	0	0	0	0	1	4	3	1	0	0	0	0					
						C	0	0	0	3	18	42	61	61	50	31	15	3	0	0					
16						C	0	8	52	125	205	257	265	226	182	125	92	55	54	104					
	377	508	505	505	522	537	520	513	531	551	542	486	402	309	241	178	150	141	128	581	353	194	111	74	57
	377	479	483	493	502	496	476	460	452	436	404	353	300	251	216	188	171	186	184	328	435	434	381	344	329
19	377	495	494	492	489	482	470	458	444	425	401	371	339	308	280	261	248	253	265	313	381	412	408	396	388
	377	484	482	491	482	477	465	449	433	417	398	377	353	331	310	295	286	288	298	325	364	393	401	399	396
	377	473	470	468	465	461	452	439	426	412	396	378	360	343	328	318	313	316	325	339	362	384	396	403	405
22	377	459	456	454	451	446	438	428	416	404	391	377	364	351	341	334	330	333	341	353	367	381	394	405	411
	377	445	443	441	437	433	427	419	409	398	387	376	366	357	349	344	342	344	350	361	372	382	394	408	416
	377	433	431	430	425	422	417	411	403	394	384	375	367	360	354	350	349	351	356	363	372	383	396	412	422
25	377	417	416	415	413	409	405	401	394	386	378	371	365	359	355	352	352	355	359	365	374	386	400	410	415

T=1800s

MORPHOR DELFT UNIVERSITY OF TECHNOLOGY PROJECT: SHANGHAI RUN: 4 first order
500*500 WET SEDIMENT
TIME= 1800. SEC

VARIABLE: CS UNIT: 0.1000E-05

	1	2	3	4	5	6	7	8	9	10	11	12	13	14	15	16	17	18	19	20	21	22	23	24	25
1																									
						C	0	0	0	0	0	0	0	0	0	0	0	0	0	0					
						C	0	0	0	0	0	0	0	0	0	0	0	0	0	0					
4						C	0	0	0	0	0	0	0	0	0	0	0	0	0	0					
						C	0	0	0	0	0	0	0	0	0	0	0	0	0	0					
						C	0	0	1	1	1	2	2	1	1	1	0	0	0	0					
7						C	1	1	2	3	4	5	5	5	4	3	1	1	0	0					
						1	2	3	6	8	11	13	14	14	11	8	5	2	1	0					
						2	4	8	13	19	25	31	33	32	27	20	13	7	3	1					
10						4	8	15	25	37	49	59	64	62	54	43	29	16	7	3					
						6	13	24	41	62	82	96	103	102	93	77	56	34	17	7					
						9	18	34	58	87	113	131	142	144	136	118	92	62	34	15					
13						13	22	39	67	100	129	154	171	179	175	160	134	98	59	27					
						22	28	43	66	95	129	166	196	212	213	201	176	139	93	45					
						54	56	64	80	106	153	202	241	260	262	247	220	180	124	61					
16						173	171	168	181	216	264	307	334	339	330	306	275	230	181	108					
	377	392	404	414	424	421	418	416	420	428	435	435	424	405	380	351	320	281	249	220	236	234	223	209	196
	377	388	358	407	416	423	427	429	431	432	430	424	412	396	377	356	334	309	289	272	280	288	290	287	286
19	377	388	397	405	412	417	420	423	425	424	422	417	409	398	385	371	355	339	325	313	312	316	320	321	324
	377	386	394	400	405	411	414	415	416	415	413	409	403	395	366	376	364	353	343	335	332	332	334	335	337
	377	385	391	396	400	403	406	407	407	406	404	400	396	390	383	375	367	359	352	346	343	341	341	342	343
22	377	383	388	392	394	397	398	399	398	397	395	392	388	384	378	372	366	360	355	350	347	345	344	345	345
	377	382	385	388	390	391	392	392	392	390	388	386	383	379	374	369	364	360	355	351	349	347	345	345	346
	377	381	383	385	385	387	387	387	386	385	383	381	378	375	371	367	363	358	355	351	348	346	345	345	346
25	377	379	381	382	383	383	383	383	382	381	379	377	374	371	368	365	361	357	354	351	348	346	345	345	345

T=1800 s

MORPHOR DELFT UNIVERSITY OF TECHNOLOGY PROJECT: SHANGHAI RUN: 4 zero order
500*500 MET SEDIMENT
TIME= 2400. SEC

VARIABLE: CS UNIT: 0.1000E-05

	1	2	3	4	5	6	7	8	9	10	11	12	13	14	15	16	17	18	19	20	21	22	23	24	25
1																									
						C	0	0	0	0	0	0	0	0	0	0	0	0	0	0					
						C	0	0	0	0	0	0	0	0	0	0	0	0	0	0					
4						C	0	0	0	0	0	0	0	0	0	0	0	0	0	0					
						C	0	0	0	0	0	0	0	0	0	0	0	0	0	0					
						C	0	0	0	0	0	0	0	0	0	0	0	0	0	0					
7						C	0	0	0	0	0	0	0	0	0	0	0	0	0	0					
						C	0	0	0	0	0	0	0	0	0	0	0	0	0	0					
						C	0	0	0	0	0	0	0	0	0	0	0	0	0	0					
10						C	0	0	0	0	0	0	0	0	0	0	0	0	0	0					
						C	0	0	0	0	0	0	0	0	0	0	0	0	0	0					
						C	0	0	0	0	0	0	0	0	0	0	0	0	0	0					
13						C	0	0	0	0	0	0	0	0	0	0	0	0	0	0					
						C	0	0	0	0	0	0	0	0	0	0	0	0	0	0					
						C	0	0	0	0	1	8	18	26	31	28	19	7	0	0					
16						C	0	6	30	63	100	135	165	180	166	163	142	81	63	28					
	377	538	538	547	575	599	591	575	557	529	497	461	429	390	352	299	259	225	189	463	391	275	195	159	143
	377	543	545	550	559	555	527	488	447	408	376	348	324	298	272	248	224	223	220	313	410	429	400	375	366
19	377	541	540	540	541	535	516	491	465	441	419	397	375	353	332	314	300	296	301	332	382	409	412	405	399
	377	545	544	542	539	529	515	496	475	455	436	418	399	380	363	349	340	339	347	366	393	413	421	421	419
	377	538	536	533	529	522	512	497	480	463	447	432	417	403	390	381	375	374	380	392	409	425	434	439	440
22	377	534	532	529	524	517	509	498	484	470	457	444	432	421	411	404	401	401	406	414	424	435	446	454	457
	377	532	530	527	522	516	509	500	489	478	466	455	444	435	428	423	421	422	426	432	437	445	455	465	471
	377	528	526	524	520	515	508	501	492	483	473	463	454	446	440	436	434	435	438	444	450	457	465	476	483
25	377	515	514	513	511	506	500	494	488	480	471	463	455	449	444	442	442	443	445	451	459	465	470	476	460

T= 2400 s

MORPHOR DELFT UNIVERSITY OF TECHNOLOGY PROJECT: SHANGHAI RUN: 4
500*500 MET SEDIMENT
TIME= 3000. SEC

VARIABLE: CS UNIT: 0.1000E-05

	1	2	3	4	5	6	7	8	9	10	11	12	13	14	15	16	17	18	19	20	21	22	23	24	25
1																									
						C	0	0	0	0	0	0	0	0	0	0	0	0	0	0					
						C	0	0	0	0	0	0	0	0	0	0	0	0	0	0					
4						C	0	0	0	0	0	0	0	0	0	0	0	0	0	0					
						C	0	0	0	0	0	0	0	0	0	0	0	0	0	0					
						C	0	0	0	0	0	0	0	0	0	0	0	0	0	0					
7						C	0	0	0	0	0	0	0	0	0	0	0	0	0	0					
						C	0	0	0	0	0	0	0	0	0	0	0	0	0	0					
						C	0	0	0	0	0	0	0	0	0	0	0	0	0	0					
10						C	0	0	0	0	0	0	0	0	0	0	0	0	0	0					
						C	0	0	0	0	0	0	0	0	0	0	0	0	0	0					
						C	0	0	0	0	0	0	0	0	0	0	0	0	0	0					
13						C	0	0	0	0	0	0	0	0	0	0	0	0	0	0					
						C	0	0	0	0	0	0	0	0	0	0	0	0	0	0					
						C	0	0	0	0	0	2	8	15	19	18	12	6	0	0					
16						C	0	7	33	69	108	143	171	181	182	157	140	89	70	23					
	377	539	539	546	573	602	598	579	556	529	501	467	432	389	349	303	267	244	216	480	417	309	230	196	181
	377	535	535	540	547	543	516	481	446	414	384	355	326	299	274	253	235	236	236	335	431	449	419	395	386
19	377	542	543	543	542	535	518	495	471	445	421	398	376	357	338	323	310	309	315	350	400	427	429	420	415
	377	547	546	543	537	528	516	499	480	460	440	421	403	387	372	361	354	354	363	383	409	428	436	437	436
	377	546	544	541	536	528	518	505	490	473	457	442	428	415	403	394	390	391	399	413	428	441	450	456	459
22	377	546	544	542	537	530	522	512	499	486	472	459	448	437	429	422	413	421	427	437	447	458	467	476	479
	377	548	546	544	540	534	527	518	508	497	486	475	465	457	450	446	444	446	450	457	466	475	485	494	498
	377	547	546	544	541	536	530	522	514	505	496	487	478	471	465	462	461	464	468	474	482	491	499	509	516
25	377	536	536	534	532	525	523	517	510	504	496	489	482	476	472	470	471	473	478	488	492	500	506	511	515

T= 3000 s

MORPHOR DELFT UNIVERSITY OF TECHNOLOGY PROJECT: SHANGHAI RUN: 4
500*500 MET SEDIMENT
TIME= 3600. SEC

VARIABLE: CS UNIT: 0.1000E-05

	1	2	3	4	5	6	7	8	9	10	11	12	13	14	15	16	17	18	19	20	21	22	23	24	25
1																									
						C	0	0	0	0	0	0	0	0	0	0	0	0	0	0					
						C	0	0	0	0	0	0	0	0	0	0	0	0	0	0					
4						C	0	0	0	0	0	0	0	0	0	0	0	0	0	0					
						C	0	0	0	0	0	0	0	0	0	0	0	0	0	0					
						C	0	0	0	0	0	0	0	0	0	0	0	0	0	0					
7						C	0	0	0	0	0	0	0	0	0	0	0	0	0	0					
						C	0	0	0	0	0	0	0	0	0	0	0	0	0	0					
						C	0	0	0	0	0	0	0	0	0	0	0	0	0	0					
10						C	0	0	0	0	0	0	0	0	0	0	0	0	0	0					
						C	0	0	0	0	0	0	0	0	0	0	0	0	0	0					
						C	0	0	0	0	0	0	0	0	0	0	0	0	0	0					
13						C	0	0	0	0	0	0	0	0	0	0	0	0	0	0					
						C	0	0	0	0	0	0	0	0	0	0	0	0	0	0					
						C	0	0	0	0	0	0	3	9	14	16	11	5	0	0					
16						C	0	4	24	54	87	118	144	158	165	150	138	92	73	21					
	377	502	500	505	529	553	552	538	522	501	478	450	420	383	349	308	276	253	220	467	414	313	236	202	186
	377	504	505	508	513	505	488	459	428	398	369	342	317	294	273	254	236	238	237	330	421	439	412	389	381
19	377	512	512	512	510	503	489	469	447	425	404	385	366	349	332	319	307	307	314	387	394	417	419	412	407
	377	515	514	512	509	502	491	477	461	443	426	409	393	379	366	356	350	350	359	379	405	421	428	429	428
	377	519	517	515	511	504	494	483	470	457	443	429	416	404	395	388	385	387	394	407	423	436	444	450	452
22	377	522	520	518	514	508	500	491	481	470	458	447	437	428	421	416	414	416	422	431	443	453	463	470	474
	377	527	525	523	519	514	508	500	492	482	473	464	456	448	443	439	438	440	445	453	462	472	481	489	494
	377	527	526	525	522	518	513	507	500	492	484	476	469	463	459	456	456	458	463	470	478	487	495	506	512
25	377	518	518	516	515	512	508	503	497	491	485	479	474	469	466	465	466	469	474	480	488	495	503	510	513

T= 3600 s

MORPHOR DELFT UNIVERSITY OF TECHNOLOGY PROJECT: SHANGHAI RUN: 4 first order
500*500 MET SEDIMENT
TIME= 3600. SEC

VARIABLE: CS UNIT: 0.1000E-05

	1	2	3	4	5	6	7	8	9	10	11	12	13	14	15	16	17	18	19	20	21	22	23	24	25
1																									
						0	0	0	0	0	0	1	1	1	1	1	2	2	2	2					
						C	0	0	0	1	1	1	1	2	2	3	4	4	4	5					
4						C	0	1	1	1	2	2	3	4	5	6	8	9	10	11					
						C	1	1	2	2	3	4	6	7	10	12	14	17	19	20					
						1	1	2	3	4	6	7	10	13	16	20	23	27	29	31					
7						1	2	3	4	6	9	12	15	19	24	29	33	37	40	42					
						2	3	4	6	9	12	16	21	27	32	38	43	48	51	53					
						2	3	5	8	12	16	21	27	34	41	47	53	59	62	64					
10						3	4	7	10	14	19	25	32	40	48	56	64	70	74	76					
						4	6	8	12	16	21	27	35	44	55	65	75	82	87	89					
						7	8	11	14	19	24	30	37	49	63	77	88	96	101	103					
13						13	15	18	22	27	33	40	50	65	80	94	106	114	119	119					
						31	34	39	47	54	63	73	86	100	114	126	134	139	139	137					
						78	88	98	112	126	139	150	161	170	178	182	183	179	168	159					
16						203	219	232	244	253	263	271	278	281	283	277	270	249	228	189					
	377	390	402	414	425	428	431	433	434	432	429	423	416	406	394	379	363	339	320	292	306	309	305	298	291
	377	389	400	411	422	430	436	439	439	436	431	425	417	407	397	386	373	360	348	337	341	348	352	352	353
19	377	389	400	410	419	427	433	437	438	438	436	432	428	421	414	407	398	389	381	374	374	376	379	381	383
	377	388	398	408	416	424	430	434	437	438	438	437	434	430	426	421	415	410	405	401	400	401	403	404	406
	377	387	397	406	414	421	427	432	435	438	439	439	438	436	434	431	428	425	422	420	420	421	422	424	426
22	377	387	396	405	412	419	425	430	435	438	440	441	441	441	440	438	437	436	435	434	435	436	438	440	442
	377	386	395	404	411	418	424	429	434	437	440	442	443	444	444	444	444	444	444	445	446	447	450	452	455
	377	386	394	402	409	416	422	428	432	436	439	442	444	445	446	447	448	449	450	451	452	455	457	460	463
25	377	385	392	400	406	413	419	424	429	433	436	439	442	444	445	447	448	450	451	453	455	457	460	463	466

T= 3600 s

4.18

Influence of the order of the model

INFLUENCE OF THE ORDER OF THE MODEL (see Fig. 4.18)

The model MORPHOR is based on an asymptotic shape of the concentration profile. This shape can be approximated by order zero or higher. A zero order solution indicates that the calculated concentration profile is identical to the equilibrium profile, as found by using the equations of Van Rijn (Appendix B).
Higher order approximations take into account a time and a distance, necessary for a momentane profile to adapt to this equilibrium profile.
As already pointed out in chapter 3, it is considered necessary to apply a first order approximation in this analysis.
In order to investigate this assumption a numerical simulation has been done with a zero order approximation. The results are shown in Fig. 4.18 and in table 4.12.

It shows that the order of the approximation is significant for the sedimentation inside the basins. A zero order approximation (mostly used in the conventional morphological programs) would never result in any accretion in the basins and is in fact unusable in this kind of sedimentation prediction.

CONCLUSION

The order of the asymptotic approximation is of significant importance. It emphasizes the importance of models like MORPHOR to predict the suspended load transport of two-dimensional problems.

influence of order N		first order	zero order
- point A	C [-]	$438 \cdot 10^{-6}$	$416 \cdot 10^{-6}$
	Tx [m2/s]	$2{,}482 \cdot 10^{-6}$	$2{,}359 \cdot 10^{-6}$
	Ty [m2/s]	$-52 \cdot 10^{-6}$	$-50 \cdot 10^{-6}$
- point B	C [-]	$161 \cdot 10^{-6}$	$3 \cdot 10^{-6}$
	Tx [m2/s]	$209 \cdot 10^{-6}$	$8 \cdot 10^{-6}$
	Ty [m2/s]	$-35 \cdot 10^{-6}$	$-53 \cdot 10^{-6}$
- point C	C [-]	$32 \cdot 10^{-6}$	$0 \cdot 10^{-6}$
	Tx [m2/s]	$-12 \cdot 10^{-6}$	$0 \cdot 10^{-6}$
	Ty [m2/s]	$2 \cdot 10^{-6}$	$0 \cdot 10^{-6}$
- point D	C [-]	$1 \cdot 10^{-6}$	$0 \cdot 10^{-6}$
	Tx [m2/s]	$0 \cdot 10^{-6}$	$0 \cdot 10^{-6}$
	Ty [m2/s]	$0 \cdot 10^{-6}$	$0 \cdot 10^{-6}$
- point E	C [-]	$88 \cdot 10^{-6}$	$0 \cdot 10^{-6}$
	Tx [m2/s]	$8 \cdot 10^{-6}$	$0 \cdot 10^{-6}$
	Ty [m2/s]	$0 \cdot 10^{-6}$	$0 \cdot 10^{-6}$
- point F	C [-]	$3 \cdot 10^{-6}$	$0 \cdot 10^{-6}$
	Tx [m2/s]	$-1 \cdot 10^{-6}$	$0 \cdot 10^{-6}$
	Ty [m2/s]	$1 \cdot 10^{-6}$	$0 \cdot 10^{-6}$
- point G	C [-]	$168 \cdot 10^{-6}$	$0 \cdot 10^{-6}$
	Tx [m2/s]	$205 \cdot 10^{-6}$	$3 \cdot 10^{-6}$
	Ty [m2/s]	$35 \cdot 10^{-6}$	$9 \cdot 10^{-6}$
- point H	C [-]	$74 \cdot 10^{-6}$	$0 \cdot 10^{-6}$
	Tx [m2/s]	$-11 \cdot 10^{-6}$	$0 \cdot 10^{-6}$
	Ty [m2/s]	$-45 \cdot 10^{-6}$	$0 \cdot 10^{-6}$

Table 4.12: values of C, Tx and Ty found for a zero order approximation and a first order approximation, for T = 3,600 s and a lay-out of 500 x 500 m

INFLUENCE OF THE TRANSPORT FORMULA

In this analysis the approach of Van Rijn (Appendix B) has been used to determine the equilibrium concentration profile.
In order to investigate the suitability of these formulas, calculations can be made using other approaches, and the results can be compared.
In this comparison the following approaches have been used:

- the results of MORPHOR;

- the formulas according to Van Rijn (Appendix B);

- the formulas according to Bijker (lit. 18);

- the formulas according to Engelund and Hansen (lit. (8), (18)).

Bijker uses the modified Kalinske-Frijlink formula:

$$S_b = \frac{B D_{50}\, \bar{u}\sqrt{g}}{C} \exp\left[\frac{-0.27\, \Delta\, \rho g\, D_{50}}{\mu \tau_c \left(1 + \frac{1}{2}\left(\xi \frac{\hat{u}_b}{u}\right)^2\right)}\right] \quad \ldots\ldots\ldots\ldots (28)$$

in which

B	=	dimensionless coefficient varying from 1 to 5	[-]
$\underline{S}_b$	=	bottom sediment transport	[m2/s]
u	=	average flow velocity	[m/s]
g	=	acceleration of gravity	[m/s2]
C	=	Chézy roughness parameter	[√m/s]
Δ	=	relative density = $(\rho s - \rho w)/\rho w$	[-]
ρ	=	density of water	[kg/m3]
D_{50}	=	average graindiameter	[m]
μ	=	ripple factor	[-]
	=	$[C/C']^{3/2}$	
C'	=	Chézy roughness parameter related to grains	
	=	$18 \log (12h/3D_{90})$	[√m/s]
τ_c	=	shear stress due to current = ρu_*^2 or $\rho g \bar{u}^2/C^2$	[N/m2]
ξ	=	wave parameter (not taken into account here)	[-]
$\hat{u}_b$	=	maximum orbital wave velocity at the bottom	[m/s]

and

$$S_s = F \cdot S_b \quad \ldots\ldots\ldots\ldots\ldots\ldots\ldots\ldots (29)$$

in which F is dependent on the suspension parameter Z,

$Z = W_s/\kappa u_*$ (see Appendix B).

The Bijker formula is valid for grain sizes in the order of 100-500 µm. It has been developed to predict long-shore sediment transport due to waves and currents.

Engelund and Hansen give the following expression for the total load transport:

$$S = 0.083 \frac{C^2}{g} \, g \Delta D_{50}^3 \left[\frac{\Delta D_{50}}{\mu h I} \right]^{-\frac{5}{2}} \ldots\ldots\ldots\ldots\ldots (30)$$

in which:

S	= total load transport	[m2/s]
C	= Chézy roughness parameter	[√m/s]
g	= acceleration of gravity	[m/s2]
Δ	= relative density	[-]
D_{50}	= average grain size	[m]
μ	= ripple factor	[-]
h	= waterdepth	[m]
I	= slope of watersurface = $\bar{u}^2/C^2h$	[-]

For each of the control-points we can compare the values for the transport rate of each of the formulas (see <u>Fig. 4.14</u>).

The average concentration in each point can be found by

$$\bar{C} = \frac{S_{tot}}{h \, \bar{u}} = \frac{Tx}{Qx} = \frac{Ty}{Qy} \ldots\ldots\ldots\ldots\ldots\ldots\ldots (31)$$

in which

S	= the total load transport as calculated by (28), (30)	[m2/s]
h	= waterdepth	[m]
u	= average velocity	[m/s]
Tx,Ty	= sediment transport in x,y direction	[m2/s]
Qx,Qy	= water discharge in x,y direction	[m2/s]

The comparison is given in table 4.13.

CONCLUSION

The transport formula of Engelund and Hansen underestimates the sediment concentration of fine graded materials in a steady flow, whereas the Bijker formula and Van Rijn's equation give more or less the same values for the main flow concentration.
Van Rijn assumes the existence of a critical shear stress, thus no transport of sediments possible for low velocity values; Bijker not includes such a phenomenon.
Since the theories on which the Bijker formula and Van Rijn's formulas are based are much alike it is expected that the results of both theories, when applied in MORPHOR, will result in an analogous sedimentation pattern. So for a comparison of the lay-out models, the formulas of Van Rijn (or Bijker) give comparable results.

	DUCHESS			MORPHOR	VAN RIJN	BIJKER	E/H
point A	h	4.615	$\bar{C}$	438.10^{-6}	370.10^{-6}	507.10^{-6}	$88.7\ .10^{-6}$
$\bar{u}$ = 1.24	Qx	5.713	Tx	$2,482.10^{-6}$	$2,113.10^{-6}$	$2,892.10^{-6}$	$50.7\ .10^{-6}$
	Qy	-0.117	Ty	-52.10^{-6}	-43.10^{-6}	-59.10^{-6}	$-10.4\ .10^{-6}$
point B	h	2.816	$\bar{C}$	161.10^{-6}	0	0	0
$\bar{u}$ = 0.15	Qx	1.296	Tx	209.10^{-6}	0	0	0
	Qy	-0.326	Ty	-35.10^{-6}	0	0	0
point C	h	2.016	$\bar{C}$	32.10^{-6}	0	0	0
$\bar{u}$ = 0.19	Qx	-0.374	Tx	-12.10^{-6}	0	0	0
	Qy	0.110	Ty	2.10^{-6}	0	0	0
point D	h	1.219	$\bar{C}$	1.10^{-6}	0	0	0
$\bar{u}$ = 0.17	Qx	-0.202	Tx	0.10^{-6}	0	0	0
	Qy	0.016	Ty	0.10^{-6}	0	0	0
point E	h	2.818	$\bar{C}$	88.10^{-6}	0	0	0
$\bar{u}$ = 0.06	Qx	-0.066	Tx	8.10^{-6}	0	0	0
	Qy	0.141	Ty	0.10^{-6}	0	0	0
point F	h	2.018	$\bar{C}$	3.10^{-6}	0	0	0
$\bar{u}$ = 0.13	Qx	-0.096	Tx	-1.10^{-6}	0	0	0
	Qy	0.248	Ty	1.10^{-6}	0	0	0
point G	h	2.824	$\bar{C}$	168.10^{-6}	0	$0.17.10^{-6}$	$0.16.10^{-6}$
$\bar{u}$ = 0.23	Qx	0.594	Tx	205.10^{-6}	0	$0.10.10^{-6}$	$0.09.10^{-6}$
	Qy	0.248	Ty	35.10^{-6}	0	$0.05.10^{-6}$	$0.05.10^{-6}$
point H	h	2.019	$\bar{C}$	74.10^{-6}	0	14.10^{-6}	$0.71.10^{-6}$
$\bar{u}$ = 0.31	Qx	-0.105	Tx	-11.10^{-6}	0	$-1.5\ .10^{-6}$	$-0.07.10^{-6}$
	Qy	-0.615	Ty	-45.10^{-6}	0	$-8.6\ .10^{-6}$	$-0.44.10^{-6}$

Table 4.13: comparison of values of $\bar{C}$, Tx and Ty as found for the different transport formulas at T = 3,600 s, for the 500 x 500 lay-out h in [m], Qx, Qy in [m2/s], C in [-] and Tx, Ty in [m2/s]

MORPHOR DELFT UNIVERSITY OF TECHNOLOGY PROJECT: SHANGHAI RUN: TEST $D_{\ell} = 100\ m^2/s$
500*500 WET SEDIMENT
TIME= 100. SEC

VARIABLE: CS UNIT: 0.1000E-05

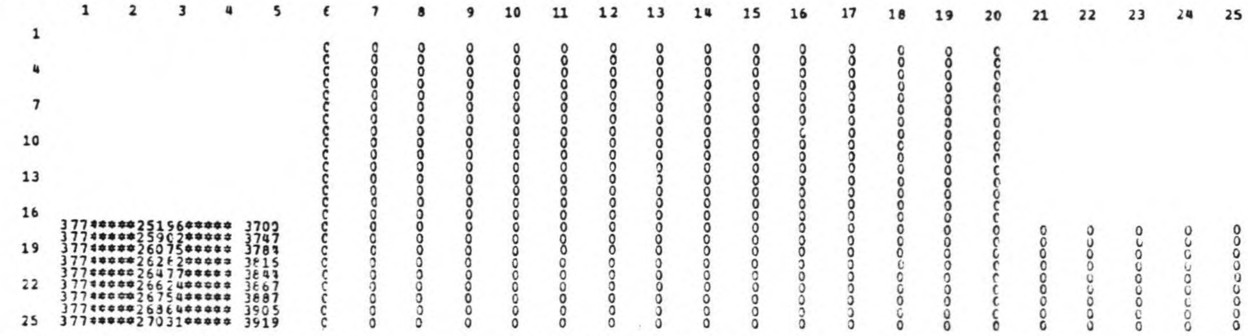

MORPHOR DELFT UNIVERSITY OF TECHNOLOGY PROJECT: SHANGHAI RUN: TEST
500*500 WET SEDIMENT
TIME= 200. SEC

VARIABLE: CS UNIT: 0.1000E-05

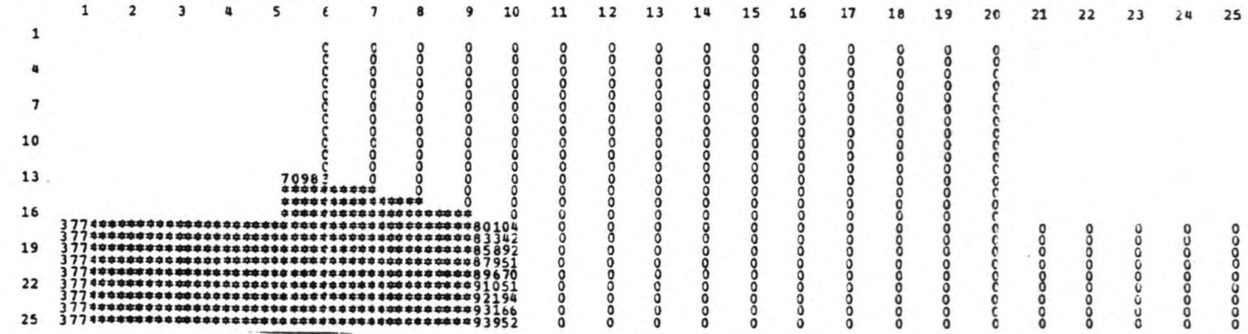

MORPHOR DELFT UNIVERSITY OF TECHNOLOGY PROJECT: SHANGHAI RUN: TEST
500*500 WET SEDIMENT
TIME= 300. SEC

VARIABLE: CS UNIT: 0.1000E-05

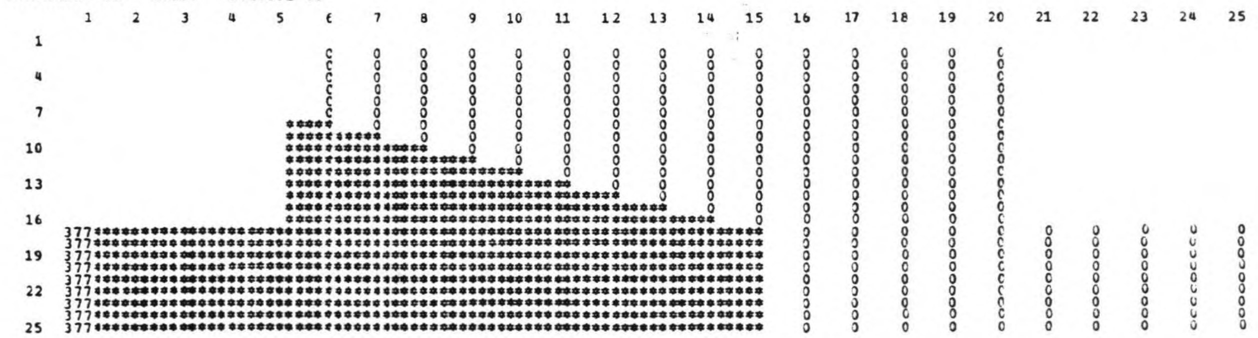

MORPHOR DELFT UNIVERSITY OF TECHNOLOGY PROJECT: SHANGHAI RUN: TEST
500*500 WET SEDIMENT
TIME= 400. SEC

VARIABLE: CS UNIT: 0.1000E-05

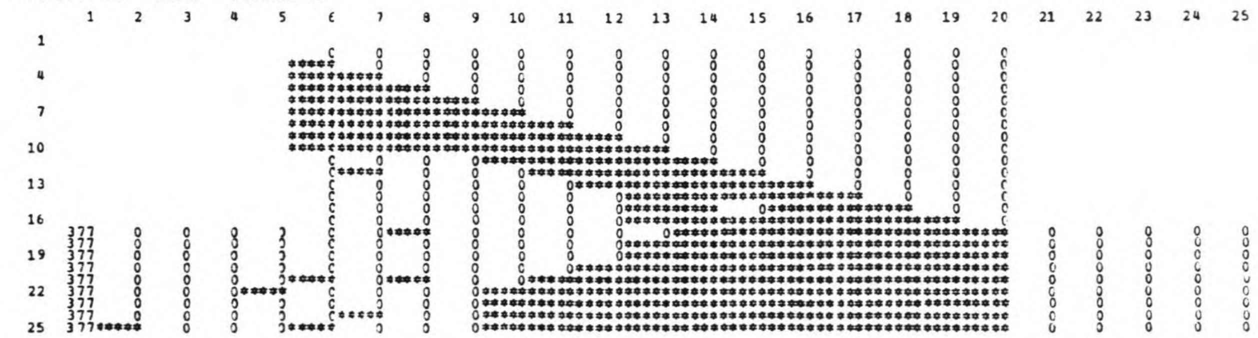

MORPHOR DELFT UNIVERSITY OF TECHNOLOGY PROJECT: SHANGHAI RUN: TEST
500*500 WET SEDIMENT
TIME= 500. SEC

VARIABLE: CS UNIT: 0.1000E-05

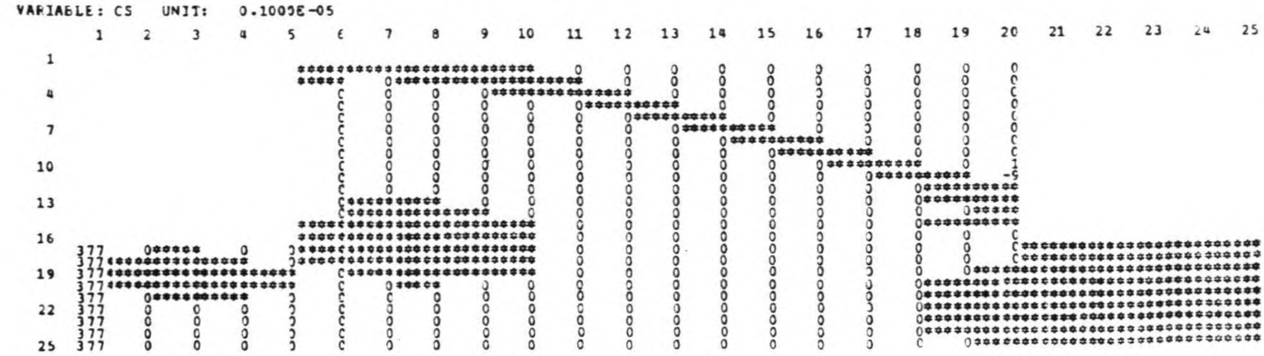

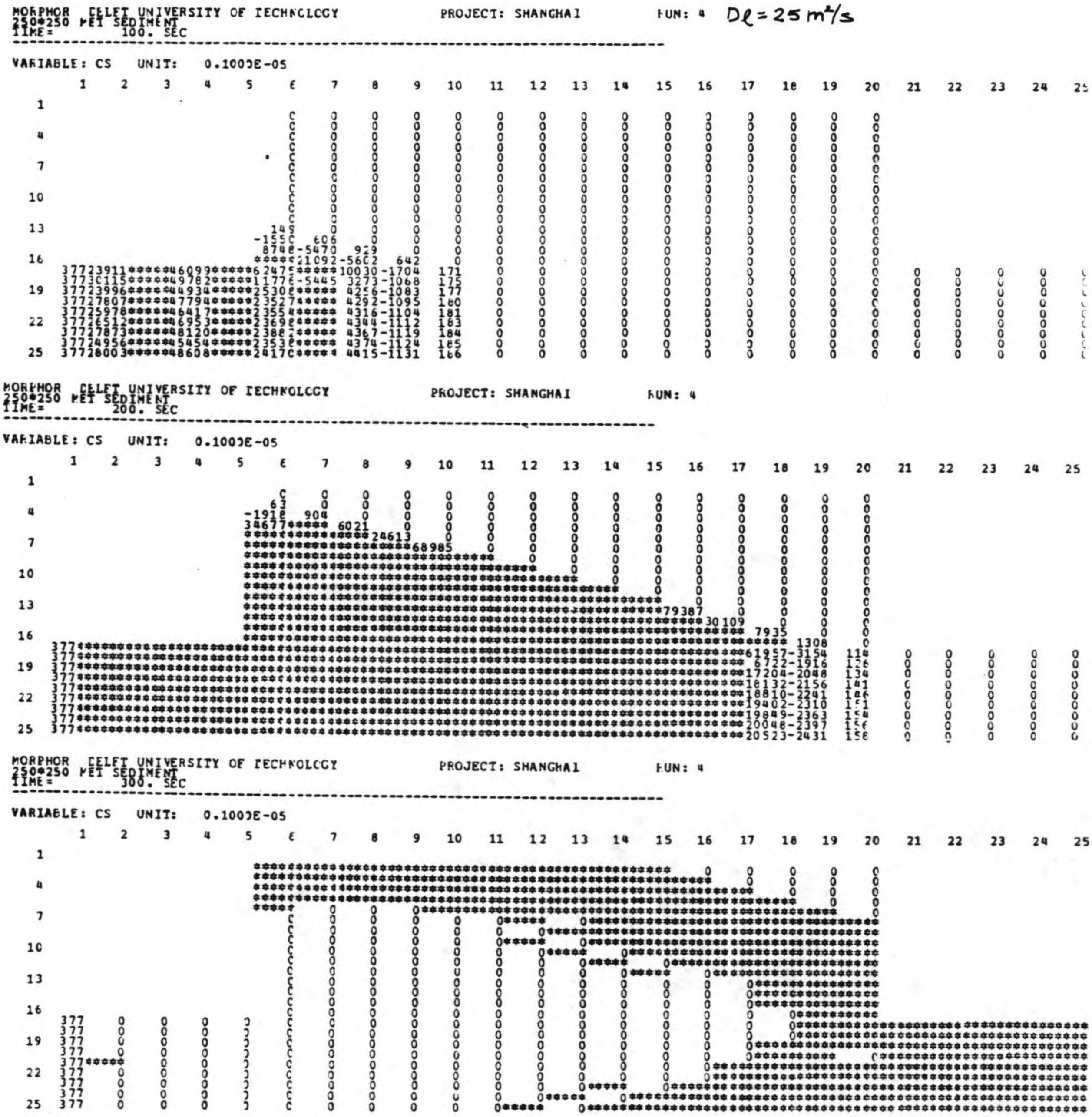

4.19

Influence of lateral diffusion

INFLUENCE OF LATERAL DIFFUSION (see Fig. 4.19)

As already pointed out in par. 3.4, the lateral diffusion is important for the stability of the calculation of the average concentration, and for the dispersion of the sediments.
In this analysis, the influence of the D_l-parameter is determined by increasing the parameter several times; it is taken D_l = 25 [m2/s] for the 500 x 500 lay-out and the 250 x 250 lay-out; and D_l = 100 m2/s for the 500 x 500 lay-out model (originally D_{500} = 2.5 and D_{250} = 1).
The results are shown in Fig. 4.19. It shows that the numerical model becomes unstable for increasing D_l-numbers, and in fact that the D_l-parameter can be chosen in a small interval only (as given in par 3.4).

CONCLUSION

The lateral diffusion parameter D_l schematizes the dispersion of the sediment in lateral direction, and can be found from an analogy with the dispersion of matter in turbulent flow. Also this parameter has to satisfy rather strict stability restrictions. As such the lateral diffusion may not be chosen too large, since this will cause instability of the calculation.

MORPHOR DELFT UNIVERSITY OF TECHNOLOGY   PROJECT: SHANGHAI   RUN: TEST (Δt = 40 s)
500*500 MET SEDIMENT
TIME=   100. SEC

VARIABLE: CS   UNIT: 0.1000E-05

	1	2	3	4	5	6	7	8	9	10	11	12	13	14	15	16	17	18	19	20	21	22	23	24	25
1																									
2						0	0	0	0	0	0	0	0	0	0	0	0	0	0	0					
3						0	0	0	0	0	0	0	0	0	0	0	0	0	0	0					
4						0	0	0	0	0	0	0	0	0	0	0	0	0	0	0					
5						0	0	0	0	0	0	0	0	0	0	0	0	0	0	0					
6						0	0	0	0	0	0	0	0	0	0	0	0	0	0	0					
7						0	0	0	0	0	0	0	0	0	0	0	0	0	0	0					
8						0	0	0	0	0	0	0	0	0	0	0	0	0	0	0					
9						0	0	0	0	0	0	0	0	0	0	0	0	0	0	0					
10						0	0	0	0	0	0	0	0	0	0	0	0	0	0	0					
11						0	0	0	0	0	0	0	0	0	0	0	0	0	0	0					
12						0	0	0	0	0	0	0	0	0	0	0	0	0	0	0					
13						0	0	0	0	0	0	0	0	0	0	0	0	0	0	0					
14						0	0	0	0	0	0	0	0	0	0	0	0	0	0	0					
15						0	0	0	0	0	0	0	0	0	0	0	0	0	0	0					
16						0	0	0	0	0	0	0	0	0	0	0	0	0	0	0					
17	377	233	125	45	15	0	0	0	0	0	0	0	0	0	0	0	0	0	0	0	0	0	0	0	0
18	377	233	126	45	15	0	0	0	0	0	0	0	0	0	0	0	0	0	0	0	0	0	0	0	0
19	377	234	127	45	15	0	0	0	0	0	0	0	0	0	0	0	0	0	0	0	0	0	0	0	0
20	377	235	127	46	17	0	0	0	0	0	0	0	0	0	0	0	0	0	0	0	0	0	0	0	0
21	377	235	128	46	17	0	0	0	0	0	0	0	0	0	0	0	0	0	0	0	0	0	0	0	0
22	377	236	128	46	17	0	0	0	0	0	0	0	0	0	0	0	0	0	0	0	0	0	0	0	0
23	377	236	129	46	17	0	0	0	0	0	0	0	0	0	0	0	0	0	0	0	0	0	0	0	0
24	377	237	129	47	17	0	0	0	0	0	0	0	0	0	0	0	0	0	0	0	0	0	0	0	0
25	377	237	129	47	17	0	0	0	0	0	0	0	0	0	0	0	0	0	0	0	0	0	0	0	0

MORPHOR DELFT UNIVERSITY OF TECHNOLOGY   PROJECT: SHANGHAI   RUN: TEST
500*500 MET SEDIMENT
TIME=   200. SEC

VARIABLE: CS   UNIT: 0.1000E-05

	1	2	3	4	5	6	7	8	9	10	11	12	13	14	15	16	17	18	19	20	21	22	23	24	25
1																									
2						0	0	0	0	0	0	0	0	0	0	0	0	0	0	0					
3						0	0	0	0	0	0	0	0	0	0	0	0	0	0	0					
4						0	0	0	0	0	0	0	0	0	0	0	0	0	0	0					
5						0	0	0	0	0	0	0	0	0	0	0	0	0	0	0					
6						0	0	0	0	0	0	0	0	0	0	0	0	0	0	0					
7						0	0	0	0	0	0	0	0	0	0	0	0	0	0	0					
8						0	0	0	0	0	0	0	0	0	0	0	0	0	0	0					
9						0	0	0	0	0	0	0	0	0	0	0	0	0	0	0					
10						0	0	0	0	0	0	0	0	0	0	0	0	0	0	0					
11						0	0	0	0	0	0	0	0	0	0	0	0	0	0	0					
12						0	0	0	0	0	0	0	0	0	0	0	0	0	0	0					
13						0	0	0	0	0	0	0	0	0	0	0	0	0	0	0					
14						0	2	0	0	0	0	0	0	0	0	0	0	0	0	0					
15						9	-2	3	0	0	0	0	0	0	0	0	0	0	0	0					
16						5	20	-3	2	0	0	0	0	0	0	0	0	0	0	0					
17	377	297	221	148	84	57	2	13	0	1	0	0	0	0	0	0	0	0	0	0	0	0	0	0	0
18	377	304	212	157	85	[illegible]	24	7	2	1	0	0	0	0	0	0	0	0	0	0	0	0	0	0	0
19	377	298	225	148	90	51	20	10	2	1	0	0	0	0	0	0	0	0	0	0	0	0	0	0	0
20	377	303	219	154	89	51	21	10	2	1	0	0	0	0	0	0	0	0	0	0	0	0	0	0	0
21	377	302	222	153	83	52	21	10	2	1	0	0	0	0	0	0	0	0	0	0	0	0	0	0	0
22	377	303	222	154	92	[illegible]	21	10	2	1	0	0	0	0	0	0	0	0	0	0	0	0	0	0	0
23	377	304	222	155	90	[illegible]	22	10	2	1	0	0	0	0	0	0	0	0	0	0	0	0	0	0	0
24	377	304	224	154	91	[illegible]	22	10	2	1	0	0	0	0	0	0	0	0	0	0	0	0	0	0	0
25	377	305	223	156	90	[illegible]	22	10	2	1	0	0	0	0	0	0	0	0	0	0	0	0	0	0	0

MORPHOR DELFT UNIVERSITY OF TECHNOLOGY   PROJECT: SHANGHAI   RUN: TEST
500*500 MET SEDIMENT
TIME=   300. SEC

VARIABLE: CS   UNIT: 0.1000E-05

	1	2	3	4	5	6	7	8	9	10	11	12	13	14	15	16	17	18	19	20	21	22	23	24	25
1																									
2						0	0	0	0	0	0	0	0	0	0	0	0	0	0	0					
3						0	0	0	0	0	0	0	0	0	0	0	0	0	0	0					
4						0	0	0	0	0	0	0	0	0	0	0	0	0	0	0					
5						0	0	0	0	0	0	0	0	0	0	0	0	0	0	0					
6						0	0	0	0	0	0	0	0	0	0	0	0	0	0	0					
7						0	0	0	0	0	0	0	0	0	0	0	0	0	0	0					
8						0	0	0	0	0	0	0	0	0	0	0	0	0	0	0					
9						0	0	0	0	0	0	0	0	0	0	0	0	0	0	0					
10						1	-1	1	0	0	0	0	0	0	0	0	0	0	0	0					
11						-4	9	-4	1	0	0	0	0	0	0	0	0	0	0	0					
12						24	-39	19	-9	2	0	0	0	0	0	0	0	0	0	0					
13						-69	153	-111	52	-13	2	0	0	0	0	0	0	0	0	0					
14						211	-399	340	-164	57	-11	2	0	0	0	0	0	0	0	0					
15						-390	679	-714	396	-141	39	-6	1	0	0	0	0	0	0	0					
16						784	-1358	1210	-641	200	-70	16	-2	0	0	0	0	0	0	0					
17	377	445	56	374	342	-1038	1777	-1364	778	-286	87	-10	3	0	0	0	0	0	0	0	0	0	0	0	0
18	377	27	804	-290	250	750	-965	972	-452	187	-41	10	0	0	0	0	0	0	0	0	0	0	0	0	0
19	377	626	-274	770	-103	-53	502	-328	220	-55	20	0	1	0	0	0	0	0	0	0	0	0	0	0	0
20	377	131	626	-150	389	102	-31	150	-24	26	4	2	1	0	0	0	0	0	0	0	0	0	0	0	0
21	377	405	140	353	90	123	110	20	39	10	7	2	1	0	0	0	0	0	0	0	0	0	0	0	0
22	377	324	260	225	152	141	62	56	26	13	7	2	1	0	0	0	0	0	0	0	0	0	0	0	0
23	377	296	343	139	245	62	114	32	34	11	7	2	1	0	0	0	0	0	0	0	0	0	0	0	0
24	377	368	205	311	91	175	50	62	24	14	7	2	1	0	0	0	0	0	0	0	0	0	0	0	0
25	377	312	315	179	212	69	101	38	33	11	8	2	1	0	0	0	0	0	0	0	0	0	0	0	0

MORPHOR DELFT UNIVERSITY OF TECHNOLOGY   PROJECT: SHANGHAI   RUN: TEST
500*500 MET SEDIMENT
TIME=   400. SEC

VARIABLE: CS   UNIT: 0.1000E-05

	1	2	3	4	5	6	7	8	9	10	11	12	13	14	15	16	17	18	19	20	21	22	23	24	25
1																									
2						0	0	0	0	0	0	0	0	0	0	0	0	0	0	0					
3						0	0	0	0	0	0	0	0	0	0	0	0	0	0	0					
4						0	0	0	0	0	0	0	0	0	0	0	0	0	0	0					
5						0	0	0	0	0	0	0	0	0	0	0	0	0	0	0					
6						-1	1	-1	0	0	0	0	0	0	0	0	0	0	0	0					
7						5	-9	7	-2	0	0	0	0	0	0	0	0	0	0	0					
8						-30	64	-52	25	-7	1	0	0	0	0	0	0	0	0	0					
9						159	-352	317	-172	61	-13	2	0	0	0	0	0	0	0	0					
10						-672	1566	-1502	908	-373	106	-19	2	0	0	0	0	0	0	0					
11						2374	-5678	5754	-3747	1726	-573	136	-21	2	0	0	0	0	0	0					
12						-6919	17098	*****	12433	-6200	2313	-642	130	-18	1	0	0	0	0	0					
13						17056	*****	46799	*****	17799	-7178	2235	-530	94	-11	1	0	0	0	0					
14						*****	92109	*****	75634	*****	17701	-5924	1563	-318	49	-5	0	0	0	0					
15						65991	*****	*****	*****	80262	*****	12340	-3453	773	-135	18	-2	0	0	0					
16						*****	*****	*****	*****	*****	55940	*****	5765	-1339	251	-36	4	0	0	0					
17	377	*****	24342	*****	*****	*****	*****	*****	*****	*****	*****	23032	-6668	1569	-294	45	-5	0	0	0	0	0	0	0	0
18	377	32803	*****	69404	*****	*****	*****	*****	*****	*****	47591	*****	4912	-1123	204	-27	3	0	0	0	0	0	0	0	0
19	377	*****	77278	*****	53610	26307	*****	*****	*****	59088	*****	9247	-2532	545	-65	11	0	0	0	0	0	0	0	0	0
20	377	30679	*****	73836	*****	9692	34249	*****	43095	*****	10934	-3606	920	-165	13	-1	0	0	0	0	0	0	0	0	0
21	377	*****	33672	*****	30634	-9618	-9582	18020	*****	8638	-3506	1090	-227	40	-2	1	0	0	0	0	0	0	0	0	0
22	377	5139	-8710	9673	-4659	-1952	7565	-8258	6032	-2962	1142	-280	64	-1	2	1	0	0	0	0	0	0	0	0	0
23	377	2482	-4776	8533	*****	11565	-9881	7236	-3952	1849	-608	200	-34	14	0	1	0	0	0	0	0	0	0	0	0
24	377	-3563	8757	*****	13719	*****	9535	-5865	3227	-1333	539	-139	51	-4	3	1	0	0	0	0	0	0	0	0	0
25	377	2147	-3560	5691	-5669	5434	-3763	2553	-1216	632	-194	95	-14	12	0	2	0	0	0	0	0	0	0	0	0

4.20

Influence of the time-step

INFLUENCE OF THE TIME STEP (see Fig. 4.20)

The time step found appropriate for calculations with DUCHESS, was also applied on MORPHOR (Δt = 40 s in case 500 * 500 m). It showed that the numerical computations became unstable (see Fig. 4.20) for time-steps of which the courant number $\sigma = 2$.

CONCLUSION

The time-step of the morphological computation is restricted by the courant number of the calculation of the average sediment concentration; this courant number should not exceed $\sigma = 1$ in order to ensure the stability of the numerical computation (see par. 3.4).

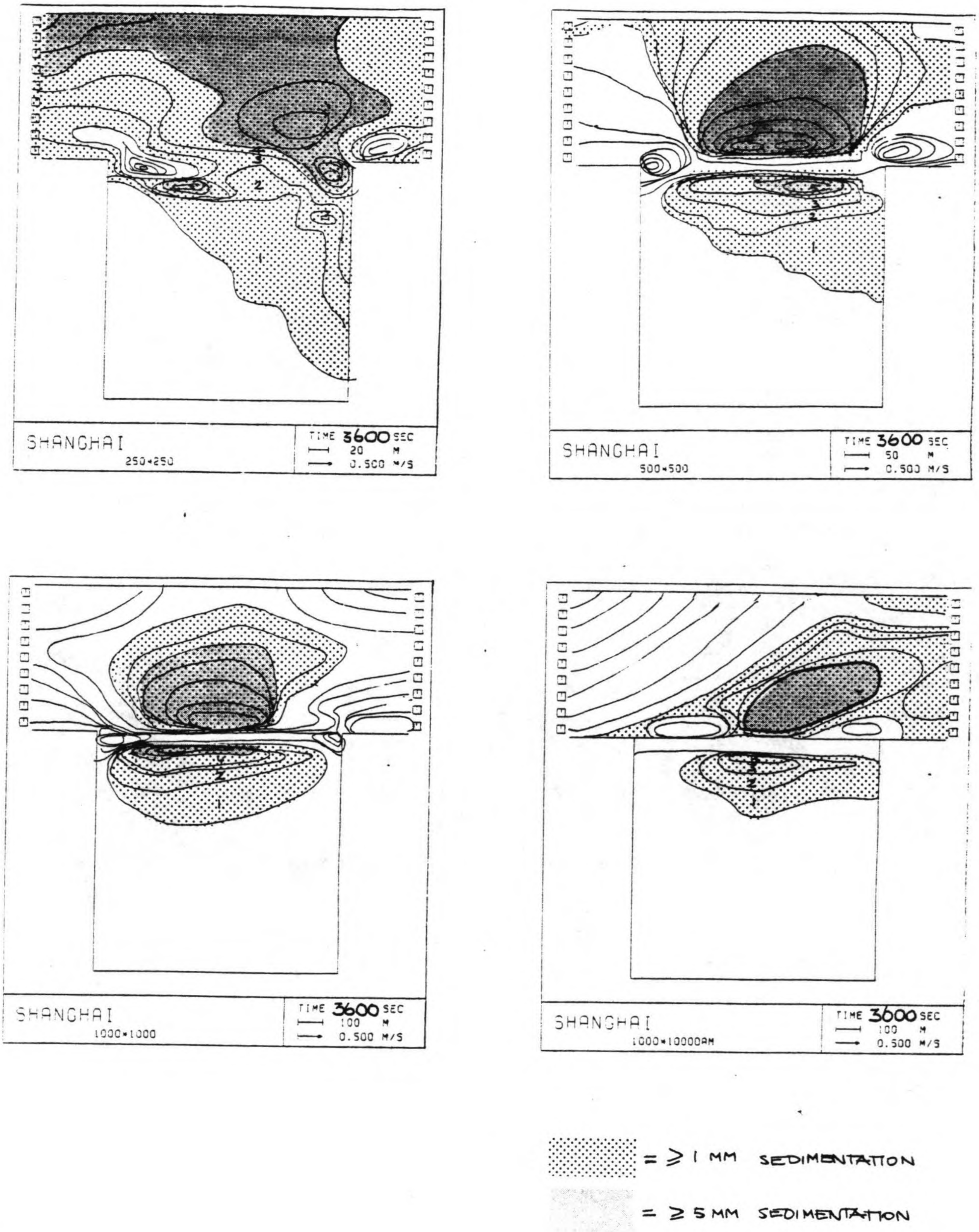

5.1

Overview of sedimentation patterns

5. CONCLUSIONS

5.1 Relation between lay-out and sedimentation

In the foregoing it has been described how the problem of determing a relation between sedimentation and lay-out is tackled in this analysis.
In chapter 3 it is described which schematization has been chosen, to find a relation between the length of the dams and sedimentation, the distance between the dams and sedimentation, and the influence of reducing the width of the opening.
In chapter 4 it is described which influence the chosen schematization of the parameters (flow and sediment) has on the results of the computation.
On the basis of the numerical results, an effort is given here to determine a relation between lay-out and sedimentation.

The results of the calculations give rise to a number of relations:

a. a relation between the area of a field and the average sedimentation per square meter;

b. a relation between the length of the dams and the average sedimentation per square meter;

c. a relation between the distance between the dams and the average sedimentation per square meter;

d. a relation between the width of the opening and the average sedimentation per square meter;

e. a relation between the total length of dikes and the average sedimentation per square meter.

The first relation can directly be taken from the results of the numerical simulations, the rest of the relations follow more or less from the first relation.

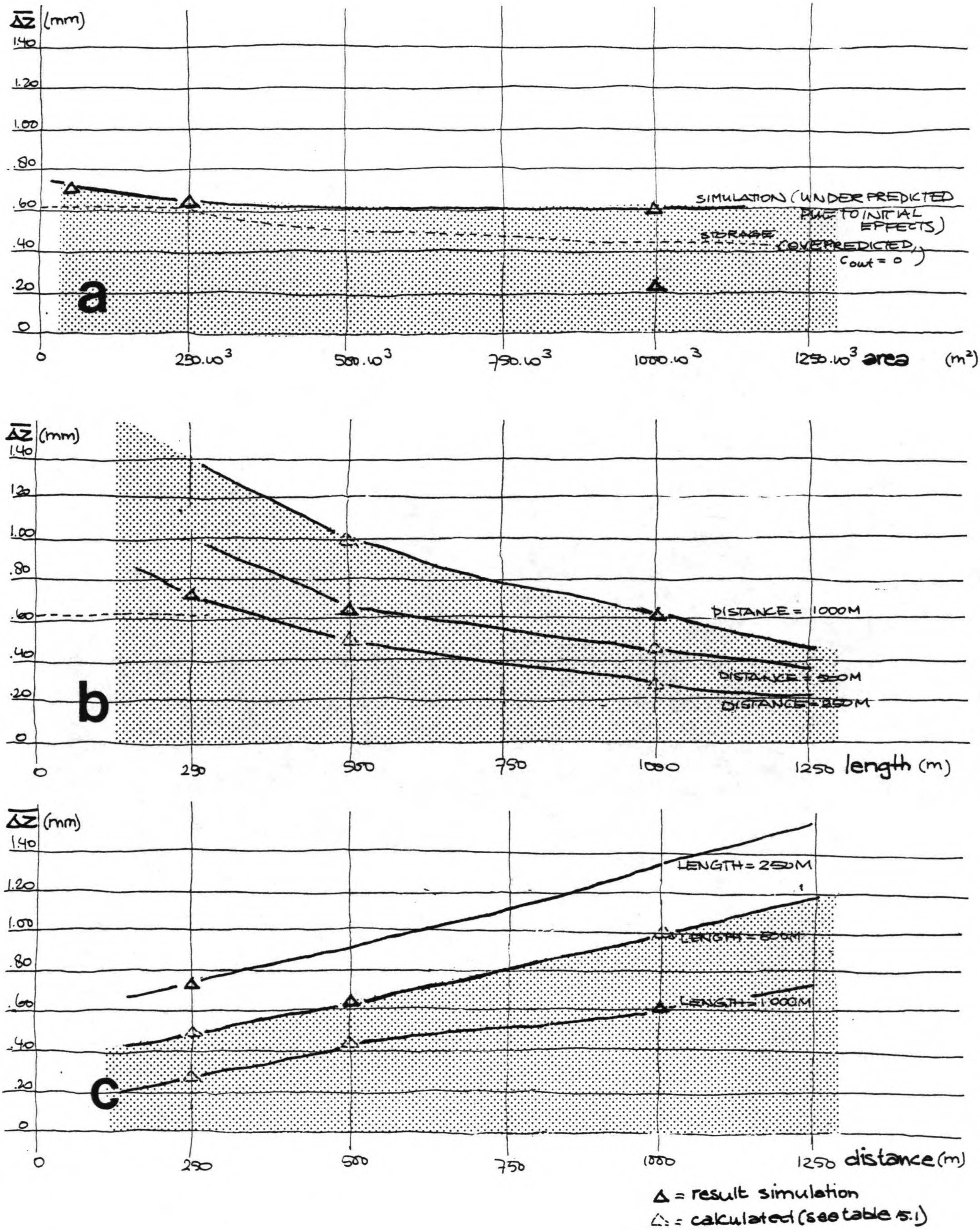

5.2

Relation between lay-out and sedimentation

LENGTH AND DISTANCE OF THE DAMS

From the results of the numerical simulations following table 5.1 can be composed; considering the fact that the exchange of water by storage is about one third of the maximum total exchange, and the exchange by eddies is about two third of the maximum exchange (in case of a reduced opening only storage causes exchange).

distance: length :	250 m	500 m	1,000 m	333 m (1,000 m)
250 m	(0.75)	?	?	?
500 m	0.50	(0.65)	1.00	0.44
1,000 m	0.30	0.45	(0.60)	(0.22)

Table 5.1: average sedimentation [mm] as a function of the distance between the dams, and the length of the field (at T = 3,600 s).
( ) = simulated

From Fig. 5.1 it can be seen that the penetration of sediments in the fields is dependent on the dimensions of the fields; but the penetration does not exceed 500 m. Also the flow pattern (see Fig. 4.3) and specifically the eddy developing is mainly determined by the first 500 m of the basins (influenced by the bottom friction).
So for lengths above 500 m, sedimentation will not increase so much anymore (only extra storage); this part of the basin functions as a "death end" and causes a decrease of the average sedimentation per square meter of basin.

In case of the other lay-outs it is not possible to predict the sedimentation for a different length, since the flow pattern in this case will be considerably different from the one calculated in the numerical simulations.

However, since the waterexchange due to the eddy-exchange forms two third of the total exchange it is expected that the extra length only causes extra storage-exchange. On this basis the figures of table 5.1. result.

The influence of the distance between the dams, the length of the dams on the average sedimentation is shown in Fig. 5.2 (relations a, b and c).

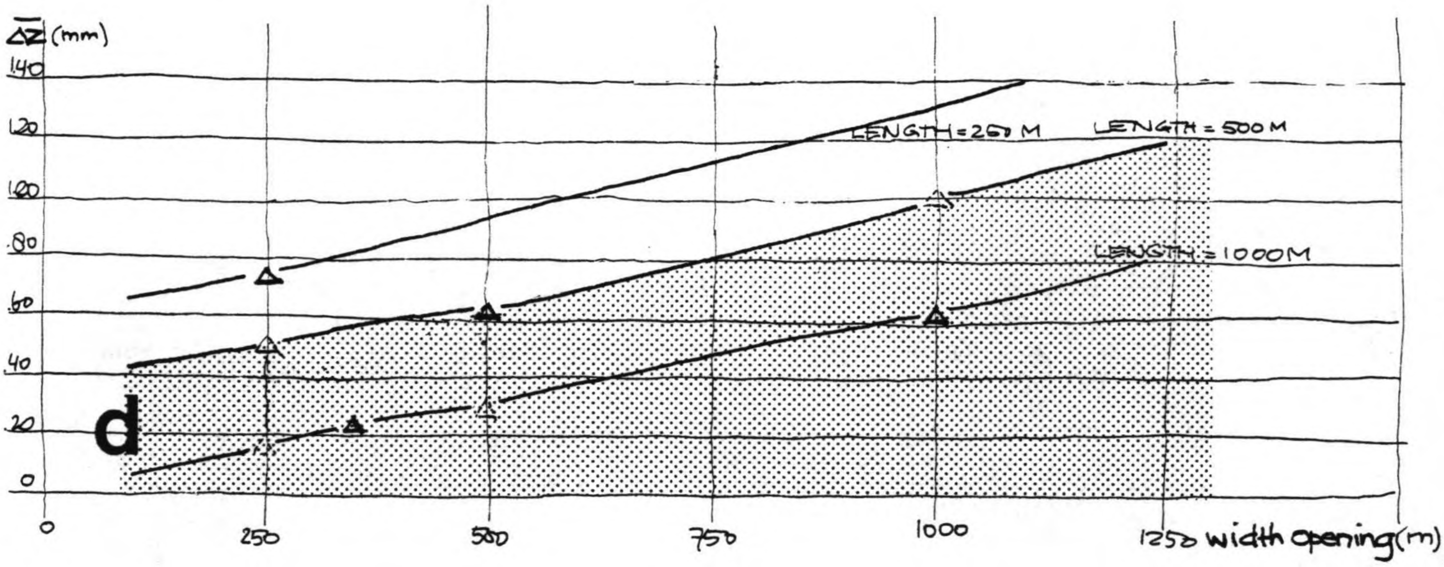

ΔZ (mm)
1.40
1.20
1.00
.80
.60
.40
.20
0
LENGTH = 250 M
LENGTH = 500 M
LENGTH = 1000 M
d
0
250
500
750
1000
1250 width opening (m)

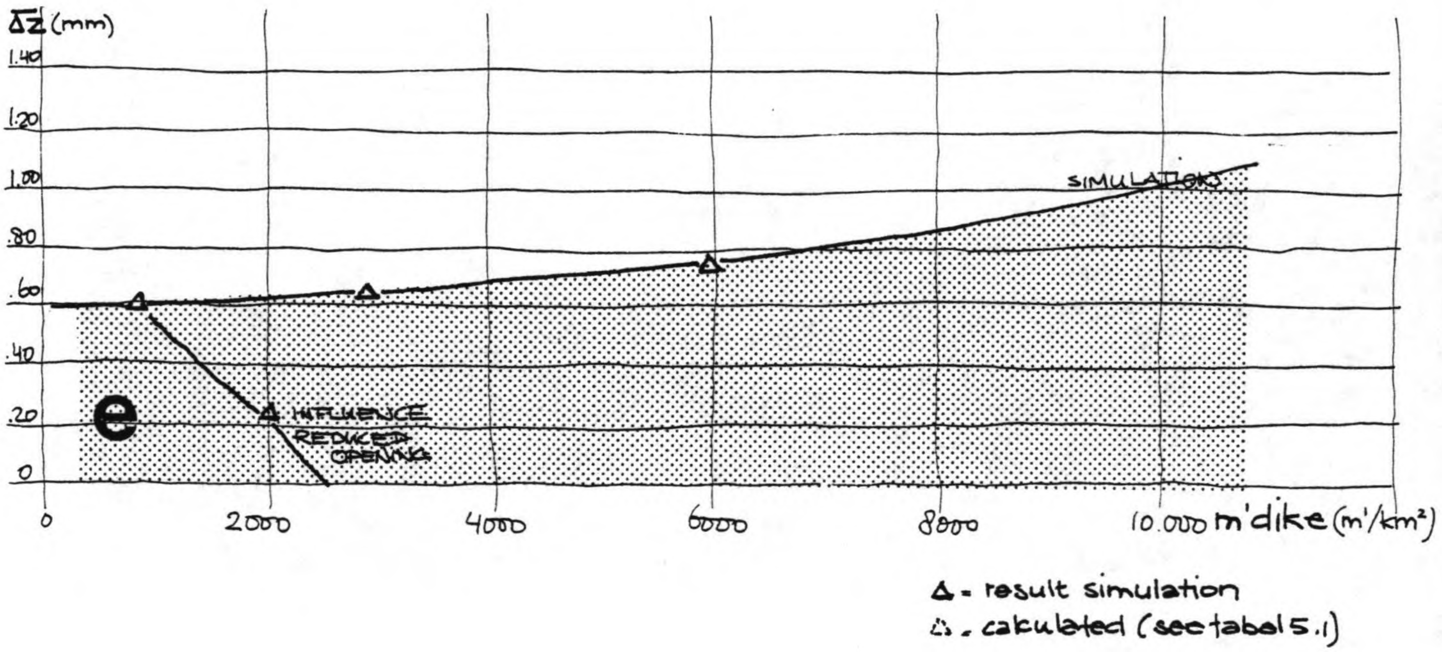

ΔZ (mm)
1.40
1.20
1.00
.80
.60
.40
.20
0
SIMULATION
INFLUENCE
REDUCED
OPENING
e
0
2000
4000
6000
8000
10.000 m'dike (m'/km²)
Δ = result simulation
Δ = calculated (see tabel 5.1)

5.2

WIDTH OF THE OPENING

From the results of the numerical computations, it shows that the sedimentation inside the field is directly related to the size of the opening at the seaward end of the basin (see Fig. 5.2) (relation d).
For the 1,000 x 1,000 m lay-out plus dam, the width of the opening is 333 m. The resulting sedimentation (considering a length of 500 m, see table 5.1) is about 0.44 mm, and in case of an opening of 250 m (considering also a length of 500 m) the sedimentation is 0.38 mm.
So the advantageous influence of increasing the distance between the dams is decreased by reducing the width of the opening (see Fig. 5.2).

However, the flow pattern outside the basin is increasingly disturbed for increasing distance between the dams (see Fig. 5.1). Already when the distance is 500 m disadvantageous erosion occurs around the dam heads, getting worse in case the distance is 1,000 m (see also the flow pattern). By introducing longitudinal dams, this situation is much improved.

TOTAL LENGTH OF DIKES IN RELATION TO THE SEDIMENTATION

In order to compare the total necessary stretch of dikes of each of the lay-out solutions an area of 1,000 x 1,000 m is considered. The total length of dikes which have to be constructed, in time, can be found by:

250 x 250 m: 6,000 m'/km2

500 x 500 m: 3,000 m'/km2

1,000 x 1,000 m: 1,000 m'/km2

1,000 x 1,000 m: 1,000 - 2,000 m'/km2, dependent on the size of
+ long. dam the opening

These figures can be related to the total expected sedimentation (relation e, see Fig. 5.2).

Since the cost of the project is directly proportional to the number of running meters dike, this relation is also illustrating the most economic solution. An increase of the total length of dikes hardly causes an increase of sedimentation. So the most economic design is the "large" lay-out, in which the distance between the cross-dams is large.

Based on the foregoing, the optimum solution, which combines a high sedimentation with a minimum length of the dikes, would be (see Fig. 5.3):

- length of the (cross-)dams: 500 m;

- distance between the dams: 1,000 m or more;

- small longitudinal dams at the end of the cross-dams to prevent erosion at the dam heads.

COMMENT

It should be kept in mind that the calculated sedimentation is nog equal to the real sedimentation. This is due to the schematization of the problem:

* the watermovement is entirely schematized; an entirely long-shore motion combined with a rise of the water-level;

* only 3,600 s of a watermovement have been simulated; the effect of initial conditions is still large (see also par. 4.2). Also the real tidal motion consists of about 6 hours rising tide (thus more sedimentation) and about 6 hours declining tide (thus some (?) loss of sedimentation);

* the effect of the waves caused by wind etc. has been neglected; this is discussed in par. 5.2 and in the following report lay-out part II (lit. [2]).

Nevertheless the results of the simulations do have some practical significance, since the lay-outs can be compared with each other. Also it shows that the expected sedimentation is stimulated by eddy developing and is larger than the storage quantity. (In case of the lay-out of 1,000 x 1,000 m plus longitudinal dams, the sedimentation is about the same as can be found by the storage quantity; due to the initial effects the total sedimentation after 3,600 s is somewhat smaller, but the increase of sedimentation during the next 3,600 s is comparable to the estimated storage quantity. This effect will be more obvious when the wave influence is taken into account; see par. 5.2.)

5.2 Influence of wind waves

In the numerical simulations, the influence of wind waves has been totally neglected. It has been supposed that the tidal motion forms the main mean of transportation of sediments from the sea to the reclamation fields.
Since the long-shore tidal current is very strong (up to 2 m/s) and the average wave height along the coastline is rather low (about 0.50 m), this assumption will be largely true: waves will not cause an extra large-scale watermovement of importance, compared with the tidal movement (during normal conditions).

In Bijker (lit. [8]) a formula is described to estimate the maximum (long-shore) current caused by breaking waves:

$$V = \frac{5\pi\sqrt{g}}{8\sqrt{2}} \; \frac{\sin\phi_o}{C_o} \; \gamma \; \frac{C}{\sqrt{fw}} \; h \; m \quad \ldots\ldots\ldots\ldots\ldots\ldots (32)$$

EXAMPLE:

normal conditions

H = 0.50 m (wave height)
T = 3 à 5 s (period)
m = 1/150 (beach slope)
h_{break} = 0.8 H = 0.40 m (waterdepth breaking waves)
ϕ_o = 15° (SE-direction)
γ = 0.8 (breaker index)
C_o = 1.56 T = 4.7 m/s
$fw = \exp\left(-5.977 + 5.213\left(\frac{a_b}{r}\right)^{-0.194}\right)$

a_b = H/(2 sinh kh) = 0.60
r = 0.05 m (roughness)
= 0.069

<u>V_{max} = 0.10 m/s</u>

extreme conditions

H_s = 2.50 m (sign. wave height)
T = 5 à 8 s (period)
m = 1/150 (slope)
h_{break} = 0.8 H = 2.0 m
ϕ_o = 15° (SE-direction)
γ = 0.8 (breaker index)
C_o = 1.56 T = 9.4 m/s
fw = friction coefficient

a_b = H/(2 sinh kh) = 2.5
r = 0.05 m (roughness)
= 0.030

<u>V_{max} = 0.32 m/s</u>

Thus the longshore current due to wave influence can be neglected during normal conditions, if compared with the tidal influence.

Another reason for the neglect of the influence of the waves, as far as the transportation of sediments is concerned, is the fact that the breakerzone, where the waves do have a dominant effect on the transport of sediments, is most of the times situated <u>in</u>side the reclamation fields. As such the waves do not contribute to the large-scale watermovement <u>along</u> the coast.

However, the waves do have an important effect on the settling and entrainment of the sediments.
The waves cause an extra shear-stress at the bottom, and thus increase the tendency of particles to go into suspension.

For example: Bijker (lit. [8]) describes a formula to estimate the shear stress caused by waves.

currents: $$\tau_c = \rho g \frac{\bar{u}^2}{C^2} \qquad (33)$$

waves : $$\tau_w = \tfrac{1}{2}\rho \, f_w \, u_b^2 \qquad (34)$$

"normal conditions":

$\bar{u}$ = 1 [m/s] (depth averaged flow velocity)
C = 50 [√m/s] (Chézy roughness parameter)
ρ = 1,000 [kg/m3] density of water
g = 10 [m/s2] acceleration of gravity

thus τ_c = 4 [N/m2]

$\hat{u}_b$ = ωH/2 sinh kh (maximum orbital velocitiy at bottom)
= 1.3 [m/s]
H = 0.5 m (average wave height)
h = 2.0 m (average water-depth)
ω = 2π/T = 2.1 [rad/s] (angular velocity)
fw = 0.04 (roughness parameter)

thus $\hat{\tau}_w$ = 57 [N/m2]

So even for "normal" conditions the shear stress caused by waves is much higher than the current shear stress.

The effect on the transport formulas and the sediment concentration will be such that the bed shear velocity u_* is (much) larger than calculated; the suspension number Z will be larger; and in general the adaption length and time of the suspended concentration will be larger than estimated by MORPHOR.

The waves will prevent the sediment particles to settle to the bottom, especially in the breaker zone.
The critical shear stress, at which particles go into suspension, was estimated at 0.16 N/m2 (u_*= 0.0125 m/s), thus even "normal" waves will completely disturb the calculated sedimentation pattern.

Concluding we find that the wave influence must be banned from the reclamation fields, otherwise the sediments will not settle (the incoming water will be of high sediment concentration, but also the outgoing water; so the storage analogy and the MORPHOR analogy both are not realistic).
This can be done by constructing a longitudinal dike along the seaward end of the reclamation fields.
The height of this dike is determined by the allowable wave transmission. In this dike also openings are necessary, to allow the tidal motion to enter the basins. The size of these openings must be small, and can be determined by wave diffraction.
These approaches are described in more detail in part II of the lay-out analysis: the effect of wind waves (lit. [2]).

CONCLUSION

The influence of the waves causes a requirement on the dike lay-out, which is in conflict with the requirement found on the basis of the tidal motion.

TIDAL MOTION : opening at seaward end should be as large as possible.

WAVE INFLUENCE: opening at seaward end should be as small as possible.

An optimum should be found between these two requirements.

N.B.: The smaller the opening size of the lay-out, the more realistic results MORPHOR will produce, since in this case the effect of waves inside the basin decreases. In case of the 1,000 x 1,000 m lay-out, with an opening size of 333 m, we already saw that the expected sedimentation inside the basin will be in the order of the storage quantity (incoming sediment concentration is high, outgoing sediment concentration is low).
Outside the basin, the results of MORPHOR can be rejected, since they are not based on the right approach.

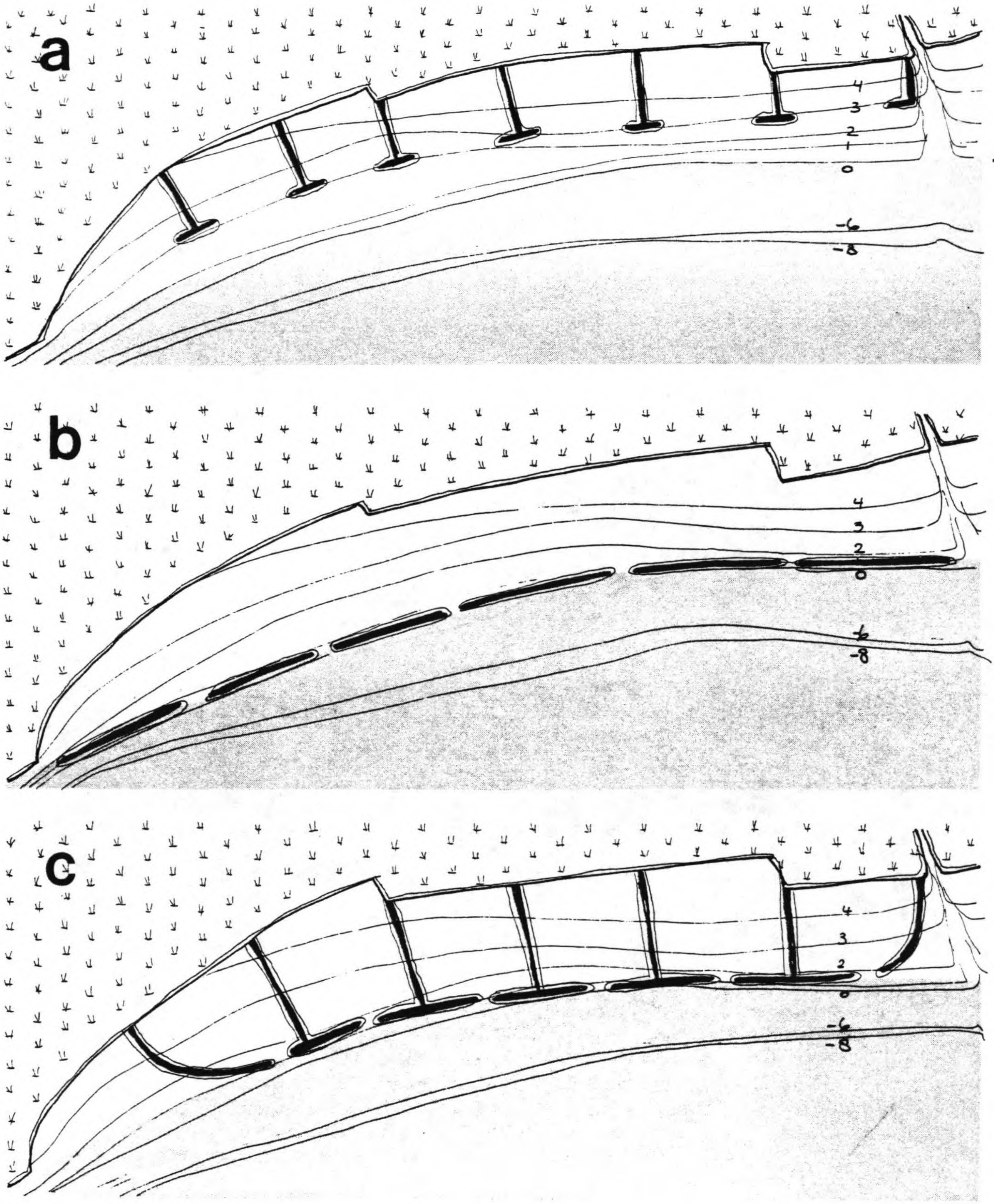

5.3

Advice on lay-out

ADVICE ON LAY-OUT OF THE RECLAMATION AREA

In Fig. 5.3 A the result for the optimum lay-out on the basis of the tidal influence is shown. Fig. 5.3. B shows the optimum lay-out based on the reduction of the wave influence (as found in the report LAY-OUT part II).

A combination results in an advice on the lay-out of the landreclamation system, based on the following remarks (see Fig. 5.3 C):

- the tidal motion is the main mean of transportation of sediments; the total amount of incoming (high concentrated) sediments is determined by storage and eddy exchange. The wave influence inside the reclamation area must be reduced sufficiently, so that the outgoing amount of sediments (transported by the tidal motion) will be low;

- the optimum length of the reclamation basin is dependent on the penetration of the high concentrated sediments. This length is about 500 m due to the tidal motion; waves will increase this length (sedimentation will take place over the total basin). Nevertheless, the length is limited due to the growth of the (reduced) waves by the wind. So the maximum length of the basin is dependent on the admissable average wave height inside the basin (report lay-out part II), estimated about 1,500 m;

- the distance between the cross-dams should be as large as possible. The maximum distance is limited by the admissable wave height caused by wind; again estimated at 1,500 m;

- the opening at the seaward end is only dependent on the allowable wave diffraction inside the basin, it should be as large as possible in order to profit from the eddy motion;

- the expected sedimentation is only dependent on the tidal motion (provided that the wave influence is reduced sufficiently); due to the limited opening it will be in the order of the storage quantity: 2 mm per tide, or 1.5 m during the first year.

In general the exact place of the dikes is also dependent on other criteria like the desired construction level (S.B.W.C. has expressed the wish to build the longitudinal part of the dike at a bottom level of + 1.00 m (Wusong level), so that the construction is in the dry during a part of the day), and budget planning. It might be economical (in order to reduce investments) to start with a low longitudinal dike at 500 m out of the coastline.

Following items are important:

- the total surface of the basins is also dependent on the size of the opening: due to storage, the water velocity through the opening may not become too large;
  since the maximum rise of the water-level is 1.2 m/hour considering a basin of 1,000 x 1,000 m, the minimum opening size is 160 m (then the filling velocity is 1 m/s). A very small opening causes accretion in front of the opening (due to contraction of the flow);

- eddy developing is advantageous for sedimentation: extra exchange of water, and an equal distribution of sediments over the area.
  The size of the eddy is limited: about 500 m diameter.
  So the total basin should not become much larger than 1,000 x 1,000 m, in order to ensure the distribution of sediments when waves are absent (the flow pattern of the "1,000 x 1,000 m plus dam"-lay-out seems a good distribution, better would be 1,000 x 500 or even 500 x 500 m; as well on the subject of eddy developing as wave reduction);

- the place of the opening is under discussion: since one wants to "catch" the incoming sediments, there is a tendency to place the opening at the upstream (of rising tide) direction (see also fig. 5.1). On the other hand the wave direction is rather random (tombolo-growth), and for the flow pattern also a central opening is advantageous.

In the report lay-out part II the wave climate at the Cao Jing district is determined, in order to find:

- the optimum width of the openings (wave diffraction);
- the optimum length and distance of the fields (allowable fetch-length);
- the optimum heigth of the dams (wave transmission).

5.3 Restrictions and recommendations

The results of this report cannot be applied in practice, because of following restrictions:

- the tidal transport of sediments must be dominating the wave induced transport;

- since the tidal motion is schematized, the sediment concentration is schematized and also the boundary conditions have been schematized, the results of the numerical simulations have no direct practical value; they can only be used to compare the effectivity of each of the solutions;

- it must be checked whether the influence of the waves is small enough to allow the tidal sedimentation pattern to develop; if the disturbances caused by the waves are large, a (completely) different approach of the problem will be necessary;

- the length of the simulations is actually too short in order to form a solid basis to estimate the actual sedimentation pattern. It seems that initial effects (in MORPHOR) play too large a part in the resulting bottom level changes.

In addition following recommendations can be done:

- determination or calculation of the wave climate at the planned reclamation area is necessary, in order to approximate the influence of the waves on the sedimentation pattern;

- the wave-climate will determine the optimum height of the dikes, and the optimum width of the openings; also it will probably result in the optimum dimensions of the fields (allowable fetch-length);

- it would be interesting to check the results of MORPHOR by some practical data; model or prototype testing are recommended in order to verify the simulations.
  For example, during the first stages of construction, intensive in situ testing should be performed, in which several lay-outs are tried, and compared afterwards;

- since the problem has been considerably schematized in this analysis, it is recommended to re-simulate the entire problem using a combined tide- and wave-influenced sediment-transport program, in which several tidal periods are calculated, and several weather circumstances.

Acknowledgements

A lot of people were more or less involved in this project, which forms a part of the feasibility study landreclamation Shanghai-province, and which was also meant to contribute to my degree of Civil Engineer at the Technical University of Delft. Although it would be too much to recall everybody involved personally, I would like to mention following persons in specific:

from the Harbour Engineering Division of Rotterdam Public Works I would like to thank Jaap de Nekker and Marjan Veltman, who assisted me during the entire project and gave advices etc. Also I would like to thank Cees van Rijt and Jaap Andeweg who shared my room and had to listen to my stories about crashing disks, systems which were breaking down, etc.

From the University of Delft I would like to thank Cees Verspuy, who assisted me with the computer-work and who enabled me to contact the right persons. Nico Booy and Simon Boer were kind enough to help me with the hard- and software; Rob Booy and dr. C. Kranenburg spent some time helping me with the eddy-phenomenon. Last but not least I would like to express my gratitude to Zheng Bing Wang who was so kind to put his programm at my disposal, and who had to spend many afternoons solving my problems with his programm. He also provided a lot of literature and good advices.

Prof. E.W. Bijker and prof. J.A. Battjes are thanked for their general assistance and the supervision.

Yvette van den Berg

Notations

Variable	Meaning	Dimension
a	reference level (boundary of the bedload material)	[m]
b	width of the flow section	[m]
b	exponent in powerlaw transport formula	[-]
c	propagation velocity of gravity waves at the surface	[m/s]
c	concentration by volume	[-]
$\bar{c}$	depth averaged concentration	[-]
c_a	concentration of the bedload at the reference level a	[-]
c_e	equilibrium concentration profile	[-]
$\overline{c_e}$	mean equilibrium concentration profile	[-]
c_m	propagation velocity of bedlevel disturbances	[m/s]
d	flow depth (= h)	[m]
g	acceleration due to gravity	[m/s^2]
h	waterdepth	[m]
i	integer related to co-ordinate level	[-]
j	integer related to time level	[-]
k	wave number = $\frac{2\pi}{L}$	[rad/s]
k_s	equivalent roughness of bottom	[m]
p_b	porosity of the bottom material	[-]
s	specific density of sediment = $\frac{\rho s}{\rho}$	[-]
s	total transport per unit width	[m^2/s]
s_b	bedload transport per unit width	[m^2/s]
s_e	equilibrium transport per unit width	[m^2/s]
s_s	suspended transport per unit width	[m^2/s]
t	time	[s]

Variable	Meaning	Dimension
u	water velocity in flow direction (x)	[m/s]
$\bar{u}$	depth averaged horizontal flow velocity	[m/s]
u_*	overall bed-shear velocity	[m/s]
u'_*	bed-shear velocity related to grains	[m/s]
$u_{*,cr}$	critical bed-shear velocity according to Shields	[m/s]
$u_\perp$	velocity normal to boundary	[m/s]
$u_{//}$	velocity parallel to boundary	[m/s]
v	water velocity normal to flow direction (y)	[m/s]
w	velocity normal to u and v (z)	[m/s]
w_s	particle fall velocity	[m/s]
x	horizontal co-ordinate (longitudinal)	[-]
y	horizontal co-ordinate (lateral)	[-]
z	vertical co-ordinate	[-]
z_a	height of reference level above the bed	[m]
z_b	elevation of the bed	[m]
B	bottomlevel	[m]
C	Chezy-coefficient related to roughness of the bed	[$\sqrt{m}/s$]
C	depth averaged concentration (MORPHOR)	[-]
C'	Chezy-coefficient related to grains	[$\sqrt{m}/s$]
C_o	Coriolis parameter (DUCHESS)	[1/s]
D	flow depth (DUCHESS)	[m]
D_b	virtual lateral diffusion coefficient	[m^2/s]
D_s	grain size of suspended sediments	[m]
D_{50}	average grain size of bed material	[m]
D_{90}	90% grain size of bed material	[m]
D_*	particle diameter parameter	[-]
E	viscosity coefficient (DUCHESS)	[m^2/s]

Variable	Meaning	Dimension
Fr	friction coefficient (DUCHESS)	[-]
H	water level (DUCHESS)	[m]
L_A	adaption length	[m]
L_*	error length	[m]
P	surface air pressure-(DUCHESS) head	[m]
Q	discharge per unit width (DUCHESS)	[m^2/s]
Qx	Q in X-direction (DUCHESS)	[m^2/s]
Qy	Q in Y-direction (DUCHESS)	[m^2/s]
R	hydraulic radius of flow	[m]
R	parameter to control numerical damping (DUCHESS) in the acceleration terms	[-]
R'	parameter to control numerical damping (DUCHESS) in the advective acceleration terms	[-]
S	total transport per unit width	[m^2/s]
S_o	initial transport per unit width	[m^2/s]
S_b	bedload transport p.u.w.	[m^2/s]
S_s	suspended transport p.u.w.	[m^2/s]
T	tidal period	[s]
T	time step MORPHOR	[s]
T_A	adaption time	[s]
Tx	transport in X-direction (MORPHOR) p.u.w.	[m^2/s]
TxT	total transport in X-direction (MORPHOR) p.u.w.	[m^2]
Ty	transport in Y-direction (MORPHOR)	[m^2/s]
TyT	total transport in Y-direction (MORPHOR) per unit width	[m^2]
T_*	error time	[s]
U	parameter concerning u = horizontal velocity in X-direction	[-]
V	parameter concerning v = horizontal velocity in Y-direction	[-]

Variable	Meaning	Dimension
W	parameter concerning w = vertical velocity in z-direction	[-]
Wx	wind shear stress in X-direction (DUCHESS)	[N/m²]
Wy	wind shear stress in Y-direction (DUCHESS)	[N/m²]
Z	verticle co-ordinate (DUCHESS)	[m]
Z	suspension parameter	[-]
Z'	modified suspension parameter	[-]
ZB	bottom level (MORPHOR)	[m]
α	pseudo-viscosity parameter $o \leq \alpha \leq 1$	[m²/s]
β	dimensionless reference level $\beta = \frac{a}{d}$	[-]
β	correction factor for the relative diffusion of sediment to water particles	[-]
γ	coefficient related to the concentration profile at the reference level = ϕ_o	[-]
δ	small parameter	[-]
ε	turbulent diffusion coefficient	[m²/s]
εf	turbulent diffusion coefficient related to fluid	[m²/s]
εs	turbulent diffusion coefficient related to sediments	[m²/s]
εz	turbulent diffusion coefficient in vertical direction	[m²/s]
ν	kinematic viscosity of water	[m²/s]
ζ	transformed vertical co-ordinate	[-]
ξ	transformed horizontal co-ordinate	[-]
κ	constant of Von Karman	[-]
λ	bedform length	[m]
λ	eigen value of (asymptotic) solution of the two dimensional convection diffusion equation	[-]

Variable	Meaning	Dimension
ρ	density of water	[kg/m³]
ρs	density of sediment	[kg/m³]
σ	courant number	[-]
σm	courant number related to bedform propagation	[-]
σs	standard deviation of grain size distribution	[-]
w	particle fall velocity	[m/s]
Δ	bedform height	[m]
Δ	relative density = $\frac{\rho s - \rho}{\rho}$	[-]
Δ	parameter related to a differential expression: Δx, Δt	[-]
φ	parameter related to the damping of the fluid turbulence caused by sediments	[-]
φ	normilized equilibrium concentration profile	[-]
ψ	bedform steepness parameter = $\frac{\Delta}{\lambda}$	[-]

List of figures

References

1. Rotterdam Public Works: Study about landreclamation

   Rotterdam Public Works
   Harbour Engineering Division 1986

2. Rotterdam Public Works: Feasibility study landreclamation at Shanghai Province: LAY-OUT part II
   1987

3. N. Booy: Users Guide for the program DUCHESS, Delft University Computer Program for 2-dimensional Horizontal Estuary and Sea surges Version II

   Delft University of Technology
   Dept. of Civil Engineering 1986

4. Z.B. Wang: Users Guide for the program MORPHOR

   Delft University of Technology
   Dept. of Civil Engineering 1986

5. N. Bahylayan: Numerical experiments on Tides and Surges with Duchess-model

   Report no. 2-85
   Delft University of Technology
   Dept. of Civil Engineering 1985

6. R. Galapatti: A depth integrated model for Suspended Transport

   Report no. 83-7
   Communications on Hydraulics
   Department of Civil Engineering
   Delft University of Technology 1983

7. R. Galapatti and C.B. Vreugdenhill: A depth integrated model for suspended sediment transport

   Journal of Hydraulic Research
   no. 4, vol. 23, page 359-377 1985

8. L. van Rijn: Sediment transport part I : bed load transport
   part II : suspended load transport
   part III: bedforms and alluvial roughness

   Journal of Hydraulic Engineering
   no. 10, vol. 140, page 1431-1457
   no. 11, vol. 110, page 1613-1641
   no. 12, vol. 110, page 1733-1754 1984

9. Z.B. Wang and J.S. Ribberink: The validity of a depth integrated model for suspended transport

Journal of Hydraulic Research
no. 1 vol. 24 page 53-67 1986

10. Instructie en Voorlichting Rekencentrum: VSPC-handleiding
H.L.P. van der Kley

Delft University of Technology
afd. der Wiskunde en Informatica 1983

11. MKO-rapport: Aanslibbing Havens deel 1: Waterbeweging

Report no. MKO-R 8307 co: 58.50-R 8321
Rotterdam Public Works
Harbour Engineering Division 1983

12. C.B. Vreugdenhill: Waterloopkundige berekeningen II

Collegedictaat B 85
Delft University of Technology
Department of Civil Engineering 1980

13. C.B. Vreugdenhill: Numerieke berekeningen in Waterbouwkunde en Hydrologie

Collegedictaat B 84 N
Delft University of Technology
Department of Civil Engineering 1985

14. R. Booy: Turbulentie in de waterloopkunde

Collegedictaat B 82
Delft University of Technology
Department of Civil Engineering 1986

15. J. Kuipers and C.B. Vreugdenhill: Calculations on two dimensional horizontal flow

Report no. S 163 part I
Delft Hydraulics Laboratory 1973

16. G.S. Stelling and L.X. Wang: Experiments and computations on unsteady separating flow in an expanding flume

Report no. 2-84
Laboratory of Fluid Mechanics
Delft University of Technology
Department of Civil Engineering 1984

17. J.P. Kalkwijk and R. Booy: Adaption of secondary flow

Delft University of Technology
Department of Civil Engineering -

18. E.W. Bijker e.o.: Harbour and Beach problems

Collegedictaat f 11 B
Delft University of Technology
Department of Civil Engineering 1978

19. J. v.d. Graaff and J. v. Overeem: Evaluation of sediment transport formulae in coastal engineering practice

Coastal Engineering group
Delft University of Technology
Department of Civil Engineering 1977

20. G.S. Stelling: On the construction of computational methods for shallow water flow problems

Ph. D. thesis
Delft University of Technology 1983

21. R. Booy and Q.X. Yu: Tussentijds verslag betreffende metingen van uitwisselingen tussen rivieren en havens

Report no. 5-86
Delft University of Technology
Department of Civil Engineering 1986

APPENDIX A

THE CLOSURE PROBLEM FOR DEPTH AVERAGED FLOW

I General

In case of a non-layered surface flow characterized by a small depth-to-length ratio, the flow features can be predicted by use of the depth integrated equations of motion. The problems usually associated with these equations concern the numerical treatment. One of the main problems is the avoidence of non-linear instability of the method. Frequently this instability is suppressed explicitely by use of smoothing process after each time step, or by adding eddy-viscosity-type terms to the equations of motion, or implicitely by use of difference schemes affected with numerical viscosity. However, these ways of avoiding non-linear instability can yield erroneous results, or at least disguise physical effects.

Vertically integrated equations of motion contain terms, derivatives of the so called effective stresses, that have to be modelled to obtain a closed system of equations. It has been shown in literature, C. Flokstra (lit. (1)), Kuipers en Vreugdenhill (lit. (2)), that these effective stresses allow the occurence of circulating flows. The existence of these stresses is a necessary, but not sufficient, condition for the generation of circulating flows.

The two dimensional equations are derived by the depth integration of the continuity equation and the so called Reynolds equations (equations of motion for turbulent flow) resulting in:

$$\frac{\partial h}{\partial t} + \frac{\partial h\bar{u}}{\partial x} + \frac{\partial h\bar{y}}{\partial y} = 0 \; \ldots\ldots\ldots\ldots \; [1]$$

$$\frac{\partial}{\partial t}(h\bar{u}) + \frac{\partial}{\partial x}(h\bar{u}^2) + \frac{\partial}{\partial y}(h\overline{uv}) + gh\frac{\partial}{\partial x}(h+p) - \frac{1}{\rho}(\tau wx - \tau bx)$$

$$\frac{1}{\rho}\;\frac{\partial}{\partial x}(h\,T_{xx}) + \frac{\partial}{\partial y}(h\,T_{xy}) = \Omega h\bar{v} \; \ldots\ldots\ldots \; [2]$$

$$\frac{\partial}{\partial t}(h\bar{v}) + \frac{\partial}{\partial x}(h\overline{uv}) + \frac{\partial}{\partial y}(h\bar{v}^2) + gh\frac{\partial}{\partial y}(h+p) - \frac{1}{\rho}(\tau wy - \tau by)$$

$$\frac{1}{\rho}\;\frac{\partial}{\partial x}(h\,T_{yx}) + \frac{\partial}{\partial x}(h\,T_{yy}) = -\,\Omega h\bar{u} \; \ldots\ldots\ldots \; [3]$$

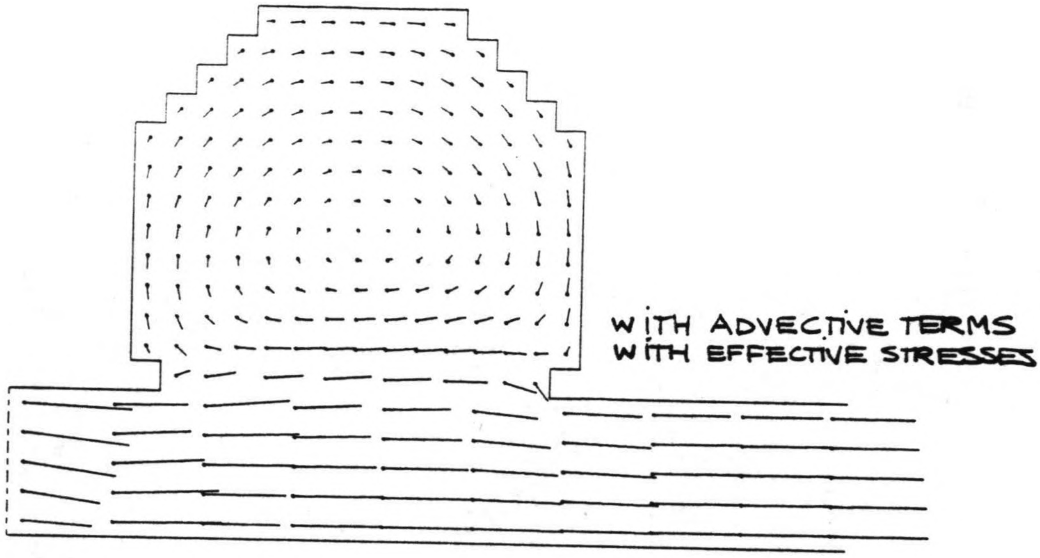
WITH ADVECTIVE TERMS
WITH EFFECTIVE STRESSES

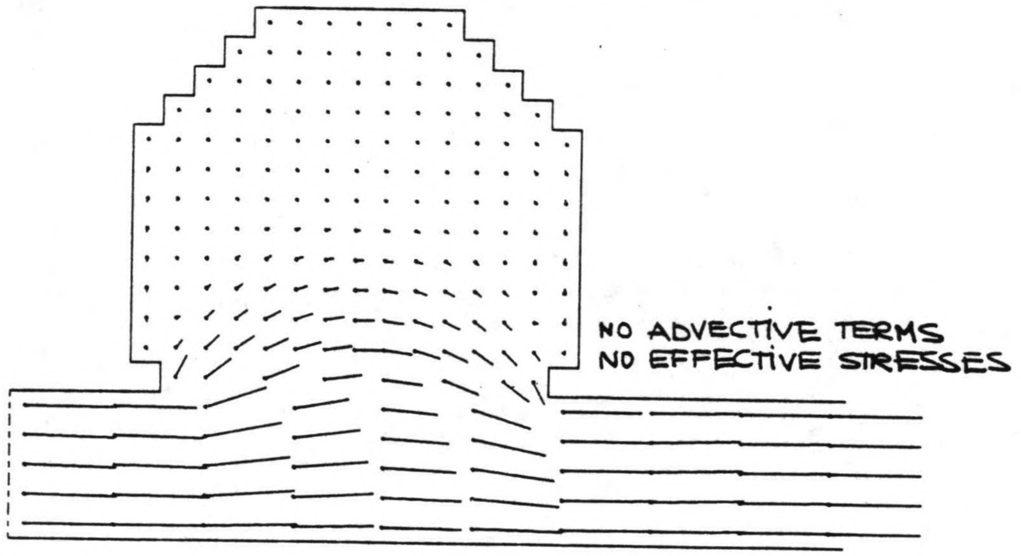
NO ADVECTIVE TERMS
NO EFFECTIVE STRESSES

1

In which

$\underline{h}$ = level of water surface
$\underline{u}$ = depth averaged velocity in X-direction
v = depth averaged velocity in Y-direction
p = atmospheric pressure at surface
τwx = wind stress component in X-direction
τbx = bottom shear stress component in X-direction

T_{xx}, T_{xy}, T_{yy} = effective stresses:

$$T_{xx} = \frac{1}{h} \int_{zb}^{h+zb} \left[2\rho\nu \frac{\partial \bar{u}}{\partial x} - \rho \overline{u'^2} - \rho(\bar{u} - u)^2 \right] dz \quad \ldots \quad [4A]$$

$$T_{xy} = \frac{1}{h} \int_{zb}^{h+zb} \left[2\rho\nu \left[\frac{\partial \bar{u}}{\partial y} + \frac{\partial \bar{v}}{\partial x} \right] - \rho\, \overline{u'v'} - \rho\, (\bar{u}-u)(\bar{v}-v) \right] dz \quad \ldots \quad [4B]$$

$$T_{yy} = \frac{1}{h} \int_{zb}^{h+zb} \left[2\rho\nu \frac{\partial \bar{v}}{\partial y} - \rho \overline{v'^2} - \rho(\bar{v}-v)^2 \right] dz \quad \ldots \quad [4C]$$

The windstress components are not investigated in this analysis, they have to be related to the wind velocity in general. For the bottom stress it is assumed that

$$\tau_{bx} = \rho \frac{g}{C^2} \bar{u} \sqrt{\bar{u}^2 + \bar{v}^2} \quad \ldots \quad [5A]$$

$$\tau_{by} = \rho \frac{g}{C^2} \bar{v} \sqrt{\bar{u}^2 + \bar{v}^2} \quad \ldots \quad [5B]$$

which implies that the direction of the bottom stress equals that of the mean velocity, and its magnitude is the same as in steady uniform flow.

C : is Chézy-value
u', v': are the fluctuations in the instantaneous velocity components in X and Y-direction
: the bar indicates a suitable averaging operation (ensemble or moving time average)
ν : is kinematic viscosity coefficient

In literature the importance of the effective stresses has been examined by means of a vorticity balance (C. Flokstra lit. [1], Kuipers and Vreugdenhill lit. [2])

the vorticity $\omega_z = \frac{\partial \bar{u}}{\partial y} - \frac{\partial \bar{v}}{\partial x}$ . . . . |6|

the result for the vorticity ω_z of the vertical mean flow:

$$\frac{\partial}{\partial t}(h\omega) + \frac{\partial}{\partial x}(\bar{u}h\omega) + \frac{\partial}{\partial y}(\bar{v}h\omega) + h(\omega-\Omega)\left(\frac{\partial \bar{u}}{\partial x} + \frac{\partial \bar{v}}{\partial y}\right)$$

$$- h\frac{\partial}{\partial y}\left(\frac{\tau wx}{\rho h} - \frac{\tau wy}{\rho h}\right) + h\frac{\partial}{\partial y}\left(\frac{\tau bx}{\rho h} - \frac{\tau by}{\rho h}\right) +$$

$$-\frac{h}{\rho}\frac{\partial}{\partial y}\,\frac{1}{h}\left(\frac{\partial}{\partial x}(h\,T_{xx}) + \frac{\partial}{\partial y}(h\,T_{xy})\right) + \frac{h}{\rho}\frac{\partial}{\partial x}\,\frac{1}{h}\left(\frac{\partial}{\partial x}(h\,T_{xy}) + \frac{\partial}{\partial y}(h\,T_{yy})\right)$$

$= 0$ . . . . [7]

Conclusions: - vorticity is generated by convergence and divergence of the mean velocity field (fourth term), by windstress, and by the stresses T_{xx}, T_{xy}, T_{xy} and T_{yy}
- vorticity is dissipated by the bottom stress term.

So the stresses T_{xx}, T_{xy} and T_{yy} influence the generation of secondary currents, such as eddies and secondary flow in riverbends etc.

The magnitude of the convective part (the convergence and divergence of the main flow) in the generation of secondary currents depends mainly on the curvature of the main flow, the stress terms depend mainly on the characteristic length of a change in velocity profile

- if the length scale is relatively small compared with the radius of curvature R (changes in velocity take place in relatively short distances) the stress terms dominate the inertial (convective) terms.

- for a flow with little curvature stress terms dominate the inertial terms, but both are unimportant compared with bottom friction.

The stresses T_{xx}, T_{xy} and T_{yy} consist of three contibutions:

- the viscous stresses
- turbulent stresses
- stresses due to depth integration of the three dimensional advective terms (the convective part of the stresses).

The magnitude of the viscous stresses plus the turbulent stresses is in the order of the bottom stress, with respect to the turbulent stresses the viscous stresses can be neglected outside the viscous sub-layer (see Flokstra, lit. [1]).

The magnitude of the last stresses is dependent on the curvature of the mean streamline, it describes the large scale transfer of momentum caused by the deviations between the local velocity (u, v) and the mean velocity ($\bar{u}$, $\bar{v}$).

Resulting:

$$T_{xx} = \frac{1}{h} \int_o^h \left[- \rho\overline{u'^2} - \rho(\bar{u} - u)^2 \right] dz \quad \text{[8A]}$$

$$T_{xy} = \frac{1}{h} \int_o^h \left[- \rho\overline{u'v'} - \rho(\bar{u} - u)(\bar{v} - v) \right] dz \quad \text{[8B]}$$

$$T_{yy} = \frac{1}{h} \int_o^h \left[- \rho\overline{v'^2} - \rho(\bar{v} - v) \right] dz \quad \text{[8C]}$$

II The turbulent stresses

The turbulent stresses are characterized by:

$$q_{xx} = - \rho \overline{u'^2}$$

$$q_{xy} = - \rho \overline{u'v'}$$

$$q_{yy} = - \rho \overline{v'^2}$$

In order to determine the magnitude of these stresses, some relation between this turbulence and the parameters u, v and h must be found.
Most of the solutions for this relation are based on the assumption that the turbulent transport is proportional to the gradients of the parameters of the mainflow, the coefficient involved is called the turbulent eddy-viscosity:

$$q_{ij} = - \overline{\rho v_i v_j} = - \rho\varepsilon \left(\frac{\partial \bar{v}_j}{\partial x_i} + \frac{\partial \bar{v}_i}{\partial x_j}\right) \quad \text{[9]}$$

ε = turbulent eddy-viscosity [m^2/s]

(see lit. [4])

This turbulent eddy-viscosity coefficient ε can be determined by different models (see Launder and Spalding (lit. [5]) Rodi (lit. [6]).

A. A constant viscosity model: ε = constant

This viscosity coefficient is based on the depth averaged characteristics of the main flow.

B. A mixing length model: $\varepsilon = l_m^2 \left| \frac{\partial u_i}{\partial x_j} \right|$

The viscosity coefficient is based on a specific turbulence length scale L_t and velocity scale V_t

$$\varepsilon_{turb} = L_t V_t \quad \text{[10]}$$

according to the thesis of Prandtl, assuming a mixing length l_m over which the "packets" of fluid retain their original properties

$$L_t = l_m \quad \text{[11A]}$$

$$V_t = l_m \left| \frac{\partial u}{\partial y} \right| \quad \text{[11B]}$$

In this model the mixing length is given by some expression, considering the boundary conditions of turbulence transfer at the bottom and the surface.

For example:

in a boundary layer (Prandtl)

$$l_m = \kappa y \quad \text{[12A]}$$

in closed pipes (Nikuradse)

$$l_m = 0.14 - 0.08 \left(1 - \frac{y}{R}\right)^2 - 0.06 \left(1 - \frac{y}{R}\right)^4 \quad \text{[12B]}$$

in open channels etc. (Bakhmetev)

$$l_m = \kappa \, h \, \frac{y}{R} \left(1 - \frac{y}{R}\right) \quad \text{[12C]}$$

R = hydraulic radius
y = co-ordinate perpendicular to boundary
(to the bottom in 12C)

C. Differential viscosity models:

ε is solved from an extra differential equation including energy dissipation by turbulence.

An example is the κ-ε-model (see lit. [5], [6]).

There are also some models that use the differential equations for the transfer of turbulence instead of a gradient type equation (eq. 9). Here only the model using constant viscosity is described, because it is most commonly used in two dimensional shallow water models.

The turbulent stresses in a constant viscosity model become:

$$T_{xx} = 2\,\rho\varepsilon\left(\frac{\partial\bar{u}}{\partial x}\right) \quad [13A]$$

$$T_{xy} = \rho\varepsilon\left(\frac{\partial\bar{u}}{\partial y} + \frac{\partial\bar{v}}{\partial x}\right) \quad [13B]$$

$$T_{yy} = 2\,\rho\varepsilon\left(\frac{\partial\bar{v}}{\partial y}\right) \quad [13C]$$

Resulting in following expressions for the effective stress components in eq [2] and [3]:

$$\frac{1}{\rho}\;\frac{\partial}{\partial x}(h\,T_{xx}) + \frac{\partial}{\partial y}(h\,T_{xy}) = \varepsilon h\left(\frac{\partial^2\bar{u}}{\partial x^2} + \frac{\partial\bar{u}^2}{\partial y^2}\right) \quad [14A]$$

and

$$\frac{1}{\rho}\;\frac{\partial}{\partial x}(h\,T_{xy}) + \frac{\partial}{\partial y}(h\,T_{yy}) = \varepsilon h\left(\frac{\partial^2\bar{v}}{\partial x^2} + \frac{\partial^2\bar{v}}{\partial y^2}\right) \quad [14B]$$

neglecting the gradients of ε and $\frac{\partial^2\bar{u}}{\partial x\partial y}$ and $\frac{\partial^2\bar{v}}{\partial x\partial y}$.

(compare the equations of DUCHESS, par. 2.1).

The value of ε is hard to find; an analogy could be seen with the dispersion of matter in a turbulent flow, where ε is analogeous to a gradient type diffusion term $D\,\frac{\partial c}{\partial x}$

$$D_b \simeq (0.1 \text{ à } 0.2)\; h|u_*| \quad [15]$$

D_b = diffusion coefficient in transverse direction

This value ε is 2 of 3 times bigger than the theoretical depth averaged diffusion coefficient: (see appendix B)

$$\overline{\varepsilon_z} = 2/3 * (1/4\ \kappa\ h|u_*|) = 0.067\ h\ u_* \quad [16]$$

which can be explained by the fact that in vertical direction the diffusion is disturbed at the bottom and surface, while this is not the case in lateral direction, exept at the closed side boundares, where some kind of slip condition must be applied (see Stelling (lit. [7]), Kuipers and Vreugdenhill (lit. [2])).

Another way to find ε is from calibration of the main flow characteristics

$$\varepsilon = \frac{-\ \overline{u'v'}}{\frac{\partial \bar{u}}{\partial y} + \frac{\partial \bar{v}}{\partial x}} \quad [17]$$

Using some assumption for the magnitude of $\overline{u'v'}$ (or by measuring). Mostly $\frac{\partial \bar{v}}{\partial x}$ is neglected compared to $\frac{\partial \bar{u}}{\partial y}$ and $\frac{\partial \bar{u}}{\partial y}$ can be related to the main flow parameters also see lit. [7].

Liepmann and Laufer (lit. [8]) and Tani (lit. [9]) found that the order of magnitude of the turbulent fluctuations were:

$$\overline{u'^2} \simeq 0.040\ \bar{u}^2 h$$

$$\overline{u'v'} \simeq 0.015\ \bar{u}^2 h$$

$$\overline{v'^2} \simeq 0.020\ \bar{u}^2 h$$

Flokstra (lit. [1]) investigated the relative importance of the contribution of the stresses T_{xx}, T_{xy} and T_{yy}, finding that the energy transfer to the circulating flow is ruled by effective stress. T_{xy}, and the turbulent stress is the only energy transferring mechanism into the circulating flow.
The con ective stresses generally transfer energy out of the flow. This agrees with the above mentioned, the effective stress constribution $- \rho\ \overline{u'v'}$ will be dominant, and at least of the same order of magnitude as the bottom stress in a shear layer (or mixing layer). Outside such a shear layer the bottom shear stress predominates the other distributions, unless the curvature of the streamline is large (see part III).

III The convective stresses

When taking into account the turbulent contributions to the effective stresses, no consideration has been given to the convection of momentum in the main flow. It refers to deviations of depth averaged flow as caused by the effect of curvature (and acceleration of coriolis). This effect causes the horizontal velocity vector to rotate over the vertical. The difference between the actual velocity and the depth averaged velocity yields the secondary flow components, in rivers giving rise to typical helical flow phenomenon. It strongly varies over the depth, but often its magnitude is small compared to the characteristic horizontal velocity. Therefore it is mostly neglected in computations. However, considering dispersion of matter of morphology of an alluvial bed, its influence is striking and it cannot be neglected at all.

Kalkwijk and Booy (lit. [10]) developed a method to approximate the generation and decay of secondary flow in steady or quasi-steady horizontal flow models.

The momentum equation in the n-direction (normal to the mainflow (in s-direction)) can be written as:

$$\frac{\partial u_n}{\partial t} + \frac{\partial u_s u_n}{\partial s} + \frac{\partial u_n^2}{\partial n} + \frac{\partial u_z u_n}{\partial z} +$$

$$+ 2\frac{u_s u_n}{R_n} + \frac{u_n^2 - u_s^2}{R_s} + \Omega\, u_s + \frac{1}{\rho}\frac{\partial p}{\partial n} +$$

$$+ \quad \text{friction terms} = 0 \quad \ldots\ldots\ldots\ldots\ldots\ldots\ldots \quad [18]$$

u_n = horizontal velocity in n-direction
u_s = horizontal velocity component in streamwise direction
u_z = vertical velocity component
R_n = radius of curvature of the depth averaged flow
R_s = radius of curvature of the streamlines of the depth averaged flow
Ω = coriolis coefficient
p = pressure

In the case of a rapidly varying main flow, more terms appear in [18].

Introducing the assumptions:

- hydrostatic pressure (nearly horizontal flow)
- neglect of friction in vertical planes
- neglect of all inertia terms exept the centrifugal term
- introducing of the eddy-viscosity concept to describe the vertical exchange of momentum by friction

yields a simplified version of equation (18) in which the essential features of secondary flow are maintained:

$$\frac{\partial u_n}{\partial t} + u_s \frac{\partial u_n}{\partial s} - \frac{u_s^2}{R_s} + \Omega\, u_s +$$

$$+ g \frac{\partial \eta}{\partial h} - \frac{\partial}{\partial z}\left(E \frac{\partial u_n}{\partial z}\right) = 0 \ldots\ldots\ldots\ldots\ldots\ldots\ldots\ldots \quad [19]$$

and the depth averaged form

$$\overline{\bar{u}_s \frac{\partial u_n}{\partial s}} - \frac{\bar{u}_s^{\,2}}{R_s} + \Omega\, \bar{u}_s + g \frac{\partial \eta}{\partial n} + \frac{\tau_h}{\rho h} = 0 \ldots\ldots\ldots\ldots \quad [20]$$

η = water level
τ_n = bottom friction
E = eddy-viscosity coefficient in vertical direction

When the water level η is eliminated from (19) and (20):

$$\frac{\partial u_n}{\partial t} + u_s \frac{\partial u_n}{\partial s} - \overline{u_s \frac{\partial u_n}{\partial s}} + \frac{\bar{u}_s^{\,2} - u_s^{\,2}}{R_s} +$$

$$+ \Omega\,(u_s - \bar{u}_s) - \frac{\partial}{\partial z}\left(E \frac{\partial u_n}{\partial z}\right) - \frac{\tau_n}{\rho h} = 0 \ldots\ldots\ldots\ldots \quad [21]$$

In the following it will be assumed that at each level the secondary flow velocities are much smaller than the main flow velocities. The viscosity can be assumed to be completely determined by the main flow. The distribution of the main flow velocity is the usual logarithmic one:

$$u_s = \bar{u}_s \left(1 + \alpha + \alpha \ln(1 + \frac{z}{h}\right) \ldots\ldots\ldots\ldots\ldots\ldots \quad [22]$$

and the viscosity pertaining to the logarithmic velocity distribution is the usual parabolic one:

$$E = - \kappa^2\, \alpha\, h\, |\, \bar{u}_s\, |\, \frac{z}{h}\left(1 - \frac{z}{h}\right) \ldots\ldots\ldots\ldots\ldots\ldots \quad [23]$$

$$\alpha = \frac{\sqrt{g}}{\kappa C} = \left(\ln\left(\frac{h}{Zo}\right) - 1\right)^{-1} = \frac{\sqrt{\tau_s/\rho}}{\bar{u}_s\ \kappa}$$

representing a friction parameter

C = Chézy coefficient
κ = constant of Von Karman = 0.4

The secondary flow caused by the effect of curvature is described by (for the effect of Coriolis another equation can be used, see Booy and Kalkwijk lit. [10].

$$\frac{\partial u_n}{\partial t} + u_s \frac{\partial u_n}{\partial s} - \overline{u_s \frac{\partial u_n}{\partial s}} + \frac{\overline{u_s}^2 - u_s^2}{R_s} - \frac{\partial}{\partial z}\left(E \frac{\partial u_n}{\partial z}\right) - \frac{\tau_n}{\rho h} = 0 \qquad \ldots\ldots\ldots\ldots\ldots [24]$$

When steady, fully developed secondary flow is assumed, all $\frac{\partial}{\partial t}$ - and all the $\frac{\partial}{\partial s}$ -terms are zero,

the relevant equation is: (driving force)

$$-\frac{\partial}{\partial z}\left(E \frac{\partial u_n}{\partial z}\right) - \frac{\tau_n}{\rho h} = -\frac{\overline{u_s}^2 - u_s^2}{R_s} \qquad \ldots\ldots\ldots\ldots\ldots [25]$$

Conditions:

- the shear stress at the surface vanishes: $\tau_n\ (z = 0) = 0$
- the velocity integrated over the depth must be zero:

$$\int_{-h}^{0} u_n \, dz = 0$$

- somewhere close to the bottom the velocity must be zero, it is assumed that the secondary velocity is equal to zero at the same depth, $z = z_0 - h$ as the main velocity.

The final solution can be written

$$u_n = 2 \frac{|\overline{u_s}|\, h}{\kappa^2 R_s} \cdot f_b\left(\frac{z}{h}, \alpha\right) \qquad \ldots\ldots\ldots\ldots\ldots\ldots\ldots [26]$$

f_b = function of $\frac{z}{h}$ and α,

being:

$$f_b\left(\frac{z}{h}, \alpha\right) = f_c\left(\frac{z}{h}, \alpha\right) + \frac{\alpha}{2} f_{b1}\left(\frac{z}{h}, \alpha\right) \qquad \ldots\ldots\ldots\ldots [27]$$

$f_c\left(\frac{z}{h}, \alpha\right)$ = function related to the secondary flow effect due to coriolis influences

$$= \int_{-1}^{\frac{z}{h}} \frac{z}{h} \ln\left(1 + \frac{z}{h}\right) d\left(\frac{z}{h}\right) + \frac{\pi^2 - 6}{6} - \alpha\left(1 + \ln\left(1 + \frac{z}{h}\right)\right) \qquad \ldots\ldots\ldots\ldots\ldots [27A]$$

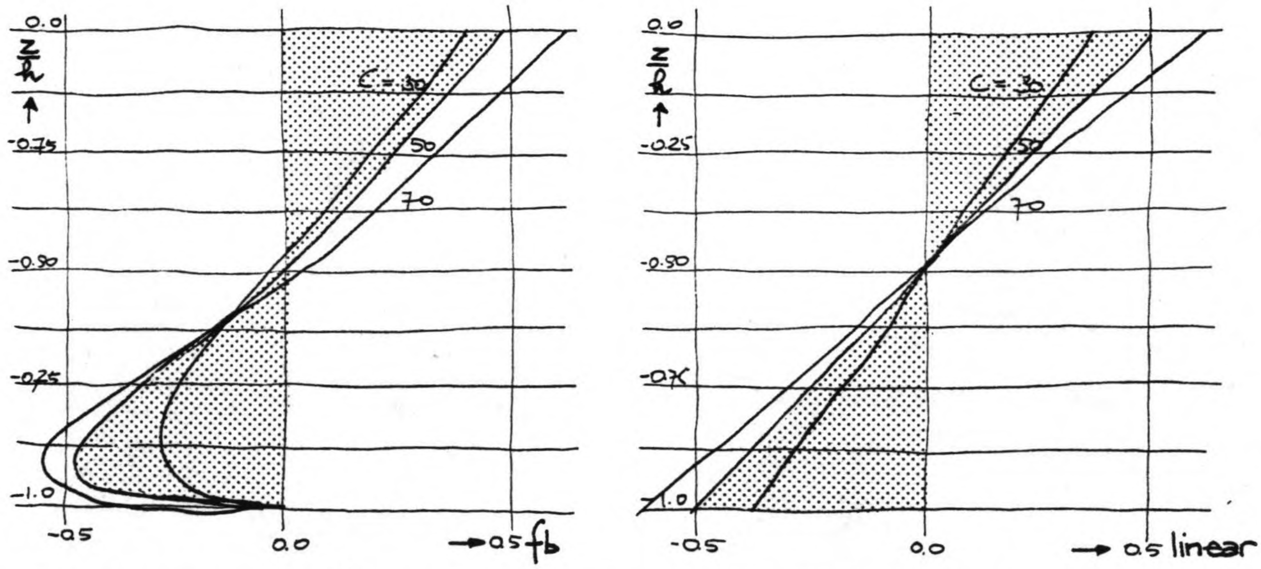

2

FUNCTIONS OF f_b AND u_n RELATED TO ROUGHNESS C (α)

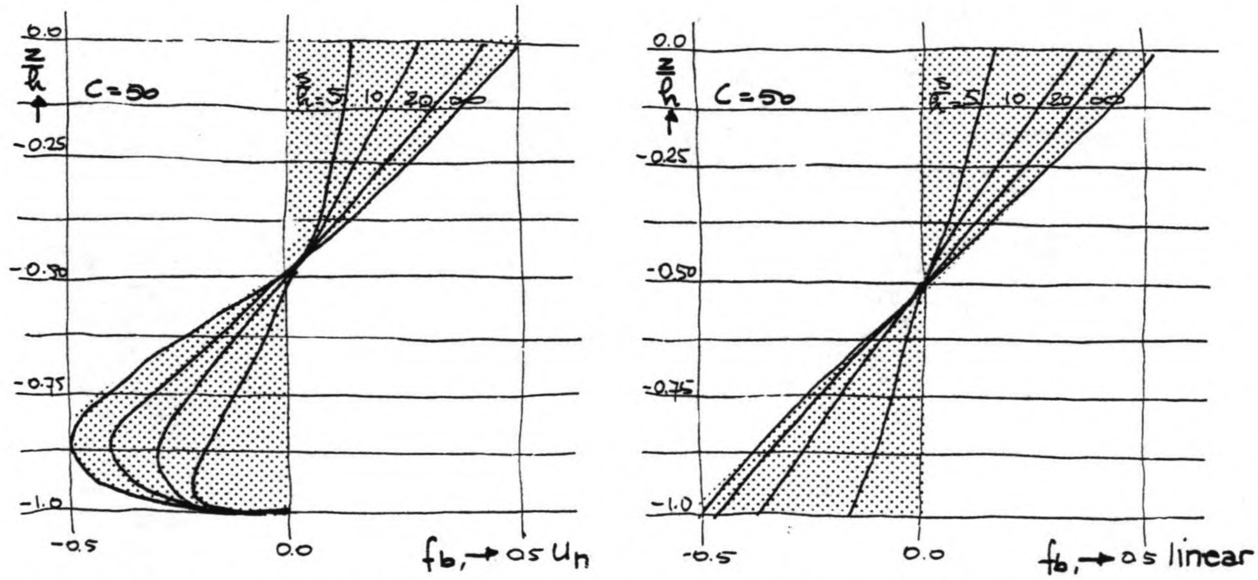

3

FUNCTIONS OF f_b AND u_n RELATED TO THE DISTANCE s`

SOURCE: BOOIJ AN KALKWIJK [17]

$f_{b1}(\frac{z}{h}, \alpha)$ = function related to secondary flow distribution due to curvature effect

$$= \int_{-1}^{\frac{z}{h}} \frac{z}{h} \ln^2(1 + \frac{z}{h})\, d\left(\frac{z}{h}\right) + 2 + 2\alpha$$

$$+ 2\alpha \ln(1 + \frac{z}{h}) \quad \text{[27B]}$$

some pictures of f_b are shown in Fig. A2 and A3, for the bottom stress it can be found:

$$\tau_h = 2\rho\alpha^2(1 - \alpha)\, \frac{h}{R_s}\, \bar{u}_s^{\,2} \quad \text{[28]}$$

LINEAR APPROXIMATIONS

The expressions for the respective secondary flows are quite complicated fucntions of $\frac{z}{h}$.

It is therefore remarkable that the profiles show an almost linear behaviour (see Figure A2). Only close to the bottom there is a rather decrease of velocities. The velocity profiles will be approximated linearly by stating that u_n varies linearly over the depth, then:

$$u_n = 2\, \frac{|\bar{u}_s|\, h}{\kappa^2 R_s}\, m_b \left(\tfrac{1}{2} + \frac{z}{h}\right) \quad \text{[29]}$$

$$m_b = \frac{m_1}{2} - \alpha m_1 + \frac{\alpha}{4} m_2 + 0\,(\alpha^2)$$

$$m_1 = 2\left(1 + \ln\left(1 + \frac{z}{h}\right)\right) = 3 \text{ (least squares)}$$

$$m_2 = \frac{4}{\alpha}\left(\frac{\alpha}{2} \ln\left(1 + \frac{z}{h}\right)\left(2 + \ln\left(1 + \frac{z}{h}\right)\right)\right) \simeq 0$$

THE ADAPTION LENGTH

The approximations given below are based on steady flow. To derive a simple expression for the dependence on the streamwise co-ordinate S other simplifications are made:

- in the term $u_s \frac{\partial u_n}{\partial s}$ u_s will be replaced by $\bar{u}_s$, only close to the bottom this leads to a relatively large error;
- u_n will be supposed to depend linear on z as in the case of fully developed flow:
- the driving force is a linear function of z with the factor $(\frac{1}{2} + \frac{z}{h})$:
- solutions are attempted of the form:

  $u_n = K(s) . u_{n\ fully\ developed}$

  K(s) is a function of s only, u_{nfd} means the secondary flow velocity in case of $\frac{\partial}{\partial s} = 0$;

- τ_n will be assumed to behave in the same way as u_n;
  $\tau_n = K(s) . \tau_{n\ fully\ developed}$.

After substituting all expressions and reducing all terms of $O(\alpha^2)$ it results:

$$\frac{R_s}{|u_s|} \frac{\frac{1-2\alpha}{2\alpha\kappa^2} d(|\bar{u}s|h \frac{K(s)}{R_s})}{ds} + K(s) = 1 \quad \ldots\ldots\ldots\ldots [30]$$

Assuming $\bar{u}_s$, R_s and h constant along a streamline

$$\frac{1-2\alpha}{2\alpha\kappa^2} \frac{d\ K(s)}{d\ \frac{s}{h}} + K(s) = 1 \quad \ldots\ldots\ldots\ldots [31]$$

then a relaxation length L can be defined, based on the elementary solution of eq. (31): $1-K(s) = C. \exp(-\lambda s/h)$

$$L = \frac{h}{\lambda} = \frac{1-2\alpha}{2\alpha\kappa^2} h \quad \ldots\ldots\ldots\ldots [32]$$

NUMERICAL SOLUTION

Kalkwijk and Booy (lit.(10)) have determined a numerical equation for the gradual adaption of secondary flow along the streamlines, incorporated in a 2D-mathematical model for unsteady nearly horizontal flow, based on all the assumptions made in the forgoing.

The results:

$$\frac{1-2\alpha}{2\alpha\kappa^2}\,\frac{h}{u_s}\left[\frac{\bar{u}_x}{u_s}\frac{\partial k}{\partial x}+\frac{\bar{u}_y}{u_s}\frac{\partial k}{\partial y}\right]+$$

$$k\left[1+\frac{1-2\alpha}{2\alpha\kappa^2}\,\frac{R_s}{u_s^2}\left(\bar{u}_x\frac{\partial\,\alpha h|\bar{u}_s|/R_s}{\partial x}+\bar{u}y\frac{\partial\,\alpha h|\bar{u}_s|/R_s}{\partial y}\right)\right]=1\quad\ldots[33]$$

This can be coupled to a 2D-horizontal flow program (for example DUCHESS) in order to take into account the convective stresses. Of course this is a very rude way to take them into account, a better way would be to incorporate these results in an expression for the convective part of T_{xx}, T_{xy} and T_{yy}. It must be stressed that eq. (33) can only be used as a correction method, after the flow pattern has been determined by some 2 DH-model.

Van Bendegom (lit. (11)) derived some expressions for the secondary flow also, based on the power law velocity profile:

$$\frac{u_s}{\bar{u}_s}=\frac{n+1}{n}\left(\frac{z}{h}\right)^{\frac{1}{n}}\quad\ldots\ldots\ldots\ldots[34A]$$

$$\frac{u_n}{\bar{u}_s}=\frac{n}{R_s\kappa^2}\left[-\frac{n(n+1)}{n+3}\left(\frac{z}{h}\right)^{\frac{1}{n}}+\frac{n^2(n+1)}{n+2}\int_0^{\left(\frac{z}{h}\right)^{\frac{1}{n}}}\frac{1-z^{n+2}}{n+z^n}\,dz\right]\quad\ldots\ldots\ldots\ldots[35A]$$

Both these equations or (26) and (29) can be used to find expressons for the convective stresses (eq. 8A .. C).
As uptill now no 2-dimensional horizontal model is available taking into account both these stresses, no further attention will be given in this analysis.

DUCHESS incorporates an approximation for the turbulent stresses, and in MORPHOR the secondary flow phenomenon is taken into account in the morphological computation.

REFERENCES APPENDIX A (the closure problem)

1. C. Flockstra: The closure problem for depth averaged dimensional flow

Publication no. 190
Delft Hydraulics Laboratory 1977

2. J. Kuipers and C.B. Vreugenhill: Calculations on two-dimensional horizontal flow

Report no. S 163 part I
Delft Hydraulics Laboratory 1973

3. J.J. Leendertse: Aspects of a computational model for long-period water wave propagation

Mem. RM-5294 PR
Rand corp. 1967

4. R. Booy: Turbulentie in de waterloopkunde

Collegedictaat B 82
Delft University of Technology 1986

5. B.E. Launders and D.B. Spalding: Lectures on mathematical models of turbulence

New York
Academic Press, London 1972

6. W. Rodi: Turbulence models and their application in hydraulics

State of the art paper
IAHR, Delft 1980

7. G.S. Stelling and L.X. Wang: Experiments and computations on unsteady separating flow in an expanding flume

Report no. 2-84
Delft University of Technology
Department of Civil Engineering 1984

8. H.W. Liepmann and J. Laufer: Investigation of free turbulent mixing

Technical Note 1257 1947

9. I. Tani, M. Luchi and H. Komoda: Experimental investigation of flow separation associated with a step or a groove

Report 364
Aeronautical Research Institute
University of Tokyo 1961

10. R. Booy and J.P. Kalkwijk: Adaption of secondary flow in nearly horizontal flow

Delft University of Technology
Department of Civil Engineering

11. L. van Bendegom: Some considerations on river morphology and river improvement

De Ingenieur 59, B1-11 1947

APPENDIX B

COMPUTATION OF THE TOTAL LOAD SEDIMENT TRANSPORT: VAN RIJN

I. Introduction

The transport of sediment particles by a flow of water can be in the form of bed-load and suspended load, depending on the size of the bed-material and the flow conditions.

Although in natural conditions there is no sharp division between the bed-load transport and suspended load transport, it is necessary to define a layer with bed-load transport for mathematical representation. Usually three modes of particle motion are distinguished:

1. rolling and sliding motion;

2. saltation motion;

3. suspended particle motion.

When the value of the bed shear velocity just exceeds the critical value for initiation of motion, the particles will be rolling and sliding or both, in contineous contact with the bed. For increasing values of the bed-shear velocity, the particles will be moving along the bed more of less by regular jumps, which are called saltations. When the value of the bed-shear velocity exceeds the fall velocity of the particles, the sediment particles can be lifted to a level at which the upward turbulent forces will be comparable with, or of higher order than, the submerged weight of the particles and as a result the particles may go into suspension.

II. The bed-load transport

In this study the approach of Bagnold is followed, which means that the motion of the bed-load particles is assumed to be dominated by gravity forces, while the effect of turbulence on the overall trajectory is supposed to be of minor importance. The dimensions of the trajectory are typically those of a saltating particle. If for given flow conditions there are sediment particles with a jump height larger than a theoretical maximum saltation height (which can be computed from the equation of motion for a bed-load particle), then these particles a e assumed to be transported as suspended load.
All particles with a jump height smaller than the maximum saltation height are transported as bed-load.

The transport rate of the bed-load (q_b) is defined as the product of particle velocity (u_b), the saltation height (δ_b) and the bed-load concentration (C_b).

$$q_b = u_b \, \delta_b \, C_b$$

In this analysis it is assumed that the bed-load transport rate can be described sufficiently accurate by two dimensionless parameters:
a dimensionless particle parameter D_*:

$$D_* = D_{50} \left[\frac{(s-1)g}{V^2} \right]^{\frac{1}{3}} \quad \ldots\ldots\ldots\ldots (1)$$

and a transport stage parameter T

$$T = \frac{(u_*')^2 - (u_{*,crs})^2}{(U_{*,crs})^2} \quad \ldots\ldots\ldots\ldots (2)$$

D_{50} = medium particle size

s = specific density = $\frac{\rho s}{\rho}$

g = acceleration of gravity

υ = kinematic viscosity = $\frac{\mu}{\rho}$

u_*' = bed shear velocity related to grains = $\frac{\sqrt{g}}{C'} \bar{u}$

C' = Chézy-value related to grains = $18 \log \frac{12R}{3D_{90}}$

$\bar{u}$ = mean flow velocity

D_{90} = 90% particle size

$u_{*,crs}$ = critical bed shear velocity according to Shields (see fig. B1)

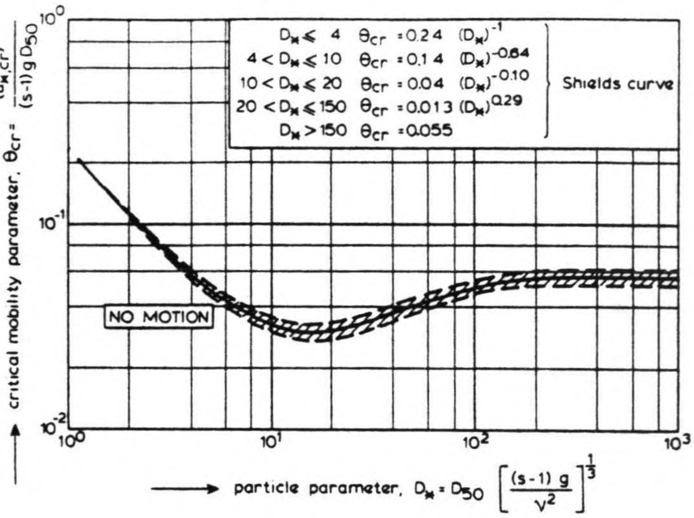

1

The introduction of the D_* and T parameter has been initiated by Ackers-White (lit. (*)) and Yalin (lit. (*)).

EQUATIONS OF MOTION

The forces acting on a saltating particle are a downward force due to its submerged weight: F_G

$$F_G = \frac{1}{6} \pi D^3 (\rho s - \rho) g \quad \ldots \quad (3)$$

and hydrodynamic fluid forces, which can be resolved in a lift force F_L and a drag force F_D.

The lift force in a shear flow is caused by the velocity gradient present in the flow (shear-effect) and by the spinning motion of the particle (Magnus-effect). For viscous flow:

$$F_L = \alpha_L \rho \nu^{0.5} D^2 V_r \left[\frac{\partial u}{\partial z}\right]^{0.5} \quad \ldots \quad (4)$$

(shear)

$$F_L = \alpha_L \rho D^3 V_r \omega \quad \ldots \quad (5)$$

(spin)

α_L = lift coefficient
ω = angular velocity of the particle
V_r = particle velocity

Saftman (lit. (*)) showed theoretically that for viscous flow the lift force due to rotation of the particles is less by an order of magnitude than that due to the shear effect, and may therefore be neglected. It is assumed that these equations are also valid for turbulent flow, the lift force is being described by eq. (4) using the α_L-coefficient as a calibration parameter.

the drag force:

$$F_D \; \tfrac{1}{2} C_D \rho A V_r^2 \quad \ldots\ldots (6)$$

C_D = drag force coefficient

$\Delta = \tfrac{1}{4} \pi D^2$ = cross-sectional area of the sphere.

Under the assumptions that
1. the particles are spherical and of uniform density;
2. the forces due to fluid accelerations are of second order.

The equations of motion can be presented as:

$$mx - \vec{F}_L \left(\frac{\dot{z}}{V_r}\right) - \vec{F}_b \left(\frac{u - \dot{x}}{V_r}\right) = 0 \quad \ldots\ldots (7)$$

$$mz - \vec{F}_L \left(\frac{u - \dot{x}}{V_r}\right) + \vec{F}_D \left(\frac{\dot{z}}{V_r}\right) + \vec{F}_G = 0 \quad \ldots\ldots (8)$$

$$v_r = \quad (u - \dot{x})^2 + \dot{z}^2$$

u = local flow velocity

<u>fig. B2</u> definition sketch of particle saltation

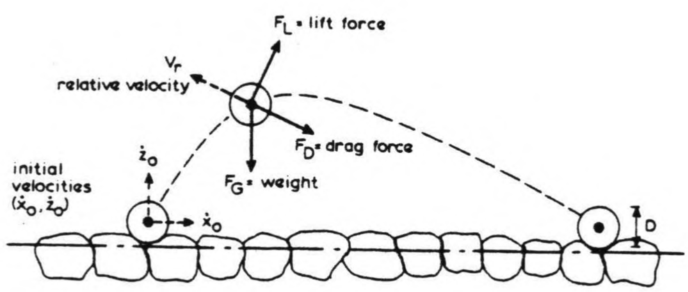

2

The total mass of the particle:

$$m = \frac{1}{6} (\rho_s + \alpha_m \rho) \pi D^3 \quad \quad (9)$$

α_m = added mass coefficient

The vertical flow velocity distribution is described by

$$u(z) = \frac{u_*}{\kappa} \ln \frac{(z)}{z_o} \quad \quad (10)$$

$z_o = 0.11 \left(\frac{\nu}{u^*}\right) + 0.03\, k_s$ = zero velocity level

k_s = equivalent roughness according to Nikuradse

κ = constant of Von Karman (= 0.4)

With this set of equations the particle motion can be solved (numerically

which Van Rijn did for various particle diameters (D = 100 µm - 2000 µm). As a result the saltation height, saltation length and the particle velocity can be computed.

Van Rijn used following assumptions:

$k_s = 2D$

$\dot{x}_o = \dot{z}_o = 2u_*$

$z_o = 0.6\ D$

$\rho_s = 2650$ kg/m3

$\nu = 1.10^{-6}$

$\alpha_m = 0.5$

$\alpha_L = 1.6$ for $\frac{u_* D}{\nu} (= R_*) \leq 5$

$\alpha_L = 20$ for $R_* \geq 70$

and $\alpha_L = 1.6 - 20$ (lineair) for $5 \leq R_* \leq 70$

$\kappa = 0.4$

SALTATION HEIGHT

The curves of the computed saltation height can be approximated with an inaccuracy of 10% by the following simple expression:

$$\frac{\delta_b}{D} = 0.3\, D_*^{\,0.7}\, T^{0.5} \qquad (11)$$

SALTATION LENGTH

The curves of the computed saltation length can be approximated with an inaccuracy of 50% by the following simple expression:

$$\frac{\lambda_b}{D} = 3\, D_*^{\,0.6}\, T^{\,0.9} \qquad (12)$$

PARTICLE VELOCITY

The particle velocity as a function of flow conditions and sediment size can be approximated with an inaccuracy of 10% by

$$\frac{u_b}{u_*} = 9 + 2.6 \log D_* - 8 \left(\frac{\theta_{cr}}{\theta}\right)^{0.5} \qquad (13)$$

or with an inaccuracy of 20% by

$$\frac{u_b}{\left[(s-1)gD\right]^{0.5}} = 1.5\, T^{0.6} \qquad (14)$$

THE BED-LOAD CONCENTRATION

In the present analysis the bed-load transport is defined as the product of the thickness of the bed-load layer, the particle velocity and the bed-load concentration.
Extensive analysis of data showed that the bed-load concentration can be expressed as:

$$\frac{c_b}{c_o} = 0.18\, \frac{T}{D_*} \qquad (15)$$

c_o = maximum bed concentration = 0.65

About 80% of the computed values (according to the set of equations (3)--(10)) are within the range of half and double value according to eq. (15). In par. 3 about suspended load eq. (15) will be modified so that it can be used to predict the reference concentration for the concentration profile.

COMPUTATION OF THE BED-LOAD TRANSPORT

Using eq. (11) (14) and (15) the bed-load for particles in the range of 200 µm - 2000 µm can be computed as:

$$\frac{q_b}{(s-1)g^{0.5} D_{50}^{1.8}} = 0.053 \frac{T^{2.1}}{D_*^{0.3}} \quad \ldots\ldots\ldots\ldots\ldots (16)$$

q_b in m2/s

The computation of the bed-load transport is as follows:

1. compute particle diameter D_* using eq. (1);

2. compute critical bed-shear velocity $u_{*,crs}$ according to Shields using fig. B1;

3. compute Chézy coefficient related to grains C' using $C' = 18 \log \frac{12R}{3D_{90}}$;

4. compute effective bed-shear velocity related to grains using $u_*^1 = \frac{\sqrt{g}\,\bar{u}}{C'}$;

5. compute transport stage parameter T using eq. (2);

6. compute bed-load transport q_b using eq. (16).

The input data are:

- mean flow velocity .... $\bar{u}$
- mean flow depth .... d
- mean flow width .... b
- particle diameters .... D_{50}, D_{90}
- density of water and sediment ρ, ρ_s
- viscosity coefficient ...... υ
- acceleration of gravity .....g

VERIFICATION

For comparison the formulas of Engelund-Hansen (lit. (*)) and Ackers-White (lit. (*)) were applied. The typical bed-load formula of Meijer-Peter-Müller (lit. (*)) was also used. Most of the flume data used for verification were selected from a compendium of solids transport compiled by Peterson and Howels (lit. (*)). Brownlie (lit. (*)) has shown that various of this databank contain serious errors, Van Rijn has eliminated these errors befor using the data in the verification analysis. Only experiments with a D_*-value larger than 12 (≈ 500 μm) were selected, assuming that for these conditions the mode of transport is mainly bed-load transport. For nearly all data the ratio (overall) bed-shear velocity and the particle fall velocity was smaller than one ($u_*/w_s < 1$). To evaluate the accuracy of the computed and measured values, a discrepancy ratio r has been used:

$$r = \frac{q_b \text{ computed}}{q_b \text{ measured}}$$

The results are given in tabel B1, it is remarked that the formulas of Engelund-Hansen were not applied to the data of Guy et al. and Shien (small particle range), because for these data the formulas will predict the total load, and not the bed-load transport.

Tabel B1

Comparison of computed and measured bed-load transport

	Source (1)	Number of tests (2)	Flow velocity, in meters per second (3)	Flow depth, in meters (4)	Particle diameter (× 10⁻⁶ m) (5)	Temperature, in degrees Centigrade (6)
Field data	Japanese Channels (Tsubaki)	12	0.63–0.93	0.20–0.73	1,330–1,440	—
	Mountain Creek (Einstein)	43	0.49–0.79	0.10–0.43	900	15–25
	Skive-Karup River (Hansen)	1	0.6	1.0	470	10
Flume data	Guy et al.	22	0.36–1.29	0.15–0.23	320	8–34
	Delft Hydraulics Laboratory	18	0.40–0.87	0.10–0.49	770	12–18
	Stein	38	0.42–1.10	0.10–0.37	400	20–26
	Meyer-Peter	18	0.45–0.88	0.11–0.21	1,000–1,500	—
	U.S.W.E.S. (sands)	48	0.44–0.58	0.10–0.20	1,000	14–18
	U.S.W.E.S. (synth. sands)	183	0.44–0.57	0.15–0.27	500–1,100	19–25
	Singh	60	0.31–0.66	0.10–0.20	600	13–20
	Znamenskaya	10	0.53–0.80	0.11–0.20	800	—
	Southampton B	73	0.31–0.70	0.15–0.46	480	22–30
	East Pakistan	21	0.44–0.70	0.15–0.30	470	25–30
	Williams	33	0.46–1.04	0.15–0.22	1,350	16–26
	Total	580				

Source	SCORES (PERCENTAGE) OF PREDICTED BED LOAD IN DISCREPANCY RANGES											
	$0.75 \le r \le 1.5$				$0.5 \le r \le 2$				$0.33 \le r \le 3$			
	Van Rijn (7)	Engelund/Hansen (8)	Ackers/White (9)	Meyer-Peter Müller (10)	Van Rijn (11)	E-H (12)	A-W (13)	MPM (14)	Van Rijn (15)	E-H (16)	A-W (17)	MPM (18)
Japanese Channels (Tsubaki)	48%	61%	83%	57%	78%	87%	91%	91%	86%	100%	100%	96%
Mountain Creek (Einstein)	28	56	21	74	54	81	67	95	84	93	98	100
Skive-Karup River (Hansen)	100	0	0	0	100	0	0	100	100	100	0	100
Guy et al.	64	—	—	51	92	—	—	87	100	—	—	100
Delft Hydraulics Laboratory	13	17	78	0	75	83	100	71	88	94	100	86
Stein	27	—	—	4	63	—	—	4	92	—	—	22
Meyer-Peter	6	82	24	6	29	94	59	41	82	94	94	76
U.S.W.E.S. (sands)	50	49	80	17	92	100	96	50	100	100	100	60
U.S.W.E.S. (synth. sands)	50	39	49	30	82	85	86	56	96	99	99	74
Singh	58	55	80	3	92	97	100	43	100	98	100	78
Znamenskaya	30	40	40	50	60	50	70	70	80	90	80	100
Southampton B	44	11	34	41	87	27	64	73	92	63	84	85
East Pakistan	10	5	10	14	29	5	10	33	62	10	29	67
Williams	20	74	23	37	71	89	60	65	97	100	82	83
Total	42%	43%	48%	23%	77%	76%	77%	58%	93%	90%	92%	76%

III. The suspended load transport

An essential part of morphological computations in the case of flow conditions with suspended sediment transport is the use of a reference concentration as a bed-boundary condition. The function for the bed-load concentration as proposed before in par. II can also be used to compute the reference concentration for the suspended load.

The bed-load transport and therefore the reference concentration at the bed are determined by particle diameter D_* (eq. (1)) and transport stage parameter T (eq. (2)).

To describe the suspended load a suspension parameter Z which expresses the influence of the upward turbulent fluid forces and the downward grantational forces is defined as:

$$Z = \frac{\omega_s}{\beta \kappa u_*} \quad \text{.......................... (17)}$$

ω_s = particle fall velocity of suspended sediment
β = coefficient related to the diffusion of sediment particles
κ = constant of Von Karman
u_* = overall bed-shear velocity

INITIATION OF SUSPENSION

Before analyzing the main hydraulic parameters which influence the suspended load, it is necessary to determine the flow conditions at which initiation of suspension will occur. Bagnold Stated in 1966 (lit. (*)) that a particle only remains in suspension, when the turbulent eddies have dominant vertical velocity components which exceed the particle fall velocity (ω_s). Assuming that the vertical velocity component (1') of the eddies are represented by the vertical turbulence intensity

($\tilde{\omega}$), the critical value of suspension can be expressed as:

$$\tilde{\omega} = \left((\omega')^2\right)^{0.5} \geq \omega_s \quad \text{.......................... (18)}$$

Detailed studies on turbulence phenomena in boundary flow suggest that the maximum value of the vertical turbulence intensity

($\tilde{\omega}$), is of the same order as the bed-shear velocity (u_*). Using these values the critical bed-shear velocity ($u_{*,crs}$) for initiation of suspension becomes

$$\frac{u_{*,crs}}{\omega_s} = 1 \quad \text{.......................... (19)}$$

Another criterion for suspension has been given by Engelund (lit. (*)). Based on rather crude stability analysis he derived:

$$\frac{u_{*,crs}}{\omega_s} = 0.25 \quad \ldots\ldots\ldots\ldots \quad (20)$$

Finally some results of experimental research at the Delft Hydraulics, Laboratory are reviewed. Van Rijn determined the critical flow conditions at which instantaneous upward turbulent motions of the sediment particles (bursts) with jump lengths of the order of 100 particle diameters were observed (lit. (*)). The experimental results can be represented by:

$$\frac{u_{*,crs}}{\omega_s} = \frac{4}{D_*} \quad \ldots \text{ for } 1 < D_* \leq 10 \quad \ldots\ldots\ldots\ldots \quad (21A)$$

and

$$\frac{u_{*,crs}}{\omega_s} = 0.4 \quad \ldots \text{ for } D_* \geq 10 \quad \ldots\ldots\ldots\ldots \quad (21B)$$

(see fig. B3)

fig. B3: initiation of suspension

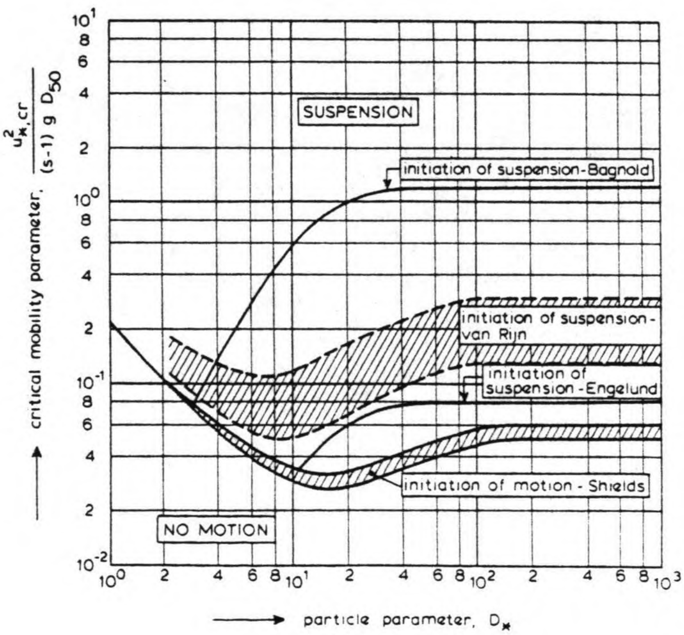

3

Summarizing it is suggested that the criterion of Bagnold may define an upper limit at which a concentration profile starts to develop, while Van Rijn's criterion defines an intermediate stage at which locally turbulent bursts of sediment particles are lifted from bed into suspension.

MATHEMATICAL DESCRIPTION

In a steady and uniform flow the vertical distribution of the sediment concentration profile can be described by:

$$(1 - c)\, c\omega_{s,m} + \varepsilon_s \frac{dc}{dz} = 0 \quad \ldots\ldots (22)$$

c = sediment concentration
$\omega_{s,m}$ = particle fall velocity in a fluid sediment mixture
ε_s = sediment diffusion coefficient
z = vertical co-ordinate

a. Particle fall velocity

The fall velocity in a clear still fluid of a solitary sand particle can be described by:

according to Stokes

$$\omega_s = \frac{1}{18} \frac{(s - 1)g\, D_s^{\,2}}{\upsilon} \quad \ldots\ldots (23A)$$

$D < 100$ mm

according to Zanke

$$\omega_s = 10 \frac{\upsilon}{D_s} \left(1 + \frac{0.01\,(s - 1)g\, D_s^{\,3}}{\upsilon^2}\right)^{0.5} - 1 \quad \ldots\ldots (23B)$$

$100\ \mu m < D < 1.000\ \mu m$

and

$$\omega_s = 1.1 \left[(s - 1)g\, D_s\right]^{0.5} \quad \ldots\ldots (23C)$$

$D > 1.000\ \mu m$

The D_s-parameter expresses the representative particle diameter of the suspended particles, which may be considerably smaller than the D_{50} of the bed material. Experiments with high sediment concentration have shown a substantial reduction of the particle fall velocity due to the presence of the surrounding particles. For normal flow conditions with particles in the range of 50-500 µm the reduced particles fall velocity can be described by a Richardson-Zaki type equation.

$$\omega_{s,m} = (1 - c)^4\, \omega_s \quad \ldots\ldots (24)$$

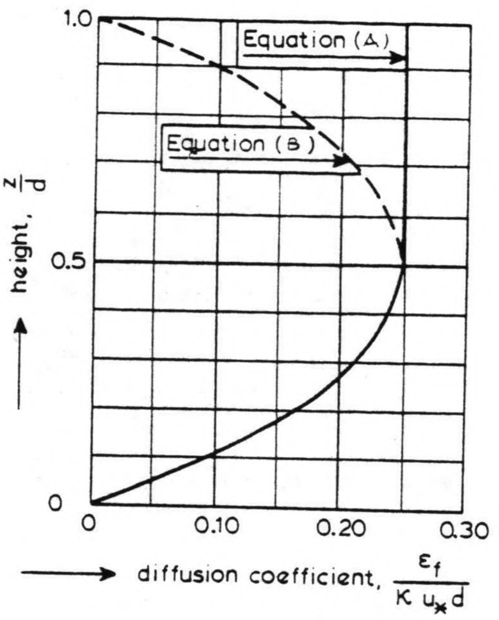
1.0
Equation (A)
Equation (B)
height, $\frac{z}{d}$
0.5
0
0
0.10
0.20
0.30
diffusion coefficient, $\frac{\varepsilon_f}{\kappa u_* d}$

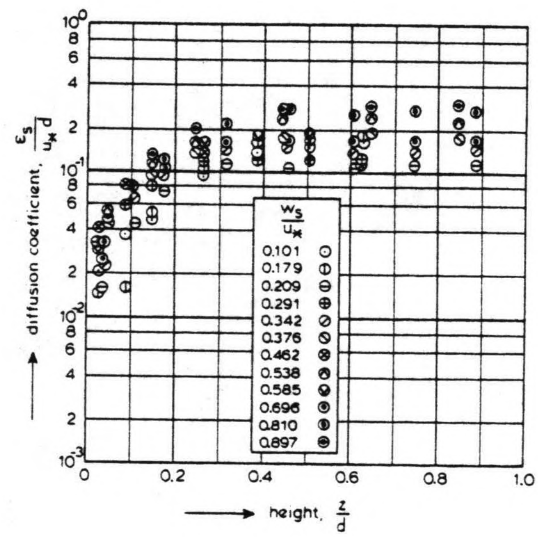
10^0
8
6
4
2
10^{-1}
8
6
4
2
10^{-2}
8
6
4
2
10^{-3}
diffusion coefficient, $\frac{\varepsilon_s}{u_* d}$
$\frac{w_s}{u_*}$
0.101
0.179
0.209
0.291
0.342
0.376
0.462
0.538
0.585
0.696
0.810
0.897
0
0.2
0.4
0.6
0.8
1.0
height, $\frac{z}{d}$

4

Van Rijn found an expression for the representative particle diameter that filled best the results from computations he made to determine the suspended load according to the size fraction method as proposed by Einstein (lit. (✱)). This method makes it possible to compute the suspended load by dividing the bed material into a number of size fractions and assuming that the fractions do not influence each other.

$$\frac{D_s}{D_{50}} = 1 + 0.011\ (\sigma_s - 1)\ (T - 25) \quad \ldots\ldots\ldots\ldots \quad (25)$$

σ_s = geometric standard deviation of the material

$$0.5\ \left(\frac{D_{84}}{D_{50}} + \frac{D_{16}}{D_{50}} \right)$$

The equation fits data rather good for $\sigma_s = 2.5$.

b. Diffusion coefficient

Usually the diffusion of fluid momentum is described by a parabolic distribution over the flow depth a: $\varepsilon_f = \frac{z}{d}\ (1 - \frac{z}{d})\ \kappa u_* d$

A parabolic constant distribution, which means a parabolic distribution in the lower half of the flow depth and a constant value in the upper half of the flow depth, is used mainly because it may give a better description of the concentration profile.

For the fluid momentum it reads

$$\varepsilon_f = \varepsilon_{fmax} = 0.25\ \kappa\ u_* d \ \ldots\ \frac{z}{d} \geq 0.5 \quad \ldots\ldots\ldots\ldots \quad (26A)$$

$$\varepsilon_f = 4\ \frac{z}{d}\ (1 - \frac{z}{d})\ \varepsilon_{fmax} \ \ldots\ \frac{z}{d} < 0.5 \quad \ldots\ldots\ldots\ldots \quad (26B)$$

The diffusion of sediment particles is related to the diffusion of fluid momentum by:

$\varepsilon_s = \beta\phi\varepsilon_f$ . . . . (see <u>fig. B4</u>) . . . . (27)

β = coefficient that describes the differences in the diffusion of a descrete sediment particle and the diffusion of a fluid particle and is assumed to be constant over the flow depth.

ϕ = coefficient which expresses the damping of the fluid turbulence by the sediment particles and is assumed to depend on the local sediment concentration.

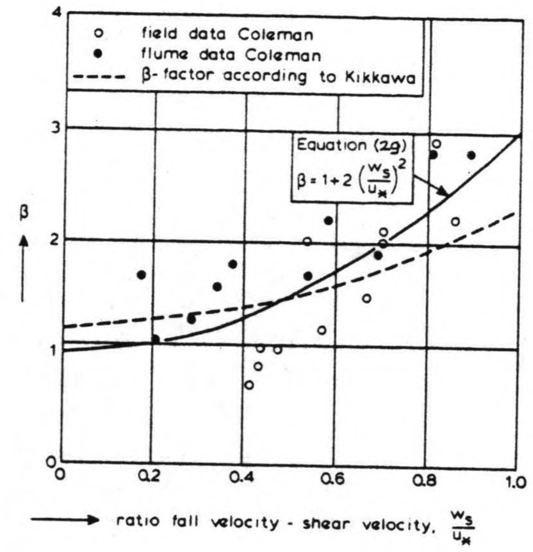
field data Coleman
flume data Coleman
β- factor according to Kikkawa
Equation (29)
$\beta = 1 + 2\left(\frac{w_s}{u_*}\right)^2$
β
ratio fall velocity - shear velocity, $\frac{w_s}{u_*}$

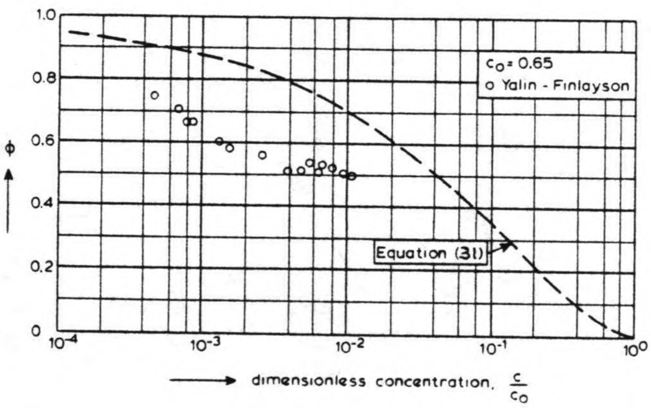
c_o = 0.65
o Yalin - Finlayson
Equation (31)
ϕ
dimensionless concentration, $\frac{c}{c_o}$

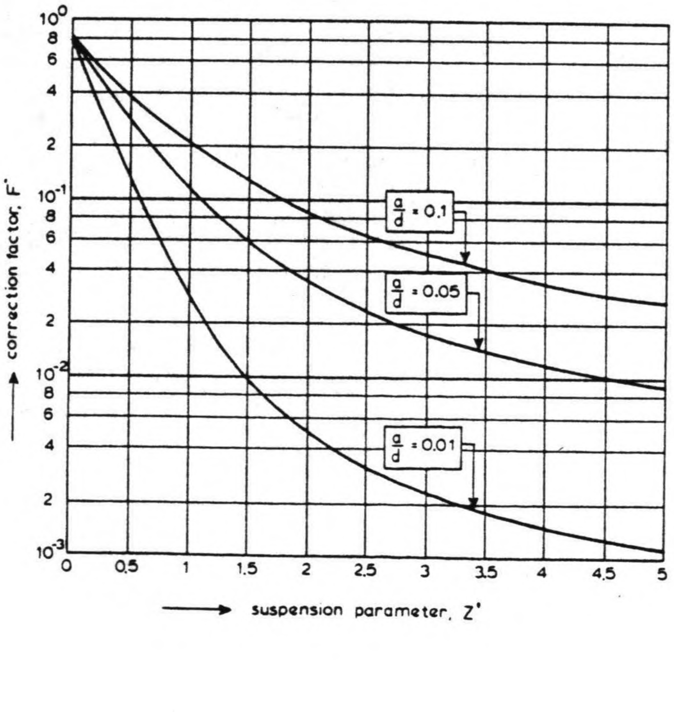
$\frac{a}{d}$ = 0.1
$\frac{a}{d}$ = 0.05
$\frac{a}{d}$ = 0.01
correction factor, F'
suspension parameter, Z'

5

The β-factor:

some investigators have concluded that $\beta < 1$ because the sediment particles cannot respond fully to be turbulent velocity fluctuations. Others have reasoned that in a turbulent flow the centrifugal forces on the sediment particles (being of higher density) would be greater than those on the fluid particles, thereby causing sediment particles to be thrown to the outside of the eddies with a consequent increase in the effective mixing length and diffusion rate, resulting in $\beta > 1$.

Coleman (lit. (*)) computed the ε_s coefficient from the following equation:

$$\omega_s c + \varepsilon_s \frac{dc}{dz} = 0 \quad \ldots\ldots (28)$$

Van Rijn used the results of Coleman to determine the β-factor being:

$$\beta = \frac{\varepsilon_{s,max}}{\varepsilon_{fmax}} = \frac{\varepsilon_{smax}}{0.25\kappa u_* d}$$

The computed β-factors can be described by

$$\beta = 1 + 2 \left[\frac{\omega_s}{u_*}\right]^2 \quad \text{for } 0.1 < \frac{\omega_s}{u_*} < 1 \quad \ldots\ldots (29)$$

According to the present results the β-factor is always larger than unity, thereby indicating a dominant influence of the centrifugal forces (see fig. B5).

The ϕ-factor:

usually the damping effect is taken into account by reducing the constant of Von Karman (κ). Apparently the mixing is reduced by the presence of a large amount of sediment particles. In view of several contradictions in literature it may be questioned if the concept of an overall constant of Von Karman for the entire velocity profile is correct for a heavy sediment laden flow. An alternative approach may be the introduction of a local constant of Von Karman dependant on the local sediment concentration.

$\kappa_m = \phi\ \kappa$ according to Yalin and Finlayson (lit. (*)).

A proper study of the influence of the sediment particle on the velocity and concentration profile requires the solution of the equatons of motion and continuity applying a first order closure (mixing length) or a second order (turbulence energy and dissipation) closure. A simplified method is introduced using a modified suspension number (see fig. B5).

$$Z' = Z + \varphi \quad \ldots \quad (30)$$

Z = suspension number according to eq. 17

φ = overall correction factor representing all additional effects (volume occupied by particles, damping of turbulence),

with an inaccuracy of $\simeq$ 25% φ is best filled by

$$\varphi = 2,5 \left[\frac{\omega_s}{u_*}\right]^{0.8} \left[\frac{C_a}{C_o}\right]^{0.4} \quad 0.01 \le \frac{\omega_s}{u_*} \le 1 \quad \ldots \quad (31)$$

c. The concentration profile

In part II a function for the bed-load concentration has been proposed (eq. 11,15). Generally however it is not attractive to use the bed-load concentration as the reference concentration for the concentration profile, because it prescribes a concentration at a level equal to the saltation height which may result in large errors for the concentration profile. Therefore a reference level, related to the bedform is introduced. Below this level all particles are considered bed-load transport:

$$q_b = c_b \, u_b \, \delta_b = c_a \, \bar{u}_a \, a \quad \ldots \quad (32)$$

c_b = bed-load concentration
u_b = velocity of bed-load particles
δ_b = saltation height
u_a = effective particle velocity
a = reference level above the bed
c_a = concentration refined to reference level

Assumed for a (= reference level)

$$a = 0.5\,\Delta \text{ or } a = k_s \quad a \ge 0.01\,d \quad \ldots \quad (33)$$

Δ = bed-form height
k_s = equivalent roughness

Then from measurement it follows

$$c_a = 0.015 \, \frac{D_{50}}{a} \, \frac{T^{1.5}}{D_*^{\,0.3}} \quad \ldots \quad (34)$$

from eq. 22 and 24. it follows

$$\frac{dc}{dz} = \frac{\omega_s \, c(1 - c)^5}{\varepsilon_s} \quad \ldots \quad (35)$$

and using the parabolic constant distribution of ε_f according to eq. 26 and ε_s according to eq. 27, the concentration profile can be obtained by integration of eq. 35.

For $\phi = 1$ and $c < c_a < 0.001$ this results in

$$\frac{c}{C_a} = \left[\frac{a\,(d - z)}{z\,(d - a)}\right]^{Z} \quad \ldots\ldots \quad \frac{z}{d} < 0.5 \quad \ldots\ldots\ldots\ldots\ldots\ldots (36A)$$

$$\frac{c}{c_a} = \left[\frac{a}{d - a}\right]^{Z} e^{-4Z(\frac{z}{d} - 0.5)} \quad \ldots\ldots\ldots \quad \frac{z}{d} \geq 0.5 \quad \ldots\ldots\ldots\ldots\ldots (36B)$$

otherwise ($\phi \neq 1$) integration can only be performed by numerical methods.

COMPUTATION OF THE SUSPENDED LOAD

In general

$$q_s = \int_a^d c\,u\,dz \ldots\ldots\ldots\ldots\ldots\ldots\ldots\ldots\ldots\ldots\ldots\ldots (37)$$

integration of (37) using eq (36, 30, 31) and $u = \frac{u_*}{\kappa}\left[\ln\left[\frac{z}{z_o}\right]\right]$

can be respresented with an inaccuracy of ≃ 25%.

$$q_s = F\,\bar{u}\,d\,c_a \ldots\ldots\ldots\ldots\ldots\ldots\ldots\ldots\ldots\ldots\ldots (38)$$

$0.3 \leq Z^1 \leq 3$

$0.001 \leq \frac{a}{d} \leq 0.1$

$$F = \frac{\left[\frac{a}{d}\right]^{Z^1} - \left[\frac{a}{d}\right]^{1.2}}{\left[1 - \frac{a}{d}\right]^{Z^1} (1.2 - Z^1)} \ldots\ldots\ldots\ldots\ldots\ldots\ldots\ldots (39)$$

$\bar{u}$ = mean flow velocity
d = flow depth
c_a = reference concentration

The input data are

$\bar{u}$ = mean flow velocity
d = mean flow depth
b = mean flow width
I = energy gradient
D_{50}, D_{90} = particle sizes of bed material
σ_s = geometric standard deviaton bed material
ν = kinematic viscosity coefficient
ρ_s = density of sediment
ρ = density of fluid
g = acceleration of gravity
κ = constant of Von Karman

The complete method consists of

1. compute particle diameter D_* using eq. (1)
2. compute criticle bed-shear velocity $u_{*,crs}$ according to Shields
3. compute transport stage parameter T using eq. (2)
4. compute reference level a using eq. (33)
5. compute reference concentration c_a using eq. (34)
6. compute representative particle size of suspended sediment D_s using eq. (25)
7. compute fall velocity of suspended sediment ω_s using eq. (23)
8. compute β-factor using eq. (29)
9. compute ϕ-factor using eq. (31)
   and $u_* = \sqrt{gdI}$
   I = slope of water level
10. compute suspension parameter Z and Z^1 using eq. (17) and (37)
11. compute F-factor using eq. (39)
12. compute suspended load transport q_s using eq. (38)

Restrictions:

for very heavy sediment laden flows the velocity profile used for eq. (38) leads to serious errors in the near bed region. Furthermore for small $\frac{u_*}{\omega_s}$ values the sediment diffusivity (ε_s) may be relatively small compared to the fluid diffusivity (ε_f) and $\beta < 1$. Ultimately the β-factor approaches zero for decreasing u_*/ω_s values.

For these reasons eq. (29) which predicts an opposite trend with an increasing β-factor (to $\beta = 3$) for decreasing $\frac{u_*}{\omega}$ values is not reliable for low flow stage, it is proposed to use eq. (29) for normal flow stages:

$$\frac{u_*}{\omega} > 2$$

and otherwise $\beta = 1$ should be used.

(fig. B5)

VERIFICATION

The suspended load transport is computed according to Van Rijn's method (eq. (38)) and also the bed-load transport (eq. (16)) $q_t = q_s + q_b$. For comparison the total load formulas of Engelund-Hansen (lit. (*)) Ackers-White (lit. (*)) and Yang (lit. (*)) were used. The accuracy of the four methods is given in terms of a discrepancy ratio (r) defined as:

$$r = \frac{q_t \text{computed}}{q_t \text{measured}}$$

Data (see table 2) were again mostly selected from a compendium of Solids Transport compiled by Peterson and Howells (lit. (*)) adjusted according to Brownlie (lit. (*)) from errors.
In addition to this databank Van Rijn has used data from the Pakistan Canals, the Middle Loup River and Niobrara River.

All washload is excluded from the data and a side wall correction method according to Vanohi-Brooks (lit. (*)) has been used.

Table 2

						SCORES (%) OF PREDICTED TOTAL LOAD DISCREPANCY RANGES											
						0.75 ≤ r ≤ 1.5				0.5 ≤ r ≤ 2				0.33 ≤ r ≤ 3			
Source (1)	Number (2)	Flow velocity, in meters per second (3)	Flow depth, in meters (4)	Particle diameter, micrometer (5)	Temperature, in degrees Celsius (6)	Van Rijn (7)	Engelund-Hansen (8)	Ackers-White (9)	Yang (10)	Van Rijn (11)	E-H (12)	A-W (13)	Yang (14)	Van Rijn (15)	E-H (16)	A-W (17)	Yang (18)
Field data																	
Various USA-Rivers (Corps-Engr.)	266	0.4–2.4	0.3–17	120–160	2–35	53%	39%	32%	6%	79%	67%	61%	24%	94%	87%	78%	44%
Middle Loup River	46	0.65–1.15	0.3–0.65	300–400	0–30	39	13	37	63	78	37	74	94	96	80	98	100
India-canals	30	0.7–1.6	1.3–3.4	90–310	10–30	30	15	27	3	60	45	48	6	90	73	70	24
Pakistan canals	87	0.6–1.3	1.4–3.6	110–290	15–35	23	37	34	13	56	71	71	29	91	94	91	48
Niobrara River	57	0.6–1.3	0.4–0.65	280	0–30	55	13	29	86	95	67	58	98	98	95	98	98
	486					45%	32%	32%	22%	76%	64%	63%	39%	94%	88%	84%	55%
Flume Data																	
Guy et al.	90	0.4–1.2	0.1–0.4	190–470	8–34	40	67	56	68	70	89	85	90	91	98	99	98
Oxford	84	0.4–1.3	0.1–0.4	100	14–30	37	20	31	45	84	38	59	89	96	70	81	96
Stein	37	0.4–1.2	0.1–0.4	400	20–30	54	73	81	56	70	95	97	97	97	97	100	100
Southampton A	33	0.4–0.8	0.15–0.3	150	15–25	64	49	46	49	85	73	79	82	97	91	94	94
Southampton B	33	0.4–0.55	0.15	480	21	18	12	82	91	81	82	96	97	94	97	100	100
Barton-Lin	20	0.4–0.95	0.15–0.4	180	15–27	35	60	30	40	65	100	50	65	100	100	100	100
	297					41%	46%	52%	59%	77%	74%	77%	89%	95%	89%	94%	98%
Total	783					43%	37%	40%	36%	76%	68%	68%	58%	94%	88%	88%	71%

LITERATURE Appendix B (Van Rijn)

1. L.C. van Rijn: Sediment Transport part I: Bed Load Transport

Journal of Hydraulic Engineering
vol. 110, no. 10
October 1984 1984

2. L.C. van Rijn: Sediment Transport part II: Suspended Load Transport

Journal of Hydraulic Engineering
vol. 110, no. 11
November 1984 1984

3. L.C. van Rijn: Sediment Transport part III: Bed Forms and Alluvial Roughness

Journal of Hydraulic Engineering
vol. 110, no. 12
December 1984 1984

* There is a more extended list of literature in each of the above mentioned articles.

APPENDIX C

A DEPTH INTEGRATED MODEL FOR SUSPENDED SEDIMENT TRANSPORT

If suspended load is the main mode of sediment transport different models are available for calculating the transport rate. The simplest one is a transport formula, which assumes local equilibrium conditions and with which the transport rate can be calculated from the local instantaneous flow conditions. For the case of two-dimensional flow (in the vertical plane) the most sophisticated model, which is based on a combination of a two-dimensional flow model and the two-dimensional convection-diffusion equation for the sediment concentration c:

$$\frac{\partial c}{\partial t} + u\frac{\partial c}{\partial x} + w\frac{\partial c}{\partial z} = w_s\frac{\partial c}{\partial z} + \frac{\partial}{\partial z}\left(\varepsilon_z\frac{\partial c}{\partial z}\right) \quad \text{. . . . (1)}$$

t = time;
c = sediment concentration;
x and z = horizontal and vertical co-ordinates;
u and w = velocity component in x- and z-direction;
w_s = fall velocity of sediment particles;
ε = turbulent diffusion coefficient for sediment transfer in vertical direction;
(see fig. C1).

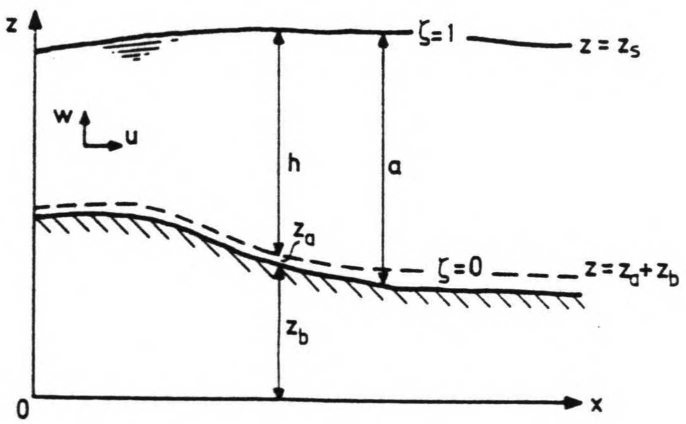

1

At the free surface ($z = z_b + a$, z_b = bottom level and a = waterdepth) the vertical sediment flux should be zero:

$$w_s c + \varepsilon \frac{\partial c}{\partial z} = 0 \quad \text{at } z = z_b + a = z_a + z_b + h \qquad (2)$$

The lower boundary condition is applied at a height z_a above the bed, suspended sediment is defined as the transport of particles above this level and transport below this level is defined to be bed load. Thus suspended sediment will be transported over a depth h given by $h = a - z_a$. If the near-bed concentration can be specified in terms of local flow and sediment parameters, the bed boundary condition that has to be applied is:

$$c = c_a \ldots \text{ at } z = z_a + z_b \qquad (3)$$

Let the flow under consideration be characterized by the horizontal length and velocity scales L and U and vertical length and velocity scales H and UH/L respectively, let E represent a scale from 10 for the turbulent diffusion coefficient ε. Equation (1) could now be written as :

$$\frac{H}{w_s T}\frac{\partial c}{\partial t'} + \frac{H}{L w_s}\left(u' \frac{dc}{dx'} + w' \frac{\partial c}{\partial z'}\right) = \frac{\partial c}{\partial z'} + \frac{E}{w_s H}\frac{\partial}{\partial z'}\left(E' \frac{\partial c}{\partial z}\right) \ldots (4)$$

wherein: $u = Uu'$;
$z = Hz'$;
$\varepsilon = E\varepsilon'$.

The order of magnitude of E is ¼ $\kappa u * H$ (κ = Von Karman constant).

$$\frac{E}{w_s H} \simeq \frac{1}{4}\frac{\kappa u * H}{w_s H} \simeq 0.005 \frac{u}{w_s} = 0(1)$$

Thus both terms on the right hand side of (4) are of 0(1) and are responsible for the vertical reajustment of concentration profiles. The magnitude of the left hand side depends on the values of

$\frac{H}{w_s T}$ and $\frac{uH}{L w_s}$.

If these parameters are small, then it is possible to construct an asymptotic solution, assumed that

$$\frac{uH}{L w_s} = \delta << 1$$

and $\frac{H}{w_s T} = \delta << 1$.

Equation (4) can be written as:

$$\delta \frac{\partial c}{\partial t'} + u' \frac{\partial c}{\partial x'} + w' \frac{\partial c}{\partial z'} = \frac{\partial c}{\partial z'} + \frac{E}{w_s H} \frac{\partial}{\partial z'} \left(E' \frac{\partial c}{\partial z'}\right) \quad (5)$$

and the solution of (1), (2) and (3) is of the type:

$$w_s \frac{\partial c_o}{\partial z} + \frac{\partial}{\partial z} \left(\varepsilon \frac{\partial c_o}{\partial z}\right) = 0 \quad (6a)$$

$$w_s \frac{\partial c_i}{\partial z} + \frac{\partial}{\partial z} \left(\varepsilon \frac{\partial c_i}{\partial z}\right) = \left(\frac{\partial}{\partial t} + u \frac{\partial}{\partial x} + w \frac{\partial}{\partial z}\right) c_{i-1} \quad (6b)$$

for $i \geq 1$

and $c = \sum_{i=0}^{n} c_i + O(\delta^{n+1})$

noting: $O(c_{i+1}) = \delta\, O(c_i)$ or $c_{i+1} \ll c_i$ . . . . (6c)

For the purpose of constructing the asymptotic series solution it is assumed that only c_o contributes to the mean concentration:

$\bar{c}_o = \bar{c}(x,t)$ . . . . (7a)
$\bar{c}_i = 0$ for all $i \geq 1$ . . . . (7b)

Introducing

$$\zeta = \frac{z - (z_a + z_b)}{h}$$, a dimensionless vertical co-ordinate;

$$\frac{\partial}{\partial \xi} = \frac{\bar{u}h}{w_s} \frac{\partial}{\partial x}$$, a transversed horizontal co-ordinate;

$$\bar{u} = \frac{1}{h} \int_{z_a+z_b}^{z_b+a} u\,dz$$, 'depth' averaged velocity;

$$a_i(\zeta) = \frac{c_e(\zeta)}{\bar{c}_e}$$, normalized eq.uilibrium concentration profile;

the complete first order solution is:

$$c = a_{11}(\zeta)\bar{c} + a_{21}(\zeta)\frac{h}{w_s}\frac{\partial\bar{c}}{\partial t} + a_{22}(\zeta)\frac{\partial\bar{c}}{\partial\xi} \quad \ldots\ldots\ldots\ldots (8)$$

the steady first order solution is:

$$c = a_{11}(\zeta)\bar{c} + a_{22}(\zeta)\frac{\partial\bar{c}}{\partial\xi} \quad \ldots\ldots\ldots\ldots (9)$$

and the nth order solution for steady uniform flow

$$c = a_{11}(\zeta)\bar{c} + a_{22}(\zeta)\frac{\partial\bar{c}}{\partial\xi} + a_{33}(\zeta)\frac{\partial^2\bar{c}}{\partial\xi^2}$$

$$= \sum_{i=0}^{n}\left[a_{i+1,\,i+1}\right](\zeta)\frac{\partial^i\bar{c}}{\partial\xi_i} \quad \ldots\ldots\ldots\ldots (10)$$

wherein the profile functions $a_{ii}(\zeta)$ for $i > 1$ are defined as:

$$\frac{\partial a_{ii}}{\partial\zeta} + \frac{\partial}{\partial\zeta}\left(\varepsilon'\frac{\partial a_{ii}}{\partial\zeta}\right) = p a_{i-1,\,i-1} \quad \ldots\ldots\ldots\ldots (11a)$$

$$\int_0^1 a_{ii}\,d\zeta = 0 \quad \ldots\ldots\ldots\ldots (11b)$$

$$\left[a_{ii} + \varepsilon'\frac{\partial a_{ii}}{\partial\zeta}\right]_{\zeta=1} = 0 \quad \ldots\ldots\ldots\ldots (11c)$$

Introducing $\varepsilon'(\zeta) = \dfrac{\varepsilon_z(\zeta)}{w_s h}$, normalized diffusion coefficient;

$p(\zeta) = \dfrac{u(\zeta)}{u}$, normalized velocity profile.

Equations (8), (9) and (10) are expressions for the concentration, which satisfies the mass-balance equation (1) and the surface boundary condition subject to the assumptions about orders of magnitude. The vertical profile functions $a_{11}(\zeta)$, $a_{21}(\zeta)$ etc. can be determined in advance if the velocity profile, the equilibrium concentration profile ϕ_0 and za/a are known (the reference level).

If the assumption of local near-bed equilibrium is used, the bed-boundary condition (3) can be reformulated in terms of the local eq.uilibrium concentration c_e as:

$$c_a = \overline{c_e}\ \phi_0(0) = \overline{c_e}\ \gamma_{11} \quad \ldots\ldots (12)$$

$$\gamma_{11} = a_{11}(0) = \phi_0(0)$$

the nth order equation for the mean concentration becomes:

$$\overline{c_e}(\xi) = \sum_{i=0}^{n} \frac{\gamma_{i+1,\,i+1}}{\gamma_{11}} \frac{a_i \bar{c}}{\overline{a\xi^i}} \quad \ldots\ldots (13)$$

or, returning to the original co-ordinates:
the first order unsteady solution:

$$\gamma_{11}\overline{c_e} = \gamma_{11}\bar{c} + \gamma_{21}\frac{h}{w_s}\frac{\partial \bar{c}}{\partial t} + \gamma_{22}\frac{\bar{u}h}{w_s}\frac{\partial \bar{c}}{\partial x} \quad \ldots\ldots (14a)$$

the first order steady solution:

$$\gamma_{11}\overline{c_e} = \gamma_{11}\bar{c} + \gamma_{22}\frac{\bar{u}h}{w_s}\frac{\partial \bar{c}}{\partial x} \quad \ldots\ldots (14b)$$

and the nth order steady solution:

$$\gamma_{11}\overline{c_e} = \gamma_{11}\bar{c} + \gamma_{22}\frac{\bar{u}h}{w_s}\frac{\partial \bar{c}}{\partial x} + \gamma_{33}\frac{\bar{u}h}{w_s}\frac{\partial}{\partial x}\frac{\bar{u}h}{w_s}\frac{\partial \bar{c}}{\partial x} + \ldots\ldots \quad \ldots (14c)$$

$\gamma_{11} = a_{11}(0)$ = value of zero order profile function;
$\gamma_{22} = a_{22}(0)$ = value of first order profile function;
$\gamma_{33} = a_{33}(0)$ = value of second order priofile function at level

$$z = z_a + z_b.$$

These are all differential equations that describe the variation of c along the X-direction, and in the case of (14a) in time. The coefficients of these equations can be determined in advance if at every point the velocity profile and the equilibrium concentration profile ϕ_0 are known. The boundary conditions for the solution of these equations have to be given in terms of c at the upstream boundary and, in case of unsteady equations, at time zero. The solution of c is a one-dimensional computation of the situation considered in 2-D. Once the depth-averaged concentration c has been determined, concentration profiles can be computed from (8), (9) or (10).

Fig. C2, C3, C4 (typical profile functions)

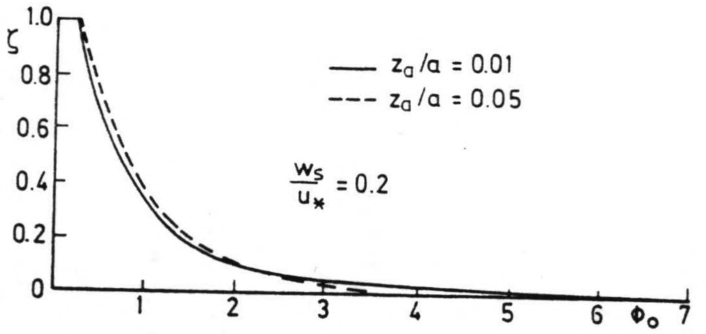

1.0
ζ
0.8
0.6
0.4
0.2
0
1
2
3
4
5
6
Φo
7
—— za/a = 0.01
--- za/a = 0.05
ws/u* = 0.2

2

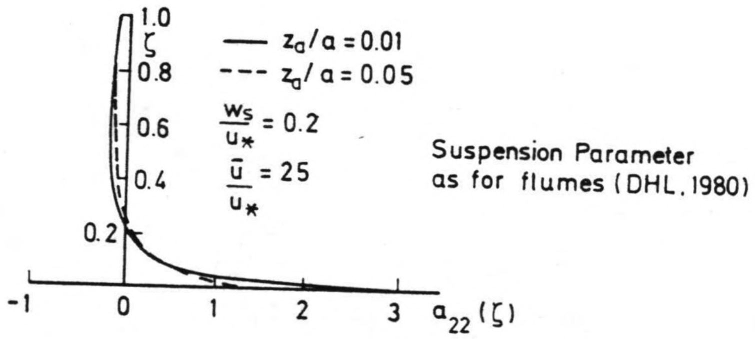

1.0
ζ
0.8
0.6
0.4
0.2
-1
0
1
2
3
a22(ζ)
—— za/a = 0.01
--- za/a = 0.05
ws/u* = 0.2
ū/u* = 25
Suspension Parameter
as for flumes (DHL, 1980)

3

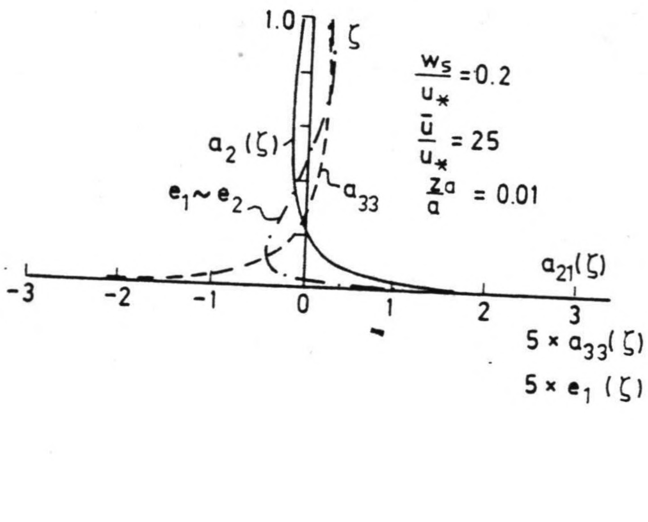

1.0
ζ
a2(ζ)
e1~e2
a33
ws/u* = 0.2
ū/u* = 25
za/a = 0.01
a21(ζ)
-3
-2
-1
0
1
2
3
5 × a33(ζ)
5 × e1 (ζ)

4

Expressions for sedimenttransport and entrainment rate

The rate of transport or suspended sediment s_s is given by:

$$s_s = \int_{z_b+z_a}^{z_b+a} ucdz = h \int_0^1 uc d\zeta \qquad (15)$$

solution zero-order: $\alpha_{ij} = \int_0^1 p.a_{ij} d\zeta$

$$s_s = \alpha_{11} \bar{u} h \bar{c} \qquad (16a)$$

solution first order:

$$s_s = \alpha_{11} \bar{u} h \bar{c} + \alpha_{21} \frac{h^2 \bar{u}}{w_s} \frac{d\bar{c}}{dt} + \alpha_{22} \frac{h^2 \bar{u}^2}{w_s} \frac{\partial \bar{c}}{\partial x} \qquad (16b)$$

or

$$s_s - s_e = \alpha_{11} \bar{u} h (\bar{c} - \bar{c}_e) + \alpha_{21} \frac{h^2 \bar{u}}{w_s} \frac{\partial \bar{c}}{\partial t} + \alpha_{22} \frac{h^2 \bar{u}^2}{w_s} \frac{\partial \bar{c}}{\partial x} \qquad (17)$$

in which

$s_e = \gamma_{11} \bar{u} h \bar{c}_e$ is the equilibrium transport

the sediment entrainment rate E is given by

$$E = \left(w_s c + \varepsilon \frac{\partial c}{\partial z}\right)_{z = \text{bottom}} \quad \text{or} \quad E = \frac{\partial (\tau h)}{\partial t} + \frac{\partial S_s}{\partial x} \qquad (18)$$

The first order expression

$$E = \frac{\partial (\bar{c} h)}{\partial t} + \frac{\partial}{\partial x} \left[\alpha_{11}\, h\, \bar{u}\, \bar{c} + \alpha_{21} \frac{h^2 \bar{u}}{w_s} \frac{\partial \bar{c}}{\partial t} + \alpha_{22} \frac{h^2 \bar{a}^2}{w_s} \frac{\partial \bar{c}}{\partial x} \right] \qquad (19a)$$

with the equivalent steady flow equation

$$E = \frac{\partial}{\partial x} \left[\alpha_{11}\, \bar{u}\, h\, \bar{c} + \alpha_{22} \frac{h^2 \bar{u}^2}{w_s} \frac{\partial \bar{c}}{\partial x} \right] \qquad (19b)$$

Most depth averaged methods consist of determining on emperical expression for the entrainment rate E to compute the concentration levels. This method used the bed boundary (12) to compute the concentration, this way the entrainment rate is computed more accurately.

Some features of interest

1. Adaption time and length

Consider a steady uniform flow where the suspended sediment is not in equilibrium. Then equation (8) may be written as:

$$\overline{c_e} = \bar{c} + T_A \frac{\partial \bar{c}}{\partial t} + L_A \frac{\partial \bar{c}}{\partial x} \qquad (20)$$

where: $$T_A = \frac{\gamma_{21}}{\gamma_{11}} \frac{h}{w_s} \qquad (21)$$

$$L_A = \frac{\gamma_{22}}{\gamma_{11}} \frac{\bar{u}h}{w_s} \qquad (22)$$

In steady uniform flow T_A and L_A will be constants and (20) will have straight characteristics in the x-t-plane. It can also be shown that $(c - c_e)$ will decay exponentially with an adaption length L_A and adaption time T_A.

The adaption length/time is defined as the interval required to decrease $(\bar{c} - c_e)$ by a factor e.

Fig. C5 (adaptation length + time)

It should also be noted that from the definition of L_A and T_A the length and time required for 95% adaption are $L_A.\ln 20$ and $T_A.\ln 20$ respectively.

The values of L_A and T_A should be compared with the dimensions of the major features of the problem under consideration, and with the mesh size of the computational grid and the time step of the calculation when a decision has to be made about the relative importance of adaptation phenomena.

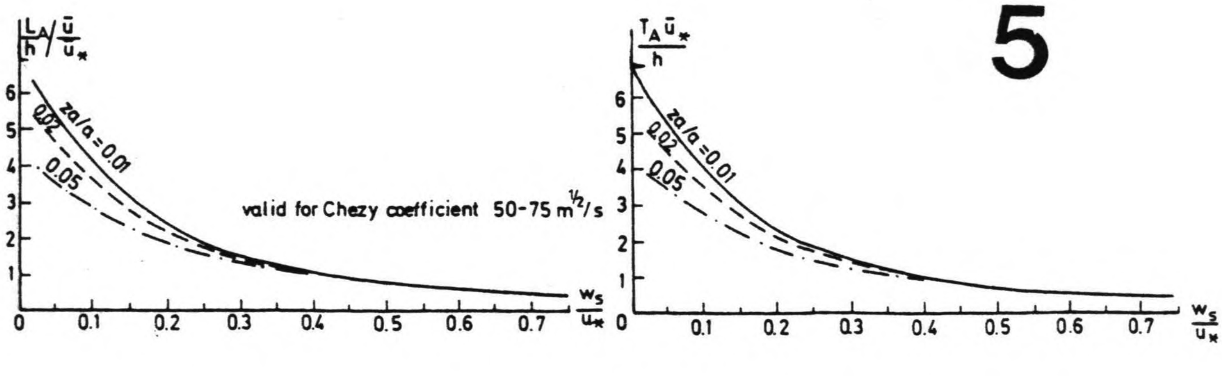

5

2. Concentration profiles

Consider a steady non-uniform flow. Then the concentration profile (first order) is (eq. (9)):

$$c = a_{11}(\zeta)\bar{c} + a_{22}(\zeta)\frac{d\bar{c}}{d\xi} \quad \ldots\ldots (9)$$

or

$$c = \phi_0(\zeta)\bar{c} + a_{22}(\zeta)\frac{\bar{u}h}{w_s}\frac{\partial\bar{c}}{\partial x} \quad \ldots\ldots (23)$$

Fig. C6 shows the typical shapes of $\phi_0(\zeta)$ and $a_{22}(\zeta)$.

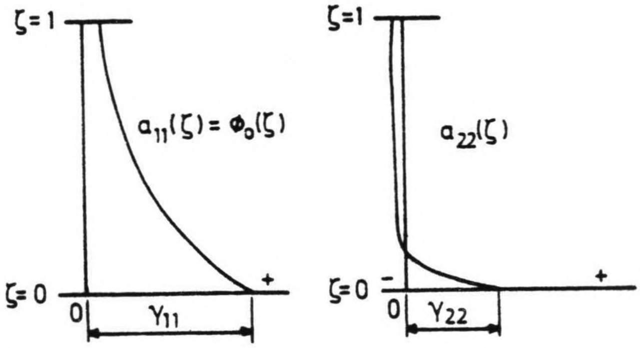

Typical Profiles

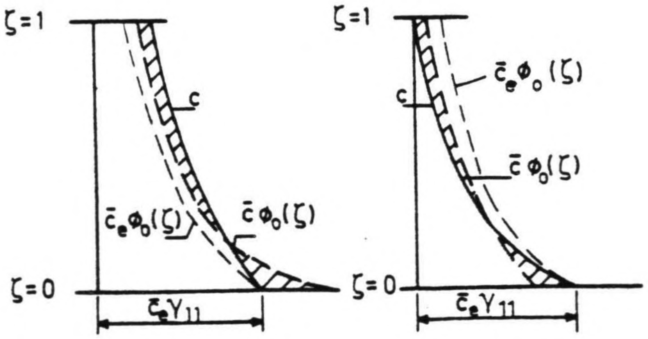

Sedimentation	**Erosion**
$\bar{c}_e < \bar{c}$	$\bar{c}_e > \bar{c}$
$c = \phi_o\,\bar{c} + a_{22}\frac{\bar{u}h}{w_s}\frac{\partial\bar{c}}{\partial x}$	$c = \phi_o\,\bar{c} + a_{22}\frac{\bar{u}h}{w_s}\frac{\partial\bar{c}}{\partial x}$
$\frac{\partial\bar{c}}{\partial x} < o$	$\frac{\partial\bar{c}}{\partial x} > o$

6

The bed-boundary condition for steady flow is:

$$\gamma_{11}\overline{c_e} = \gamma_{11}\bar{c} + \gamma_{22}\frac{\bar{u}h}{w_s}\frac{\partial\bar{c}}{\partial x} \quad \ldots\ldots\ldots\ldots\ldots\ldots\ldots (14b)$$

$$\text{or } \frac{\bar{u}h}{w_s}\frac{\partial\bar{c}}{\partial x} = \frac{\gamma_{11}}{\gamma_{22}}(\overline{c_e} - \bar{c}) \quad \ldots\ldots\ldots\ldots\ldots\ldots\ldots (24)$$

Figure C6 also shows how the concentration profile is modified during

a. sedimentation: $\bar{c} - \overline{c_e} > 0 \quad \frac{\partial\bar{c}}{\partial x} < 0;$

b. erosion : $\bar{c} - \overline{c_e} < 0 \quad \frac{\partial\bar{c}}{\partial x} > 0.$

The zero-order profile ϕ_o has about the standard shape as originally derived by Rouse (lit. (6)).
The first order correction a_{22}, which is the main contribution of the present theory, is seen to give a steeper profile if $\partial c/\partial x > 0$, if, roughly speaking, the concentration is below equilibrium. Conversely, the profile is flattened if $\frac{dc}{cx} < 0$, i.e. in case of sedimentation.
It is obvious that $d\bar{c}/dx$ should not be too large numerically, as negative concentration would result. This is related to the basic assumption for the present theory that the length scale should be sufficiently large.
When the solution is convergent, higher order solutions will give better approximations of the true concentration profile.

3. Validity of the approximation

The solution is base on the assumption that c_i is an order of magnitude smaller that c_{i-1}. Therefore the first order steady solution (eq. (9)):

$$\left| a_{22}(\zeta)\frac{\bar{u}h}{w_s}\frac{\partial\bar{c}}{\partial x} \right| << |a_{11}(\zeta)\bar{c}| \quad \ldots\ldots\ldots\ldots\ldots\ldots (25)$$

or

$$\left| \frac{a_{22}}{a_{11}}\frac{\bar{u}h}{cw_s}\frac{\partial\bar{c}}{\partial x} \right| << 1.$$

The largest value of a_{22}/a_{11} (fig. C6) appears to occur at $\zeta = 0$:

$$\left| \frac{\gamma_{22}}{\gamma_{11}} \frac{\bar{u}h}{cw_s} \frac{\partial \bar{c}}{\partial x} \right| << 1$$

substituting from (19):

$$\left| \frac{\overline{c_e} - \bar{c}}{c} \right| << 1.$$

Therefore the error in the solution will increase as the local mean concentration moves away from the mean equilibrium concentration. The worst case is when $\bar{c} = 0$.

4. Adaption from zero concentration

Notwithstanding foregoing conclusion, the analysis was applied to a steady uniform flow where the initial mean concentration was zero. The solution could be obtained analytically because of the constant coefficients. Fig. C7 shows the decay of $(\bar{c}_e - \bar{c})/\bar{c}_e$ for two values of w_s/u_*.

The first and second order analytical solutions as well as the numerical solution of the two-dimensional mass balance equations (1) are shown. It can be seen that while errors of adaption rate are present when $\bar{c}$ is small, the comparison improves considerably as c increases.

It should be mentioned here that when the mean concentration is zero, the first order solution (9) will give negative values in the upper part of the flow. Agreement between the full numerical solution and the asymptotic solution (from point of view of the adaption rate) is quite reasonable for $(\bar{c}_e - \bar{c})/\bar{c}_e < 0.5$ or $\dfrac{c_e - c}{c} < 1.$

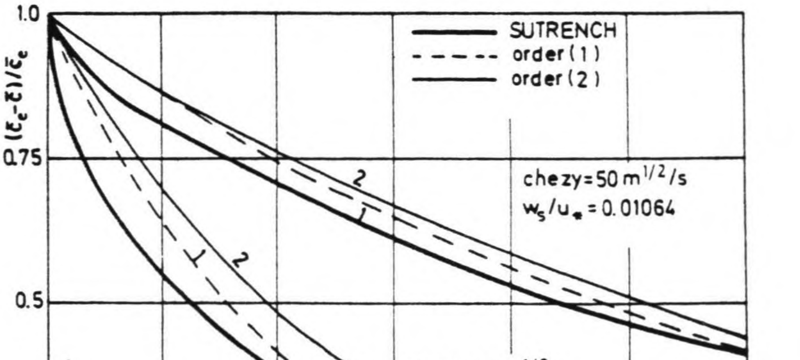

7

5. Alternative bed-boundary condition

The boundary condition as described before assumes that the value of the concentration c_a at $z = z_a + z_b$ is known in advance. If this value is the same as the equilibrium value then, for example, the first order steady equation

$$\gamma_{11}\overline{c_e} = \gamma_{11}\overline{c} + \gamma_{22}\frac{\overline{u}h}{w_s}\frac{\partial\overline{c}}{\partial x}$$

may be derived.

If an alternative boundary condition, i.e. that the concentration gradient at $z = z_a + z_b$ is equal to the equilibrium value, is used the first order steady solution would yield

$$\left.\frac{\partial a_{11}}{\partial\zeta}\right|_{\zeta=0}\overline{c_e} = \left.\frac{\partial a_{11}}{\partial\zeta}\right|_{\zeta=0}\overline{c} + \frac{\overline{u}h}{w_s}\left.\frac{\partial a_{22}}{\partial\zeta}\right|_{\zeta=0}\frac{\partial\overline{c}}{\partial x}$$

Galapatti shows that this reduces to

$$\gamma_{11}\overline{c_e} = \gamma_{11}\overline{c} + (\gamma_{22} + \alpha_{11})\frac{\overline{u}h}{w_s}\frac{\partial\overline{c}}{\partial x}$$

Therefore, the use of this boundary condition will lead to larger adaptation lengths than before. For very fine sediment ($w_s \rightarrow 0$) it can be shown that $\alpha_{11} \rightarrow 1$ while γ_{22}/w_s remains finite. So the adaption length will become infinite.

6. Formulae for coefficients

Each coefficient is built up from eight constants a_i, b_i from $i = 1$ to 4. The values of a_i and b_i required to compute eleven coefficients for each combination of values of w_s/u_* and $\bar{u}/u_*$ are given later in this appendix. The formulae to be used are as follows.

$\kappa = 1 \quad \gamma_{21}/\gamma_{11} = (w_s/u_*)\exp(f)$

$\kappa = 2 \quad \gamma_{22}/\gamma_{11} = (w_s/u_*)\exp(f)$

$\kappa = 3 \quad \gamma_{33}/\gamma_{11} = (w_s/u_*)^2\exp(f)$

$\kappa = 4 \quad \mu_1/\gamma_{11} = w_s f/u_*$

$\kappa = 5 \quad \mu_1/\gamma_{11} = w_s f/u_*$

$\kappa = 6 \quad \alpha_{11} = f$

$\kappa = 7 \quad \alpha_{21} = (w_s/u_*)$

$\kappa = 8 \quad \alpha_{22} = (w_s/u_*)$

$\kappa = 9 \quad \alpha_{33} = (w_s/u_*)$

$\kappa = 10 \quad \lambda_1 = w_s f/u_*$

$\kappa = 11 \quad \lambda_2 = w_s f/u_*$

where

$$f = \sum_{i=1}^{4} \left(a_i + b_i \frac{u_*}{\bar{u}}\right)\left(\frac{w_s}{u_*}\right)^{i-1}$$

where a_i and b_i are obtained from the tables c1 to c3 for the corresponding value of κ for $z_a/d = 0.01$, 0.02 and 0.05. The computations were based on the suspension parameter for natural channels.

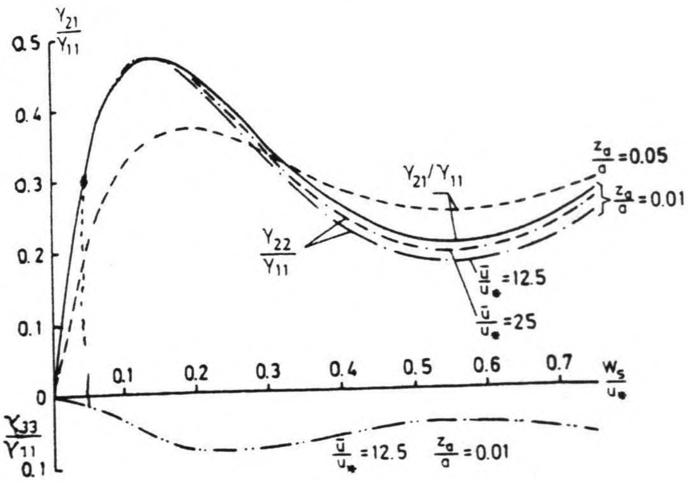

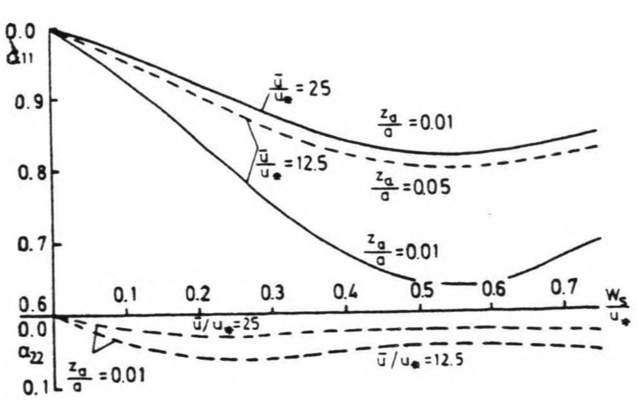

8

z_a/d = 0.01 for natural channels

k	a_1	b_1	a_2	b_2	a_3	b_3	a_4	b_4
1	1.9779	0.000	-6.3214	0.000	3.256	0.00	0.193	0.00
2	1.9782	0.543	-6.3255	-3.331	3.272	0.40	0.181	1.79
3	1.0944	5.632	-4.3437	-13.537	-2.844	15.34	3.812	-5.77
4	-0.0109	-0.808	-4.8698	-11.761	12.161	39.05	-8.041	-30.26
5	-0.0107	-0.819	-4.8663	-12.471	12.150	40.93	-8.033	-31.56
6	1.0000	0.114	0.0000	-7.995	-0.000	2.04	0.000	3.48
7	0.0000	-3.852	0.0001	3.763	-0.000	5.25	-0.012	-7.03
8	-0.0098	-4.254	-0.0382	5.325	0.042	3.52	-0.012	6.52
9	0.0004	-0.006	-0.0245	4.787	0.068	-11.27	-0.049	7.34
10	0.0007	-0.307	-0.0547	13.221	0.135	-26.98	-0.088	14.75
11	0.0008	-0.311	-0.0585	13.370	0.143	-27.28	-0.093	14.91

Table C1

z_a/d = 0.02 for natural channels

k	a_1	b_1	a_2	b_2	a_3	b_3	a_4	b_4
1	1.7883	0.000	-5.7793	0.000	2.860	0.00	0.226	0.00
2	1.7887	0.570	-5.7832	-3.000	2.872	0.56	0.217	1.43
3	0.9619	4.942	-4.3581	-10.455	-2.423	11.06	3.440	-3.70
4	-0.0177	-0.565	-4.1797	-9.906	10.487	31.50	-6.955	-23.95
5	-0.0175	-0.680	-4.1743	-10.959	-10.470	34.28	-6.9.42	-25.85
6	1.0000	0.091	0.0000	-7.040	-0.000	3.16	-0.000	1.76
7	0.0000	-3.372	0.0000	4.239	-0.000	2.16	0.000	-4.48
8	0.0084	-3.715	-0.0313	5.522	0.036	0.68	-0.012	-3.98
9	-0.0003	0.006	-0.0189	3.780	0.052	-8.98	-0.037	5.89
10	0.0005	-0.212	-0.0420	-10.435	0.105	-22.13	-0.070	-12.64
11	0.0006	-0.216	-0.0472	-10.637	0.116	-22.55	-0.076	-12.88

Table C2

$z_a/d = 0.05$ for natural channels

k	a_1	b_1	a_2	b_2	a_3	b_3	a_4	b_4
1	1.4856	0.000	- 4.9986	0.000	2.306	0.00	0.247	0.00
2	1.4859	0.576	- 5.0016	- 2.416	2.314	0.72	0.242	0.91
3	0.6944	4.006	- 4.2619	- 6.914	- 1.902	6.62	2.895	- 1.77
4	- 0.0198	- 0.300	- 3.1905	- 7.145	7.985	21.48	- 5.280	- 15.91
5	- 0.0195	- 0.320	- 3.1820	- 8.745	7.960	25.64	- 5.262	- 18.72
6	1.0000	0.059	0.0000	- 5.363	- 0.000	3.48	0.000	0.30
7	0.0000	- 2.535	- 0.0000	9.937	- 0.000	- 0.47	0.000	- 1.85
8	0.0059	- 2.776	- 0.0206	4.777	0.024	- 1.45	- 0.009	- 1.49
9	- 0.0002	0.013	- 0.0113	2.412	0.030	- 5.73	- 0.022	3.75
10	0.0002	- 0.110	- 0.0252	6.710	0.064	- 14.83	- 0.044	8.87
11	0.0004	- 0.115	- 0.0320	6.973	0.079	- 15.40	- 0.053	9.21

Table C3

CALCULATION OF BED-LEVEL CHANGE

1. <u>General</u>

The solution of the depth averaged equations that are developed here requires the prior knowledge of the coefficients γ_{ij}, α_{ij} etc. as well as the main equilibrium concentration C_e. It can be seen that all the coefficients could be obtained if the following quantities are known:

a. z_a: the level where the bottom boundary is applied, this is determined by the dimensionless quantitiy

$$\frac{z_a}{d} \text{ or } \frac{z_a}{h} = \beta$$

b. the normalized velocity profile p (ζ). If the flow is assumed to be fully rough the shape of p (ζ) can be shown to depend on only the parameters

$$f_* = \frac{\kappa \bar{u}}{u_*} \qquad \text{and } \beta;$$

c. the normalized equilibrium concentration profile $\phi_o(\zeta)$, this profile can be shown to depend on the parameters

$$\frac{w_s}{u_*} \text{ and } \beta.$$

2. Unsteady flow calculation

If the porosity of the bed is p_b and the storage term $\frac{\partial(ch)}{\partial t}$ is negligible, the rate of change in the bed z_b could be expressed as

$$\frac{\partial z_b}{\partial t} + \frac{1}{(1 - p_b)} \frac{\partial s_s}{\partial x} + \frac{\partial s_b}{\partial x} = 0 \quad \dots\dots (26)$$

s_s = suspended transport
s_b = bed-load transport

then if the effects of the changing shape of the velocity profile and the equilibrium profile are neglected, the basic equation that governs the first order variation of the mean concentration is

$$\gamma_{11} \overline{c_e} = \gamma_{11} \bar{c} + \gamma_{21} \frac{h}{w_s} \frac{\partial \bar{c}}{\partial t} + \gamma_{22} \frac{\bar{u}h}{w_s} \frac{\partial \bar{c}}{\partial x} \quad \dots\dots (14a)$$

which may also be written as

$$\overline{c_e} = \bar{c} + L_A \frac{\partial \bar{c}}{\partial x} + T_A \frac{\partial \bar{c}}{\partial t} \quad \dots\dots (20)$$

$$\text{where } L_A = \frac{\gamma_{22}}{\gamma_{11}} \frac{\bar{u}h}{w_s} \quad \dots \quad T_A = \frac{\gamma_{21}}{\gamma_{11}} \frac{h}{w_s} \quad \dots\dots (21)(22)$$

A six-point scheme is used for expressing these equations in finite difference form

$$\frac{\partial \bar{c}}{\partial t} = \frac{c_i^{j+1} - c_i^j}{\Delta t} \quad \dots\dots (27a)$$

$$\frac{\partial c}{\partial x} = \frac{(1 - \theta) \left[c_{i+1}^j - c_{i-1}^j\right] + \theta \left[c_{i+1}^{j+1} - c_{i-1}^{j+1}\right]}{2\Delta x} \quad \dots\dots (27b)$$

$$\bar{c} = (1 - \theta) \; c_i^j + \theta \; c_i^{j+1} \quad \dots\dots (27c)$$

$$\bar{c}_e = (1 - \theta) \; c_{e_i}^j + \theta \; c_{e_i}^{j+1} \quad \dots\dots (27d)$$

$$T_A = (1 - \theta)\, T_i^j + \theta\, T_i^{j+1} \quad \ldots\ldots\ldots\ldots\ldots\ldots\ldots\ldots\ldots\ldots (27e)$$

$$L_A = (1 - \theta)\, L_i^j + \theta\, L_i^{j+1} \quad \ldots\ldots\ldots\ldots\ldots\ldots\ldots\ldots\ldots\ldots (27f)$$

As $\bar{u}$, h, u_* etc. are known on beforehand, C_e, T_A and L_A could be calculated from (27) using the fitted relations to obtain γ_{21} and γ_{22} for each point (i,j).

This can also be written as

$$a_i^j = b_{i-1}^j * c_{i-1}^{j+1} + b_i^j * c_i^{j+1} + b_{i-1}^j * c_{i+1}^{j+1} \qquad \underline{2 \le i \le n-1} \quad \ldots (28a)$$

where $b_{i-1}^j = - \dfrac{\theta L_A}{2\Delta x}$

$b_i^j = \dfrac{T_A}{\Delta t}$

$b_{i+1}^j = \dfrac{\theta L_A}{2\Delta x}$

$$a_i^j = \overline{c_e} + \frac{T_A}{\Delta t} c_i^j - (1 - \theta)\, c_i^j - (1 - \theta)\, \frac{L_A}{2\Delta x}\, c_{i+1}^j - c_{i-1}^j$$

$a_i^j = b_i^j\, c_i^{j+1} + b_2^j\, C_2^{j+1} + b_0^j\, c_0^{j+1}$ <u>as upstream boundary</u> ... (28b)

c_0^j and c_0^{j+1} is known

where $b_i^j = \dfrac{T_A}{\Delta t} + \theta \qquad b_0 = \dfrac{L_A}{2\Delta x}$

$b_2^j = \dfrac{\theta L_A}{2\Delta x}$

$$a_i^j = \overline{c_e} + \frac{T_A}{\Delta t} c_i^j - (1 - \theta)\, c_i^j - (1 - \theta)\, \frac{L_A}{2\Delta x}\, c_2^j - c_0^j$$

and $a_n^j = b_{n-1}^j\, c_{n-1}^{j+1} + b_n^j\, c_n^{j+1}$ <u>as downstream boundary</u> ... (28c)

$$b_{n-1}^j = \frac{- L_A\theta}{\Delta x} + \frac{T_A}{2\Delta t} + \frac{\theta}{2}$$

$$b_n^j = \frac{T_A}{2\Delta t} + \frac{\theta}{2} + \frac{L_A\theta}{\Delta x}$$

$$a_n^j = \overline{c_e} - \frac{TA}{2\Delta t}(c_n^j - c_{n-1}^j) + \frac{LA}{\Delta x}(1-\theta)(c_n^j - c_{n-1}^j)$$

$$+ \frac{(1-\theta)(c_n^j + c_{n-1}^j)}{2}$$

Equations (28a,b,c) represent a set of h simultaneous equations for c_i^{j+1} from i = 1 to n. a_i^j is known if the concentrations c_i^j at the previous time step are known. The solution requires the inversion of a tn-diagonal matrix. The boundary conditions required are:

a. C_0^j for all values j(t) (upstream condition)

b. c_i^0 for all values i(x) (initial condition)

Once the mean concentration is obtained, the sediment transport rate can be calculated from (16b)

$$s_s = \alpha_{11}\,\bar{u}\,h\,\bar{c} + \alpha_{21}\frac{h^2\bar{u}}{w_s}\frac{\partial\bar{c}}{\partial t} + \alpha_{22}\frac{h^2\bar{u}^2}{w_s}\frac{\partial\bar{c}}{\partial x} \quad \text{(16b)}$$

$$\frac{\partial\bar{c}}{\partial x} = \frac{c_{i+1}^j - c_{i-1}^j}{2\Delta x} \quad \text{(29a)}$$

$$\frac{\partial\bar{c}}{\partial t} = \frac{c_i^{j+1} - c_i^{j-1}}{2\Delta t} \quad \text{(29b)}$$

the entrainment rate is obtained from (18) using

$$\frac{\partial(\bar{c}h)}{\partial t} = \frac{(c_i^{j+i}\,h_i^{j+i} - c_i^{j-i}\,h_i^{j-i})}{2\Delta t} \quad \text{(30)}$$

$$E = \frac{\partial(\bar{c}h)}{\partial t} + \frac{\partial s_s}{\partial x} \quad \text{(18)}$$

3. Quasi steady flow

The first order equation governing the mean concentration in a flow when the roughness is assumed to remain constant is (see Galapatti (lit. (1))

$$\gamma_{11}\,\overline{c_e} + \quad \gamma_{11} + (\mu_1 + \frac{\mu_2}{f_*})\frac{\bar{u}}{w_s}\frac{\partial h}{\partial x} \quad \bar{c} + \gamma_{22}\frac{\bar{u}h}{w_s}\frac{\partial c}{\partial x} \quad \text{(31)}$$

with $\frac{\partial f_*}{\partial x} = \frac{1}{h}\frac{\partial h}{\partial x}$ and $f_* = \frac{\kappa \bar{u}}{u_*}$

and μ_1, μ_2 according to figure C9, this to take into account the vertical velocity and the changes of shape of both the velocity profile p and the equilibrium concentration which may also be expressed as

$$\overline{c_e} = (1 + G_A \frac{\partial h}{\partial x})\,\bar{c} + L_A \frac{\partial \bar{c}}{\partial x} \quad \ldots\ldots\ldots\ldots\ldots (32)$$

where $G_A = (\mu_1 + \frac{\mu_2}{f_*})\,\frac{\bar{u}}{\gamma_{11}\, w_s}$

Equation (31) is solved at each time level independently.

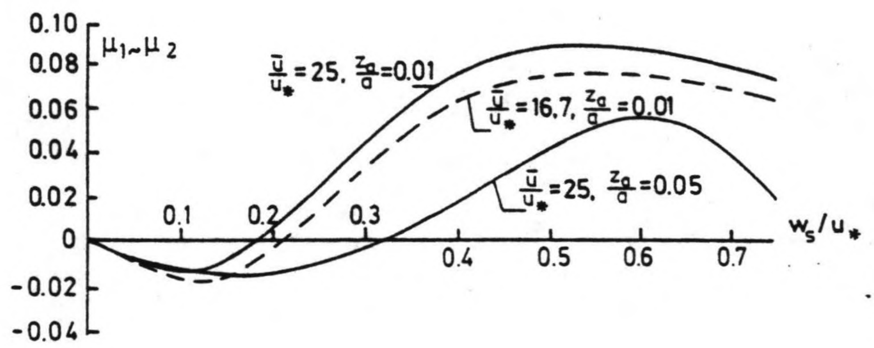

9

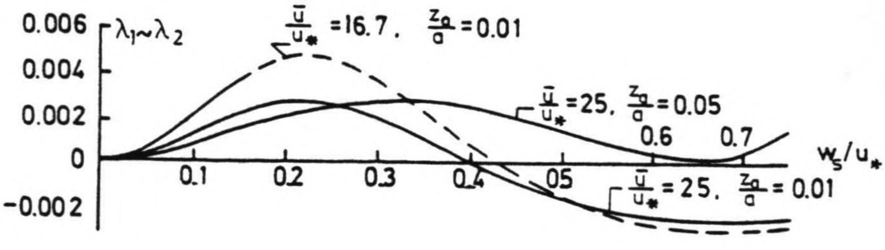

10

The following difference scheme was used to set up the simultaneous equations to solve c_i^j from i = 1 to h

$$\frac{\partial \bar{c}}{\partial x} = \frac{c_{i+1}^j - c_{i-1}^j}{2\Delta x} \qquad (33a)$$

$$\frac{\partial h}{\partial x} = \frac{h_{i+1}^j - h_{i-1}^j}{2\Delta x} \qquad (33b)$$

$$G_A = G_{A\,i}^j \qquad (33c)$$

$$L_A = L_{A\,i}^j \qquad (33d)$$

$$\overline{c_e} = c_{e\,i}^j \qquad (33e)$$

Substituting equation 33a t/m 33e in 32 will yield n-1 equations in c_j^i for i = 1, n. the last equation is obtaned by writing the differential equation for $x = (n - \frac{1}{2})\,\Delta x$

$$\frac{\partial \bar{c}}{\partial x} = \frac{c_n^j - c_{n-1}^j}{\Delta x} \qquad (34a)$$

$$\frac{\partial h}{\partial x} = \frac{h_n^j - h_{n-1}^j}{\Delta x} \qquad (34b)$$

$$G_A = \frac{G_{A\,n}^j + G_{A\,n-1}^j}{2} \quad \text{etc.} \qquad (34c)$$

Therefore it is possible to express (31) as h simultaneous equations for c_i^j = 1 to h. C_o is the known boundary condition.

Once c_i^j is known, the sediment transport rate is calculated from

$$s_s = \bar{u}h \left[\left[\alpha_{11} + \left(\lambda_1 + \frac{\lambda 2}{f_*}\right) \frac{\bar{u}}{w_s} \frac{\partial h}{\partial x} \right] \bar{c} + \alpha_{22} \frac{\bar{u}h}{w_s} \frac{\partial \bar{c}}{\partial x} \right] \qquad (35)$$

by expressing it in finite difference form

λ_1 and λ_2 from Galapatti <u>fig. C10</u>

The new bed level is calculated from

$$z_{b\,i}^{j+1} = z_{b\,i}^{j} - \frac{1}{(1 - p_b)} \; \frac{s_{j+1}^{j} - s_{j-1}^{j}}{2\Delta x} \; t \; +$$

$$0.5\alpha \, (z_{b\,i+1}^{j} - 2\, z_{b\,i}^{j} + z_{b\,i-1}^{i}) . \; . \; . \; . \; . \; . \; . \; . \; . \; . \; . \; . \; . \; . \; . \; (36)$$

The term with the α is an artificially introduced "pseudoviscosity" term. The smallest possible value of α compatible with stability is used. Once the new bed profile is known it is possible to compute the new flow field etc. using an appropriate procedure. Hence u_i^{j+1}, h_2^{j+1} etc. may be obtained.

fig. C11

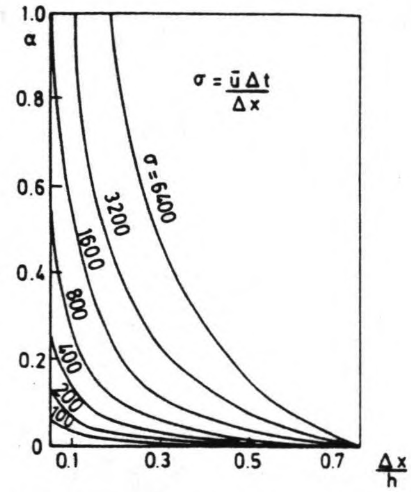

11

Fig. C11 shows the minimum values of α required to obtain stability for all K for various values of $\frac{\Delta x}{h}$ and the courant number $\sigma = \frac{u\Delta t}{\Delta x}$

$$\kappa = \frac{2\pi}{\lambda} \; ; \; \lambda = \text{length bedform disturbance}$$

VALIDITY OF THE MODEL

For practical application a high order solution is not interesting. In fact only the first order solution can generally be used in practice. Therefore the validity of first order solution has to be studied as done by Wang (lit. (3)). It can be shown that the deviation between the first order estimation and the exact value of the solution of the asymptotic relationship depends mainly on $\frac{w_s}{u_*}$ and this deviation increases as $\frac{ws}{u_*}$ increases.
It should be holed that the adaption length of the mean concentration has the order of magnitude $\frac{uh}{w_s}$ (see fig. C5).
Directly downstream of a stepwise change in the bed boundary condition or a stepwise change of the concentration profile (initial condition) the asymptotic model is not valid.
This distance where the model is not valid has the same order of magnitude as the adaption length of the function

$$f(\xi) = \frac{A_2 \exp(\lambda_2 \xi)}{A_1 \exp(\lambda_1 \xi)} = \frac{A_2}{A_1} \exp((\lambda_2 - \lambda_1)\xi) \quad \ldots\ldots\ldots (37)$$

because the exact n^{th} order solution for steady uniform flow of eq. (1)

$$p(\zeta) \frac{\partial c}{\partial \xi} = \frac{\partial c}{\partial \zeta} + \frac{\partial c}{\partial \zeta} (\varepsilon^{1} \frac{\partial c}{\partial \zeta}) \quad \ldots\ldots\ldots (38)$$

consists of

$$c\ (\xi, \zeta) = c_e(\zeta) + \sum_{1=1}^{\infty} A_i \exp(\lambda_i \xi)\phi_i\ (\zeta) \quad \ldots\ldots\ldots (39)$$

in which ϕ_i is an eigen function with the corresponding eigen value λ_i

and the n^{th} order solution of the asymptotic model converges to one component

$$c(\xi,\zeta) = c_e(\zeta) + A_1 \exp(\lambda_1 \xi)\phi_1(\zeta) \quad \ldots\ldots\ldots (40)$$

consequently, the model is not generally valid. However the components of eq. (39) that do not occur in (40) will decrease more rapidly than the first component because

$|\lambda_1| < |\lambda_2| < |\lambda_3|$ etc.

By using the approximations $p \simeq 1$ and $\varepsilon_z \simeq 0.1(u_* h)$ it can be shown that the adaption length of the error function $f(\xi)$ which is defined as the value at which $f(\xi)$ is decreased by a factor e, has the order of $\frac{uh}{u_*}$.

Therefore the model is only valuable if $\frac{w_s}{u_*}$ is small because otherwise the adaption length of the mean concentration will have the same order of magnitude as the length of the region in which the model is not valid. A maximum value of $\frac{w_s}{u_*}$ for validity of the first order solution is estimated as 0.3 to 0.4.

For the general case, viz. unsteady non-uniform flow, the validity of the model has not been studied. However, based on the analysis done by Z.B. Wang (lit. (4)) it can be expected that the model is valid if the following three requirements are satisfied:

1. the time scale of the flow variation is much larger than $\frac{h}{u_*}$;
2. the length scale of the flow variation is much larger than $\frac{uh}{u_*}$;
3. the factor $\frac{w_s}{u_*}$ is small (< 0.3)

CONCLUSIONS

A simple transport formula can only be applied if the adaption time and length of the depth averaged (mean) concentration is small compared with the time/length scale of the problem under consideration. On the other hand, a two-dimensional model to solve the basic equation (1) is expensive since it requires a lot of computation work. This is especially true in case of morphological computations in which predictions over a period of several years are necessary, and for three-dimensional applications (estuaries).

In order to avoid the disadvantages of the two models, attemptions have been made by different researchers to develop cheaper alternatives such as depth integrated models. Generally these models are based on the integration of equation (1) over the depth averaged concentration $\underline{c}$. An extra emperical relation is needed for the rate of sediment exchange between the flow and the bed (entrainment rate).

A new approach has been carried out by Galapatti (lit. (1)), who developed a depth integrated model based on a asymptotic solution of equation (1). The main concept of this model is:

1. with an asymptotic solution of eq (1) the concentration field c(x,z,t) is expressed in the unknown depth average concentration c(x,t);

2. by applying the bed boundary condition a solution is found for the depth averaged concentration c(x,t);

3. when c(x,t) has been solved, the concentration field can be found by substituting c(x,t) in the asymptotic solution.

Compared with other depth integrated models this model has two important advantages:

1. no empirical relation is used during the derivation of the model;

2. all possible bed boundary conditions can be used in the model.

Literature Appendix C (a depth integrated model)

1. Galapatti, R., A depth integrated model for suspended transport

Report 83-7
Communications on Hydraulics
Delft University of Technology 1983

2. Galapatti, R. and Vreugdenhill, C.B., A depth integrated model for suspended transport

Journal of Hydraulic Research
Vol 23 no. 4 1985

3. Wang, Z.B. and Ribbernik, J.S., The validity of a depth integrated model for suspended sediment transport

Journal of Hydraulic Research
Vol 24 no. 1 1986

4. Wang, Z.B., The validity of a Depth Integrated Model for Suspended Sediment Transport and the Extension of this Model to Tidal Rivers

Report 84-10
Department of Civil Engineering
Delft University of Technology 1984

5. Kerssens, P.J.M., Adaption Length for Suspended Sediment Verticals

Afstudeerverslag
Department of Civil Engineering
Delft University of Technology 1974

6. Rousse, H, Modern Conceptions of the Mechanics of Turbulence

Trans. ASCE
Page 532-536 1937

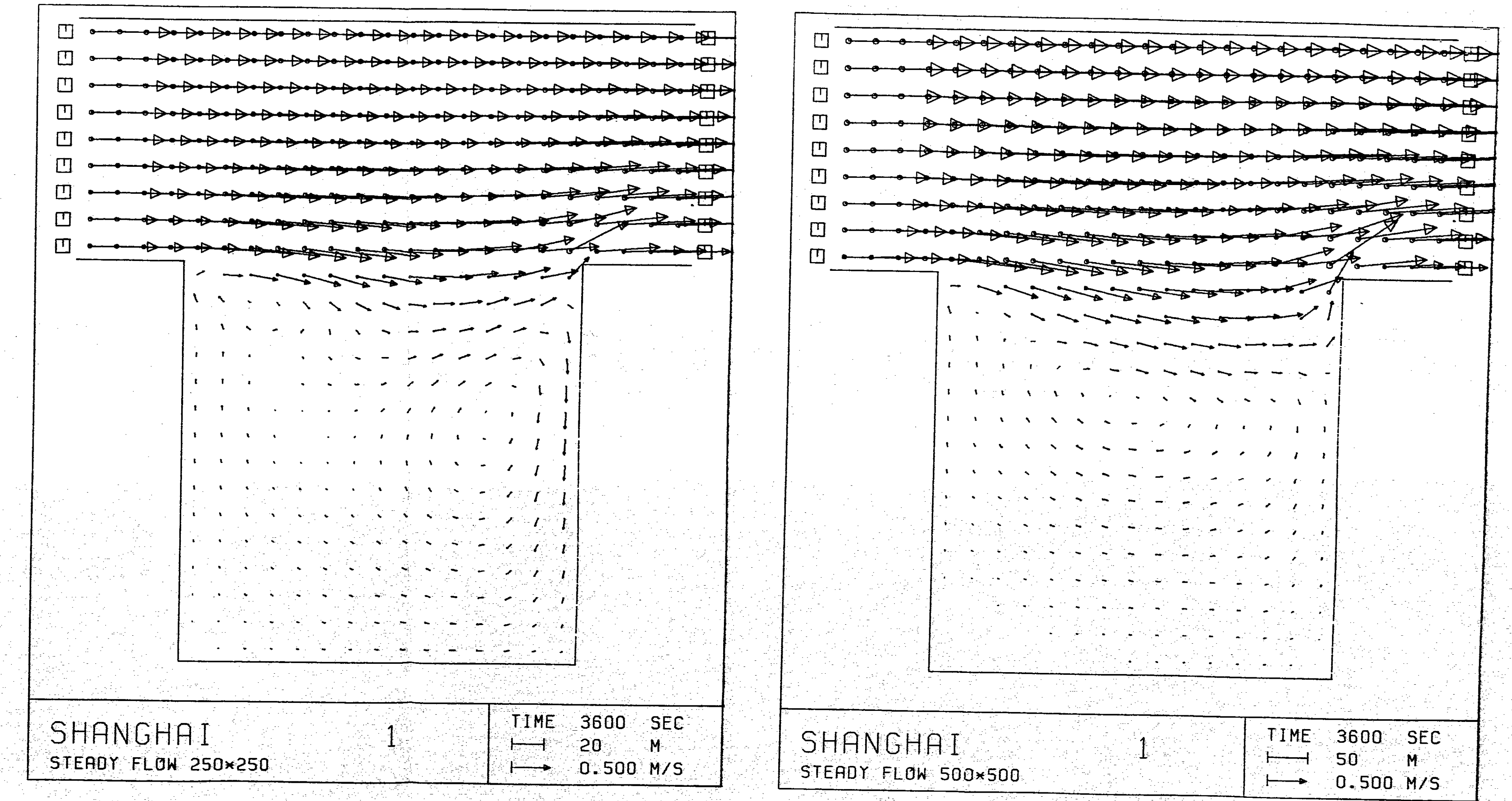

Results steady-flow computations

4.1

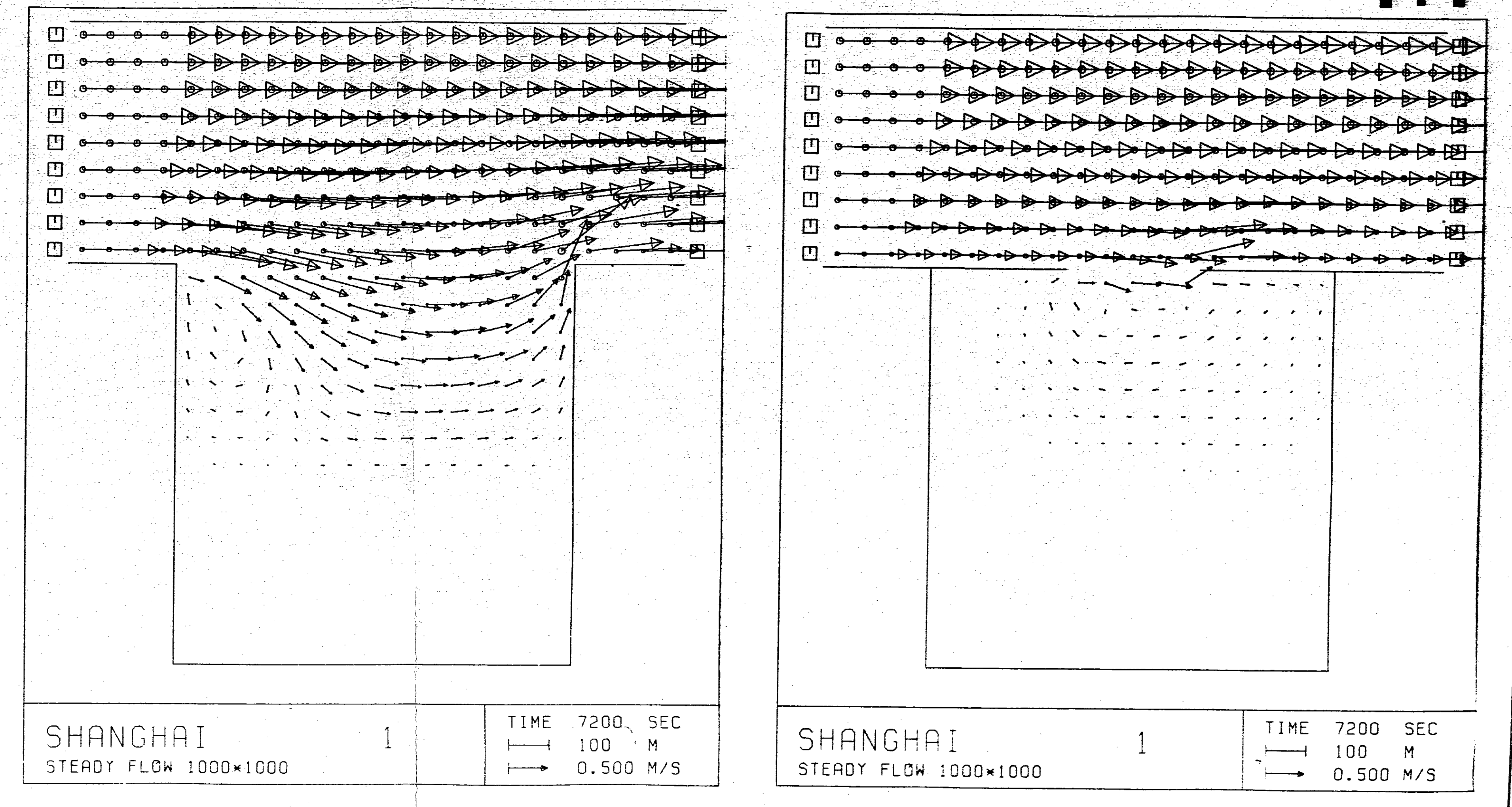

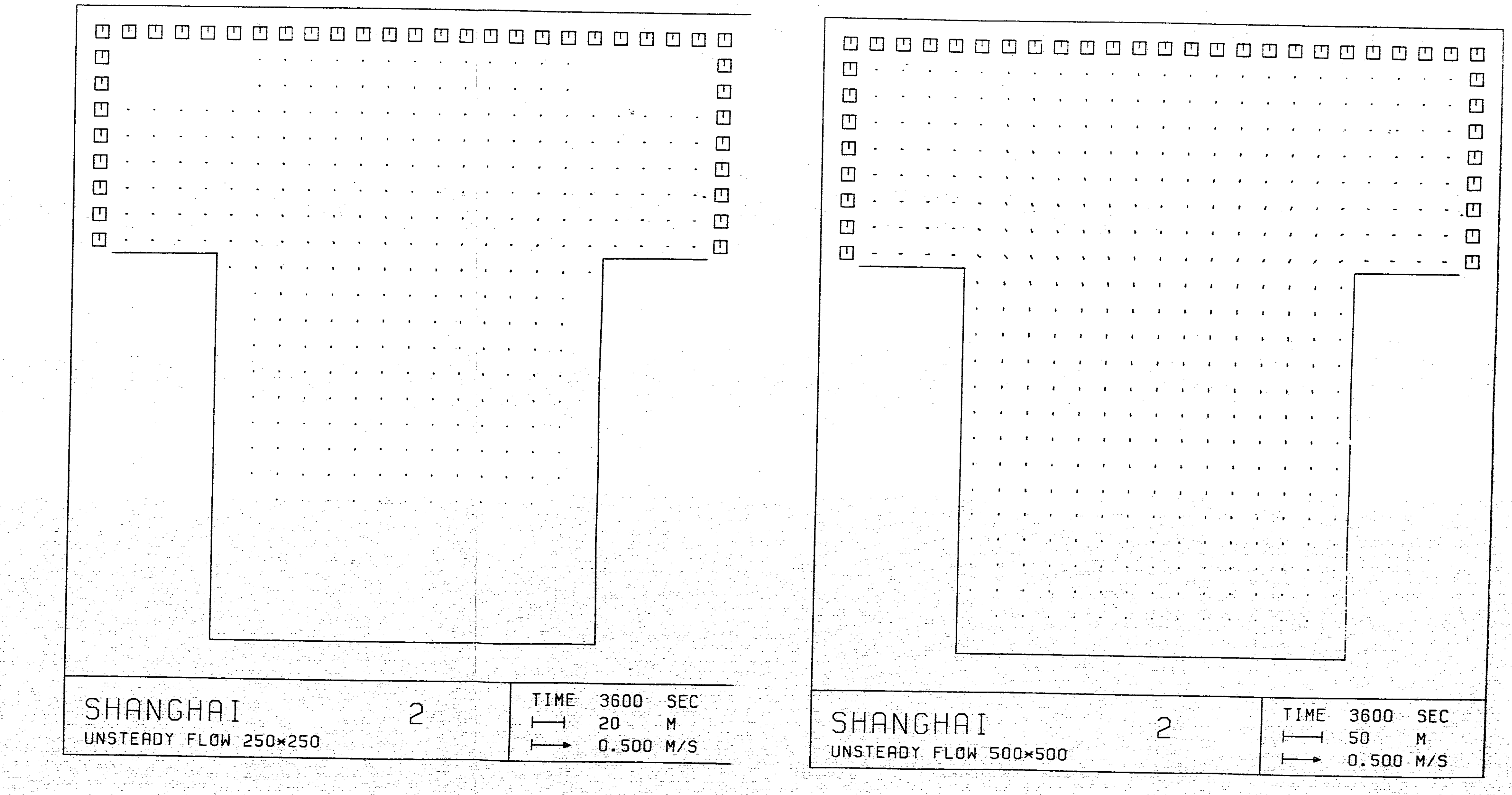

Results unsteady-flow computations 4.2

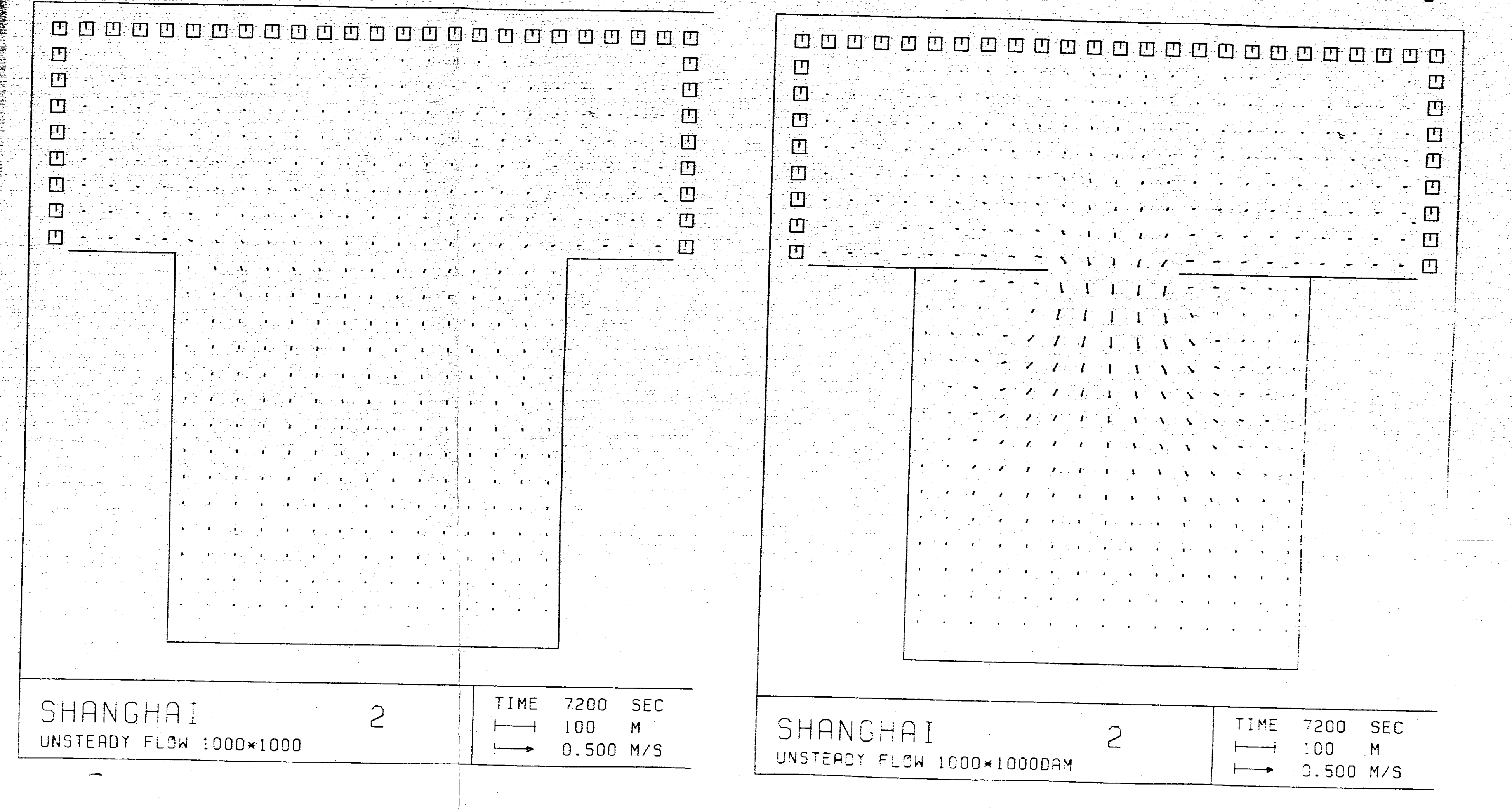

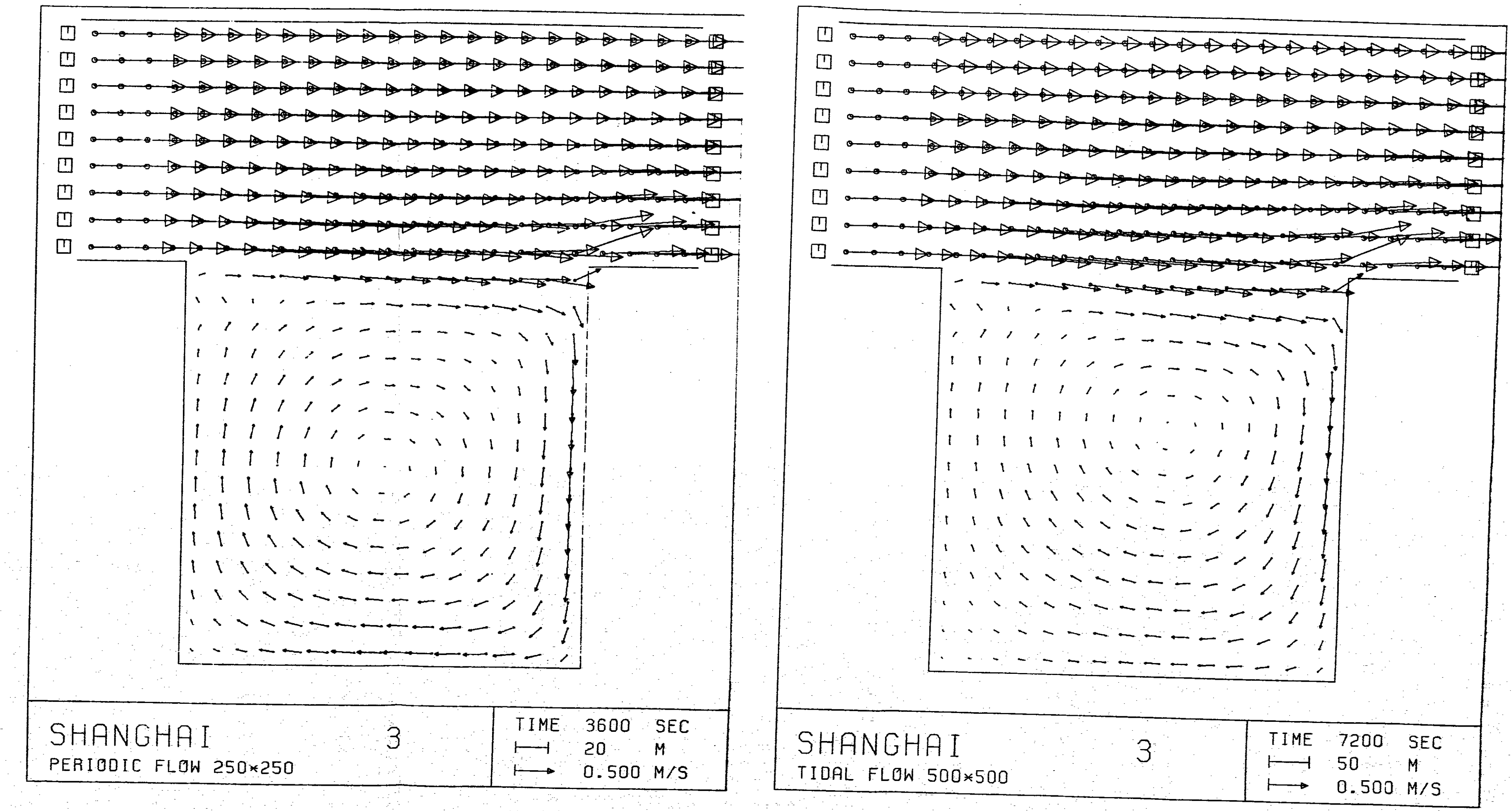

Results tidal-flow computations

4.3